UNIVERSITEIT GENT

FACULTY OF PHARMACEUTICAL SCIENCES
DRUG Quality & Registration (DRUQUAR) Lab

TO WHAT EXTENT DO CELL-PENETRATING PEPTIDES SELECTIVELY CROSS THE BLOOD-BRAIN BARRIER?

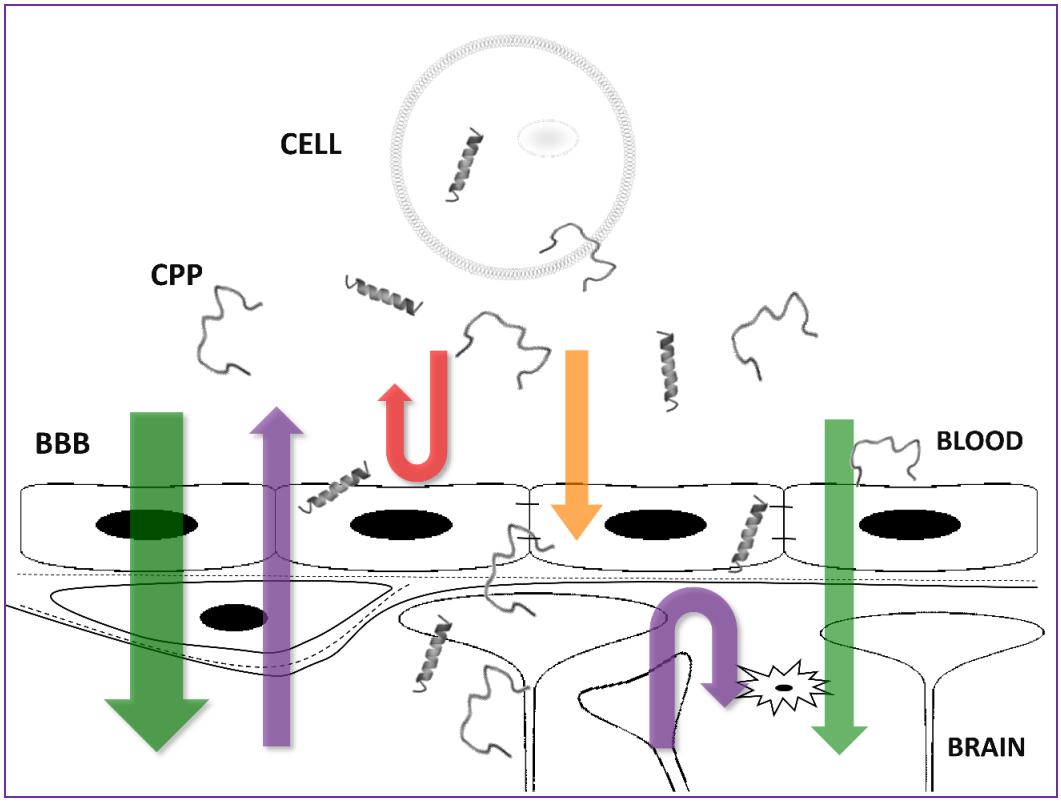

Thesis submitted to obtain the degree of Doctor in Pharmaceutical Sciences

Sofie STALMANS

Promotor
Prof. Dr. Bart DE SPIEGELEER

UNIVERSITEIT GENT

FACULTY OF PHARMACEUTICAL SCIENCES
Drug Quality & Registration (DruQuaR) Lab

TO WHAT EXTENT DO CELL-PENETRATING PEPTIDES SELECTIVELY CROSS THE BLOOD-BRAIN BARRIER?

Sofie STALMANS
Master of Science in Drug Development

Promoter
Prof. Dr. Bart DE SPIEGELEER

2015

Thesis submitted to obtain the degree of
Doctor in Pharmaceutical Sciences

COPYRIGHT

Ghent, 25 September 2015

The promotor	The author
Prof. Dr. Bart De Spiegeleer	Sofie Stalmans

ACKNOWLEDGEMENTS

During this Ph.D. project, I was helped and supported by many people and I'm very grateful for that. Therefore, I would like to address some words to them.

First of all, I'm very thankful to my *promotor, Prof. Dr. Bart De Spiegeleer*. It was your contagious enthusiasm and scientific dedication that persuaded me to start this Ph.D. at DruQuaR. During the last four years, I learned so much from our endless discussions, but also from your sharing of your long-lasting experience in the pharmaceutical world. I really appreciate you always took your time to advise and help me with my research. I also thank you for your encouragements and to always drive me to bring my work at a higher level. It was an honor to me to work under your guidance.

I also wish to thank the members of the *reading and examination committee*, *i.e.* Prof. Dr. Kevin Braeckmans as chairman, Prof. Dr. Christophe Stove, Prof. Dr. Albert Gjedde, Prof. Dr. Jos Hoogmartens (all members of the reading committee), Prof. Dr. Dieter Deforce, Prof. Dr. Luc Leybaert, Prof. Dr. Guy De Tré and Dr. Kathelijne Peremans, for critically reviewing this work. The interesting and dynamic discussions definitely helped to improve the quality of this thesis.
I thank *Ghent University*, its *faculty of Pharmaceutical Sciences* and the *DruQuaR* lab for the use of their facilities and *Doctoral Schools* for the educational support. This work would not have been possible without the financial support of the *Special Research Fund* (BOF number 01D38811), which I greatly acknowledge.

I'm grateful to my *former DruQuaR co-workers*, Dr. Sylvia Van Dorpe, Dr. Jente Boonen, Elien Vangheluwe and the previous lab technicians, for helping me to familiarize at the lab during the first months. I thank Dr. Sylvia Van Dorpe, Dr. Evelien Wynendaele, Nathalie Bracke, Bert Gevaert and Mathieu Verbeken for teaching me the blood-brain barrier transport experiment techniques, for your help during the experiments and with the care for the animals. Thanks Matthias, Kirsten and Sileshi for the nice atmosphere at the desk. I'm also grateful to my *present collegues*: Dr. Evelien Wynendaele, Dr. Matthias D'Hondt, Mathieu Verbeken, Sultan Suleman, Nathalie Bracke, Lieselotte Veryser, Lien Taevernier, Bert Gevaert, Frederick Verbeke, Han Yao, Xiaolong Xu, Sileshi Belew Yohannes and Yorick Janssens. Due to you all, I really enjoyed my stay at DruQuaR. Thanks for the help with experiments, writing manuscripts and reports and scientific discussions, but also for all the laughs, joyful evening activities and of course, the memorable DruQuaR weekends. I really hope the finishing of this Ph.D. is not a goodbye to you all!

Furthermore, I would like to thank the people that I worked with during collaborating projects. I acknowledge *Prof. Dr. Guy De Tré, Prof. Dr. Antoon Bronselaer* and *Joachim Nielandt* (Ghent University, Department of Telecommunications and Information Processing, TELIN) for their help with the adjustments to the Brainpeps database and help with modeling and classification strategies. I'm grateful to *Dr. Kathelijne Peremans* and *Dr. Eva Vandermeulen* (Ghent University, Department of Veterinary Medical Imaging and Small Animal Orthopaedics) for their help with the logistics of the blood-brain barrier transport experiments and for being always ready to help. I appreciate the comments and suggestions of *Yvan Saeys* (Ghent University - VIB, Inflammation Research Center) on the study of the classification of blood-brain barrier influx of peptides. I'm thankful to *Prof. Dr. Jean Paul Remon and Dr. Maxime Willems* for the fruitful collaboration project on the stability study of cyclophosphamide during flatworm carcinogenicity assays. I also express my gratitude to *Prof. Dr. Ralf Hoffmann* and *Dr. Daniel Knappe* (University of Leipzig, Center for Biotechnology and Biomedicine) for the collaboration project on the short, proline-rich antimicrobial peptides and to *Prof. Dr. David Craik* (University of Queensland, Institute for Molecular Bioscience) for the constructive cooperation on the disulfide-rich (cyclic) peptides.

Last, but foremost, I wish to thank my family and friends for their kindness, support and interest in my work. The dinners, lovely chats, family weekends and short trips provided the necessary distraction and made me realize that there was more than work in life. Finally, I would like to thank four special people: mama, papa, my brother Jan and Pieter. Thanks for your love, your patience, especially during the last half year, care, encouraging words and for being always there for me. You really are the best!

Sofie

LIST OF ABBREVIATIONS AND SYMBOLS

3D	3-Dimensional
Aβ	Amyloid beta
ABC	ATP-Binding Cassette
AD	Alzheimer's Disease
AJ	Adherens Junction
AMP	Antimicrobial Peptide
ATMP	Advanced Therapy Medicinal Product
ATP	Adenosine Triphosphate
a.u.	Arbitrary/absorbance unit
BBB	Blood-Brain Barrier
BBB_{in}	Blood-Brain Barrier influx
BEH	Ethylene Bridged Hybrid
BLI	Kier Benzene-Likeliness Index
BMEC	Brain Microvessel Endothelial Cells
BRCP	Breast Cancer Resistance Protein
BSA	Bovine Serum Albumin
BUI	Brain Uptake Index
C_{18}	Octadecyl carbon chain-bonded silica
CA	Carrier-Added
CAPH	Cationic Amphipathic Polyproline Helix
CD	Capillary Depletion
CHMP	Committee for Medicinal Products for Human use
CNS	Central Nervous System
CLSM	Confocal Laser Scanning Microscopy
COPD	Chronic Obstructive Pulmonary Diseases
CP	Cell-Penetrating
CPP	Cell-Penetrating Peptide
Cx	Connexin
DOTA	1,4,7,10-tetraazacyclododecane-1,4,7,10-tetraacetic acid
DNA	Deoxyribonucleic Acid
EC	Extracellular
EFGCP	European Forum for Good Clinical Practice

EFPIA	European Federation of Pharmaceutical Industries and Associations
EMA	European Medicines Agency
EPAR	European Public Assessment Report
ESI	Electrospray Ionization
EU	European Union
FA	Formic Acid
FACS	Fluorescence-Assisted Cell Sorting
FDA	Food and Drug Administration
FITC	Fluorescein Isothiocyanate
Fmoc	9-Fluorenylmethyloxycarbonyl
GATS	Geary 2D-Autocorrelation
GEG	Geriatric Expert Group
GIP	Geriatric Investigation Plan
GJ	Gap Junction
GLP	Good Laboratory Practices
GLUT-1	Glucose Transporter-1
GMP	Good Manufacturing Practices
GMWP	Geriatric Medicines Working Party
GVP	Good Pharmacovigilance Practices
HCA	Hierarchical Cluster Analysis
HEPES	4-(2-hydroxyethyl)-1-piperazineethanesulfonic acid
HIV	Human Immunodeficiency Virus
HPLC	High Performance Liquid Chromatography
HRQOL	Health Related Quality Of Life
IC	Intracellular
ICH	International Conference on Harmonization
ICR-CD-1	Institute for Cancer Research, Caesarean Derived-1
ID	Identifier
IFN-γ	Interferon gamma
IgG	Immunoglobulin G
IND	Investigational New Drug
IV	Intravenous
JAM	Junctional Adhesion Molecule
K	Net brain clearance
K_1	Unidirectional blood-to-brain clearance

K_{in}	Unidirectional brain influx rate
k_{out}	Efflux rate constant
LC	Liquid Chromatography
LDL	Low Density Lipoprotein
LOD	Limit Of Detection
LR	Lactated Ringer
LRP	Low-density lipoprotein Receptor-related Protein
MALDI	Matrix-Assisted Laser Desorption/Ionization
MAP	Model Amphipathic Peptide
MLR	Multiple Linear Regression
MoRSE	3D-Molecule Representation of Structures based on Electron diffraction
MRI	Magnetic Resonance Imaging
MRP	Multidrug Resistance-associated Protein
Mp	Mean atomic polarizability
MS	Mass Spectrometry
M&S	Modeling & Simulation
MTR	Multiple Time Regression
MW	Molecular Weight
NBD	Nitrobenzoxadiazole
NCA	No-Carrier-Added
n_p	Peak capacity
NSAID	Non-Steroidal Anti-Inflammatory Drug
P	Permeability
PASS	Post-Authorization Safety Studies
PC	Principal Component
PCA	Principal Component Analysis
PDA	Photodiode Array
PDCO	Paediatric Committee
PNA	Peptide Nucleic Acid
Pgp	P-glycoprotein
Ph. Eur.	European Pharmacopoeia
pI	Isoelectric point
PIL	Product Information Leaflet
PIP	Paediatric Investigation Plan
Ph.D.	Doctor of Philosophy

PhVWP	Pharmacovigilance Working Party
PK/PD	Pharmacokinetics/Pharmacodynamics (modeling)
PMDA	Pharmaceutical and Medical Devices Agency
POT	Proton-coupled Oligopeptide Transporter
PRAC	Pharmacovigilance Risk Assessment Committee
PrAMP	Short, Proline-Rich Antimicrobial Peptide
PTS	Peptide Transport System
Q&A	Questions & Answers
QALY	Quality Adjusted Life Years
QC	Quality Control
QR	Quick Response
QSPR	Quantitative Structure-Property Relationship
RAGE	Receptors for Advanced Glycation End products
R&D	Research & Development
RLU	Relative Light Units
RNA	Ribonucleic Acid
ROS	Reactive Oxygen Species
RP	Reversed-Phase
SAR	Structure-Activity Relationship
SEM	Standard Error of the Mean
SI	Signal Intensity
siRNA	Short interfering Ribonucleic Acid
SmPC	Summary of the Product Characteristics
S/N	Signal-to-Noise ratio
SPE	Solid-Phase Extraction
SPPS	Solid-Phase Peptide Synthesis
SST	System Suitability Test
SVM	Support Vector Machine
$t_{1/2}$	Half-life
$t_{1/2,brain}$	Brain half-time disappearance
TAMRA	5-Carboxytetramethylrhodamine
Tat	Trans-activating transcriptional activator
TEER	Trans-Endothelial Electrical Resistance
TFA	Trifluoroacetic Acid
TJ	Tight Junction

TNF-α	Tumor Necrosis Factor-alpha
TOC	Total Organic Carbon
TOF	Time-Of-Flight
TP10	Transportan 10
U(H)PLC	Ultra (-High) Performance Liquid Chromatography
USA	United States of America
UV	Ultraviolet
V_0	Vascular brain distribution volume
V_g	Brain tissue distribution volume
V_i	Initial (vascular) brain distribution volume
WCX	Weak Cation eXchange
WHIM	Weighted Holistic Invariant Molecular
WHO	World Health Organization

TABLE OF CONTENTS

CHAPTER I

INTRODUCTION

"It is not the answers you give, but the questions you ask."

Voltaire
(°1694 - †1778, French Enlightenment writer, historian and philosopher)

CHAPTER I

INTRODUCTION

1. CELL-PENETRATING PEPTIDES

The ability of peptides to traverse the phospholipid bilayer of cell membranes was discovered more than 20 years ago, when it was demonstrated that the Trans-activator of transcription (Tat) protein of the Human Immunodeficiency Virus (HIV) and, a few years later, the third helix of the Antennapedia transcription factor protein of *Drosophila Melanogaster* were able to enter cells [1-5]. Since then, hundreds of studies have described peptides crossing cellular membranes, which are most commonly called *cell-penetrating peptides (CPPs)*. These CPPs are extensively investigated to act as intracellular delivery tools for (non-) covalently attached bioactive cargoes like siRNA, double stranded DNA, antisense oligonucleotides, peptides, proteins, nanoparticles, liposomes and small molecules [4-7]. Successful developmental applications have already been reported for CPPs coupled to therapeutic cargoes for treatment of cancer, muscular dystrophy, cardiology, antiprion diseases, as well as bacterial and viral infections [4]. Beside their use as carrier for intracellular delivery, CPPs can also exert a biological activity themselves [6,8-10]. Studies on the biological effect of CPPs, which can be toxic or of therapeutic interest, are limited. Generally, CPPs are considered to have a low toxicity profile as demonstrated both *in vivo* and *in vitro*, making them such interesting vectors for hydrophilic macromolecules [4,11-13].

Cell-penetrating peptides constitute a structural diverse group of peptides, characterized by a relatively short sequence of less than 40 amino acids. They can be classified based on their origin resulting in the *protein-derived, chimeric or synthetic CPP subgroups*, with chimeric implying a fusion peptide being an unnatural, multifunctional construct of at least two different peptides [14,15]. Cell-penetrating peptides derived from heparin-binding proteins, DNA and/or RNA-binding proteins, homeoproteins (a family of transcription factors containing a conserved DNA-binding motif), signal peptides, antimicrobial peptides and viral proteins have already been identified. In some cases, the cell-penetrating property of the CPPs is linked to the function of the native protein or peptide, like for viral proteins to gain cell entry, but sometimes the role of the CPP sequence in the parent protein or peptide is unknown [6]. Cell-penetrating peptides are mostly described as short, cationic peptide

sequences, but actually they show a great sequence variety. When classified based on their physicochemical properties, traditionally three major classes can be distinguished: the *cationic, amphipathic and hydrophobic CPPs* [6]. The cationic CPPs are characterized by a stretch of positive charges derived from arginine and lysine residues in their sequence. The second group comprises the amphipathic CPPs. Primary amphipathic peptides are featured by a hydrophilic and hydrophobic part in their sequence, while for the secondary amphipathic peptides the hydrophobic and hydrophilic amino acids become separated through formation of a helix structure. The hydrophobic CPPs are rich in apolar amino acids and have a low net charge. However, a clear overlap exists between these chemical groups, emphasizing that CPPs represent a chemically diverse group of peptides [6]. In Table 1, some examples of CPPs from the different classes and origin can be found.

Table 1: Examples of CPPs.

Name	Sequence	Chemical class	Origin	Reference
Tat 47-57	YGRKKRRQRRR	Cationic	Protein (viral)	[16]
SynB3	RRLSYSRRRF	Cationic	Protein (antimicrobial)	[17]
Oligo-arginine	R_n (n = 6-12)	Cationic	Synthetic	[18]
Penetratin	RQIKIWFQNRRMKWKK	Cationic	Protein (DNA-binding)	[3]
pVEC	LLIILRRRIRKQAHAHSK	Amphipathic (secondary)	Protein	[19]
TP10	AGYLLGKINLKALAALAKKIL	Amphipathic (primary)	Chimeric	[20]
K-FGF	AAVLLPVLLAAP	Hydrophobic	Peptide (signal)	[21]
Bip	VPTLK	Hydrophobic	Protein (DNA-binding)	[22]

Although CPPs are intensively investigated, the exact cellular uptake mechanism of these peptides remains elusive. A variety of methods is used to determine the cellular uptake mechanism and subcellular localization of CPPs. Both biological methods, using cell cultures, and biophysical methods, using model membranes and molecular modeling, are applied. In biological methods, CPPs are mainly fluorescently labeled and their uptake is indirectly quantified using fluorimetry or fluorescence-assisted cell sorting (FACS), and the cellular localization is studied using confocal microscopy [23]. Beside these fluorescence-based methods, functional assays in which the biological activity of the conjugated cargo is detected and matrix-assisted laser desorption/ionization-time-of-flight mass spectrometry (MALDI-TOF MS), allowing to directly quantify the internalized CPPs, are also widely applied [5,23]. Chromatographic separation techniques are no standard method to study the cellular uptake of peptides, and if used, the peptides are chemically modified [24,25]. The mechanism of uptake is evaluated using an inhibitor of one or more of the possible influx pathways [23]. Moreover, available studies differ in the applied experimental conditions like the cell line used, the extracellular peptide concentration, coupled cargo and label, temperature and incubation time [5]. These different parameters are known to influence the uptake of CPPs, complicating to draw general conclusions on the influx efficacy, used influx mechanism and the structural features determining cellular influx [5,23]. Currently, a consensus exists that both *endocytosis*, which is energy-dependent, and a *direct penetration mechanism*, which is energy-independent, are involved,

whether or not simultaneously occurring, depending on the applied conditions [4,5,23]. In addition, the involvement of receptors in the uptake of CPPs was recently demonstrated [26]. From the limited available structure-activity relationship (SAR) studies, it can be concluded that the number and density of positive charges, hydrogen bonding, presence of hydrophobic α-helical structures, thus the secondary structure, as well as the peptide length determine the cellular uptake of peptides [23,27-29].

In Figure 1, an overview of the different endocytosis-dependent and direct penetration mechanisms is shown [30]. Endocytosis, which is a natural process that occurs in all cells, is subdivided in macropinocytosis, endocytosis dependent on the coat proteins clathrin or caveolin and endocytosis independent of these coat proteins [23]. Endocytosis is triggered by an electrostatic interaction between the cationic CPPs and the negatively charged proteoglycans of the cell surface or through direct interaction with the plasma membrane [5]. Direct translocation involves the destabilization of the plasma membrane following an interaction of the CPP and the cell membrane either by an hydrophobic or electrostatic interaction [5,23]. Subsequently, the peptide folds on the lipid bilayer and internalizes using different mechanisms, *i.e.* inverted micelle model, through pore formation, including the barrel stave or toroidal pore model, or carpet-like model, depending on the peptide concentration, peptide sequence and composition of the cell membrane [23]. Endocytosis is assumed to be the main mechanism at lower peptide concentrations. When a certain concentration threshold is reached, which depends again on the cell type, the CPP sequence and the attached cargo, the CPPs enters the cell through direct penetration [23].

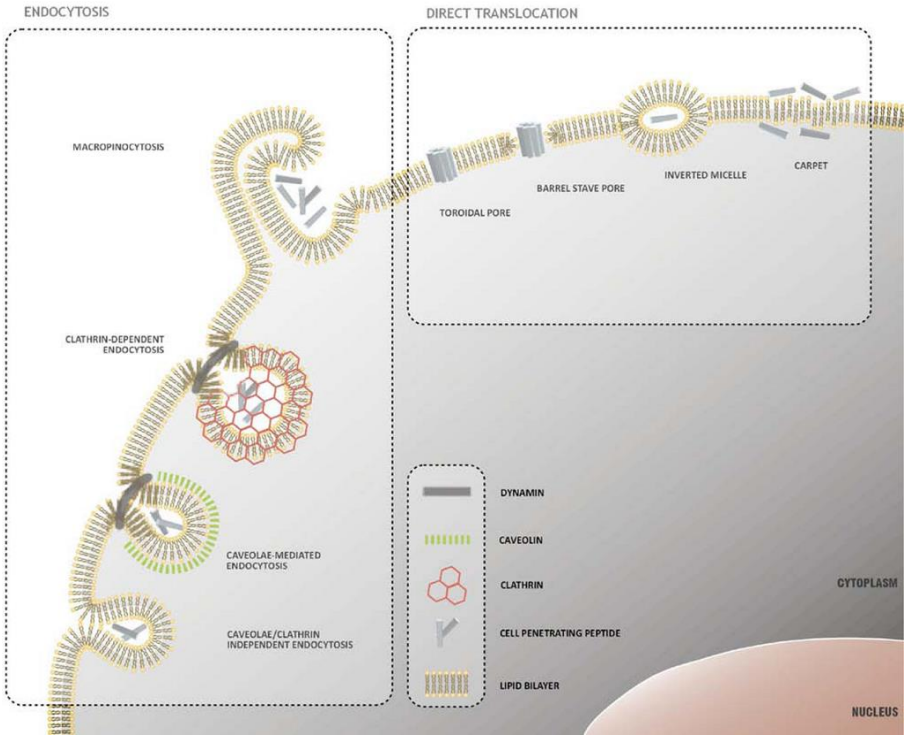

Figure 1: Overview of the proposed mechanisms for cellular influx of CPPs (adopted from Trabulo *et al.* [30]).

2. BLOOD-BRAIN BARRIER

In the central nervous system (CNS), neurons communicate through a combination of chemical signals, *i.e.* neurotransmitters, and electrical signals like synaptic and action potentials within complex networks [31,32]. Therefore, a strict regulation of the local microenvironment around synapses, glial cells and neurons is required for reliable neural signaling. This need for homeostasis is argued to be the strongest evolutionary pressure driving the development of CNS barriers [31-33]. The existence of these barriers was already demonstrated in 1885 by Paul Ehrlich, who described how dye injection resulted in staining of peripheral organs, but not of the brain and spinal cord [34,35]. Later, Ehrlich's student Edwin Goldmann confirmed these findings by showing that injection of trypan blue in the cerebrospinal fluid stained the cells of the CNS but not in the periphery [34,36].

In the CNS, three brain barriers can be distinguished: (1) the *blood-brain barrier (BBB)* constituted by the endothelial cells lining the brain capillaries, (2) the blood-cerebrospinal fluid barrier formed by the epithelial cells of the choroid plexus facing the cerebrospinal fluid and (3) the arachnoid barrier provided by the avascular arachnoid epithelium underlying the dura [31]. These three interfaces form a *physical barrier*, with tight junctions sealing the endothelial cells that also lack fenestrations and show limited transcellular transport of ions, water, solutes, macromolecules and blood cells, as well as a *transport barrier*, fulfilled by the specific transporters which strictly regulate the transport of solutes, ions, and macromolecules [31-33]. Intra- and extracellular enzymes are capable of metabolizing (toxic) molecules during transit, forming an *enzymatic barrier*. Finally, specialization of the endothelial cells and other residing cells helps to regulate the transport of leucocytes, contributing to the *immunological barrier* [31,32,37].

The *tight junctions* between the cerebral endothelial cells are the key feature of the BBB, restricting the paracellular diffusion of ions, polar solutes and water between endothelial cells and blocking the transport of macromolecules. The restriction of paracellular transport is accomplished by the high trans-endothelial electrical resistance (TEER) of the BBB [31,33,37]. The junctional complexes between the endothelial cells comprise both the *tight junctions (TJs)* and *adherens junctions (AJs)*, as well as the *gap junctions (GJs)* (Figure 2). In the adherens junctions, cadherin proteins span the cleft between endothelial cells and are intracellularly linked with the scaffold proteins α-, β- and γ-catenin. Adherens junctions give structural support by holding endothelial cells together and are essential for the formation of tight junctions. Occludin and claudin proteins span the intercellular cleft and form the tight junctions together with the junctional adhesion molecules (JAMs), which are assumed to act as cell-adhesion molecules for leukocytes. These proteins are intracellularly anchored with scaffolding and regulatory proteins like ZO-1, ZO-2, ZO-3, cingulin, afadin (AF-6) and 7H6

antigen. The association with these adaptor proteins ensures the stabilization of the tight junctions as well as the dynamic regulation of the junction opening or closure, either directly, through linking claudin and occludin with the actin filaments of the cytoskeleton, and indirectly, via binding to second-order adaptor proteins [31,33]. Connexin (Cx) proteins also constitute an important part of the junctional complex. These proteins form gap junction channels, directly connecting the cytoplasm of adjacent endothelial cells, and are assembled by head-to-head docking of two half gap junction channels or hemi-channels (CxHC, see Figure 2). The connexin hemi-channels allow contact between the cytosol and the extracellular space. Although connexins are rather unexplored, studies indicate their involvement in the junction complex having important regulatory functions, allowing autocrine and paracrine signaling and direct transfer of nutrients, metabolites, ions and signaling molecules [33].

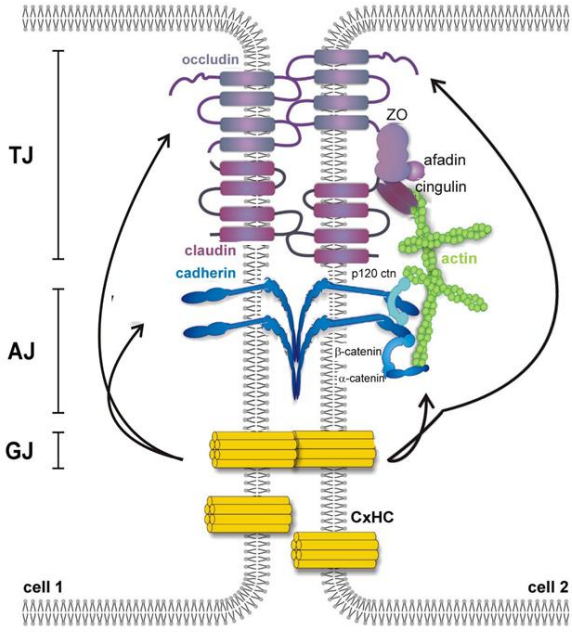

Figure 2: Junctional complexes between the endothelial cells of the BBB with TJ are the tight juctions, AJ the adherens junctions and GJ the gap junctions (adapted from De Bock *et al.* [33]).

Several cellular and non-cellular components interact with the cerebral endothelial cells and are involved in the development and maintenance of the BBB. This interplay is called the *neurovascular unit* (Figure 3) and comprises the cerebral endothelial cells, as well as pericytes, astrocytes, neurons, microglial cells and leucocytes. The structural and functional support of the BBB is further accomplished by the extracellular matrix and basement membrane ensheating the brain capillaries [31,32,37,38]. *Pericytes* contribute to the vessel stability and regulate the capillary diameter and hence blood flow. These cells also control the integrity and function of the BBB by enhancing the formation of tight junctions between endothelial cells [31,32,37,38]. *Astrocytes* also modulate the BBB tight junctions: *in vitro* co-culture experiments indicated an improved barrier function if brain

endothelial cells were co-cultured with astrocytes, probably by secretion of soluble factors like interleukin-6, glial cell line-derived neurotrophic factor and fibroblast growth factor 2 [37]. Beside, astrocytes also provide nutrition for neurons, regulate brain and electrolyte metabolism, control immune reactions and carry out the clearance and recycling of neurotransmitters [37,38]. *Microglia* are the CNS-resident immune cells and play a critical role in the immune responses of the CNS, while circulating *leukocytes* are involved in the surveillance and immune protection of the CNS [32,38]. The *extracellular matrix* consists of the interstitial matrix and *basement membrane*, which is formed by extracellular matrix molecules secreted by the endothelial cells, pericytes and astrocytes [37]. The basement membrane holds the cells of the neurovascular unit in their place and regulates the intercellular communication [37].

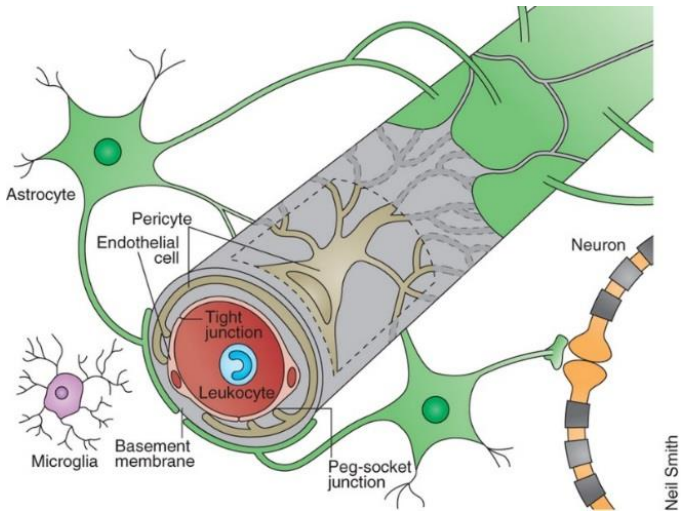

Figure 3: Cellular interplay at the neurovascular unit of the central nervous system (adopted from Obermeier *et al.* [37]).

At the BBB, several routes of transport exist for different types of molecules. Lipophilic compounds, like the blood gases oxygen and carbon dioxide, can cross the BBB by *passive diffusion*, with the rate of brain entry is correlated with their lipid solubility [31,32]. *Solute carriers* in the luminal and abluminal membranes regulate the transport of ions, nutrients and molecules essential for normal brain function like amino acids, glucose (GLUT-1), nucleosides, monocarboxylic acids, as well as clear waste products from the brain [32]. The ATP-binding cassette (ABC) transporters, like Multidrug Resistance-associated Proteins (MRPs), *e.g.* P-glycoprotein (Pgp), and Breast Cancer Resistance Proteins (BRCPs), are active efflux pumps mainly present in the luminal membrane that transport a diversity of lipophilic compounds out of the brain. They fulfill an important neuroprotective role as they remove potential neurotoxic compounds, as demonstrated for several drugs [31,32]. The transcytosis mechanism of macromolecules like proteins and peptides via endocytosis is less clear. Both *adsorptive-mediated* and *receptor-mediated transcytosis* are identified and are further described in the next section [31,32].

3. BLOOD-BRAIN BARRIER TRANSPORT OF PEPTIDES

Historically, peptides were believed not to cross the BBB. Despite this general skepticism, Kastin and Banks initiated their research on the BBB transport of peptides in the mid-1970s following the observation that pituitary peptide hormones outside the brain had effects on behavior [39,40]. At that time, the brain uptake index (BUI) was traditionally used to study the *in vivo* BBB transport, although this method was lacking sensitivity, illustrated by the example of morphine which could not be reliably detected by BUI although it has a pronounced CNS effect [39,41]. During BUI experiments, a single pass uptake from blood over a few seconds is measured rendering this method suitable for compounds showing a rapid uptake in the brain like glucose [42,43]. Only very small fractions of peripherally delivered peptides reach the brain parenchyma, which could not be detected using the BUI method [38]. The introduction of the multiple time regression (MTR) analysis method, combined with a graphical evaluation of the brain uptake data [44,45] and perfusion methods [46-48], both using radioactively labeled peptides, allowed sensitive and accurate determination of the BBB influx kinetics of (slowly penetrating) peptides [39,41,42]. Since then, numerous studies have described the ability of peptides to cross the BBB. Quantitative data on the BBB transport of peptides are compiled in the Brainpeps database, managed by our research group in collaboration with the database research group (TELIN) of our university, and the resulting data of this Ph.D. project were used to update the database [49]. It was in fact noted that BBB transport data of peptides are scattered in literature and suffer from, as observed for the studies on CPPs, a wide variety of used methods and experimental set-ups. However, overall, the available data persuasively prove that peptides do cross the BBB, demonstrating that its barrier function is not fixed but can be modulated and regulated and is affected by developmental, physiological and pathological events [31,50]. For example, the BBB is involved in the regulation of feeding as ingestive peptides interact with the BBB [51]. Although peptides cross the BBB in small amounts, their high specificity and potency renders them to be functionally active leading to possible therapeutic applications [52].

Both saturable and non-saturable transport systems are identified for peptides when crossing the BBB from *blood-to-brain*. *Saturable* transport systems, showing inhibition at higher doses, are endocytosis-driven and thus energy-requiring, which can be receptor-, adsorptive- or carrier-mediated [53,54]. The intracellular trafficking of the peptides in the endothelial cells, as well the exocytosis mechanism are still elusive [53,54]. *Receptor-mediated transcytosis* is triggered by a specific interaction between the peptide and a receptor at the luminal face of the brain endothelial cells, followed by an endocytotic uptake, movement across the cytoplasm of the endothelial cell and exocytosis at the abluminal side [53]. At the BBB, a receptor has already been demonstrated for

insulin, transferrin and low density lipoproteins (LDL) [42,54]. *Adsorptive-mediated transcytosis* of peptides at the BBB follows an electrostatic interaction between positive charges of the peptide and negative charges present on the plasma membrane [42,55]. The BBB is well "equipped" for this transport mechanism: both the luminal and abluminal membranes as well as the basal membrane are negatively charged, facilitating both the endocytosis and exocytosis of (cationic) peptides. The brain capillary endothelium is enriched in clathrin-coated pits, which are involved in the endocytosis process. The density of mitochondria in cerebral endothelial cells is about five times higher than in other endothelial cells, which increases the energy potential of the BBB, enabling the energy-requiring adsorptive-mediated transcytosis process [55]. Both receptor- and adsorptive-mediated transcytosis are time- and concentration-dependent, with the receptor-mediated transport mechanism being characterized by a higher specificity, higher affinity and lower capacity compared to adsorptive-mediated transcytosis [53,55]. *Carrier-mediated transcytosis* involves an interaction of the peptide with a transporter on the endothelial cell surface [56,57]. Carrier-mediated transcytosis can be both energy-dependent and -independent [56]. For some peptides, the used transporter has been identified such as for the enkephalin analogs, biphalin and DPDPE, all opioid peptides, which are assumed to cross the BBB by the large neutral amino acid carrier (system L), as well as by an unknown transporter other than system L [57]. For other peptides, the exact identification of the involved transporter is lacking and a generic name is attributed (Peptide Transport System (PTS)) [58]. Another possible mechanism for BBB transport of peptides is *fluid-phase endocytosis*, involving no specific interaction but the peptide is simply present in the extracellular fluid at the site where the plasma membrane invaginates to form an endocytotic vesicle. The peptide bathing in the extracellular fluid is captured within the lumen of the budding caveolar vesicle and enters the brain capillary endothelial cell [55,59]. However, caveolae rarely occur at the BBB, thus the use of this transport system is presumed to be limited at the BBB [55]. Beside the saturable transport systems, peptides also can cross the BBB by *passive diffusion*, which is non-saturable and currently assumed to be used by the majority of the peptides [42]. The rate of diffusion depends on the physicochemical properties like lipophilicity and is inversely related with the size, number of hydrogen bonds and the square root of the molecular weight [42]. Peptide transport from *brain-to-blood* involves both specific, *saturable carrier-mediated transport systems*, as well as *non-saturable*, non-specific transport of peptides out of the brain by reabsorption of the peptide in the circulation of the cerebrospinal fluid [60]. As for the brain influx transporters, efflux transport systems are poorly characterized, but use of Pgp, PTS-transporters and proton-coupled oligopeptide transport (POT) family has already been reported [58].

4. BLOOD-BRAIN BARRIER AND AGING

The aging process is associated with a gradual change of multiple physiological, biological, physical and social functions [61]. At the BBB, several important structural and functional changes occur, ultimately resulting in an increased BBB permeability. With age, the BBB also becomes more susceptible for external factors like disease, *e.g.* hypertension, and drugs [62-66]. In Table 2, an overview is provided of the molecular mechanisms contributing to the age-related BBB dysfunction [66].

Table 2: Molecular mechanisms of BBB disruption, caused by aging and age-associated diseases (adopted from Popescu *et al.* [66]).

Mechanism	Cause
Increased oxidative stress	Aging
Microglia activation	Aging
Increased transport of TNF-α through BBB	Aging
Decreased expression of GLUT-1	Aging, diabetes
Iron accumulation	Aging, high cholesterol, Parkinson's disease
Decreased activity of Pgp	Aging, Alzheimer's, Parkinson's disease
Decreased estrogen level	Aging
Reduced sensitivity to insulin	Aging
Decreased occludin expression	Diabetes
Decreased ZO-1 expression	Diabetes
Decreased ZO-2 expression	Hypertension
Increased endothelia-monocytes interaction	Diabetes
Activation of δPKC	Hypertension
Alteration of adherens and tight junctions function	Stroke
RAGE up-regulation	Aging, Alzheimer's disease
LRP down-regulation	Aging, Alzheimer's disease

δPKC = δ protein kinase C; RAGE = receptor for advanced glycation end products; LRP = low-density lipoprotein receptor-related protein; RAGE and LRP = involved in the transport of amyloid β in and out of the brain.

Aging is associated with a heightened peripheral inflammation leading to increased TNF-α levels at the BBB, resulting in vascular inflammation [62]. Increased levels of TNF-α suppress the expression of junctional protein complexes like occludin and ZO-1, causing loosening of the tight junctions [66,67]. Disruption of the BBB is also associated with microglial activation, which together with the accumulated iron in both glial cells and astrocytes, form a source of oxidative stress to the cells of the neurovascular unit [66,68,69]. Moreover, aging is associated with decreased estrogen levels, which is known to have protective function on the BBB endothelial cells [66]. Alterations in transporter functions, like of the glucose transporter GLUT-1 and of Pgp, cause an imbalanced uptake or efflux of compounds as demonstrated for glucose and amyloid β (Aβ), that shows accumulation in the aged brain [62,66]. The resulting increased permeability of the BBB in turn enables passage of pro-inflammatory compounds and cells, as well of toxic compounds, which further enhances the BBB dysfunction.

Alterations in BBB permeability can also be attributed to several diseases with high incidence rates in the elderly population like Alzheimer's and Parkinson's disease as shown in Table 2 [66]. Moreover, for these disorders, a pathogenic link between the BBB dysfunction and the onset or the progression of the disease has been demonstrated [62,66,70]. Changes of the BBB permeability, either due to aging or disease, also impact the brain pharmacokinetics of (peptide) drugs, which can complicate the treatment of CNS disorders and can cause CNS adverse drug reactions if not appropriately dosed [70]. This stresses the importance of including the elderly patient in clinical trials, especially those with (neurodegenerative) comorbidities.

5. STUDY OBJECTIVES

Cell-penetrating peptides are a class of peptides that traverse cellular bilayers. It is also generally accepted that peptides are able to cross the BBB. As CPPs are mainly investigated for their carrier functionality, studies evaluating, mostly qualitatively, the BBB transport of CPPs *in vivo* and *in vitro*, focus on CPPs coupled to cargoes of different chemical nature. This BBB transport is indirectly estimated by measuring the pharmacological effect of the attached cargo or by *in vivo* imaging and fluorescence microscopy techniques using (fluorescently) labeled peptides. Beside their application as carriers, CPPs can also be formed endogenously through metabolization of proteins and also can possess biological activity. It is of general importance to know whether this group of peptides is able to enter the brain and hence might exert CNS effects on their own. **Therefore, the main goal of this research project was to quantitatively investigate whether uncoupled CPPs selectively cross the BBB *in vivo* and whether this is related to their cell-penetrating properties.**

In order to answer the central question of this research project, following objectives were set:

(1) Select model peptides representative for the chemically and functionally diverse group of CPPs.

Cell-penetrating peptides are a chemically diverse group of peptides, showing a varying extent of cellular uptake which is influenced by multiple factors like the cell line used, extracellular concentration, attached label and incubation temperature. The exploration of the chemical space is performed to classify CPPs according to their structural characteristics. Selection of model peptides is also based on their cellular influx properties. As a plethora of experimental set-ups and methods is used to investigate these peptides, an approach to globally estimate the extent of cellular uptake is investigated. By combining the knowledge on the chemical and functional properties of these peptides, the structural features that determine the cellular uptake of peptides can be identified.

(2) Define a method that allows the overall and objective comparison of peptides regarding their BBB transport, based on the exploration of already available quantitative BBB transport data of peptides.

Numerous studies have already described the ability of peptides to cross the BBB. Quantitative BBB transport data of peptides scattered in literature, are compiled in the Brainpeps database. From the exploration of this database, it became clear that the BBB influx is evaluated using a diversity of techniques and inherently is expressed using different BBB influx response types. Available quantitative data are used to propose a method that enables the comparison of peptides regarding their BBB transport despite differences in used response types, aiming at an objective and overall evaluation of the obtained BBB transport results of CPPs during this research.

(3) Evaluate the quality of the peptides investigated for their BBB transport characteristics, using a chromatographic system optimized for analysis of cationic peptides.

In order to obtain reliable research outcomes, it is imperative that the quality of the externally purchased peptides is verified. Currently, analysis of the cationic CPPs is hardly described and an initial analysis of the cationic CPPs using our traditional liquid chromatography (LC) systems indicated analytical difficulties. Moreover, the evaluation of the impurity profile of the CPPs used during cellular uptake studies is often ignored throughout biomedical literature, which might explain the discrepancy in study results. Therefore, we want to comparatively investigate selected chromatographic and detection systems to solve the analytical quality control (QC) challenges for this group of peptides.

(4) Characterize the BBB transport of a chemically and functionally diverse set of CPPs.

Several studies have demonstrated the ability of CPPs, mostly coupled to cargoes, to reach the brain parenchyma. The question is whether this is a general characteristic of CPPs. Therefore, the BBB transport of uncoupled CPPs is quantitatively evaluated in order to verify whether cell-penetrating properties of peptides inherently imply the ability to cross the BBB. For investigation of the BBB transport studies, CPPs will be selected, as well as “new” CPPs like the short, proline-rich antimicrobial peptides (PrAMPs) and disulfide-rich (cyclic) peptides, which are biofunctional peptides that also possess cell-penetrating properties.

(5) Explore the regulatory status of the development of geriatric medicines.

The aging process is associated with gradual changes of several physiological, biological, physical and social functions. Changes of organ functions, like the increase in BBB permeability, affect the pharmacokinetics of drugs and should be taken into account when developing geriatric medicines. As with the current demographic trend of an aging population, the geriatric patients will soon outweigh the other population subgroups, and therefore, it was evaluated what

regulatory framework is currently provided for the development of geriatric medicines. This study fits into the DruQuaR tradition to include a regulatory-oriented aspect of the Ph.D. research.

6. THESIS OUTLINE

The coherence of the different aspects covered in this research are outlined in Figure 4. Chapters of this thesis are logically ordered, but to ensure a fluent reading, each chapter is presented as a stand-alone text, with the introduction delineating the specific context of that section.

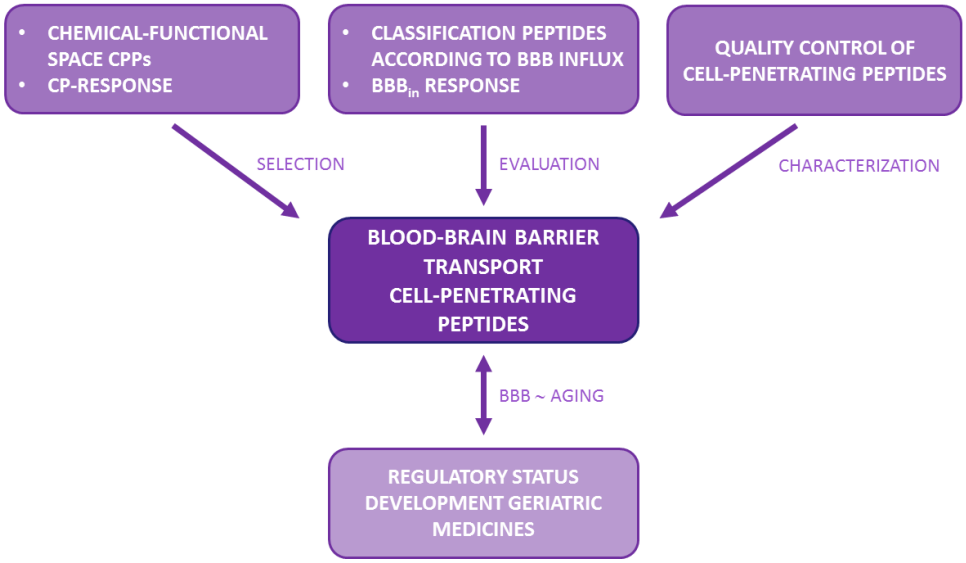

Figure 4: Thesis outline.

In **Chapter II**, a database is built consisting of peptides, quantitatively investigated for their cellular uptake. Using chemo-molecular descriptors, numerically expressing the peptide structure, the chemical space of the CPPs is explored applying multivariate data analysis techniques. The cell-penetrating (CP) response is introduced, which is a unified response expressing the extent of cellular uptake of peptides independent of the experimental set-up and method used to investigate the peptide. A quantitative structure-property relationship (QSPR) study is performed, using the new CP-response, to identify the structural features determining cell-penetrating properties of peptides.

Chapter III describes the method for an objective and overall comparison of peptides regarding their BBB influx. Therefore, four different BBB influx response types were selected for which quantitative data are available in the Brainpeps database. Based on the distribution of the available data, a classification system and derived unified BBB influx reponse (BBB_{in}) is proposed and its use and possible applications are demonstrated.

Prior to performing the BBB transport studies, the quality of the used peptides is verified, which is described in **Chapter IV**. Five chromatographic systems are used to perform the quality control of five cationic CPPs and to identify the most suitable C_{18}-chromatographic method for the quality control (QC) of these cationic peptides. The use of single quad MS detectors during QC of these peptides is indicated.

Chapter V comprises the *in vivo* BBB transport study of five CPPs, selected based on the different identified CPP-subgroups and CP-response described in Chapter II, as well as of four PrAMPs and three disulfide-rich (cyclic) peptides, which are "new" CPPs that are demonstrated to fit in the chemical space of the "traditional" CPPs. The brain influx and efflux characteristics, as well as the parenchymal/capillary distribution and tissue distribution are investigated. The *in vitro* metabolic stability in serum and several tissue homogenates is also verified. For the CPPs, the regional brain distribution and possible brain influx mechanism is evaluated. Finally, the obtained BBB transport characteristics are linked with the cell-penetrating properties of the selected peptides.

At last, in **Chapter VI**, the current regulatory status for the development of geriatric medicines is provided. The views of the different involved stakeholders are explained and the current challenges encountered in this field are identified. While this study is not immediately related to the laboratory-based experimental research of the previous chapters, it is a pertinent regulatory issue which is to some extent linked to the BBB functionality.

7. REFERENCES

[1] Frankel A, Pabo CO. Cellular Uptake of the Tat Protein from Human Immunodeficiency Virus. *Cell* 1988; **55**: 1189-1193.

[2] Green M, Loewenstein PM. Autonomous Functional Domains of Chemically Synthesized Human Immunodeficiency Virus Tat Trans-activator Protein. *Cell* 1988; **55**: 1179-1188.

[3] Derossi D, Joliot AH, Chassaing G, Prochiantz A. The 3rd Helix of the Antennapedia Homeodomain Translocates through Biological-Membranes. *J. Biol. Chem.* 1994; **269**: 10444-10450.

[4] Copolovici DM, Langel K, Eriste E, Langel Ü. Cell-Penetrating Peptides: Design, Synthesis, and Applications. *ACS Nano* 2014; **8**: 1972-1994.

[5] Bechara C, Sagan S. Cell-penetrating peptides: 20 years later, where do we stand? *FEBS Lett.* 2013; **587**: 1693-1702.

[6] Milletti F. Cell-penetrating peptides: classes, origin, and current landscape. *Drug Discov. Today* 2012; **17**: 850-860.

[7] Rizzuti M, Nizzardo M, Zanetta C, Ramirez A, Corti S. Therapeutic applications of the cell-penetrating HIV-1 Tat peptide. *Drug Discov. Today* 2015; **20**: 76-85.

[8] Brugnano J, Ward BC, Panitch A. Cell penetrating peptides can exert biological activity: a review. *Biomol. Concepts* 2010; **1**: 109-116.

[9] Verdurmen WPR, Brock R. Biological responses towards cationic peptides and drug carriers. *Trends Pharmacol. Sci.* 2011; **32**: 116-124.

[10] Howl J, Matou-Nasri S, West DC, Farquhar M, Slaninova J, Östenson C-G, Zorko M, Östlund P, Kumar S, Langel Ü, McKeating J, Jones S. Bioportide: an emergent concept of bioactive cell-penetrating peptides. *Cell. Mol. Life Sci.* 2012; **69**: 2951-2966.

[11] Saar K, Lindgren M, Hansen M, Eiriksdottir E, Jiang Y, Rosenthal-Aizman K, Sassian M, Langel Ü. Cell-penetrating peptides: A comparative membrane toxicity study. *Anal. Biochem* 2005; **345**: 55-65.

[12] Kilk K, Mahlapuu R, Soomets U, Langel Ü. Analysis of *in vitro* toxicity of five cell-penetrating peptides by metabolic profiling. *Toxicology* 2009; **265**: 87-95.

[13] Khafagy E-S, Kamei N, Nielsen EJB, Nishio R, Takeda-Morishita M. One-month subchronic toxicity study of cell-penetrating peptides for insulin nasal delivery in rats. *Eur. J. Pharm. Biopharm.* 2013; **85**: 736-743.

[14] Lindgren M, Langel Ü. Classes and Prediction of Cell-Penetrating Peptides. In *Cell-Penetrating Peptides: Methods and Protocols* (Ed: Langel Ü), Humana Press Inc., **2011**, pp. 3-19.

[15] Mezö G, Hudecz F. Synthesis of Linear, Branched, and Cyclic Peptide Chimera. In Peptide Synthesis and Applications (Ed: Howl J), Humana Press Inc., **2005**, pp. 63-76.

[16] Vivès E, Brodin P, Lebleu B. A truncated HIV-1 Tat protein basic domain rapidly translocates through the plasma membrane and accumulates in the cell nucleus. *J. Biol. Chem.* 1997; **272**: 16010-16017.

[17] Rousselle C, Clair P, Lefauconnier JM, Kaczorek M, Scherrmann JM, Temsamani J. New advances in the transport of doxorubicin through the blood-brain barrier by a peptide vector-mediated strategy. *Mol. Pharmacol.* 2000; **57**: 679-686.

[18] Tünnemann G, Ter-Avetisyan G, Martin RM, Stöckl M, Herrmann A, Cardoso MC. Live-cell analysis of cell penetration ability and toxicity of oligo-arginines. *J. Pept. Sci.* 2008; **14**: 469-476.

[19] Elmquist A, Lindgren M, Bartfai T, Langel Ü. VE-Cadherin-Derived Cell-Penetrating Peptide, pVEC, with Carrier Functions. *Exp. Cell Res.* 2001; **269**: 237-244.

[20] Soomets U, Lindgren M, Gallet X, Hällbrink M, Elmquist A, Balaspiri L, Zorko M, Pooga M, Brasseur R, Langel Ü. Deletion analogues of transportan. *Biochim. Biophys. Acta* 2000; **1467**: 165-176.

[21] Lin YZ, Yao SY, Veach RA, Torgerson TR, Hawiger J. Inhibition of nuclear translocation of transcription factor NF-kappa B by a synthetic peptide containing a cell membrane-permeable motif and nuclear localization sequence. *J. Biol. Chem.* 1995; **270**: 14255-14258.

[22] Gomez JA, Gama V, Yoshida T, Sun W, Hayes P, Leskov K, Boothman D, Matsuyama S. Bax-inhibiting peptides derived from Ku70 and cell-penetrating pentapeptides. *Biochem. Soc. Trans.* 2007; **35**: 797-801.

[23] Madani F, Lindberg S, Langel Ü, Futaki S, Gräslund A. Mechanisms of Cellular Uptake of Cell-Penetrating Peptides. *J. Biophys.* 2011; **2011**: 414729.

[24] Oehlke J, Scheller A, Wiesner B, Krause E, Beyermann M, Klauschenz E, Melzig M, Bienert M. Cellular uptake of an α-helical amphipathic model peptide with the potential to deliver polar compounds into the cell interior non-endocytically. *Biochym. Biophys. Acta* 1998; **1414**: 127-139.

[25] Holm T, Netzereab S, Hansen M, Langel Ü, Hällbrink M. Uptake of cell-penetrating peptides in yeasts. *FEBS Lett.* 2005; **579**: 5217-5222.

[26] Ezzat K, Helmfors H, Tudoran O, Juks C, Lindberg S, Padari K, El-Andaloussi S, Pooga M, Langel Ü. Scavenger receptor-mediated uptake of cell-penetrating peptide nanocomplexes with oligonucleotides. *FASEB J.* 2012; **26**: 1172-1180.

[27] Mitchell DJ, Kim DT, Steinman L, Fathman CG, Rothbard JB. Polyarginine enters cells more efficiently than other polycationic homopolymers. *J. Pept. Res.* 2000; **56**: 318-325.

[28] Elmquist A, Hansen M, Langel Ü. Structure-activity relationship study of the cell-penetrating peptide pVEC. *BBA-Biomembranes* 2006; **1758**: 721-729.

[29] Mueller J, Kretzschmar I, Volkmer R, Boisguerin P. Comparison of Cellular Uptake Using 22 CPPs in 4 Different Cell Lines. *Bioconjugate Chem.* 2008; **19**: 2363-2374.

[30] Trabulo S, Cardoso AL, Mano M, Pedroso de Lima MC. Cell-Penetrating Peptides – Mechanisms of Cellular Uptake and Generation of Delivery Systems. *Pharmaceuticals* 2010; **3**: 961-993.

[31] Abbott NJ, Patabendige AAK, Dolman DEM, Yusof SR, Begley DJ. Structure and function of the blood-brain barrier. *Neurobiol. Dis.* 2010; **37**: 13-25.

[32] Abbott NJ. Blood-brain barrier structure and function and the challenges for CNS drug delivery. *J. Inherit. Metab. Dis*. 2013; **36**: 437-449.

[33] De Bock M, Vandenbroucke RE, Decrock E, Culot M, Cecchelli R, Leybaert L. A new angle on blood-CNS interfaces: A role for connexins? *FEBS Lett.* 2014; **588**: 1259-1270.

[34] Serlin Y, Shelef I, Knyazer B, Friedman A. Anatomy and physiology of the blood-brain barrier. *Semin. Cell Dev. Biol.* 2015; **38**: 2-6.

[35] Ehrlich P. Das sauerstufbudurfnis des organismus. In *Eine Farbenanalytische Studie*, Hirschwald, **1885**.

[36] Goldmann E. Vitalfärbung am zentralnervensystem - Beitrag zur Physio-Pathologie des Plexus chorioideus und der Hirnhäute, Königl. Akademie der Wissenschaften, **1913**.

[37] Obermeier B, Daneman R, Ransohoff RM. Development, maintenance and disruption of the blood-brain barrier. *Nat. Med.* 2013; **19**: 1584-1596.

[38] Zlokovic BV. The Blood-Brain Barrier in Health and Chronic Neurodegenerative Disorders. *Neuron* 2008; **57**: 178-201.

[39] Banks WA. Peptides and the blood-brain barrier. Peptides 2015; doi: 10.1016/j.peptides.2015.03.010.

[40] Kastin AJ, Banks WA, Marks N, Olson RD. Dissociative effects of CNS peptides with some unusual applications in RIA, In *Physiological peptides and new trends in radioimmunology*, Elsevier/North-Holland Biomedical Press, **1981**, pp. 89-99.

[41] Banks WA, Kastin AJ. Bidirectional passage of peptides across the blood-brain barrier, In *Progress in Brain Research* (Eds: Ermisch A, Landgraf R, Rühle H-J), Elsevier Science, **1992**, pp. 139-147.

[42] Kastin AJ, Pan W. Peptide transport across the blood-brain barrier. In *Progress in Drug Research* (Eds Prokai L, Prokai-Tatrai K), Birkhäuser Verlag, **2003**, pp. 79-100.

[43] Oldendorf WH. Brain uptake of radio-labelled amino acids, amines and hexoses after arterial injection. *Am. J. Physiol.* 1971; **221**: 1629-1639.

[44] Gjedde A. High- and low-affinity transport of D-glucose from blood to brain. *J. Neurochem.* 1981; **36**: 1463-1471.

[45] Patlak CS, Blasberg RG, Fenstermacher JD. Graphical evaluation of blood-to-brain transfer constants from multiple-time uptake data. *J. Cerebr. Blood F. Met.* 1983; **3**: 1-7.

[46] Takasato Y, Rapoport SI, Smith QR. An in situ brain perfusion technique to study cerebrovascular transport in the rat. *Am. J. Physiol.* 1984; **247**: H484-H493.

[47] Zlokovic BV, Begley DJ, Djuricic BM, Mitrovic DM. Measurement of Solute Transport Across the Blood-Brain Barrier in the Perfused Guinea Pig Brain: Method and Application to N-Methyl-α-Aminoisobutyric Acid. *J. Neurochem.* 1986; **46**: 1444-1451.

[48] Barrera CM, Banks WA, Kastin AJ. Passage of Tyr-MIF-1 From Blood to Brain. *Brain Res. Bull.* **1989**; 23: 439-442.

[49] Van Dorpe S, Bronselaer A, Nielandt J, Stalmans S, Wynendaele E, Audenaert K, Van De Wiele C, Peremans K, Hsuchou H, De Tré G, De Spiegeleer B. Brainpeps: the blood-brain barrier peptide database. *Brain Struct. Funct.* 2012; **217**: 687-718.

[50] Banks WA, Kastin AJ. Passage of peptides across the blood-brain barrier: pathophysiological perspectives. *Life Sci.* 1996; **59**: 1923-1943.

[51] Kastin AJ, Pan W. Blood-Brain Barrier and Feeding: Regulatory Roles of Saturable Transport Systems for Ingestive Peptides. *Curr. Pharm. Design* 2008; **14**: 1615-1619.

[52] McGonigle P. Peptide therapeutics for CNS indications. *Biochem. Pharmacol.* 2012; **83**: 559-566.

[53] Pan W, Kastin AJ. Why study transport of peptides and proteins at the neurovascular interface. *Brain Res. Rev.* 2004; **46**: 32-43.

[54] Gabathuler R. Approaches to transport therapeutic drugs across the blood-brain barrier to treat brain diseases. *Neurobiol. Dis.* 2010; **37**: 48-57.

[55] Hervé F, Ghinea N, Scherrmann J-M. CNS Delivery Via Adsorptive Transcytosis. *AAPS J.* 2008; **10**: 455-472.

[56] Egleton RD, Davis TP. Bioavailability and Transport of Peptides and Peptide Drugs into the Brain. *Peptides* 1997; **18**: 1431-1439.

[57] Tamai I, Tsuji A. Transporter-Mediated Permeation of Drugs Across the Blood-Brain Barrier. *J. Pharm. Sci.* 2000; **89**: 1371-1388.

[58] Banks WA. Critical roles of efflux systems in health and disease, In *Efflux transporters and the blood-brain barrier* (Ed: Taylor EM), Nova Publishers, **2005**.

[59] Smith MW, Gumbleton M. Endocytosis at the blood-brain barrier: From basic understanding to drug delivery strategies. *J. Drug Target.* 2006; **14**: 191-214.

[60] Banks WA, Kastin AJ, Michals EA, Barrera CM. Stereospecific Transport of Tyr-MIF-1 Across the Blood-Brain Barrier by Peptide Transport System-1. *Brain Res. Bull.* 1990; **25**: 589-592.

[61] Stegemann S, Ecker F, Maio M, Kraahs P, Wohlfart R, Breitkreutz J, Zimmer A, Bar-Shalom D, Hettrich P, Broegmann B. Geriatric drug therapy: Neglecting the inevitable majority. *Ageing Res. Rev.* 2010; **9**: 384-398.

[62] Marques F, Sousa JC, Sousa N, Palha JA. Blood-brain barriers in aging and Alzheimer's disease. *Mol. Neurodegener.* 2013; **8**: 38.

[63] Mooradian AD. Effect of Aging on the Blood-Brain Barrier. *Neurobiol. Aging* 1988; **9**: 31-39.

[64] Shah GN, Mooradian AD. Age-related changes in the blood-brain barrier. *Exp. Gerontol.* 1997; **32**: 501-519.

[65] Farrall AJ, Wardlaw JM. Blood-brain barrier: Ageing and microvascular disease – systematic review and meta-analysis. *Neurobiol. Aging* 2009; **30**: 337-352.

[66] Popescu BO, Toescu EC, Popescu LM, Bajenaru O, Muresanu DF, Schultzberg M, Bogdanovic N. Blood-brain barrier alterations in ageing and dementia. *J. Neurol. Sci.* 2009; **283**: 99-106.

[67] Elahy M, Jackaman C, Mamo JCL, Lam V, Dhaliwal SS, Giles C, Nelson D, Takechi R. Blood-brain barrier dysfunction developed during normal aging is associated with inflammation and loss of tight junctions but not with leukocyte recruitment. *Immun. Ageing* 2015; **12**: 2.

[68] Ward RJ, Zucca FA, Duyn JH, Crichton RR, Zecca L. The role of iron in brain ageing and neurodegenerative disorders. *Lancet Neurol.* 2014; **13**: 1045-1060.

[69] Minogue AM, Jones RS, Kelly RJ, McDonald CL, Connor TJ, Lynch MA. Age-associated dysregulation of microglial activation is coupled with enhanced blood-brain barrier permeability and pathology in APP/PS1 mice. *Neurobiol. Aging* 2014; **35**: 1442-1452.

[70] Banks WA. Drug delivery to the brain in Alzheimer's disease: Consideration of the blood-brain barrier. *Adv. Drug Deliv. Rev.* 2012; **64**: 629-639.

CHAPTER II

CHEMICAL-FUNCTIONAL DIVERSITY IN CELL-PENETRATING PEPTIDES

"The voyage of discovery lies not in seeking new horizons, but in seeing with new eyes"

Marcel Proust
(°1871 - †1922, French novelist)

Parts of this chapter were published:

Stalmans S, Wynendaele E, Bracke N, Gevaert B, D'Hondt M, Peremans K, Burvenich C, De Spiegeleer B. Chemical-Functional Diversity in Cell-Penetrating Peptides. *PLOS ONE* 2013; **8**: e71752.

ABSTRACT

Cell-penetrating peptides (CPPs) are a promising tool to overcome cell membrane barriers. They have already been successfully applied as carriers for several problematic cargoes, like *e.g.* plasmid DNA and (si)RNA, opening doors for new therapeutics. Cellular uptake studies of these peptides suffer from inconsistencies in used techniques and other experimental conditions, leading to uncertainties about their uptake mechanisms and structural properties. To clarify the structural characteristics influencing the cell-penetrating properties of peptides, the chemical-functional space of peptides, already investigated for cellular uptake, was explored. For 186 peptides, a new cell-penetrating (CP) response was proposed, based upon the scattered quantitative results for cellular influx available in the literature. Principal component analysis (PCA) and a quantitative structure-property relationship study (QSPR), using chemo-molecular descriptors and our newly defined CP-response, learned that besides typical well-known properties of CPPs, *i.e.* positive charge and amphipathicity, the shape, structure complexity and the 3D-pattern of constituting atoms influence the cellular uptake capacity of peptides.

CHAPTER II

CHEMICAL-FUNCTIONAL DIVERSITY IN CELL-PENETRATING PEPTIDES

Main focus in this chapter:

- To explore the chemical-functional space of cell-penetrating peptides.
- To present a unified response for cell-penetrating properties of peptides allowing their direct comparison.
- To identify structural properties that determine cellular uptake of peptides.

1. DIVERSITY ASPECTS OF CELL-PENETRATING PEPTIDES

Since the discovery about 20 years ago by Frankel and Pabo that the Tat protein of the human immunodeficiency virus (HIV-1) can enter cells [1], cell-penetrating peptides (CPPs) are an increasingly growing part of fundamental and applied biomedical research. Throughout the literature, cell-penetrating peptides are traditionally defined as containing less than 40 amino acids, characterized by a net positive charge, which are able to cross cell barriers without causing significant membrane damage [2]. This property makes CPPs suitable to deliver hydrophilic macromolecules into the cell interior and to the different cellular compartments *in vitro* and *in vivo* [3]. They have already been successfully applied as carriers for cell membrane-impermeable cargoes like plasmid DNA, oligonucleotides, short interfering RNA ((si)RNA), peptide-nucleic acids (PNA), proteins and other peptides, small molecules and liposome nanoparticles [4]. This implies that doors have been opened to new efficient (peptide) drugs [5].

During the last decade, several hundreds of CPPs have already been reported in the literature. In contrast to the traditional definition, CPPs actually present a chemically diverse group of peptides, showing a variety in constituent amino acids and 3D-structure. Three major classes can be distinguished: cationic, amphipathic and hydrophobic CPPs. This structural diversity accounts for the difference in uptake mechanism and level under different conditions between the groups of CPPs. Moreover, coupling the CPP to a cargo can also influence the level and mode of uptake into the cell [6]. Only a few structure-activity relationship (SAR) studies have tried to reveal which structural

features are crucial for cellular uptake [7-16]. Hydrophobic α-helical structures seem to be important, as well as the positive charges from basic amino acids, with arginine favored over lysine. Although equally contributing to the overall charge, the guanidinum group of arginine can donate two hydrogen bonds compared to one by lysine. Other factors apparently influencing cellular uptake are the peptide length and the conformation of the structure, which was demonstrated by the difference in cellular influx for pVEC and its scrambled analogue [2,17]. The latter showed a reduced uptake into the cell, probably due to the loss of the N-terminal hydrophobic domain [7]. The influence of the peptide length was demonstrated for the SV40 T antigen, which showed an increase in cellular influx by adding a N-terminal sequence [17].

The available SAR studies only cover a limited set out of the diverse group of CPPs. Moreover, some publications show contradictory results [8,9], possibly due to different experimental set-ups. This impedes drawing general conclusions about the structural features important for cellular uptake. Furthermore, the uptake mechanism of the different CPP groups is still under debate. Today, endocytosis (energy-dependent) and direct penetration (energy-independent) are suggested to be the two major cellular uptake mechanisms. Depending on the experimental conditions, CPPs use two or more different mechanisms [2].

One approach for predicting CPPs is trial and error, which implies identifying sequences of a suitable length and rich in positive charges in a protein structure [18]. Another approach are the Sandberg expanded z-descriptors, used by Hällbrink *et al.* [19]. They calculated the bulk property values for a training set of known CPPs and known non-penetrating peptides and averaged over the total number of amino acids. The most relevant descriptors were Z1, Z2 and Z3, describing respectively lipophilicity, steric bulk properties and polarity, the latter having the highest predictive power. Cell-penetrating properties of new sequences were predicted based on whether their bulk property values fall within preset intervals, derived from the values of the training set. Z-descriptors make it possible to predict cell-penetrating properties *in silico*, but a major disadvantage is that the sum of descriptors is calculated, hereby neglecting the order of the amino acids. Moreover, the Tat peptide was not considered a CPP by their search criteria [19]. Another way to predict CPPs is data mining, which is based on finding similarity patterns in a large set of (experimental) data [18]. Artificial neural networks have already been used by Karelson and Dobchev to predict CPPs, based on quantitative structure-activity relationship (QSAR) derived features of a training set of about 100 known (non-) penetrating peptides [20]. Sanders *et al.* used support vector machine (SVM) classifiers, based on primary features derived from the biochemical properties of 111 known CPPs and 34 non-CPPs, to predict cell-penetrating properties [21]. The authors could experimentally confirm the cell-penetrating ability of the SVM-classified CPPs. As primary biochemical properties of peptides were

used, their classifiers provided insight in the structural requirements for cellular penetration, *e.g.* positional preference for certain amino acids, like positively charged and aromatic residues.

One can conclude that, although CPPs have been studied for over 20 years, a lot of structural and mechanistic properties still need to be unraveled. Furthermore, it is obvious that the variety of techniques and experimental conditions used to quantify the cellular uptake of CPPs, impedes to directly compare their extent of uptake. Together with the fact that the CPPs differ structurally and mechanistically, controversies about the uptake mechanisms and artifactual results in the past [22], make it difficult to predict whether a peptide is cell-penetrating or not.

In this article, we explored the chemical space of a set of 186 peptides, for which quantitative data for cellular uptake are available, by use of chemo-molecular descriptors, which numerically express the peptide structure. In addition, we defined a new cell-penetrating (CP)-response, in order to compare the cell-penetrating properties of these peptides in a one-merit figure. This CP-response allows the use and comparison of experimental data obtained with a different experimental set-up. By combining the chemical descriptors and the CP-responses, biomolecular modeling and clustering of peptides was performed. Our results confirm already described determining features for cellular uptake, but also provide new insights in structural requirements for cellular uptake of peptides.

2. MULTIVARIATE DATA ANALYSIS METHODS

Data

Articles describing the uptake of CPPs covering the period 2007 – March 2012, were gathered using the search engines Web of Knowledge, Google and PubMed. The terms “cell penetrating peptides”, “uptake cell penetrating peptides”, “protein transduction domain” each separately, as well as “cellular uptake”, “characterization”, “kinetics”, “quantification cellular uptake” and “studying uptake”, using the Boolean operator “AND” were used. Specific names of known CPPs (*e.g.* penetratin) were also included as search terms. More publications were obtained by searching in the reference list of suitable articles and reviews. This resulted in publications dating before 2007 (1998-2006). Only those were withheld, where the experimental set-up was correct, *i.e.* use of non-fixed cells and removing or quenching of extracellular bound peptide [22]. Moreover, the publications should contain quantitative data or graphs expressing the cellular uptake of CPPs. When no quantitative data were explicitly mentioned in the text, these data were deduced from the available graphs.

Calculating chemo-molecular descriptors

Before the chemo-molecular descriptors of the 186 selected peptides could be calculated, the MM+ *in vacuo* optimized structure of the peptides (not amidated), representing the most fundamental peptide structure, was drawn and optimized using HyperChem 8.0 (Hypercube, Gainesville, FL, USA). The geometry optimization was obtained by the molecular mechanics force field method using the Polak–Ribière conjugate gradient algorithm with a root mean square gradient of 0.1 kcal/(Å × mol) as stop criterion. Afterwards, these Cartesian coordinate matrices were used to calculate more than 3000 descriptors, using Dragon 5.5 (Talete, Milan, Italy), HyperChem 8.0 and MarvinSketch 5.10.3 (ChemAxon, Budapest, Hungary) software programs. The specific peptide descriptor LogSumAA, introduced by our research group, was also included in the descriptor set [23]. The non-discriminative descriptors, *i.e.* constant for all peptides, and one of two highly correlated descriptors, calculated using the Pearson correlation coefficient (absolute correlation > 0.95), were eliminated, resulting in a final 186 × 454 data matrix for the original descriptors. When all descriptors were divided by the molecular weight, a data matrix of 186 × 416 was obtained. Next, the data were transformed by z-scaling, ensuring equal contribution of each descriptor to the resulting model [24].

Multivariate data analysis

Multivariate data analyses of the data matrix of descriptors were performed using Principal Component Analysis (PCA) and Hierarchical Cluster Analysis (HCA) with SIMCA-P+ 12.0.0.0 (Umetrics AB, Umeå, Sweden) and SPSS Statistics 20.0.0 (IBM Corp., Armonk, NY, USA) software programs, respectively. Average-linkage HCA clustering was performed using the Euclidean distance as the dissimilarity criterion. After a first PCA analysis of the data set, feature selection was performed by selecting the descriptors having a predicted variation value of more than 0.30, resulting in a 186 × 248 data matrix. For the descriptor set divided by the molecular weight, a 186 × 210 matrix was obtained.

Multiple Linear Regression (MLR) analysis of the chemo-molecular descriptors, using SPSS Statistics 20.0.0, was performed to build a predictive model for cellular uptake of CPPs. The stepwise method was performed during the MLR process to identify the most significant descriptors using the following criteria: probability of F to enter ≤ 0.05 and probability of F to remove ≥ 0.10. After eliminating 12 outliers identified by the Grubbs outlier test ($\alpha = 0.05$), the CP-responses of 174 peptides were used to build the model (information about the outliers see Table S2 of the Supplementary Information). In order to identify the descriptors robustly influencing the CP-response, a noise factor of 0.90, 0.95, 1.00, 1.05 or 1.10 was randomly introduced into the CP-responses. The *in silico* noised responses cover a variability with a range of 20%, an arbitrarily

assigned value lower than the experimental variability of the CP-responses, but this introduced variability allowed the identification of robust descriptors, which was the purpose of this robustness test.

Statistics

All statistical analyses of the data were performed using SPSS Statistics 20.0.0 software. Throughout this article, the median of data sets was used as the best measure for central tendency for not normally distributed data.

3. EXPLORATION OF THE CHEMICAL-FUNCTIONAL SPACE OF CELL-PENETRATING PEPTIDES

Data

Studies were selected if protocols were used in which the cellular uptake was determined in non-fixed cells and after removing or quenching of extracellular bound peptide according to Richard *et al.* [22]. Only pure peptides, not coupled to cargoes or to fatty acid chains, were withheld for this study. At last, we selected only those peptides for which standardizing to the cellular influx of penetratin was possible, allowing to calculate the CP-response for cellular uptake. Finally, a data set of 186 peptides was obtained, showing high to no or (very) low cellular uptake [7,9,11-13,16,17,25-69] (see Table S1 of the Supplementary Information). The different studies showed a remarkable variety in used techniques and operational parameters to test cellular uptake (Table 1).

Inherent to the different techniques used, the protocols of the experiments varied between research groups. This may explain the inconsistent cellular uptake results for some CPPs in the literature, like Tat 48-60, which normally demonstrates a cellular uptake within the same range as penetratin and R9, but was not in reference [17]. The model amphipathic peptide (MAP) showed an unusual low uptake in the study of Wada *et al.*, which is explained by the cell-specific uptake of this CPP [52].

Table 1. Experimental differences between studies for cellular uptake of peptides.

Operational parameter	Examples					
Technique	Spectrofluorometry		MALDI-TOF MS		Confocal laser scanning microscopy (CLSM)	
	RP-HPLC		Flow cytometry (FACS)		Atomic Absorption Spectrometry	
	Scintillometry		Splice correction assay		Quantitative analysis of CLSM images	
	Fluorescence microscopy					
Positive control	No		Tat 48-60		TP10	
	Penetratin		Tat 47-57		Transportan	
	MAP		R9		YGR6	
	pVEC		D-R9		R8	
Negative control	No		Dextran		Perforin	
	No peptide used		YDEGE		STRRSAMAPR	
	Green fluorescent peptide		YDEEGGG		APRTPGGRR	
Units of quantitative data	µM or nM		pmol or nmol/mg cell protein		SI/mg cell protein	
	ng/mg cell protein		a.u.		Fold change in GeoMean fluorescence	
	Mean fluorescence intensity		RLU/mg		Mean fluorescence intensity/mg cell protein	
	Fold/basal fluorescence		Relative fluorescence intensity		Relative cellular uptake (to control)	
	% of total peptide		% of added peptide		% cellular uptake	
	Cellular fluorescence		Fold change in FITC medium			
Label	FITC		5,6-carboxyfluorescein		2-aminobenzoic acid	
	Biotin		Deuterium		Rhodamine	
	NBD		TAMRA		Alexa 488	
	^{Ga}DOTA		Texas Red		^{125}I	
Cell line	AEC	BMC	HaCaT	HEK293	MC57	*S. cerevisiae*
	HBCEC	CHO (-K1)	Caco-2	HL60	A549	*C. albicans*
	bEnd	U2OS	Cos-7	MDCK	A431	*E. coli*
	MCF-7	Jurkat	MOLT-4	HeLa	Hela pLuc705	*B. megaterium*
	NIH-3T3	RAW264.7	BA/F3	K562	BT-20	N2a
	KB	RAW	U373 MG	Daudi	Sf9	MDA-MB-231
	HT-29	SKMel37	DAMI	A549	U251	KG1a
	TF-1	ESC	NC	Sca-1^{+}Lin^{-}	HEK293	L929
	Calu-3	MDA	HER	TM12	CCRF-CEM	
Incubation concentration	10 nM	200 nM	0.1 µM	0.33 µM	0.4 µM	0.8 µM
	1 µM	1.8 µM	2 µM	2.5 µM	3 µM	3.1 µM
	3.5 µM	4 µM	4.5 µM	5 µM	6 µM	6.3 µM
	7.5 µM	10 µM	12.5 µM	15 µM	20 µM	25 µM
	30 µM	40 µM	50 µM	100 µM	110 µM	200 µM
	400 µM	800 µM	1.6 mM			

Defining a CP-response

Because of the variety in experimental settings throughout the literature, the cellular uptake results of the available CPPs are difficult to be directly compared and are expressed using different units, as listed in Table 1. Therefore, a CP-response, a unified response expressing the cellular uptake efficiency of CPPs, would be of great help to obtain a clear overview of the cellular influx capacities of the available CPPs.

Penetratin, one of the first discovered CPPs and often described in the literature, is the most used positive control in uptake studies of other peptides. Therefore, penetratin was considered as a general positive control and used to normalize the responses for cellular uptake. Before a CP-response could be defined, several assumptions were made: (1) cell and label differences were neglected. As shown in Table 1, about 50 different cell lines and 12 different labels were used. The different nature of the labels was not considered when chemically defining the peptide structure. (2)

The uptake of the negative control was considered to be negligible. (3) The maximal values of cellular uptake during an experiment were used to cope with a possible time effect. (4) If a positive control was used in a study, it was considered as an internal standard and could be used to average variations in operational parameters. Finally, (5) a linear correlation between the extracellular and intracellular peptide concentration was assumed, although it cannot be excluded that there is a specific concentration effect [37,39,41,42,60]. This last assumption was necessary, because to calculate the CP-response, the quantitative value for cellular uptake was first corrected for the incubation (extracellular) concentration resulting in a concentration normalized response. Then, the latter response was normalized to the positive control penetratin, according to the following equation:

$$\frac{P_{CPP}/C_{CPP}}{P_{pen}/C_{pen}} \quad (1)$$

where P_{CPP}/C_{CPP} and P_{pen}/C_{pen} are the concentration-normalized influx responses for a CPP and penetratin respectively in the same study.

As already mentioned before, not all studies included penetratin as a positive control. When another positive control than penetratin was used, the median of all available ratios of that alternative positive control over penetratin was used to normalize the response to penetratin:

$$\frac{P_{CPP}/C_{CPP}}{P_{PC}/C_{PC}} \times \text{responsefactor} \quad (2)$$

where P_{CPP}/C_{CPP} is the concentration normalized influx response for a CPP, P_{PC}/C_{PC} for a positive control in the same study different from penetratin and the response factor is the median of all ratios of the concentration normalized responses of the positive control over the concentration normalized responses of penetratin, *i.e.* the median CP-response of the positive control, as expressed in formula (1) (Table 2).

Table 2. Overview of the used positive controls in studies for cellular uptake of peptides and their median CP-response (response factor).

Positive control	CP-response
MAP	2.05
Penetratin	1.00
pVEC	1.31
R9	1.00
Tat 47-57	0.31
Tat 48-60	0.22
TP10	1.64

A third possibility was that no positive control was used in the cellular uptake study. Then, the CP-response was calculated using the following equation:

$$\frac{P_{CPP}/C_{CPP}}{\overline{P_{pen}/C_{pen}}} \quad (3)$$

with P_{CPP}/C_{CPP} being the concentration normalized influx response for a CPP and $\overline{P_{pen}/C_{pen}}$ the median of all concentration normalized influx responses of penetratin, obtained using the same technique as the considered influx response (*i.e.* having the same unit).

If more than one CP-response was available for a peptide, the median CP-response was calculated. Over all peptides, the CP-response ranged from 0.001378 to 2.744. The ranking of the peptides based on their CP-response, roughly corresponded with those found in the literature, *e.g.* the CP-response increased as follows: Tat 48-60 < R9 ≈ penetratin < pVEC < TP10 < MAP < transportan. This was in agreement with the overall study conclusions: Tat 48-60 mostly showed the lowest cellular influx [17,26,30,31,33,34,38], followed by R9 and penetratin [17,25,26,28,30-34,38]. The peptides pVEC, TP10, MAP and transportan showed higher cellular influx than Tat 48-60, penetratin and R9. Transportan mostly showed a higher cellular influx than TP10 [10,28]. Moreover, as a proof of concept, we investigated all manuscripts providing the quantitative data for cellular influx for the 186 peptides and compiled for each peptide how the authors estimated (subjectively) their cell-penetrating properties (see Table S3 of the Supplementary Information). In these studies, five classifications could be distinguished: no CPP, low CPP (described as low CPP, low efficient, low effective, slow, nearly unmeasurable), medium CPP (described as medium CPP, efficient, effective) and high CPP (described as high CPP, highly, extremely effective, extremely efficient, rapid). When the authors only described the peptide as cell-penetrating, without any scaling or subjective ranking, these peptides were classified as CPP. Next, the distribution of the CP-responses in the five different classes was evaluated using box-and-whisker plots (see Figure 1). The median CP-response increased over the different classes from no CPP over low CPP, medium CPP and CPP to high CPP, indicating that peptides having a high or low calculated CP-response were also estimated in the same way by the researchers. From Figure 1 can be concluded that the researchers who investigated peptide 80 (MitP) were rather pessimistic when evaluating the uptake data: the authors concluded a medium cellular uptake, while a high CP-response was calculated. This comparative analysis thus demonstrated the validity of the CP-response, being indicative for the extent of cell-penetration of a peptide, as well as showed the use of this unified response during the evaluation of quantitative data for cellular uptake of peptides.

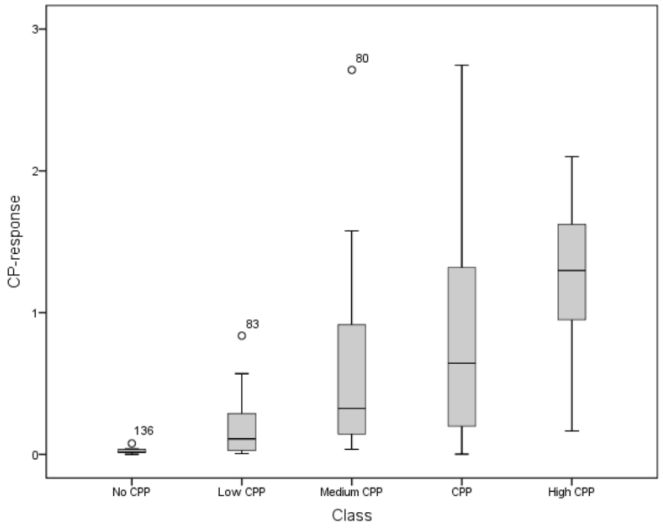

Figure 1. Distribution of the CP-responses in five different CPP classes as defined by the authors. The median CP-response increases from class no to high CPP, showing the validity of the CP-response to rank peptides according to their cell-penetrating properties.

Exploration of the chemical space of cell-penetrating peptides

To determine the chemical space of a set of 186 peptides, which were investigated for cell-penetrating properties, a PCA and HCA analysis of their calculated descriptors was performed. The scores plot of the first and the second principal component (PC) of the calculated PCA model explained already 62.6% of the total variability (Table 3).

Table 3. Summary of the PCA analysis of the original descriptors, describing the eigenvalues of the covariance matrix, the total variance explained (cumulative R^2) and the predictive ability (cumulative Q^2).

Principal Component	Eigenvalue	Cumulative R^2	Cumulative Q^2
1	86.9	0.467	0.448
2	29.5	0.626	0.602
3	12.1	0.691	0.639
4	11.6	0.753	0.701
5	5.74	0.784	0.720
6	5.16	0.812	0.743
7	4.42	0.836	0.764
8	3.53	0.854	0.781
9	2.58	0.868	0.789
10	2.17	0.880	0.797
11	1.94	0.890	0.807

Based on the dendrogram of the HCA analysis and the scores plot of the first two PCs of the PCA analysis, the 186 peptides were categorized into six main clusters, which could be subdivided into eight subclusters (Figure 2).

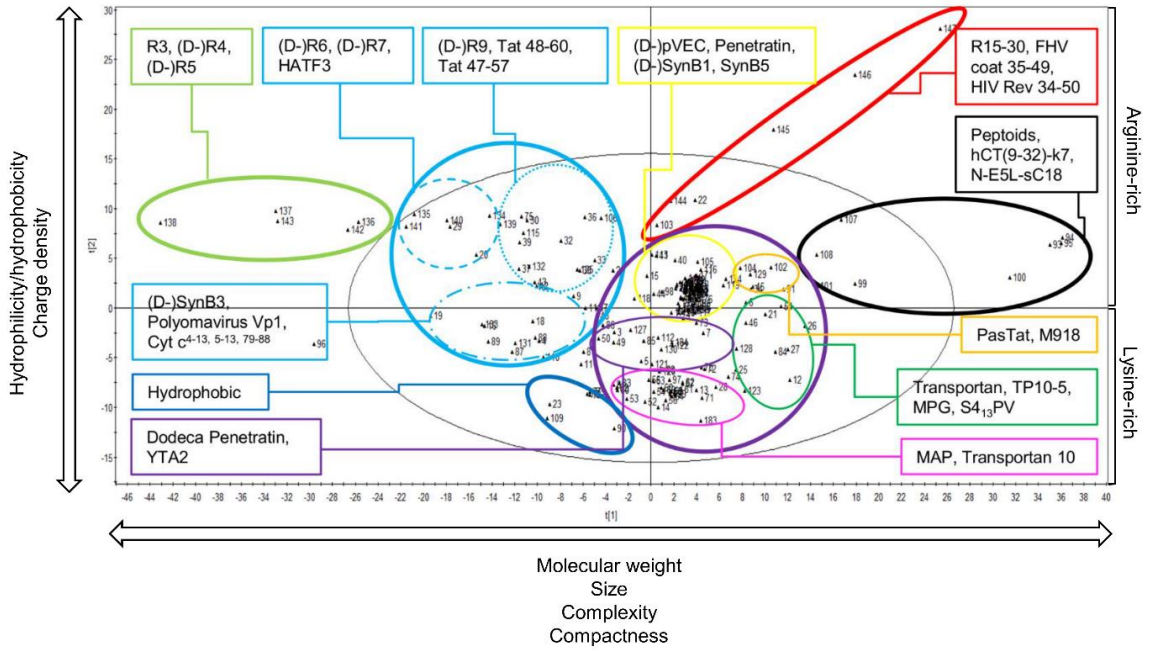

Figure 2. Scores plot of the first versus the second principal component of the PCA analysis of 186 peptides (represented by the black triangles). The six main clusters of peptides are indicated by a bold line, while the eight subclusters are encircled by a thin line. Along the principal axes, examples of descriptors strongly influencing the principal components are indicated as derived from the loadings plot.

The loadings plot, which displays the relationship among the variables, can be used to explain interesting patterns in the scores plot, *i.e.* which variables or descriptors determine the observed clusters of peptides [24]. The loadings plot indicated that the first principle component (PC1) is mainly influenced by the mass, shape and connectivity of the peptides, while the second principle component (PC2) was determined by hydrophilicity and lipophilicity. In Figure 2, the peptides with high molecular weight (MW), surface area, molecular volume and number of hydrogen acceptor atoms were situated on the right along the horizontal axis and inherently these peptides had a higher number of peptide bonds (represented by the descriptors nRCONHR and C-040). The peptides on the right were also characterized by a more voluminous, complex and less compact structure. On the other side of the horizontal axis, the smaller, more symmetrical and compact peptides were located. On the PC2 axis, peptides mainly consisting of hydrophilic amino acids, like the basic arginine and lysine residues, represented by the high pI values of these peptides, were situated at the top. When descending to the bottom, the peptides turn more hydrophobic, indicated by higher log P values, hydration energy and BLI values (Kier Benzene Likeliness index), the latter describing the extent of molecular aromaticity.

The light green cluster at the left in the scores plot represented short oligo-arginines (R3-R5), showing a very low median CP-response of 0.0769. The light blue subclusters contained cationic peptides, which differed in charge and peptide length (increasing from the left to the right). The light

blue dashed-dotted subcluster (*e.g.* SynB3 and polyomavirus Vp1), showed a low median CP-response of 0.0392, while the dashed (*e.g.* R6, R7 and HATF3) and dotted (*e.g.* R9 and Tat 48-60) light blue subclusters had a mediocre cellular influx with median CP-responses of 0.323 and 0.464, respectively. The yellow and orange subclusters, which were centrally located in the PCA scores plot, formed mixed clusters, as they contained both cationic and amphipathic peptides. The pink and purple amphipathic subclusters had median CP-responses of 0.181 and 0.302, respectively. The yellow subcluster (*e.g.* pVEC and penetratin), orange subcluster (*e.g.* PasTat and M918) and the dark green subcluster (*e.g.* transportan and MPG) had the highest values for the median CP-response, ranging from 0.511 to 0.729 and 0.798, respectively. These peptides were cationic and/or amphipathic and are composed of 15-27 amino acids. Remarkably, the group of peptides, showing a high CP-response could be subdivided in two groups: those having a positive PC2 value, which were mainly arginine rich (yellow and orange subcluster) and those having a negative PC2 value (dark green subcluster), which were mainly lysine rich. Although it was previously stated that arginine residues are favorable over lysine for cellular influx [2], our data did not confirm this statement. Peptides showing the highest CP-response had a high charge density or show amphipathicity. The latter peptides were centrally located in the scores plot and were rich in sulfur-containing residues, especially methionine, as well as in aromatic amino acids.

The hydrophobic peptides, which are alanine, glycine, leucine, proline and valine rich, were located at the bottom of the scores plot and showed a mediocre, but significant influx (median CP-response of 0.354). The peptides of the red cluster were highly charged and showed a high CP-response (median of 0.764). The cluster was mainly composed of oligo-arginines of more than 15 residues, which are known for their cellular toxicity [12]. The black cluster consisted of voluminous, high molecular weight peptides, *i.a.* some peptoid structures, showing a very low cellular influx (median CP-response of 0.166).

As PC1 was mainly dominated by the molecular weight, the same PCA analysis was performed, but using all descriptors divided by the molecular weight in order to neutralize its MW size-effect, although some descriptors were already corrected for the MW. However, this modification of the descriptors did not provide additional information. The calculated PCA model resulted in similar clusters of CPPs (see Table S4 and Figure S1 of the Supplementary Information).

Functional diversity of cell-penetrating peptides

Using our newly defined CP-response and the calculated chemo-molecular descriptors of the peptides, a stepwise MLR model was constructed to predict the cell-penetrating ability of peptides. In order to find the descriptors most robustly influencing the CP-response, new datasets were

created by introducing a random response noise covering 20% of variability (MLR1 to MLR10). For these data sets, MLR analyses were performed allowing to identify the descriptors that significantly, based upon inclusion into the MLR model, and robustly influence the CP-response, *i.e.* descriptors which were withheld in more than half of the MLR-models (Table 4).

Table 4. Overview of the most robust descriptors influencing the CP-responses in the 11 MLR data sets.

	MLR	**MLR_1**	**MLR_2**	**MLR_3**	**MLR_4**	**MLR_5**	**MLR_6**	**MLR_7**	**MLR_8**	**MLR_9**	**MLR_{10}**	**Mean**
R^2	0.621	0.589	0.493	0.515	0.619	0.617	0.508	0.587	0.525	0.572	0.615	0.569
Adjusted R^2	0.577	0.545	0.458	0.478	0.578	0.572	0.471	0.542	0.487	0.532	0.567	0.528
Descriptor	**Coefficients[1]**											**#**
B04[N-N]	0.175	0.285	0.287	0.298	0.228	0.154	0.183	0.251	0.203	0.305	0.187	11
GATS5m	0.401	0.573	0.321	0.298	0.541	0.435	0.389	0.443	0.396	0.612	0.670	11
G2e	-0.184	-0.141	-0.186	-0.221	-0.205	-0.186	-0.218	-0.226	-0.215	-0.177	-0.181	11
nCt	0.465	0.482	0.570	0.547	-	0.453	0.491	0.588	0.555	0.215	-	9
nROR	0.244	0.198	-	-	0.322	0.231	-	-	-	0.300	0.320	6
T(N..S)	0.912	0.461	-	-	0.897	0.940	-	-	-	0.799	0.607	6
G3u	-0.184	-0.137	-	-	-0.224	-0.183	-	-	-	-0.190	-	5
Mp	0.548	0.352	-	-	0.525	0.553	-	0.307	-	-	-	5
Mor15p	-0.656	-	-	-	-0.791	-0.673	-	-	-	-0.366	-0.275	5
Mor26m	-0.319	-	-0.202	-0.209	-0.361	-0.318	-	-	-0.191	-0.305	-	7
GATS7e	-	-	0.922	1.066	-	-	1.127	1.233	1.143	-	-	5
GATS7p	-	-	-0.682	-0.761	-	-	-0.798	-0.944	-0.806	-	-	5
Mor16p	-	-0.316	-0.385	-0.419	-	-	-0.478	-0.482	-0.391	-	-0.301	7
Mor27m	-	-	-0.410	-0.404	-	-	-0.327	-0.298	-0.387	-	-	5
Mor27e	-	-	0.248	0.291	-	-	0.202	0.217	0.274	-	-	5

[1]For each model, the coefficients of the significant descriptors are indicated.

In Table 5, the meaning of these robust descriptors influencing the cell-penetrating properties are listed.

Table 5. Meanings of the robust descriptors influencing significantly the CP-response of peptides.

Descriptor	**Meaning**	**Class**
B04[N-N]	Presence/absence of N-N at topological distance 4	2D binary fingerprints
GATS5m	Geary autocorrelation - lag 5/weighted by atomic masses	2D autocorrelations
G2e	2st component symmetry directional WHIM index/weighted by atomic Sanderson electronegativities	WHIM[1] descriptors
nCt	Number of total tertiary C (sp^3)	Functional group counts
nROR	Number of ethers (aliphatic)	Functional group counts
T(N..S)	Sum of topological distances between N..S	Topological descriptors
G3u	3rd component symmetry directional WHIM index/unweighted	WHIM descriptors
Mp	Mean atomic polarizability (scaled on Carbon atom)	Constitutional descriptors
Mor15p	3D-MoRSE - signal 15/weighted by atomic polarizabilities	3D-MoRSE[2] descriptors
Mor26m	3D-MoRSE - signal 26/weighted by atomic masses	3D-MoRSE[2] descriptors
GATS7e	Geary autocorrelation - lag 7/weighted by atomic Sanderson electronegativities	2D autocorrelations
GATS7p	Geary autocorrelation - lag 7/weighted by atomic polarizabilities	2D autocorrelations
Mor16p	3D-MoRSE - signal 16/weighted by atomic polarizabilities	3D-MoRSE[2] descriptors
Mor27m	3D-MoRSE - signal 27/weighted by atomic masses	3D-MoRSE[2] descriptors
Mor27e	3D-MoRSE - signal 27/weighted by atomic Sanderson electronegativities	3D-MoRSE[2] descriptors

[1]Weighted Holistic Invariant Molecular descriptors

[2]3D-Molecular Representation of Structures based on Electron diffraction

The descriptor B04[N-N] is a 2D-binary fingerprint descriptor, representing the presence or absence of the specific atom pair N-N at a topological distance of four bonds. Our models indicated that the presence of such an N-N pair has a positive influence on the CP-response. When looking at the amino acid structures, this N-N bond at topological distance four is found in asparagine and histidine residues. The latter is a weak α-helix former and thus may be important to establish the secondary amphipathic structure of peptides [70]. The GATS5m, GATS7p and GATS7e descriptors are Geary 2D-autocorrelation descriptors, which describe the topology of the peptide in association with atomic masses (m), polarizabilities (p) and Sanderson electronegativities (e). At specific path length (lag) five, the atomic masses have a high positive contribution to the cell-penetrating properties, while at lag seven, a positive (weighted by atomic Sanderson electronegativities) or negative (weighted by atomic polarizabilities) influence on our CP-response was observed. GATS7e shows the dispersion of electronegative atoms at a topological distance equal to seven bonds in a peptide, while the value of GATS7p shows the importance of atomic polarizabilities over the same topological distance. Peptides having high (GATS5m and GATS7e) or low (GATS7p) values of these descriptors, were rich in basic amino acids, arginine and lysine, as well as the aromatic amino acid tryptophan.

3D-Molecule Representation of Structures based on Electron diffraction (3D-MoRSE) descriptors are 3D-molecular descriptors derived from scattering transform functions, reflecting various physicochemical properties, like atomic polarizability (signals 15 and 16), atomic masses (signals 26 and 27) and atomic electronegativity (signal 27) [71]. From these 3D-MoRSE descriptors could be derived that the position of these physicochemical properties in the 3D-space is crucial for cell-penetrating properties. Based on these descriptors, a favorable cellular influx was predicted for the amphipathic and/or cationic subclusters of the PCA analysis, *i.e.* the dark green, pink, purple and yellow subclusters. Moreover, the peptides belonging to the dark green and yellow subclusters showed the highest median CP-response, which was also predicted based on their values of the robust 3D-MoRSE descriptors. 3D-descriptors characterizing the symmetry of the peptides also robustly influenced the CP-response: the symmetry-directional WHIM descriptors G2e (weighted by atomic Sanderson electronegativities) and G3u (unweighted) negatively influenced the cell-penetrating properties, indicating that the cellular influx of peptides increased with decreasing peptide symmetry [71]. Peptides containing branched and hydrophobic amino acids, *e.g.* valine, leucine and isoleucine, as indicated by the descriptor nCt, accounting for the number of tertiary carbon atoms showed a higher CP-response. Also the T(N..S) descriptor referring to the presence of sulfur-containing amino acids, and the mean atomic polarizability (Mp) contributed positively to the cellular penetration. Methionine (α-helix former) as well as the hydrophobic amino acids (favor β strands) are important for establishing a secondary amphipathic structure. Finally, the nROR descriptor, which was an unexpected robust descriptor, also positively influenced the CP-response.

The cationic amphiphilic polyproline helices (CAPHs) contain such ether functions to link the hydrophobic and hydrophilic residues. Although the MLR analysis did not directly point to the importance of a positive charge for cellular uptake, the information contained in the robust descriptors indicated its influence as well as of a secondary amphipathic structure.

4. EVALUATION OF THE CP-RESPONSE AND THE CHEMICAL SPACE OF CELL-PENETRATING PEPTIDES

Studies of the cellular uptake of CPPs demonstrate a great variety in experimental conditions, as illustrated in Table 1. These differences in used techniques and operational parameters, are at least partly responsible for discrepancies in conclusions about the cellular uptake of certain CPPs, like *e.g.* the uptake mechanism. In Table S3, the available information on the mechanism of cellular uptake of our selected peptides is listed. There are three main mechanisms of cellular entry: (1) direct penetration, which can be subdivided into (a) inverted micelle formation, (b) pore formation, (c) carpet-like model, (d) membrane thinning and (e) nucleation zones. The second mechanism is (2) endocytosis, with subcategories (a) macropinocytosis, (b) dependent on coat proteins and (c) independent on coat proteins. Some publications also define a third mechanism: (3) energy-dependent, but not endocytosis (exact mechanism not specified by authors) [2,12,72,73]. From Table S3 can be derived that the different studies on the uptake mechanism of CPPs show an inconsistency in cellular uptake mechanism. Cell-penetrating peptides use different mechanisms of entry, either simultaneously or as function of experimental factors, like the extracellular concentration, cell line, presence of a cargo, incubation time and temperature [2,42,44].

Clearly, there is an urgent need for harmonization of the experimental conditions in the investigations of cellular uptake of peptides, like other authors have already suggested in the past [18,20]. Especially, the use of a standard positive control or controls, *e.g.* penetratin, is recommended, as it allows to neutralize to some extent the differences in experimental conditions. Therefore, we defined a CP-response, a unified response which allows the comparison of experimental data of the cellular influx of peptides. Several assumptions were made, which cause, together with the existing experimental variations, some variability in our CP-response. Nevertheless, the hitherto described CPPs can be compared using this CP-response and new conclusions about the structure-activity modeling of these peptides can be drawn.

As a first assumption, cell and label differences were neglected, as a wide range of cell lines and detection labels are used throughout the literature. It is clear that different cell lines have different membrane characteristics, influencing the used mechanism and quantity of cellular uptake of CPPs [17,22,25,27,30,32-34,37,38,40,41,43-45,53,55,56,58,64-67]. The correlation between the incubated

cell line and the cellular uptake properties of CPPs deserves a more thorough investigation, but was outside the scope of this study. We also assumed penetratin as a general positive control, because it is quite often used and is well characterized, being one of the first described CPPs. It was also necessary to correct the uptake responses for the incubation concentration, as there exists a clear relationship between the extra- and intracellular concentration of CPPs. Therefore, we assumed a simple linear relationship, justified by the fact that only a few studies have already investigated the internalization dependence on the extracellular peptide concentration, not allowing more complex models to be used. For most CPPs, there is indeed a correlation between the intracellular and the extracellular concentration [37,39,41,42,60]. On the other hand, some peptides, like R9, hLF and Tat 47-57, show a sudden sharp increase in intracellular concentration, when a certain extracellular concentration is reached [41,42]. Still, for other peptides, the extracellular concentration needs to exceed a threshold concentration before cellular uptake takes place. Some authors explain this phenomenon by the fact that the uptake mechanism of CPPs depends on the extracellular concentration [42]. Moreover, Hällbrink *et al.* [74] showed that the uptake of CPPs may also be dependent on the peptide-to-cell ratio, as demonstrated for MAP and penetratin. Besides, some CPPs show toxic effects starting from a certain extracellular concentration [37,39]. Taking the above findings in consideration, we visualized the intracellular versus extracellular concentration curve for CPPs as a sigmoid (see Figure 3), characterized by a threshold value for influx, which was for all available peptide data about 1 μM. When the threshold is reached, the intracellular concentration increases in function of the extracellular concentration, followed by flattening of the curve until a plateau value for intracellular concentration is reached, possibly due to cell death. The threshold value for influx is CPP and cell line dependent. For most CPPs however, only one extracellular concentration is investigated, which makes it impossible to reconstruct the full sigmoid curve dependence. We applied a linear model, realizing that this approach is an over-simplification, leading to increased variability and bias. It is clear that studying the correlations between intracellular and extracellular concentration, would give more insights into the uptake mechanisms of the peptides, as well as into the toxicity profile.

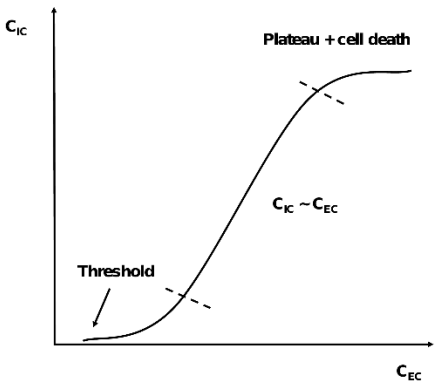

Figure 3. Supposed dependence of the intracellular CPP concentration on the extracellular concentration when performing cellular influx studies.

Our data set contained peptides showing very low to high cellular influx (CP-response of 0.001378 to 2.744), indicating that our data set covered a sufficiently wide range of CP-responses. Moreover, the ranking of the peptides based on the CP-responses, corresponds roughly with those found in the literature, when considering the most studied and compared CPPs. This indicates that our approach is a valuable quantitative way to assess CPP properties, which was also demonstrated by the evaluation of the distribution of the CP-responses in the five different classes of CPPs as defined by the authors. From Figure 1 can be derived that the medium CP-response increases over the different classes from no CPP to high CPP. Still there exists a clear overlap in CP-responses between the different classes. The lower whiskers of the distribution of the medium CPP, CPP and high CPP classes are extended to almost zero response, indicating that they also contain non- or low-penetrating peptides, according to our proposed CP-response. We evaluated the peptides composing these lowest values and concluded that they can often be explained by an incorrect descriptive conclusion of the authors. Possible reasons are that the classification was based on experiments without trypsinization, while also experiments with trypsinization of the cells were performed, or that much higher incubation concentrations than normally applied are used in order to reach cellular uptake, leading to low CP-responses as they are concentration corrected [17,51]. Nevertheless, this observed consistency strengthens the value of our CP-response.

The exploration of the chemical space of the 186 peptides, investigated for cell-penetrating properties, confirmed some known features about CPPs, supporting our approach, but also revealed some new insights in the structural diversity of these peptides. The molecular weight, surface area, molecular volume, the number of hydrogen bond acceptors, hydrophobicity and charge determined the main clusters in the PCA analysis. These characteristics join with previous findings about important properties for cellular influx, *i.a.* z-scales used by Hällbrink *et al.* [19]. However, our PCA analysis indicated that also the shape and complexity of the structure differ within the group of CPPs. In the scores plot of the PCA analysis (Figure 2), there was a clear trend in symmetry, complexity and

compactness of the structure: extremes for these descriptors give low CP-responses for the peptides. From this exploration of the chemical space of CPPs, it can be derived that not only the constituent amino acids determine cell-penetrating properties but also their position. This contrasts the current general opinion that the 3D-structure is not significantly influencing the cellular uptake, except for the secondary amphipathic CPPs [6]. Moreover, our 3D-structures are calculated based on a theoretical phase, *i.e.* MM+ *in vacuo* optimized structures according to Hyperchem molecular mechanics, which is independent from its biological medium and interactions.

The light green cluster in Figure 2 consists of oligo-arginines of up to five arginines and shows a very low to negligible CP-response, consistent with the conclusions of Mitchell *et al.* [12]. On the other hand, based on the characteristics of the clusters with the highest unified response, high density of positive charges and amphipathicity favor cellular uptake. The amphipathic peptides were located centrally in the scores plot of the PCA analysis and were characterized by a high extent of sulfur-containing residues, as well as aromatic amino acids. These features are indeed important for establishing a secondary amphipathic structure. According to Chou and Fasman, methionine is a strong α-helix former, while the aromatic amino acids, phenylalanine and tryptophan favor the formation of β strands by contributing to hydrophobic interactions when establishing this secondary structure [70].

Although MLR only captures a linear correlation between descriptors [21], it gives us valuable information about which descriptors significantly influence cellular uptake. By adding a random noise around our calculated CP-response, the descriptors most robustly influencing the CP-response, *i.e.* those descriptors which were incorporated in more than half of the obtained MLR models, were identified. This MLR analysis revealed that a positive charge, represented by the basic amino acids arginine and lysine, and an amphipathic structure are discriminating properties for cellular influx of peptides. We also identified the symmetry and the compactness of the peptide structure as determining. Furthermore, the 3D-MoRSE descriptors indicate that certain patterns in the molecular structure influence whether a peptide is efficiently cell-penetrating or not. This refers to an amphipathic structure, or more in general, to recurrent functional groups, like *e.g.* the guanidinium group of arginine. Indeed, based on the 3D-MoRSE descriptors, a favored cellular influx is predicted for the amphipathic peptides. The results of the MLR analysis correspond well with the identified important features for cellular uptake during the exploration of the chemical space of the 186 peptides.

Cell-penetrating peptides form a chemically diverse group of peptides, as we demonstrated during the PCA analysis, and are traditionally classified into three chemically different groups [6]: (1) cationic CPPs (C), which contain a stretch of positive charges and whose 3D-structure is not an amphipathic helix. (2) Amphipathic CPPs (A), which are characterized by a hydrophobic and hydrophilic part by

adopting a helix structure. Amphipathic peptides may have a cationic nature (AC) or their hydrophilic part can be neutral, anionic or polar (A). The (3) hydrophobic CPPs (H) are peptides containing only apolar residues, with low net charge or that have hydrophobic amino acid groups that are crucial for cellular uptake. Cationic CPPs may also have a hydrophobic (CH) or amphipathic nature (AC). In Table S3, the chemical classes of the individual peptides of our data set are listed and schematically visualized in Figure 4. Using this chemical classification method, there is a clear overlap demonstrated for the different classes, especially for the amphipathic-cationic peptides.

We believe that our CP-response, as a more objective and quantitative measure for cellular penetration, will foster the discussion of the cellular uptake mechanisms, as well as the definition and the classification of the CPPs.

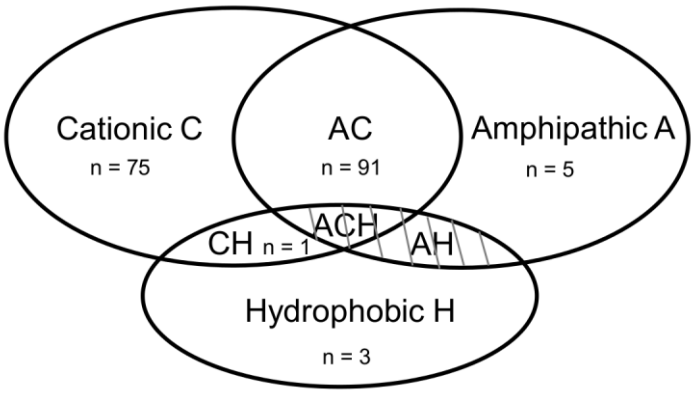

Figure 4. Schematic representation of the CPP chemical classes from our data set. The number of peptides attributed to the different classes is indicated.

5. CONCLUSIONS

When gathering quantitative data for cellular influx of peptides, it was clear that harmonization of these studies is highly needed. By defining a CP-response, the quantitative evaluation of the cellular influx characteristics of 186 peptides was possible. This CP-response, together with chemo-molecular descriptors of the peptides, was used to explore the chemical-functional space of CPPs. Our study indicated that besides already reported CPP-determining features, like *i.a.* positive charge and amphipathicity, also the shape, complexity and compactness of the structures, play an import role for influx into the cell. As our CP-response is a more objective and quantitative measure for cellular penetration of peptides, it will help to classify these peptides, to unravel the different uptake mechanisms, as well as to establish a common evaluation tool.

6. REFERENCES

[1] Frankel AD, Pabo CO. Cellular uptake of the tat protein from human immunodeficiency virus. *Cell* 1988; **55**: 1189-1193.

[2] Madani F, Lindberg S, Langel Ü, Futaki S, Gräslund A. Mechanisms of Cellular Uptake of Cell-Penetrating Peptides. J. Biophys. 2011; **2011**: 414729.

[3] Jarver P, Langel Ü. Cell-penetrating peptides – A brief introduction. *BBA-Biomembranes* 2006; **1758**: 260-263.

[4] Lindgren M, Langel Ü. Classes and Prediction of Cell-Penetrating Peptides. In *Cell-Penetrating Peptides: Methods and Materials* (Ed: Langel Ü). Humana Press, **2011**, pp. 3-19.

[5] Vergote V, Burvenich C, Van de Wiele C, De Spiegeleer B. Quality specifications for peptide drugs: a regulatory-pharmaceutical approach. *J. Pept. Sci.* 2009; **15**: 697-710.

[6] Milletti F. Cell-penetrating peptides: classes, origin, and current land scape. *Drug Discov. Today* 2012; **17**: 850-860.

[7] Elmquist A, Hansen M, Langel Ü. Structure-activity relationship study of the cell-penetrating peptide pVEC. *BBA-Biomembranes* 2006; **1758**: 721-729.

[8] Fischer PM., Zhelev NZ, Wang S, Melville JE, Fåhraeus R, Lane DP. Structure-activity relationship of truncated and substituted analogues of the intracellular delivery vector Penetratin. *J. Peptide Res.* 2000; **55**: 163-172.

[9] Drin G, Mazel M, Clair P, Mathieu D, Kaczorek M, Temsamani J. Physico-chemical requirements for cellular uptake of pAntp peptide: Role of lipid-binding affinity. *Eur. J. Biochem.* 2001; **268**: 1304-1314.

[10] Soomets U, Lindgren M, Gallet X, Hällbrink M, Elmquist A, Balaspiri L, Zorko M, Pooga M, Brasseur R, Langel Ü. Deletion analogues of transportan. *BBA-Biomembranes* 2000; **1467**: 165-176.

[11] Song J, Kai M, Zhang W, Zhang J, Liu L, Zhang B, Liu X, Wang R. Cellular uptake of transportan 10 and its analogs in live cells: Selectivity and structure-activity relationship studies. *Peptides* 2011; **32**: 1934-1941.

[12] Mitchell DJ, Kim DT, Steinman L, Fathman CG, Rothbard JB. Polyarginine enters cells more efficiently than other polycationic homopolymers. *J. Pept. Res.* 2000; **56**: 318-325.

[13] Scheller A, Oehlke J, Wiesner B, Dathe M, Krause E, Beyermann M, Melzig M, Bienert M. Structural Requirements for Cellular Uptake of α-Helical Amphipathic Peptides. *J. Pept. Sci.* 1999; **5**: 185-194.

[14] Vivès E, Brodin P, Lebleu B. A Truncated HIV-1 Tat Protein Basic Domain Rapidly Translocates through the Plasma Membrane and Accumulates in the Cell Nucleus. *J. Biol. Chem.* 1997; **272**: 16010-16017.

[15] Vivès E, Granier C, Prevot P, Lebleu B. Structure-activity relationship study of the plasma membrane translocating potential of a short peptide from HIV-1 Tat protein. *Lett. Pept. Sci.* 1997; **4**: 429-436.

[16] Wender PA, Mitchell DJ, Pattabiraman K, Pelkey ET, Steinman L, Rothbard JB. The design, synthesis, and evaluation of molecules that enable or enhance cellular uptake: Peptoid molecular transporters. *P. Natl. Acad. Sci. USA* 2000; **97**: 13003-13008.

[17] Mueller J, Kretzschmar I, Volkmer R, Boisguerin P. Comparison of Cellular Uptake Using 22 CPPs in 4 Different Cell Lines. *Bioconjugate Chem.* 2008; **19**: 2363-2374.

[18] Hansen M, Kilk K, Langel Ü. Predicting cell-penetrating peptides. *Adv. Drug Deliver. Rev.* 2008; **60**: 572-579.

[19] Hällbrink M, Kilk K, Elmquist A, Lundberg P, Lindgren M, Jiang Y, Pooga M, Soomets U, Langel Ü. Prediction of Cell-Penetrating Peptides. *Int. J. Pept. Res. Ther.* 2005; **11**: 249-259.

[20] Karelson M, Dobchev D Using artificial neural networks to predict cell-penetrating compounds. *Expert Opin. Drug Dis.* 2011; **6**: 783-796.

[21] Sanders WS, Johnston CI, Bridges SM, Burgess SC, Willeford KO. Prediction of Cell-Penetrating Peptides by Support Vector Machines. *PLOS Comput. Biol.* 2011; **7**: e1002101.

[22] Richard JP, Melikov K, Vivès E, Ramos C, Verbeure B, Gait MJ, Chernomordik LV, Lebleu B. Cell-penetrating Peptides: A reevaluation of the mechanism of cellular uptake. *J. Biol. Chem.* 2003; **278**: 585-590.

[23] D'Hondt M, Gevaert B, Stalmans S, Van Dorpe S, Wynendaele E, Peremans K, Burvenich C, De Spiegeleer B. Reversed-phase fused-core HPLC modeling of peptides. *J. Pharm. Anal.* 2013; **3**: 93-101.

[24] Eriksson L, Johansson E, Kettaneh-Wold N, Trygg J, Wikström C, Wold S. *Multi- and Megavariate Data Analysis: Part I – Basic Principles and Applications*, second revised and enlarged edition. Umetrics AB, **2006**, pp. 39-101.

[25] Elmquist A, Lindgren M, Bartfai T, Langel Ü. VE-Cadherin-Derived Cell-Penetrating Peptide, pVEC, with Carrier Functions. *Exp. Cell Res.* 2001; **269**: 237-244.

[26] Lundberg P, Langel Ü. Uptake Mechanisms of Cell-Penetrating Peptides Derived from Alzheimer's Disease Associated Gamma-Secretase Complex. *Int. J. Pept. Res. Ther.* 2006; **12**: 105-114.

[27] Holm T, Netzereab S, Hansen M, Langel Ü, Hällbrink M. Uptake of cell-penetrating peptides in yeasts. *FEBS Lett.* 2005; **579**: 5217-5222.

[28] Lindgren ME, Hällbrink MM, Elmquist AM, Langel Ü. Passage of cell-penetrating peptides across a human epithelial cell layer *in vitro*. *Biochem. J.* 2004; **377**: 69-76.

[29] Palm C, Jayamanne M, Kjellander M, Hällbrink M. Peptide degradation is a critical determinant for cell-penetrating peptide uptake. *BBA-Biomembranes* 2007; **1768**: 1769-1776.

[30] El-Andaloussi S, Järver P, Johansson HJ, Langel Ü. Cargo-dependent cytotoxicity and delivery efficacy of cell-penetrating peptides: a comparative study. *Bioch. J.* 2007; **407**: 285-292.

[31] Burlina F, Sagan S, Bolbach G, Chassaing G. Quantification of the Cellular Uptake of Cell-Penetrating Peptides by MALDI-TOF Mass Spectrometry. *Angew. Chem. Int. Edit.* 2005; **44**: 4244-4247.

[32] El-Andaloussi S, Johansson HJ, Holm T, Langel Ü. A Novel Cell-Penetrating Peptide, M918, for Efficient Delivery of Proteins and Peptide Nucleic Acids. *Mol. Ther.* 2007; **15**: 1820-1826.

[33] Fischer R, Köhler K, Fotin-Mleczek M, Brock R. A Stepwise Dissection of the Intracellular Fate of Cationic Cell-penetrating Peptides. *J. Biol. Chem.* 2004; **279**: 12625-12635.

[34] Jones SW, Christison R, Bundell K, Voyce CJ, Brockbank SMV, Newham P, Linday MA. Characterisation of cell-penetrating peptide-mediated peptide delivery. *Brit. J. Pharmacol.* 2005; **145**: 1093-1102.

[35] Walrant A, Correia I, Jiao C-Y, Lequin O, Bent EH, Goasdoué N, Lacombe C, Chassaing G, Sagan S, Alves ID. Different membrane behaviour and cellular uptake of three basic arginine-rich peptides. *Biochim. Biophys. Acta* 2011; **1808**: 382-393.

[36] Maiolo JR, Ferrer M, Ottinger EA. Effects of cargo molecules on the cellular uptake of arginine-rich cell-penetrating peptides. *BBA-Biomembranes* 2005; **1712**: 161-172.

[37] Oehlke J, Scheller A, Wiesner B, Krause E, Beyermann M, Klauschenz E, Melzig M, Bienert M. Cellular uptake of an α-helical amphipathic model peptide with the potential to deliver polar compounds into the cell interior non-endocytically. *BBA-Biomembranes* 1998; **1414**: 127-139.

[38] Sugita T, Yoshikawa T, Mukai Y, Yamanada N, Imai S, Nagano K, Yoshida Y, Shibata H, Yoshioka Y, Nakagawa S, Kamada H, Tsunoda S-I, Tsutsumi Y. Comparative study on transduction and toxicity of protein transduction domains. *Brit. J. Pharmacol.* 2008; **153**: 1143-1152.

[39] Drin G, Cottin S, Blanc E, Rees AR, Temsamani J. Studies on the Internalization Mechanism of Cationic Cell-Penetrating Peptides. *J. Biol. Chem.* 2003; **278**: 31192-31201.

[40] Johansson HJ, El-Andaloussi S, Holm T, Mäe M, Jänes J. Characterization of a Novel Cytotoxic Cell-Penetrating Peptide Derived From p14ARF Protein. *Mol. Ther.* 2008; **16**: 115-123.

[41] Duchardt F, Ruttekolk IR, Verdurmen WPR, Lortat-Jacob H, Bürck J, Hufnagel H, Fischer R, van den Heuvel M, Löwik DWPM, Vuister GW, Ulrich A, de Waard M, Brock R. A Cell-penetrating Peptide Derived from Human Lactoferrin with Conformation-dependent Uptake Efficiency. *J. Biol. Chem.* 2009; **284**: 36099-36108.

[42] Duchardt F, Fotin-Mleczek M, Schwarz H, Fischer R, Brock R. A Comprehensive Model for the Cellular Uptake of Cationic Cell-penetrating Peptides. *Traffic* 2007; **8**: 848-866.

[43] Verdurmen WPR, Bovee-Geurts PH, Wadhwani P, Ulrich AS, Hällbrink M, van Kuppevelt TH, Brock R. Preferential Uptake of L- versus D-Amino Acid Cell-Penetrating Peptides in a Cell Type-Dependent Manner. *Chem. Biol.* 2011; **18**: 1000-1010.

[44] Alves ID, Bechara C, Walrant A, Zaltsman Y, Jiao C-Y, Sagan S. Relationships between Membrane Binding, Affinity and Cell Internalization Efficacy of a Cell-Penetrating Peptide: Penetratin as a Case Study. *PLOS ONE* 2011; **6**: e24096.

[45] Jones S, Howl J. Enantiomer-Specific Bioactivities of Peptidomimetic Analogues of Mastoparan and Mitoparan: Characterization of Inverso Mastoparan as a Highly Efficient Cell Penetrating Peptide. *Bioconjugate Chem.* 2011; **23**: 47-56.

[46] Jones S, Holm T, Mäger I, Langel Ü, Howl J. Characterization of Bioactive Cell Penetrating Peptides from Human Cytochrome c: Protein Mimicry and the Development of a Novel Apoptogenic Agent. *Chem. Biol.* 2010; **17**: 735-744.

[47] Paramelle D, Subra G, Vezenkov LL, Maynadier M, André C, Enjalbal C, Calmès M, Garcia M, Martinez J, Amblard M. A Straightforward Approach for Cellular-Uptake Quantification. *Angew. Chem. Int. Edit.* 2010; **49**: 8240-8243.

[48] Fischer R, Waizenegger T, Köhler K, Brock R. A quantitative validation of fluorophore-labelled cell-permeable peptide conjugates: fluorophore and cargo dependence of import. *BBA-Biomembranes* 2002; **1564**: 365-374.

[49] Kalafut D, Anderson TN, Chmielewski J. Mitochondrial targeting of a cationic amphiphilic polyproline helix. *Bioorg. Med. Chem. Lett.* 2012; **22**: 561-563.

[50] Geisler IM, Chmielewski J. Dimeric Cationic Amphiphilic Polyproline Helices for Mitochondrial Targeting. *Pharm. Res.* 2011; **28**: 2797-2807.

[51] Gomez JA, Chen J, Ngo J, Hajkova D, Yeh I-J, Gama V, Miyagi M, Matsuyama S. Cell-Penetrating Penta-Peptides (CPP5s): Measurement of Cell Entry and Protein-Transduction Activity. *Pharmaceuticals* 2010; **3**: 3594-3613.

[52] Wada S-i, Tsuda H, Okada T, Urata H. Cellular uptake of Aib-containing amphipathic helix peptide. *Bioorg. Med. Chem. Lett.* 2011; **21**: 5688-5691.

[53] Palm C, Netzereab S, Hällbrink M. Quantitatively determined uptake of cell-penetrating peptides in non-mammalian cells with an evaluation of degradation and antimicrobial effects. *Peptides* 2006; **27**: 1710-1716.

[54] Neundorf I, Rennert R, Hoyer J, Schramm F, Löbner K, Kitanovic I, Wölfl S. Fusion of a Short HA2-Derived Peptide Sequence to Cell-Penetrating Peptides Improves Cytosolic Uptake, but Enhances Cytotoxic Activity. *Pharmaceuticals* 2009; **2**: 49-65.

[55] Takayama K, Nakase I, Michiue H, Takeuchi T, Tomizawa K, Matsui H, Futaki S. Enhanced intracellular delivery using arginine-rich peptides by the addition of penetration accelerating sequences (Pas). *J. Control. Release* 2009; **138**: 128-133.

[56] Nakase I, Hirose H, Tanaka G, Tadokoro A, Kobayashi S, Takeuchi T, Futaki S. Cell-surface Accumulation of Flock House Virus-derived Peptide leads to Efficient Internalization via Macropinocytosis. *Mol. Ther.* 2009; **17**: 1868-1876.

[57] Walther C, Ott I, Gust R, Neundorf I. Specific Labeling With Potent Radiolabels Alters the Uptake of Cell-Penetrating Peptides. *Biopolymers* 2009; **92**: 445-451.

[58] Manceur A, Wu A, Audet J. Flow cytometric screening of cell-penetrating peptides for their uptake into embryonic and adult stem cells. *Anal. Biochem.* 2007; **364**: 51-59.

[59] Foged C, Franzyk H, Bahrami S, Frokjaer S, Jaroszewski JW, Nielsen HM, Olsen CA. Cellular uptake and membrane-destabilising properties of α-peptide/β-peptoid chimeras: lessons for the design of new cell-penetrating peptides. *Biochim. Biophys. Acta* 2008; **1778**: 2487-2495.

[60] Åmand HL, Fant K, Nordén B, Esbjörner EK. Stimulated endocytosis in penetratin uptake: Effect of arginine and lysine. *Bioch. Bioph. Res. Com.* 2008; **371**: 621-625.

[61] Bodor N, Tóth-Sarudy E, Holm T, Pallagi I, Vass E, Buchwald P, Langel Ü. Novel, cell-penetrating molecular transporters with flexible backbones and permanently charged side-chains. *J. Pharm. Pharmacol.* 2007; **59**: 1065-1076.

[62] Östlund P, Kilk K, Lindgren M, Hällbrink M, Jiang Y, Budihna M, Cerne K, Bavec A, Östenson C-G, Zorko M, Langel Ü. Cell-Penetrating Mimics of Agonist-Activated G-Protein Coupled Receptors. *Int. J Pept. Res. Ther.* 2005; **11**: 237-247.

[63] Aubry S, Aussedat B, Delaroche D, Jiao C-Y, Bolbach G, Lavielle S, Chassaing G, Sagan S, Burlina F. MALDI-TOF mass spectrometry: A powerful tool to study the internalization of cell-penetrating peptides. *BBA- Biomembranes* 2010; **1798**: 2182-2189.

[64] Letoha T, Gaál S, Somlai C, Venkei Z, Glavinas H, Kusz E, Duda E, Czajlik A, Peták F, Penke B. Investigation of penetratin peptides. Part 2. *In vitro* uptake of penetratin and two of its derivatives. *J. Pept. Sci.* 2005; **11**: 805-811.

[65] Takeshima K, Chikushi A, Lee K-K, Yonehara S, Matsuzaki K. Translocation of Analogues of the Antimicrobial Peptides Magainin and Buforin across Human Cell Membranes. *J. Biol. Chem.* 2003; **278**: 1310-1315.

[66] Myrberg H, Lindgren M, Langel Ü. Protein Delivery by the Cell-Penetrating Peptide YTA2. *Bioconjugate Chem.* 2007; **18**: 170-174.

[67] Martin I, Teixidó M, Giralt E. Design, Synthesis and Characterization of a New Anionic Cell-Penetrating Peptide: SAP(E). *ChemBioChem*. 2011; **12**: 896-903.

[68] Lindgren M, Gallet X, Soomets U, Hällbrink M, Bråkenhielm E, Pooga M, Brasseur R, Langel Ü. Translocation Properties of Novel Cell Penetrating Transportan and Penetratin Analogues. *Bioconjugate Chem.* 2000; **11**: 619-626.

[69] Balayssac S, Burlina F, Convert O, Bolbach G, Chassaing G, Lequin O. Comparison of Penetratin and Other Homeodomain-Derived Cell-Penetrating Peptides: Interaction in a Membrane-Mimicking Environment and Cellular Uptake Efficiency. *Biochemistry* 2006; **45**: 1408-1420.

[70] Chou PY, Fasman GD. Secondary structural prediction of proteins from their amino acid sequence. *Trends Biochem. Sci.* 1977; **2**: 128-131.

[71] Todeschini R, Consonni V. Descriptors from Molecular Geometry. In *Handbook of Chemoinformatics: From Data to Knowledge in 4 Volumes*, First edition (Ed: Gasteiger J), Wiley-VCH Verlag GmbH & Co, **2003**, pp. 1004-1033.

[72] Trabulo S, Cardoso AL, Mano M, Pedroso de Lima MC. Cell-Penetrating Peptides – Mechanisms of Cellular Uptake and Generation of Delivery Systems. *Pharmaceuticals* 2010; **3**: 961-993.

[73] Alves ID, Walrant A, Bechara C, Sagan S. Is There Anybody in There? On The Mechanism of Wall Crossing of Cell Penetrating Peptides. *Curr. Protein Pept. Sci.* 2012; **13**: 658-571.

[74] Hällbrink M, Oehlke J, Papsdorf G, Bienert M. Uptake of cell-penetrating peptides is dependent on peptide-to-cell ratio rather than on peptide concentration. *BBA-Biomembranes* 2004; **1667**: 222-228.

SUPPLEMENTARY INFORMATION

Table S1. Overview of the 186 (non-) CPPs, including their CP-response.

Peptide ID	Peptide name	Sequence	Number of AA	CP-response	Ref.[1]
1	pVEC	LLIILRRRIRKQAHAHSK	18	1.318	17, 25, 27, 53, 66
2	Tat 48-60	GRKKRRQRRRPPQ	13	0.221	17, 26, 34, 38, 66
3	APH-1 (85-98)	VFRFAYYKLLKKA	13	0.188	26
4	APH-1 (236-246)	LRSIQRSLLCK	11	0.039	26
5	Nicastrin (38-53)	RKIYIPLNKTAPCVR	15	0.345	26
6	Nicastrin (414-434)	RRPNQSQPLPPSSLQRFLRAR	21	0.016	26
7	Nicastrin (616-635)	RLPRCVRSTARLARALSPAF	20	0.031	26
8	Presenilin-1 (97-109)	VATIKSVSFYTRK	13	0.008	26
9	Presenilin-1 (305-317)	AQRRVSKNSKYNA	13	0.016	26
10	D-pVEC	lliilrrrirkqahahsk	18	0.824	7, 27, 53
11	$(KFF)_3K$	KFFKFFKFFK	10	1.837	27
12	*Transportan*	*GWTLNSAGYLLGKINLKALAALAKKIL*	*27*	*(4.357)*	*17, 28, 68*
13	TP10	AGYLLGKINLKALAALAKKIL	21	1.641	28, 30, 32, 34, 66
14	MAP	KLALKLALKALKAALKLA	18	1.716	13, 17, 29, 37, 53
15	Syn B1	RGGRLSYSRRRFSTSTGR	18	0.063	17, 39
16	Polyomavirus Vp_1	APKRKSGVSK	10	0.028	17
17	Bac1-15	RRIRPRPPRLPRPRP	15	0.035	17
18	NF-κB	VQRKRQKLMP	10	0.025	17
19	SV40-T antigen	PKKKRKV	7	0.028	17
20	$HATF_3$	ERKKRRRE	8	0.023	17
21	hCT(9-32)	LGTYTQDFNKFHTFPQTAIGVGAP	24	0.024	17
22	HIV-1 Rev (34-50)	TRQARRNRRRRWRERQR	17	1.460	17, 38, 56
23	Integrin	VTVLALGALAGVGVG	15	0.549	17
24	DPV6	GRPRESGKKRKRKRLKP	17	0.073	17
25	$S4_{13}PV$	ALWKTLLKKVLKAPKKKRKV	20	0.781	17
26	Pep-1	KETWWETWWTEWSQPKKKRKV	21	0.105	17
27	MPG	GALFLGWLGAAGSTMGAWSQPKKKRKV	27	1.065	17
28	Poly-P (SAP)	VRLPPPVLRPPPVLRPPP	18	0.027	17
29	R7	RRRRRRR	7	0.395	12, 16, 17, 36
30	R9	RRRRRRRRR	9	1.000	17, 31, 33, 41, 42, 47, 63
31	pVEC scrambled	IAARIKLRSRQHIKLRHL	18	0.101	7, 17
32	Tat 47-57	YGRKKRRQRRR	11	0.309	30, 33, 42, 58
33	Tat 48-59	GRKKRRQRRRPP	12	0.192	31, 63
34	*M918*	*MVTVLFRRLRIRRACGPPRVRV*	*22*	*(7.158)*	*32*
35	Penetratin	RQIKIWFQNRRMKWKK	16	1.000	33, 39, 44
36	R11	RRRRRRRRRRR	11	0.211	34
37	RL9	RRLLRRLRR	9	0.134	35
38	RW9	RRWWRRWRR	9	1.301	35
39	R7W	RRRRRRRW	8	1.687	36
40	VP22	NAKTRRHERRRKLAIER	17	0.161	38
41	D-Syn B1	rggrlsysrrrfststgr	18	0.089	39
42	Syn B3	RRLSYSRRRF	10	0.126	39
43	D-Syn B3	rrlsysrrrf	10	0.185	39
44	Syn B5	RGGRLAYLRRRWAVLGR	17	1.159	39
45	ARF (1-22)	MVRRFLVTLRIRRACGPPRVRV	22	1.641	40
46	ARF (1-22) scrambled	FVTRGCPRRLVARLIRVMVPRR	22	1.296	40
47	ARF (2-14)	VRRFLVTLRIRRA	13	0.950	40
48	ARF (2-14) scrambled	RVRILARFLRTRV	13	0.173	40
49	ARF (19-31)	RVRVFVVHIPRLT	13	1.382	40
50	ARF (19-31) scrambled	VIRVHFRLPVRTV	13	0.259	40
51	hLF	KCFQWQRNMRKVRGPPVSCIKR *(disulfide 2-19)*	22	0.952	41
52	MAP (II)	KALAALLKKLAKLLAALK	18	0.181	13

Peptide ID	Peptide name	Sequence	Number of AA	CP-response	Ref.[1]
53	MAP (III)	KLALKLALKALKAALK	16	0.115	13
54	MAP (VII)	KLALKLALKALQAALQLA	18	0.022	13
55	MAP (VIII)	KLALQLALQALQAALQLA	18	0.243	13
56	MAP (XI)	LKTLATALTKLAKTLTTL	18	0.177	13
57	MAP (XIII)	LKTLTETLKELTKTLTEL	18	0.052	13
58	MAP (XV)	RQIKIWFQNRRMKWKK	16	0.104	13
59	KLA 1	KLALKLALKAWKAALKLA	18	0.085	13
60	KLA 2	KLALKAALKAWKAAAKLA	18	0.008	13
61	KLA 11	KITLKLAIKAWKLALKAA	18	0.025	13
62	KLA 5	KIAAKSIAKIWKSILKIA	18	0.036	13
63	KLA 12	KALAKALAKLWKALAKAA	18	0.079	13
64	KLA 13	KLALKLALKWAKLALKAA	18	0.008	13
65	KLA 14	KLLAKAAKKWLLLALKAA	18	0.015	13
66	KLA 9	KLLAKAALKWLLKALKAA	18	0.023	13
67	KLA 10	KALKKLLAKWLAAAKALL	18	0.115	13
68	KLA 15	KLAAALLKKWKKLAAALL	18	0.120	13
69	KLA 8	KALAALLKKWAKLLAALK	18	0.181	13
70	TP10-1	AGYLLGPINLKALAALAKKIL	21	1.223	11
71	TP10-2	AGYLLGKINLKPLAALAKKIL	21	0.749	11
72	TP10-3	AAYLLAKINLKALAALAKKIL	21	1.243	11
73	TP10-4	AGYLLGKINLRALAALARRIL	21	1.263	11
74	TP10-5	AGYLLGKINLKKLAKL(Aib)KKIL[2]	21	2.141	11
75	D-R9	rrrrrrrrr	9	1.389	12, 43
76	MP	INLKALAALAKKIL	14	0.570	45
77	*iMP*	*inlkalaalakkil*	*14*	*(3.602)*	*45*
78	rMP	LIKKALAALAKLNI	14	0.352	45
79	riMP	likkalaalaklni	14	0.288	45
80	MitP	INLKKLAKL(Aib)KKIL[2]	14	2.712	45, 46
81	iMitP	inlkklakl(Aib)kkil	14	2.272	45
82	rMitP	LIKK(Aib)LKALKKLNI	14	0.531	45
83	riMitP	likk(Aib)lkalkklni[2]	14	0.837	45
84	Cyt c^{77-101}	GTKMIFVGIKKKEERADLIAYLKKA	25	0.179	46
85	Cyt c^{86-101}	KKKEERADLIAYLKKA	16	0.006	46
86	Cyt c^{79-92}	KMIFVGIKKKEERA	14	0.013	46
87	Cyt c^{79-88}	KMIFVGIKKK	10	0.006	46
88	Cyt c^{4-13}	EKGKKIFIMK	10	0.013	46
89	Cyt c^{5-13}	KGKKIFIMK	9	0.069	46
90	MTS	AAVALLPAVLLALLAP	16	0.315	48
91	*P14LRR*	*see fig. 1 reference 49*	-	*(7.958)*	*49*
92	P11LRR	see fig. 1 reference 49	-	1.623	49, 50
93	*(P10LRR-Gly)$_2$-C5*	*see fig. 2 reference 50*	-	*(84.034)*	*50*
94	*(P10LRR-β-Ala)$_2$-C5*	*see fig. 2 reference 50*	-	*(66.648)*	*50*
95	*(P10LRR-ABUA)$_2$-C5*	*see fig. 2 reference 50*	-	*(73.892)*	*50*
96	VPTLK	VPTLK	5	0.002	51
97	*MAP(Aib)*	*KL(Aib)LKL(Aib)LK(Aib)LKA(Aib)LKL(Aib)[2]*	*18*	*(125.240)*	*52*
98	sC18	GLRKRLRKFRNKIKEK	16	0.166	54
99	hCT(18-32)-k7	KFHTFPQTAIGVGAP KKRKAPKKKRKFA↵	28	0.183	54, 57
100	N-E5L-hCT(18-32)-k7	*GLLEALAELLE*KFHTFPQTAIGVGAP KKRKAPKKKRKFA↵	39	0.364	54
101	N-E5L-sC18	GLLEALAELLEGLRKRLRKFRNKIKEK	27	0.150	54
102	N-E5L-Tat 48-60	GLLEALAELLEGRKKRRQRRRPPQ	24	0.507	54
103	*FHV coat (35-49)*	*RRRRNRTRRNRRRVR*	*15*	*(4.127)*	*56*
104	*PasTat*	*FFLIPKGGRKKRRQRRRPPQ*	*20*	*(4.426)*	*55*
105	BMV Gag (7-25)	KMTRAQRRAAARRNRWTAR	19	0.288	56
106	HTLV-II Rex (4-16)	TRRQRTRRARRNR	13	0.288	56
107	Human cJun (252-279)	RIKAERKRMRNRIAASKSRKRKLERIAR	28	2.744	56
108	Human cFos (139-164)	KRRIRRERNKMAAAKSRNRRRELTDT	26	0.199	56
109	K-FGF (Kaposi fibroblast growth factor)	AAVLLPVLLAAP	12	0.200	58
110	PreS2-TLM (PreS2-derived translocatory motif)	PLSSIFSRIGDP	12	0.224	58

Peptide ID	Peptide name	Sequence	Number of AA	CP-response	Ref.[1]
111	PTD4 (Protein transduction domain 4)	PIRRRKKLRRLK	12	0.658	58
112	α-peptide/β-peptoid chimera 2	see fig. 1 reference 59	-	0.185	59
113	α-peptide/β-peptoid chimera 6	see fig. 1 reference 59	-	2.040	59
114	α-peptide/β-peptoid chimera 8	see fig. 1 reference 59	-	2.102	59
115	$hArg_8$ ($Homoarginine_8$)	see fig. 1 reference 59	-	0.464	59
116	PenArg	RQIRIWFQNRRMRWRR	16	1.810	60
117	PenLys	KQIKIWFQNKKMKWKK	16	0.041	60
118	aca-[$Lys(Nys^+)$-aca]$_4$-$Lys(Nys^+)$	aca-[$Lys(Nys^+)$-aca]$_4$-$Lys(Nys^+)^3$	-	0.001	61
119	aca-[$Lys(Nys^+)$-aca]$_6$-$Lys(Nys^+)$	aca-[$Lys(Nys_+)$-aca]$_6$-$Lys(Nys^+)^3$	-	0.005	61
120	M511	FLGKKFKKYFLQLLK	15	0.599	62
121	M551	KGKFQLYLKLKFKFL	15	0.240	62
122	G53-1	IVIAKLKANLMCKTCRLAK	19	0.150	62
123	G53-2	AIGVNYLVKFIKVIAIVIAKLKA	23	0.839	62
124	*Kno ref. 63 (Knotted-1 homeodomain third helix)*	*KQIKINNWFINQRKRHWK*	*18*	*(7.358)*	*63*
125	R6/W3	RRWWRRWRR	9	0.910	63
126	$Phe^{6,14}$-penetratin	RQIKIFFQNRRMKFKK	16	0.727	64
127	Dodeca-penetratin	RQIKIWFRKWKK	12	1.154	64
128	MG2d (Magainin 2 analogue)	GIGKFLHSAKKWGKAFVGQIMNC	23	0.798	65
129	BF2d (Buforin 2 analogue)	TRSSRAGLQWPVGRVHRLLRKGGC	24	0.953	65
130	YTA2	YTAIAWVKAFIRKLRK	16	1.545	66
131	K9	KKKKKKKKK	9	0.119	12
132	H9	HHHHHHHHH	9	0.068	12
133	O9	OOOOOOOOO	9	0.068	12
134	R8	RRRRRRRR	8	0.639	12, 16
135	R6	RRRRRR	6	0.194	12, 16
136	R5	RRRRR	5	0.077	12, 16
137	R4	RRRR	4	0.074	12
138	R3	RRR	3	0.055	12
139	D-R8	rrrrrrrr	8	1.577	12
140	D-R7	rrrrrrr	7	1.071	12
141	D-R6	rrrrrr	6	0.323	12
142	D-R5	rrrrr	5	0.115	12
143	D-R4	rrrr	4	0.098	12
144	R15	RRRRRRRRRRRRRRR	15	1.345	12
145	R20	RRRRRRRRRRRRRRRRRRRR	20	0.764	12
146	R25	RRRRRRRRRRRRRRRRRRRRRRRRR	25	0.400	12
147	R30	RRRRRRRRRRRRRRRRRRRRRRRRRRRRRR	30	0.109	12
148	[Ala_1]pVEC	ALIILRRRIRKQAHAHSK	18	0.304	7
149	[Ala_2]pVEC	LAIILRRRIRKQAHAHSK	18	0.507	7
150	[Ala_3]pVEC	LLAILRRRIRKQAHAHSK	18	0.406	7
151	[Ala_4]pVEC	LLIALRRRIRKQAHAHSK	18	0.659	7
152	[Ala_5]pVEC	LLIIARRRIRKQAHAHSK	18	0.456	7
153	[Ala_6]pVEC	LLIILARRIRKQAHAHSK	18	2.433	7
154	[Ala_7]pVEC	LLIILRARIRKQAHAHSK	18	1.115	7
155	[Ala_8]pVEC	LLIILRRAIRKQAHAHSK	18	2.129	7
156	[Ala_9]pVEC	LLIILRRRARKQAHAHSK	18	0.760	7
157	[Ala_{10}]pVEC	LLIILRRRIAKQAHAHSK	18	1.470	7
158	[Ala_{11}]pVEC	LLIILRRRIRAQAHAHSK	18	1.774	7
159	[Ala_{12}]pVEC	LLIILRRRIRKAAHAHSK	18	1.420	7
160	[D-Ala_{13}]pVEC	LLIILRRRIRKQaHAHSK	18	1.825	7
161	[Ala_{14}]pVEC	LLIILRRRIRKQAAAHSK	18	0.558	7
162	[D-Ala_{15}]pVEC	LLIILRRRIRKQAHaHSK	18	1.115	7
163	[Ala_{16}]pVEC	LLIILRRRIRKQAHAASK	18	1.521	7
164	[Ala_{17}]pVEC	LLIILRRRIRKQAHAHAK	18	2.129	7
165	[Ala_{18}]pVEC	LLIILRRRIRKQAHAHSA	18	2.079	7
166	retro-pVEC	KSHAHAQKRIRRRLIILL	18	0.406	7
167	Ap1	AQIKIWFQNRRMKWKK	16	0.289	9

Peptide ID	Peptide name	Sequence	Number of AA	CP-response	Ref.[1]
168	Ap2	RAIKIWFQNRRMKWKK	16	1.333	9
169	Ap3	RQAKIWFQNRRMKWKK	16	0.111	9
170	Ap4	RQIAIWFQNRRMKWKK	16	0.511	9
171	Ap5	RQIKAWFQNRRMKWKK	16	0.244	9
172	Ap6	RQIKIAFQNRRMKWKK	16	0.222	9
173	Ap7	RQIKIWAQNRRMKWKK	16	0.089	9
174	Ap8	RQIKIWFANRRMKWKK	16	0.778	9
175	Ap9	RQIKIWFQARRMKWKK	16	0.978	9
176	Ap10	RQIKIWFQNARMKWKK	16	0.400	9
177	Ap11	RQIKIWFQNRAMKWKK	16	0.242	9
178	Ap12	RQIKIWFQNRRAKWKK	16	0.644	9
179	Ap13	RQIKIWFQNRRMAWKK	16	0.378	9
180	Ap14	RQIKIWFQNRRMKAKK	16	0.356	9
181	Ap15	RQIKIWFQNRRMKWAK	16	0.411	9
182	Ap16	RQIKIWFQNRRMKWKA	16	0.444	9
183	SAP (E)	VELPPPVELPPPVELPPP	18	0.007	67
184	Eng (Engrailed-2 homeodomain third helix)	SQIKIWFQNKRAKIKK	16	1.235	69
185	Hox (HoxA-13 homeodomain third helix)	RQVTIWFQNRRVKEKK	16	0.500	69
186	*Kno ref. 69 (Knotted-1 homeodomain third helix)*	*KQINNWFINQRKRHWK*	*16*	*(11.118)*	*69*

Peptides whose unified response is an (extreme) outlier are indicated in italic. Their CP-responses were not considered during data evaluation.

[1]References are listed in the reference list of this chapter.

[2]Aib = alpha amino-isobutyric acid.

[3]Aca = $NH_2(CH_2)_5CO$-; Lys(Nys^+) = Redox amino acid = Lys with 1,4-dihydrotriognelline side chain.

Table S2. List of CPPs of which CP-response is an outlier.

Peptide ID	Peptide Name	Reference	Details
12	Transportan	17	In reference 17, transportan showed higher cell-specificity for HeLa cells, resulting in a higher response for cellular influx in comparison with other results for transportan.
34	M918	32	In the quantitative uptake assay, M918 showed a 7 times higher influx than penetratin.
91	P14LRR	49	P14LRR showed an about 20 times higher uptake than Tat 47-57, the positive control.
93	$(P10LRR\text{-}Gly)_2$-C5	50	The dimeric cationic amphiphilic polyproline helices showed an about 200 times higher uptake responses than the positive control Tat 47-57.
94	$(P10LRR\text{-}\beta\text{-}Ala)_2$-C5	50	
95	$(P10LRR\text{-}ABUA)_2$-C5	50	
97	MAP(Aib)	52	The internal positive control MAP showed a much lower influx response in the tested A549 cells (*cfr*. cell-specificity).
103	FHV Coat (35-49)	56	FHV coat (35-49) showed a 21 times higher cellular uptake than the positive control Tat 48-60.
104	PasTat	55	PasTat has a 20 times higher uptake than the positive control Tat.
124	Kno *(ref 63)*	63	Kno has a 7 times higher uptake than the positive control penetratin.
186	Kno *(ref 69)*	69	Kno has a 10 times higher uptake than the positive control penetratin.

Table S3. Classification of (non-) CPPs based on chemical class, literature data and their uptake mechanisms.

Peptide ID	Peptide name	Chemical class[1]	CP-response	Ref.[2]	Literature evaluation[3]	Comment	Uptake mechanism[4]	Comment
1	pVEC	AC	1.318	17	High CPP	-	2	Unspecified
				25	CPP	≥ penetratin	1 and 2	Unsure
				27	CPP	> $(KFF)_3K$ and penetratin	Not available	-
				53	CPP	≥ MAP, > penetratin	Not available	-
				66	CPP	= YTA2, > Tat 48-60, TP10, penetratin	1 and 2	Unspecified
2	Tat 48-60	C	0.221	17	Medium CPP	-	2	Unspecified
				26	CPP	< penetratin, APH (85-98), nicastrin (38-53)	2a	-
				34	CPP	= TP10 < penetratin < R11	2b	-
				38	CPP	> VP22, < HIV Rev (34-50) and penetratin	2a	-
				66	CPP	= TP10, > Tat 48-60, < pVEC and YTA2	1 and 2	Unspecified
3	APH-1 (85-98)	AU (AC)	0.188	26	CPP	> Tat 48-60, < penetratin and nicastrin (38-53)	2a	-
4	APH-1 (236-246)	AU (AC)	0.039	26	No CPP	-	Not applicable	-
5	Nicastrin (38-53)	AU (AC)	0.345	26	CPP	> Tat 48-60, < penetratin and APH (85-98)	2a	-
6	Nicastrin (414-434)	AU (C)	0.016	26	No CPP	-	Not applicable	-
7	Nicastrin (616-635)	AU (AC)	0.031	26	No CPP	-	Not applicable	-
8	Presenilin-1 (97-109)	AU (AC)	0.008	26	No CPP	-	Not applicable	-
9	Presenilin-1 (305-317)	AU (AC)	0.016	26	No CPP	-	Not applicable	-
10	D-pVEC	AC	0.824	7	CPP	≈ pVEC	2b > 2a	-
				27	CPP	≥ pVEC	Not available	-
				53	CPP	≥ pVEC	Not available	-
11	$(KFF)_3K$	AU (AC)	1.837	27	CPP	Less efficient than pVEC because of degradation	Not available	-
12	*Transportan*	*AC*	*(4.357)*	*17*	*High CPP*	-	*2*	*Unspecified*
				28	*CPP*	*> TP10*	*Not available*	-
				68	*CPP*	-	*1*	*Unspecified*
13	TP10	AC	1.641	28	CPP	< transportan	Not available	-
				30	CPP	> penetratin >> Tat 47-57	Not available	-
				32	CPP	< M918	2a and 2b	-
				34	CPP	= Tat 48-60, < penetratin < R11	Not available	-
				66	CPP	= penetratin, > Tat 48-60, < pVEC and YTA2	1 and 2	*Unspecified*
14	MAP	AC	1.716	13	CPP	-	1 and 2	-
				17	High CPP	-	2	*Unspecified*
				29	CPP	-	1 and 2	Unspecified
				37	CPP	-	1 and 2	Unsure
				53	CPP	≥ pVEC, > penetratin	Not available	-
15	Syn B1	AC	0.063	17	Medium CPP	-	2	Unspecified
				39	CPP	-	2c	-
16	Polyomavirus Vp_1	AU (C)	0.028	17	Low CPP	Nearly unmeasurable uptake	2	Unspecified
17	Bac1-15	AU (C)	0.035	17	Medium CPP	-	2	Unspecified
18	NF-κB	C	0.025	17	Low CPP	Nearly unmeasurable uptake	2	Unspecified
19	SV40-T antigen	C	0.028	17	Low CPP	Nearly unmeasurable uptake	2	Unspecified
20	$HATF_3$	C	0.023	17	Low CPP	Nearly unmeasurable uptake	2	Unspecified
21	hCT(9-32)	A	0.024	17	Low CPP	Nearly unmeasurable uptake	2	Unspecified
22	HIV-1 Rev (34-50)	C	1.460	17	High CPP	-	2	Unspecified
				38	CPP	> penetratin > Tat 48-60 > VP22	2a	-
				56	CPP	-	Not available	-
23	Integrin	H	0.549	17	Medium CPP	-	2	Unspecified
24	DPV6	C	0.073	17	Medium CPP	-	2	Unspecified
25	$S4_{13}PV$	AC	0.781	17	High CPP	-	2	Unspecified

Peptide ID	Peptide name	Chemical class[1]	CP-response	Ref.[2]	Literature evaluation[3]	Comment	Uptake mechanism[4]	Comment
26	Pep-1	AC	0.105	17	Medium CPP	-	2	Unspecified
27	MPG	AC	1.065	17	Medium CPP	-	2	Unspecified
28	Poly-P (SAP)	AC	0.027	17	Low CPP	Nearly unmeasurable uptake	2	Unspecified
29	R7	C	0.395	12	CPP	> R6, < R8-9	3	-
				16	CPP	> R6, < R8-9	Not available	-
				17	High CPP	-	2	Unspecified
				36	CPP	< R7W	1 and 2	Unspecified, 2 = dominant mechanism
30	R9	C	1.000	17	High CPP	-	2	Unspecified
				31	CPP	-	Not available	-
				33	CPP	-	2	Unspecified
				35	High CPP	One of the most efficient known CPPs	1 and 2	Unspecified
				41	High CPP	Rapid	1e and 2	Unspecified
				42	CPP	-	1e, 2a and 2b	-
				43	CPP	-	1 < 2	Unspecified
				47	CPP	-	Not available	-
				63	CPP	-	Not available	-
31	pVEC scrambled	AU	0.101	7	Low CPP	<< pVEC , not efficient	2b > 2a	-
				17	Medium CPP	-	2	Unspecified
32	Tat 47-57	C	0.309	30	CPP	<< penetratin < TP10	1 and 2	Unspecified
				33	CPP	-	2	Unspecified
				42	CPP	-	1e, 2a and 2b	-
				58	CPP	> K-FGF and PreS2-TLM	Not available	-
33	Tat 48-59	C	0.192	31	CPP	< penetratin < R9	Not available	-
				63	CPP	-	Not available	-
34	*M918*	*AC*	*(7.158)*	*32*	*High CPP*	*Excellent novel CPP, > penetratin and TP10*	*2a*	-
35	Penetratin	C	1.000	17	High CPP	-	2	Unspecified
				29	CPP	-	2	Unspecified
				32	CPP	-	2a and 2b	-
				33	CPP	-	2	Unspecified
				39	CPP	-	2c	-
				42	CPP	-	1e, 2a and 2b	-
				44	CPP	-	1 and 2	Unspecified
				60	CPP	-	2a	-
				64	CPP	-	2b	-
36	R11	C	0.211	34	CPP	> penetratin > Tat 48-60, TP10	Not available	-
37	RL9	AC	0.134	35	Low CPP	Poor	1 and 2	Unspecified
38	RW9	AC	1.301	35	High CPP	One of the most efficient known CPPs	1 and 2	Unspecified
39	R7W	C	1.687	36	CPP	Efficient	1 and 2	Unspecified, 2 = dominant
40	VP22	AU (C)	0.161	38	CPP	< Tat 48-60 < penetratin < HIV Rev (34-50)	2a	-
41	D-Syn B1	AC	0.089	39	CPP	-	2c	-
42	Syn B3	AU (C)	0.126	39	CPP	-	2c	-
43	D-Syn B3	AU (C)	0.185	39	CPP	-	2c	-
44	Syn B5	AU (AC)	1.159	39	CPP	-	2c	-
45	ARF (1-22)	AC	1.641	40	High CPP	≈ TP10	2b	-
46	ARF (1-22) scrambled	AU	1.296	40	High CPP	≈ TP10	2b	-
47	ARF (2-14)	AC	0.950	40	High CPP	≈ TP10	Not available	-
48	ARF (2-14) scrambled	AU	0.173	40	Low CPP	-	Not available	-
49	ARF (19-31)	AC	1.382	40	High CPP	≈ TP10	Not available	-
50	ARF (19-31) scrambled	AU	0.259	40	Low CPP	-	Not available	-
51	hLF	AC	0.952	41	High CPP	Rapid	1e and 2	2 unspecified
52	MAP (II)	AC	0.181	13	CPP	-	1 and 2	Unspecified
53	MAP (III)	AC	0.115	13	CPP	≈ MAP	1 and 2	Unspecified
54	MAP (VII)	AC	0.022	13	Low CPP	Slow	1 and 2	Unspecified
55	MAP (VIII)	A	0.243	13	CPP	> MAP	1 and 2	Unspecified
56	MAP (XI)	AC	0.177	13	CPP	≈ MAP	1 and 2	Unspecified
57	MAP (XIII)	A	0.052	13	CPP	≈ MAP	1 and 2	Unspecified
58	MAP (XV)	AC	0.104	13	CPP	≈ MAP	1 and 2	Unspecified
59	KLA 1	AC	0.085	13	CPP	-	1 and 2	Unspecified
60	KLA 2	AC	0.008	13	Low CPP	Slow	1 and 2	Unspecified
61	KLA 11	AC	0.025	13	Low CPP	Slow	1 and 2	Unspecified
62	KLA 5	AC	0.036	13	Low CPP	Slow	1 and 2	Unspecified

Peptide ID	Peptide name	Chemical class[1]	CP-response	Ref.[2]	Literature evaluation[3]	Comment	Uptake mechanism[4]	Comment
63	KLA 12	AC	0.079	13	CPP	-	1 and 2	Unspecified
64	KLA 13	AC	0.008	13	Low CPP	Slow	1 and 2	Unspecified
65	KLA 14	AC	0.015	13	Low CPP	Slow	1 and 2	Unspecified
66	KLA 9	AC	0.023	13	Low CPP	Slow	1 and 2	Unspecified
67	KLA 10	AC	0.115	13	CPP	-	1 and 2	Unspecified
68	KLA 15	AC	0.120	13	CPP	-	1 and 2	Unspecified
69	KLA 8	AC	0.181	13	CPP	-	1 and 2	Unspecified
70	TP10-1	AC	1.223	11	CPP	< TP10	1d	-
71	TP10-2	AC	0.749	11	CPP	< TP10	1d	-
72	TP10-3	AC	1.243	11	CPP	< TP10	1d	-
73	TP10-4	AC	1.263	11	CPP	< TP10	1d	-
74	TP10-5	AC	2.141	11	CPP	> TP10	1d	-
75	D-R9	C	1.389	12	CPP	Effective, (> (D-)R6-8)	3	-
				43	CPP	< R9	1 > 2	Unspecified
76	MP	AC	0.570	45	Low CPP	Low efficient	1	Unspecified
77	*iMP*	*AC*	*(3.602)*	*45*	*High CPP*	*Highly efficient, (> MitP, penetratin)*	*1*	*Unspecified*
78	rMP	AC	0.352	45	Low CPP	Low efficient	Not applicable	-
79	riMP	AC	0.288	45	Low CPP	Low efficient	Not applicable	-
80	MitP	AC	2.712	45	Medium CPP	Efficient	1	Unspecified
				46	CPP	-	Not available	-
81	iMitP	AC	2.272	45	CPP	Strong propensity for cell penetration	Not available	-
82	rMitP	AC	0.531	45	Low CPP	Low efficient	Not available	-
83	riMitP	AC	0.837	45	Low CPP	Low efficient	Not available	-
84	Cyt c^{77-101}	AU (C)	0.179	46	High CPP	Extremely/very efficient	Not available	-
85	Cyt c^{86-101}	AU (C)	0.006	46	CPP	-	Not available	-
86	Cyt c^{79-92}	AU (C)	0.013	46	Not available	-	Not available	-
87	Cyt c^{79-88}	AU (C)	0.006	46	Not available	-	Not available	-
88	Cyt c^{4-13}	AU (C)	0.013	46	Not available	-	Not available	-
89	Cyt c^{5-13}	AU (C)	0.069	46	Not available	-	Not available	-
90	MTS	H	0.315	48	CPP	-	Not available	-
91	*P14LRR*	*AC*	*(7.958)*	*49*	*High CPP*	*Highly efficient class of CPPs*	*1*	*Unspecified*
92	P11LRR	AC	1.623	49	High CPP	Highly efficient class of CPPs	1 and 2	Unspecified
				50	CPP	-	1 and 2	Unspecified
93	*(P10LRR-Gly)$_2$-C5*	*AC*	*(84.034)*	*50*	*CPP*	*Uptake far superior to P11LRR and Tat 47-57*	*1 and 2*	*Unspecified*
94	*(P10LRR-β-Ala)$_2$-C5*	*AC*	*(66.648)*	*50*	*CPP*	*Uptake far superior to P11LRR and Tat 47-57*	*1 and 2*	*Unspecified*
95	*(P10LRR-ABUA)$_2$-C5*	*AC*	*(73.892)*	*50*	*CPP*	*Uptake far superior to P11LRR and Tat 47-57*	*1 and 2*	*Unspecified*
96	VPTLK	CH	0.002	51	CPP	-	Unknown	-
97	*MAP(Aib)*	*AC*	*(125.240)*	*52*	*High CPP*	-	*Not available*	-
98	sC18	AC	0.166	54	High CPP	Highly efficient	1 and 2	Unspecified
99	hCT(18-32)-k7	AU	0.183	54	CPP	-	2	Unspecified
				57	Medium CPP	Effective	Not available	-
100	N-E5L-hCT(18-32)-k7	AU	0.364	54	CPP	Faster and efficienter than hCT(18-32)-k7	Unclear	-
101	N-E5L-sC18	AC	0.150	54	CPP	Faster and efficienter than sC18	Unclear	-
102	N-E5L-Tat 48-60	AU (C)	0.507	54	CPP	Faster and efficienter than Tat 48-60	Unclear	-
103	*FHV coat (35-49)*	*C*	*(4.127)*	*56*	*High CPP*	*High efficient CPP and superior cellular uptake > Tat 48-60*	*2a*	-
104	*PasTat*	*C*	*(4.426)*	*55*	*CPP*	-	*Not available*	-
105	BMV Gag (7-25)	C	0.288	56	CPP	-	Not available	-
106	HTLV-II Rex (4-16)	C	0.288	56	CPP	-	Not available	-
107	Human cJun (252-279)	C	2.744	56	CPP	-	Not available	-
108	Human cFos (139-164)	C	0.199	56	CPP	-	Not available	-
109	K-FGF (Kaposi fibroblast growth factor)	H	0.200	58	CPP	< arginine-rich peptides: Tat 47-57, penetratin and PTD4	Not available	-
110	PreS2-TLM (PreS2-derived translocatory motif)	A	0.224	58	CPP	< arginine-rich peptides: Tat 47-57, penetratin and PTD4	Not available	-

Peptide ID	Peptide name	Chemical class[1]	CP-response	Ref.[2]	Literature evaluation[3]	Comment	Uptake mechanism[4]	Comment
111	PTD4 (Protein transduction domain 4)	C	0.658	58	CPP	> peptides: K-FGF and PreS2-TLM	Not available	-
112	α-peptide/β-peptoid chimera 2	AU	0.185	59	Medium CPP	Possesses efficient cellular uptake properties superior to well-described CPPs, ≈ Tat 47-57	1 and 2	Unspecified
113	α-peptide/β-peptoid chimera 6	AU	2.040	59	High CPP	Possesses efficient cellular uptake properties superior to well-described CPPs, > Tat 47-57	1 and 2	Unspecified
114	α-peptide/β-peptoid chimera 8	AU	2.102	59	High CPP	Possesses efficient cellular uptake properties superior to well-described CPPs, > Tat 47-57	1 and 2	Unspecified
115	$hArg_8$ ($Homoarginine_8$)	C	0.464	59	Medium CPP	Possesses efficient cellular uptake properties superior to well-described CPPs, ≈ Tat 47-57	1 and 2	Unspecified
116	PenArg	C	1.810	60	CPP	> penetratin > PenLys	2a	-
117	PenLys	C	0.041	60	CPP	< penetratin < PenArg	2a	-
118	aca-[Lys(Nys^+)-aca]$_4$-Lys(Nys^+)	AU	0.001	61	No CPP	-	Not applicable	-
119	aca-[Lys(Nys^+)-aca]$_6$-Lys(Nys^+)	AU	0.005	61	Low CPP	-	Not available	-
120	M511	AU (AC)	0.599	62	CPP	-	Not available	-
121	M551	AU (C)	0.240	62	CPP	-	Not available	-
122	G53-1	AU (AC)	0.150	62	Low CPP	-	Not available	-
123	G53-2	AU (AC)	0.839	62	CPP	-	Not available	-
124	*Kno ref. 61 (Knotted-1 homeodomain third helix)*	*C*	*(7.358)*	*63*	*CPP*	-	*Not available*	-
125	R6/W3	AC	0.910	63	CPP	-	Not available	-
126	$Phe^{6.14}$-penetratin	AU (C)	0.727	64	CPP	< penetratin	2b	-
127	Dodeca-penetratin	AU (AC)	1.154	64	CPP	≈ penetratin	2b	-
128	MG2d (Magainin 2 analogue)	AC	0.798	65	CPP	-	1b	-
129	BF2d (Buforin 2 analogue)	AC	0.953	65	CPP	-	Not available	-
130	YTA2	AC	1.545	66	CPP	= pVEC, > Tat 48-60, TP10, penetratin	1 and 2	Unspecified
131	K9	C	0.119	12	Low CPP	Not effective	Not available	-
132	H9	C	0.068	12	Low CPP	Not effective	Not available	-
133	O9	C	0.068	12	Low CPP	Not effective	Not available	-
134	R8	C	0.639	12	Medium CPP	Effective CPP (> R6-7, < R9)	3	-
				16	CPP	> R6-7, < R9	Not available	-
135	R6	C	0.194	12	Medium CPP	Effective CPP, < R7-9	3	-
				16	CPP	< R7-9	Not available	-
136	R5	C	0.077	12	Low CPP	Not effective CPP	Not available	-
				16	No CPP	-	Not applicable	-
137	R4	C	0.074	12	Low CPP	Not effective CPP	Not available	-
138	R3	C	0.055	12	Low CPP	Not effective CPP	Not available	-
139	D-R8	C	1.577	12	Medium CPP	Effective CPP, > (D-)R6-7, < (D-) R9	3	-
140	D-R7	C	1.071	12	Medium CPP	Effective CPP, > (D-)R6, < (D-) R8-9	3	-
141	D-R6	C	0.323	12	Medium CPP	Effective CPP, < (D-)R7-9	3	-
142	D-R5	C	0.115	12	Low CPP	Not effective CPP	Not available	-
143	D-R4	C	0.098	12	Low CPP	Not effective CPP	Not available	-
144	R15	C	1.345	12	Medium CPP	Effective CPP, > R6-9, but toxic	3	-
145	R20	C	0.764	12	Medium CPP	Effective CPP, < R9, R15, but toxic	3	-
146	R25	C	0.400	12	Low CPP	Not effective CPP, < R7, R9, R15, but toxic	Not available	-
147	R30	C	0.109	12	Low CPP	Not effective CPP	Not available	-
148	[Ala_1]pVEC	AC	0.304	7	CPP	Significant < pVEC	2b > 2a	-

Peptide ID	Peptide name	Chemical class[1]	CP-response	Ref.[2]	Literature evaluation[3]	Comment	Uptake mechanism[4]	Comment
149	[Ala_2]pVEC	AC	0.507	7	CPP	Significant < pVEC	2b > 2a	-
150	[Ala_3]pVEC	AC	0.406	7	CPP	Significant < pVEC	2b > 2a	-
151	[Ala_4]pVEC	AC	0.659	7	CPP	Significant < pVEC	2b > 2a	-
152	[Ala_5]pVEC	AC	0.456	7	CPP	Significant < pVEC	2b > 2a	-
153	[Ala_6]pVEC	AC	2.433	7	CPP	Significant > pVEC	2b > 2a	-
154	[Ala_7]pVEC	AC	1.115	7	CPP	≈ pVEC	2b > 2a	-
155	[Ala_8]pVEC	AC	2.129	7	CPP	Significant > pVEC	2b > 2a	-
156	[Ala_9]pVEC	AC	0.760	7	CPP	Significant > pVEC	2b > 2a	-
157	[Ala_{10}]pVEC	AC	1.470	7	CPP	≈ pVEC	2b > 2a	-
158	[Ala_{11}]pVEC	AC	1.774	7	CPP	≈ pVEC	2b > 2a	-
159	[Ala_{12}]pVEC	AC	1.420	7	CPP	≈ pVEC	2b > 2a	-
160	[D-Ala_{13}]pVEC	AC	1.825	7	CPP	≈ pVEC	2b > 2a	-
161	[Ala_{14}]pVEC	AC	0.558	7	CPP	Significant > pVEC	2b > 2a	-
162	[D-Ala_{15}]pVEC	AC	1.115	7	CPP	≈ pVEC	2b > 2a	-
163	[Ala_{16}]pVEC	AC	1.521	7	CPP	≈ pVEC	2b > 2a	-
164	[Ala_{17}]pVEC	AC	2.129	7	CPP	Significant > pVEC	2b > 2a	-
165	[Ala_{18}]pVEC	AC	2.079	7	CPP	≈ pVEC	2b > 2a	-
166	retro-pVEC	AC	0.406	7	CPP	Significant > pVEC	2b > 2a	-
167	Ap1	C	0.289	9	Low CPP	< penetratin	Unclear	-
168	Ap2	C	1.333	9	CPP	> penetratin	Unclear	-
169	Ap3	C	0.111	9	Low CPP	< penetratin	Unclear	-
170	Ap4	C	0.511	9	Low CPP	< penetratin	Unclear	-
171	Ap5	C	0.244	9	Low CPP	< penetratin	Unclear	-
172	Ap6	C	0.222	9	Low CPP	< penetratin	Unclear	-
173	Ap7	C	0.089	9	Low CPP	< penetratin	Unclear	-
174	Ap8	C	0.778	9	CPP	≈ penetratin	Unclear	-
175	Ap9	C	0.978	9	CPP	≈ penetratin	Unclear	-
176	Ap10	AC	0.400	9	Low CPP	< penetratin	Unclear	-
177	Ap11	C	0.242	9	Low CPP	< penetratin	Unclear	-
178	Ap12	C	0.644	9	CPP	< penetratin	Unclear	-
179	Ap13	C	0.378	9	Low CPP	< penetratin	Unclear	-
180	Ap14	C	0.356	9	Low CPP	< penetratin	Unclear	-
181	Ap15	C	0.411	9	Low CPP	< penetratin	Unclear	-
182	Ap16	C	0.444	9	Low CPP	< penetratin	Unclear	-
183	SAP (E)	A	0.007	67	Low CPP	Not highly efficient	2b	-
184	Eng (Engrailed-2 homeodomain third helix)	C	1.235	69	CPP	-	Not available	-
185	Hox (HoxA-13 homeodomain third helix)	C	0.500	69	CPP	-	Not available	-
186	*Kno ref. 67 (Knotted-1 homeodomain third helix)*	*C*	*(11.118)*	*69*	*High CPP*	*High uptake efficiency*	*Not available*	-

Peptides whose unified response is an (extreme) outlier are indicated in italic. Their CP-responses were not considered during data evaluation.

[1]Chemical classes of CPPs: A = amphipathic, C = cationic, H = hydrophobic, AC = intersection amphipathic-cationic, CH = intersection cationic-hydrophobic and AU = author unclassified. If AU, the recommended chemical class, according to ref. 6, is indicated between brackets.

[2]References are listed in the reference list of this chapter.

[3]Literature evaluation = how the authors of the study estimated the cellular influx capacity of the investigated peptides: no, low, medium or high CPP. CPP alone means not specified by the authors.

[4]1 = direct penetration with 1a = inverted micelles, 1b = pore formation, 1c = carpet like model, 1d = membrane thinning and 1e = uptake through nucleation zones; 2 = endocytosis with 2a = macropinocytosis, 2b = endocytosis dependent on coat proteins (clathrin, caveolae or lipid raft mediated) and 2c = endocytosis independent on coat proteins; 3 = energy-dependent mechanism, but not endocytosis (not further specified by authors) [according to ref. 2,12,72,73].

Table S4. Summary of the PCA analysis of the descriptors divided by the molecular weight, describing the eigenvalues of the covariance matrix, the total variance explained (cumulative R^2) and the predictive ability (cumulative Q^2).

Principal Component	Eigenvalue	Cumulative R^2	Cumulative Q^2
1	73.7	0.396	0.371
2	41.8	0.621	0.596
3	12.7	0.689	0.655
4	8.28	0.734	0.678
5	7.95	0.777	0.715
6	6.27	0.810	0.749
7	4.44	0.834	0.771
8	3.18	0.851	0.781
9	2.75	0.866	0.792
10	2.53	0.880	0.803
11	2.08	0.891	0.807
12	1.62	0.900	0.803
13	1.44	0.907	0.807

Figure S1. Scores plot of the first versus the second principal component of the PCA analysis of 186 peptides after dividing their descriptors by the molecular weight. The colors of the clusters correspond with the clusters found in the scores plot of the PCA analysis using the original descriptors (Figure 2). For each cluster, some examples of peptides are indicated.

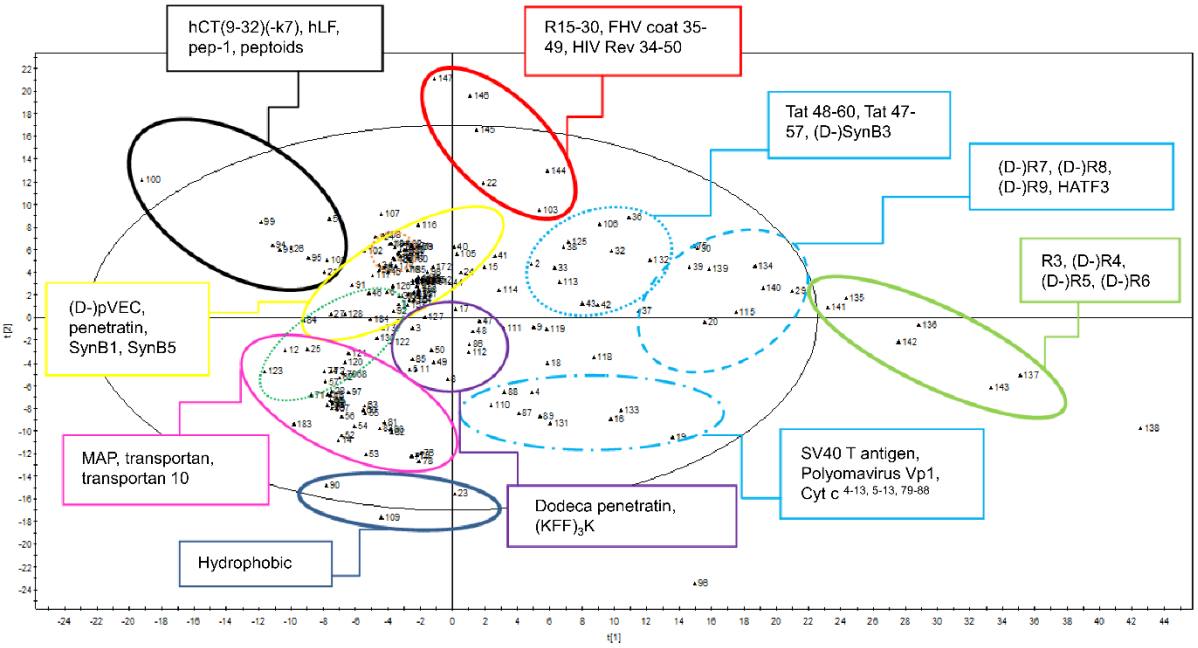

CHAPTER III

CLASSIFICATION OF PEPTIDES ACCORDING TO THEIR BLOOD-BRAIN BARRIER INFLUX

"The end of our exploring will be to arrive at where we started and to know the place for the first time."

Thomas Stearns Eliot
(°1888 - †1965, American essayist and poet)

Parts of this chapter were published:

Stalmans S, Gevaert B, Wynendaele E, Nielandt J, De Tré G, Peremans K, Burvenich C, De Spiegeleer B. Classification of Peptides According to Their Blood-Brain Barrier Influx. *Protein Peptide Lett.* 2015; **22**: 768-775.

ABSTRACT

An increasing number of studies demonstrate the ability of peptides to cross the blood-brain barrier (BBB), opening perspectives for a new class of therapeutics for central nervous system diseases. However, information on the BBB transport of peptides suffers from a wide variety in used methods and experimental set-ups. Therefore, it is currently difficult, if not impossible, to classify peptides according to their BBB influx characteristics. To allow direct comparison of BBB influx results of peptides, we introduce a classification method and unified response for BBB influx transport of peptides. First, the results of BBB influx response types (*i.e.* K_{in} (MTR), K_{in} (Perfusion), $P_{in\ vitro}$ and $P_{in\ vivo}$), which quantitatively express brain influx, were classified into five classes of BBB influx magnitude based on the distribution of these results for the individual response types. Then, these classes were converted to a BBB_{in}-response, representing a scaled value ranging from zero (no influx) to ten (high influx), independent from the BBB influx response type from which it was derived. This unified response can immediately be applied for new BBB influx results of peptides and represents a ballpark figure for BBB influx allowing direct comparison and ranking of peptides independent of the response type.

CHAPTER III

CLASSIFICATION OF PEPTIDES ACCORDING TO THEIR BLOOD-BRAIN BARRIER INFLUX

Main focus in this chapter:

- To introduce a classification method and unified response, BBB_{in}, for the BBB influx properties of peptides.
- To present possible applications of this classification system for peptides.

1. BLOOD-BRAIN BARRIER TRANSPORT OF PEPTIDES

Peptide drugs are exponentially gaining interest from the pharmaceutical industry, with already more than one hundred commercialized peptide drugs. Peptides fill the gap between small molecules and protein biologics, which currently are the two main classes of successful drugs. Therefore, peptides combine the advantages of both drug classes, *i.e.* the high specificity of the protein biologics for *in vivo* targets, causing high potency and few side-effects, and the smaller size, making them more accessible and cheaper to manufacture [1]. However, the widespread therapeutic applicability of peptides is limited due to their undesirable physicochemical properties, such as higher molecular weight and hydrophilicity compared to small molecules. These properties, together with their poor *in vivo* stability and rapid (renal) clearance, cause a low bioavailability, poor membrane permeability, short half-life and potential immunogenicity [1-3]. Several strategies are being applied to engineer the peptides in order to overcome these problems, making peptide therapeutics one of the fastest growing segments in the pharmaceutical industry [2-4].

Current marketed small molecules for the treatment of central nervous system (CNS) disorders, like schizophrenia, anxiety, depression and autism, suffer from serious side effects and significant efficacy limitations. Moreover, the development of safer and more effective therapies for these psychiatric disorders has slowed down [5-7]. Because of their high specificity and potency, peptides are promising therapeutics for CNS disorders [5]. Historically, peptides were believed not to reach the brain parenchyma, but in the 1970s the first reviews were published in which the ability of peptides

to cross the blood-brain barrier (BBB) was demonstrated [8,9]. Since then, numerous studies have described the BBB transport of peptides [9,10]. Brainpeps, the BBB peptide database, was constructed to collect these quantitative BBB transport data of peptides which are scattered in literature [11]. A multitude of methods and experimental protocols is used to assess the BBB behavior of peptides, impeding the comparison, ranking or classification of peptides according to their BBB influx characteristics. Moreover, very few BBB transport studies of peptides incorporate control compounds, considered as system suitability tests (SST) allowing standardization. In the literature, inulin, sucrose and bovine serum albumin (BSA), as vascular markers which do not cross the BBB, are most frequently proposed [12]. On the other hand, a positive control as SST is lacking in the majority of the BBB transport studies. This makes meaningful quantitative comparisons between influx properties very difficult, if not, impossible. Therefore, it was strongly suggested to include also a positive BBB permeability peptide in the experiments and dermorphin has been suggested to fulfill this role, being a universally available, well-characterized, pure, stable and easily-labeled peptide [11]. This standardization procedure would allow easier comparison of data between different research groups and methods as the correction of BBB transport results by the controls compensates for experimental differences. Clearly, there is a need for one universal measure for BBB influx transport of peptides. Therefore, we present here a classification method and unified response, BBB_{in}, which is a ballpark figure for BBB influx of peptides, using a straightforward calculation method. Our BBB influx classification and BBB_{in}-response are an elegant way to compare peptides regarding their overall BBB influx behavior and transcends the differences in experimental set-up and techniques.

2. CLASSIFICATION METHOD FOR BLOOD-BRAIN BARRIER INFLUX DATA OF PEPTIDES

BBB influx data

All data were gathered from the most recent Brainpeps database (http://brainpeps.ugent.be), which contains quantitative data of BBB transport of peptides available in literature [11]. Four different response types, expressing quantitatively BBB influx, were selected based on the availability of more than three experimental results. Reported negative response values were converted to zero, *i.e.* its physical-theoretical boundary. In total, 115 peptides were included in this study, containing up to 55 amino acids in their sequence. This arbitrary cut-off point for peptides is somewhat higher than the mostly used (arbitrary) cut-off of 50 amino acids applied throughout the literature in order to include borderline cases.

The original studies reporting the selected BBB influx responses can be found in the Brainpeps database and are not listed in the reference list. The used identification numbers of the peptides correspond with those in Brainpeps.

Method for classification and calculation of BBB_{in}-response

To define a BBB_{in}-response, the available data for the different selected BBB influx response types were evaluated by a box-and-whisker plot using SPSS Statistics 22 (IBM, Brussels, Belgium). This software was also used to calculate the 25, 50 and 75 percentiles, of which the weighted average percentiles were used in this study. Based on these percentiles and whiskers, reflecting the distribution of the experimental data for a specific influx response, the data were classified into five BBB influx classes: very low (lowest value – 25 percentile), low (25 – 50 percentile), medium (50 – 75 percentile), high (75 percentile – higher whisker) and very high influx (> higher whisker). The five-cluster principle represents a simple, but sufficiently detailed classification system. The classes were assigned a response score, BBB_{in}, as follows (between brackets the BBB_{in}-range is indicated for a class): class 1 = score 1 [0,2]; class 2 = score 3]2,4]; class 3 = score 5]4,6]; class 4 = score 7]6,8] and class 5 = score 9]8,10]. Several BBB_{in} data were sometimes available for one peptide, as well as within the same influx response as from different influx response types. Therefore, an overall BBB_{in}-response was calculated, which was obtained by calculating the median BBB_{in}-response of the peptide within each response type. Then, the median BBB_{in}-response was calculated over all BBB influx response types available for the peptide. The median was preferred over the mean, being less sensitive to outliers.

Evaluation of classification

The approach to classify and score the peptides according to their BBB_{in}-intensity was evaluated by comparing our result with the appreciation of the BBB transport by the authors who investigated the peptides. A positive correspondence was concluded in case of the same classification or only one class difference. If there was more than one class difference, a negative correspondence was reported. When authors only concluded the peptide crossed the BBB or if the BBB transport was described to be significantly higher than the vascular marker, without any more appreciation details, this was interpreted as low to medium BBB influx.

3. BBB_{IN}, AN INDEPENDENT MEASURE FOR BLOOD-BRAIN BARRIER INFLUX OF PEPTIDES

Influx responses

The unidirectional influx rate (K_{in}), represents the influx rate of peptides that are relatively stable in blood and slowly cross the BBB [10]. K_{in} actually represents the clearance of blood from the peptides after a single passage of the brain, expressed in units of volume per time [11]. Two K_{in} responses can be distinguished: K_{in} (MTR) obtained by performing a multiple time regression (MTR) experiment after intravenous injection (n = 76) and K_{in} (Perfusion) obtained by performing an *in situ* brain perfusion experiment (n = 21). Two permeability responses were included as well, representing the rate at which a peptide moves from blood to the brain with units of distance per time [11]. Both *in vitro* (n = 44) and *in vivo* (n = 6) BBB permeability (P) data were available: all $P_{in\ vitro}$ data were acquired using a brain microvessel endothelial cell culture model (BMEC), while $P_{in\ vivo}$ data were calculated after *in situ* brain perfusion experiments in rats. An overview of the data is given in the Supplementary Information (Table S1-S4). During a MTR experiment, peptides are intravenously injected and the solute concentration or radioactivity is determined at different time points in brain and serum. The same measurements are performed during the *in situ* brain perfusion method, but a perfusion fluid replaces the animal's circulating blood. The peptide, at a known concentration, is perfused into the carotid artery for a defined time interval and directly delivered to the brain via the perfusion fluid. During both *in vivo* methods, the BBB system is intact, which is a general advantage compared to the *in vitro* methods. The use of a perfusion buffer during the *in situ* brain perfusion method allows to control constituting components, which simplifies data interpretation, *e.g.* less metabolization of peptides due to absence of metabolizing enzymes in the perfusion fluid. However, the MTR method represents the "golden standard" for evaluating the BBB transport of peptides [12]. Thus, each of the four selected BBB influx responses is looking at BBB influx from a slightly different viewpoint and hence giving a slightly different information aspect.

Classification and calculation of BBB_{in}-response

For each of the selected BBB influx response types, the data distribution was evaluated using a box-and-whisker plot. In Figure 1, the classification of the K_{in} (Perfusion) data is presented.

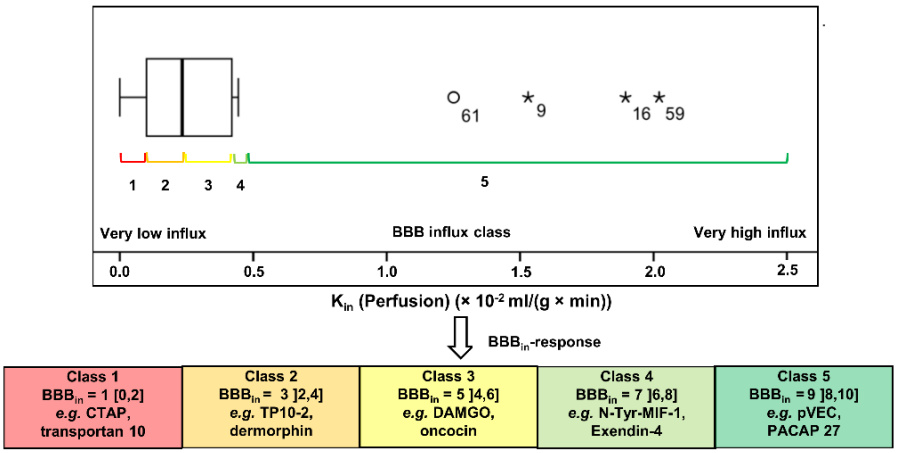

Figure 1. Classification of the BBB influx data.
The classification of the K_{in} (Perfusion) data are presented as an example. At the top, the box-and-whisker plot of the K_{in} (Perfusion) data is shown and data were classified into five BBB influx classes based on the 25, 50 and 75 percentiles as well as the lower and higher whisker. Peptides with outlying K_{in} (Perfusion) data constitute class 5. Then, BBB influx classes were converted to the BBB_{in}-response by attributing the mid-value of the corresponding BBB_{in}-range of the obtained BBB influx class, illustrated in the lower part of the figure.

Five BBB influx classes, ranging from very low over medium to very high BBB influx, were calculated, with class 1 to 4 were determined by the 25, 50 and 75 percentiles as well as the lower and higher whisker. BBB influx class 5 comprised the peptides with outlying BBB influx data (Figure 1). In Table 1, the limits of the five classes are listed for each influx response type. This table was used to classify peptides based on their BBB influx properties and can be used to classify newly obtained BBB transport data. The classification of the individual peptides can be found in the Supplementary Information (Table S1-S4).

Table 1. Classification of peptides based on BBB influx response data.
The ranges of the different BBB influx classes are determined by the calculated 25, 50 and 75 percentiles as well as the lower and higher whiskers calculated for the data of each individual BBB influx response type. Class 5 contains all data above the higher whisker, *i.e.* the outlying values.

BBB influx response type	Number of peptides	Class 1 Very low influx	Class 2 Low influx	Class 3 Medium influx	Class 4 High influx	Class 5 Very high influx	Unit
K_{in} (MTR)	76	$[0; 1.83 \cdot 10^{-4}]$	$]1.83 \cdot 10^{-4}; 3.78 \cdot 10^{-4}]$	$]3.78 \cdot 10^{-4}; 9.37 \cdot 10^{-4}]$	$]9.37 \cdot 10^{-4}; 2.10 \cdot 10^{-3}]$	$]2.10 \cdot 10^{-3}; \infty[$	ml/(g × min)
K_{in} (Perfusion)	21	$[0; 9.30 \cdot 10^{-4}]$	$]9.30 \cdot 10^{-4}; 2.34 \cdot 10^{-3}]$	$]2.34 \cdot 10^{-3}; 4.32 \cdot 10^{-3}]$	$]4.32 \cdot 10^{-3}; 1.25 \cdot 10^{-2}]$	$]1.25 \cdot 10^{-2}; \infty[$	ml/(g × min)
$P_{in\ vitro}$	44	$[0; 1.74 \cdot 10^{-5}]$	$]1.74 \cdot 10^{-5}; 3.44 \cdot 10^{-5}]$	$]3.44 \cdot 10^{-5}; 8.21 \cdot 10^{-5}]$	$]8.21 \cdot 10^{-5}; 1.53 \cdot 10^{-4}]$	$]1.53 \cdot 10^{-4}; \infty[$	cm/s
$P_{in\ vivo}$	6	$[0; 4.75 \cdot 10^{-8}]$	$]4.75 \cdot 10^{-8}; 9.50 \cdot 10^{-8}]$	$]9.50 \cdot 10^{-8}; 4.34 \cdot 10^{-7}]$	$]4.34 \cdot 10^{-7}; 5.65 \cdot 10^{-7}]$	$]5.65 \cdot 10^{-7}; \infty[$	cm/s

For 15 peptides, BBB influx data were available for more than one BBB influx response type (Table 2). It concerns peptides already extensively investigated for their BBB transport properties. Five of these peptides, *i.e.* exendin-4, adrenomedullin, endomorphin-2, biphalin and urocortin II, showed divergent classification based on the different BBB influx response types, *i.e.* the classification range was more than one class. For exendin-4, adrenomedullin, biphalin and urocortin II, the range of

classification based on the different BBB influx responses was two classes (indicated as "+/-" in Table 2). An important discrepancy between the techniques used to obtain the BBB influx responses of exendin-4, adrenomedullin and urocortin II, is that during MTR, peptides are intravenously injected, causing an increased possibility of metabolization and protein binding. In contrast, during *in situ* brain perfusion studies, peptides are perfused in serum-free buffers. Thus differences in methodologies used in the different BBB influx response types explain deviating classification.

There is only one peptide with a classification range greater than two (indicated as "-" in Table 2), *i.e.* endomorphin-2, which showed a higher classification based on the K_{in} (MTR) data (*i.e.* 4) compared to $P_{in\ vitro}$ data (*i.e.* 1). In the study of endomorphin-2 where the MTR method was used to characterize the BBB transport properties, the proposed control peptide dermorphin was investigated as well, allowing to "standardize" the experimental values [13]. We thus compared the dermorphin K_{in} results obtained in that study with the overall K_{in} results obtained, and observed a significantly higher K_{in} result for dermorphin in the concerned study (*i.e.* $2.2 \cdot 10^{-3}$ ml/(g × min)) compared to the other values reported (range from $1.6 \cdot 10^{-4}$ ml/(g × min) to $3.6 \cdot 10^{-4}$ ml/(g × min), with a median value of $2.7 \cdot 10^{-4}$ ml/(g × min)) [values from Brainpeps database]. Thus, the higher result of dermorphin in the concerned study (class 5 compared to class 1 or 2 for other results) indicates that the obtained BBB influx data are generally higher, which might be due to biological factors like increased stress or older age of the mice. This illustrates one of the applications of our classification method of BBB influx data of peptides: it allows the evaluation of obtained experimental data on the BBB transport of peptides and the comparison with other already available data.

Table 2. Correspondence of classification of peptides based on their BBB influx properties for which data are available for more than one type of BBB influx responses. A positive correspondence (+) is concluded if the classification range was ≤ 1. If the classification range is 2 classes, the correspondence is indicated as "+/-" and if the classification range was ≥ 3, a negative correspondence (-) is concluded.

Peptide name	BBB influx class				Correspond?
	K_{in} (MTR)	K_{in} (Perfusion)	$P_{in\ vitro}$	$P_{in\ vivo}$	
PACAP 38	5	5	-	-	+
VIP	3	2	-	-	+
Exendin-4	3	5	-	-	+/-
F^{13}, Y^{19}-MCH	1	1	-	-	+
Adrenomedullin	3	1	-	-	+/-
Urocortin I	1	1	-	-	+
[Tyr^{10}] Secretin-27	4	3	-	-	+
Endomorphin-2	4	-	1	-	-
Biphalin	-	2	4	3	+/-
DPDPE	-	2	3	-	+
Urocortin II	3	5	-	-	+/-
Peptide YY	3	2	-	-	+
p-[Cl-$Phe^{4'4'}$] biphalin	-	3	4	4	+
CTAP	1	2	-	-	+
Insulin detemir	1	1	-	-	+

To obtain a response type-independent overall measure for BBB influx of peptides, the BBB influx classes were converted to a BBB_{in}-response, which is a scaled value estimating the BBB influx properties of peptides, ranging from zero (no influx) to ten (high influx). This BBB_{in}-response could be calculated for each peptide enabling direct comparison of peptides regarding their blood-to-brain transport characteristics. The conversion from class to BBB_{in}-response is given in Figure 1. In the Supplementary Information (Table S5), the overall BBB_{in}-responses of the included peptides are listed. Although MTR is currently the "golden standard" method for evaluation of the BBB influx of peptides, it is currently not clear how much weight has to be justifiably attributed to K_{in} (MTR) compared to the other BBB influx response types. Therefore, at this moment, the contribution of the different response types to the overall BBB_{in}-response was not weighed.

Evaluation of the classification

For two-thirds (n = 10) of the peptides having data available for more than one influx response type (n = 15), the classification based on these different response types corresponded well, indicating the appropriateness of the classification. Moreover, our BBB influx classification of peptides was verified by comparing our result with the appreciation by the original authors, which is visualized in Figure 2.

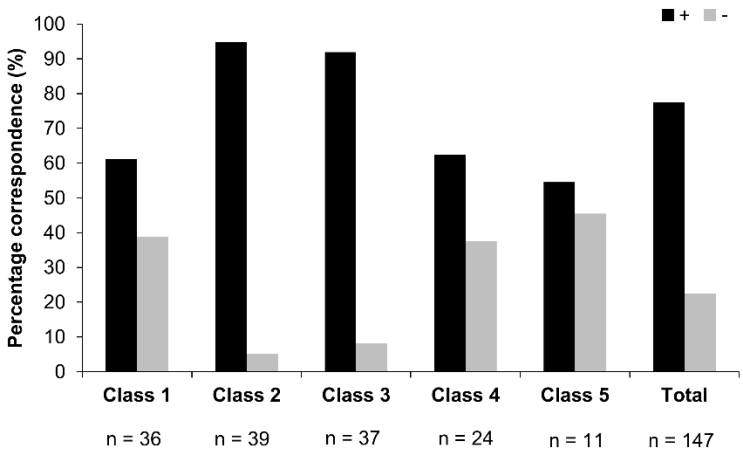

Figure 2. Evaluation of correspondence between BBB influx classes and appreciation by the original authors. A positive correspondence was attributed if the authors concluded the same classification, allowing one class difference. If the calculated influx class and the estimation of the authors differed more than one influx class, a negative correspondence was concluded.

The comments of the authors on the individual BBB influx response data are listed in the Supplementary Information (Table S1-S4). This cross-verification indicated a 75% correspondence between our classification method, based on all available BBB influx responses for peptides, and the appreciation of the BBB influx of the peptides by the authors who investigated the peptides. The observed 75% correspondence between our classification method and the authors' conclusions thus justified our classification approach.

Application of the BBB_{in}-response

In the selected data set, seven groups of peptides could be identified based on their biological functionality. In Figure 3, the distribution of the BBB_{in}-response within these different groups is visualized.

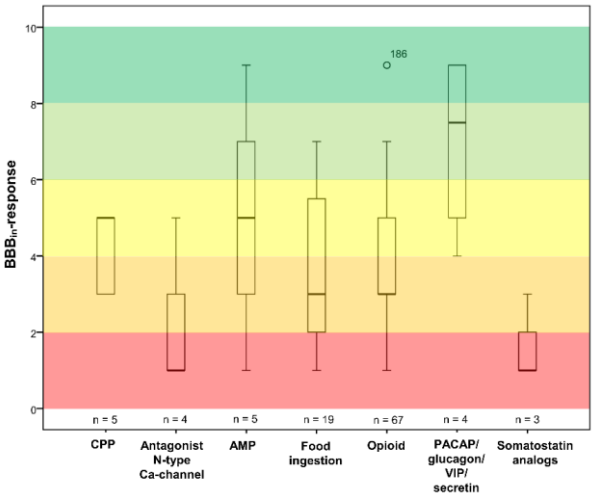

Figure 3. Distribution of the BBB_{in}-responses, visualized using a box-and-whisker plot, in the seven groups of peptides identified in the investigated data set based on their biological function. The number of peptides per group are indicated under the box-and-whisker plots.

The PACAP/glucagon/VIP/secretin family showed the highest BBB influx (median high BBB influx). This group of peptide hormones is widely distributed in the body, but especially in the brain and gut and displays pleiotropic physiological functions, *i.a.* neurotransmitter, neuromodulatory and neurotrophic properties [14]. The high median BBB_{in}-response indicates that peripherally synthesized peptides can reach the brain as well, which also has therapeutic implications [14]. The antimicrobial (AMP) and cell-penetrating peptides (CPP), which are rich in basic arginine and/or lysine residues, had a median medium BBB influx [15,16]. Cationization of peptides has already been demonstrated to improve brain uptake, as the positive charges enable to use an adsorptive-mediated transcytosis mechanism to cross the BBB [17]. However, we could not demonstrate a saturable influx mechanism for CPPs when we investigated their BBB transport characteristics of five representative peptides, which is further elaborated in **Chapter V**. For the opioid peptides, which can alleviate centrally mediated pain, a low median BBB_{in}-response was calculated. This result was expected as these peptides suffer from a low brain influx and significant efflux out of the brain due to their structural characteristics, resulting in poor net BBB transport [18]. Several strategies are now explored to enhance their brain influx [18]. The food ingestion peptides also show a low median brain influx. This group of peptides is involved in the regulation of feeding. Some of these peptides enter the brain using a simple passive diffusion, while others use a saturable transport system. Due to their regulatory function, this transport system can be influenced by fluctuations in blood levels of

nutrients, resulting in a varying extent of brain influx [19]. Finally, the somatostatin analogs had a very low median brain influx, which can be explained by a serum-related factor, like protein-binding or an aggregation-promoting factor limiting the brain influx of these peptides [20].

When the distribution of the BBB_{in}-response was evaluated in function of the used transport type to cross the BBB, there was no difference determined between the peptides using a saturable or non-saturable mechanism (Figure 4).

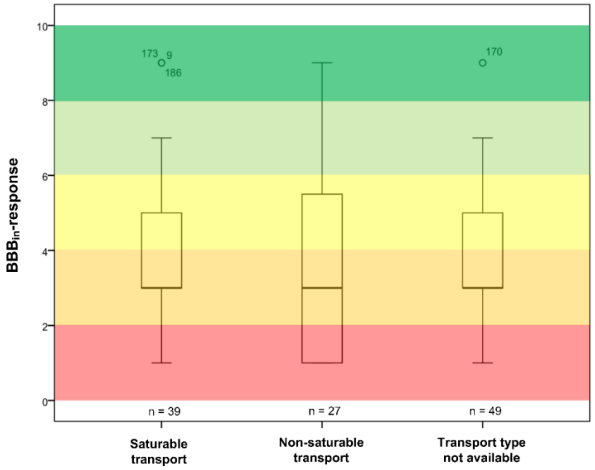

Figure 4. BBB_{in}-response distribution in function of used transport type to cross the BBB. The number of peptides per transport type group are indicated under the box-and-whisker plots.

4. APPLICATION OF THE CLASSIFICATION METHOD AND BBB_{IN}-RESPONSE

Historically, peptides were believed not to cross the BBB as a result of the unsuitability of the traditional techniques, like the brain uptake index (BUI) which is not sensitive enough to measure the influx of the slowly BBB-penetrating peptides [21]. However, during the last decades, numerous studies have demonstrated the ability of peptides to overcome the BBB [22-25]. Currently, a variety of methods is used to describe the BBB influx properties of peptides, which are numerically expressed using different BBB influx response types. Moreover, in most BBB transport studies, a negative and/or positive control are not included, making it very difficult, if not impossible, to globally compare the brain influx of peptides [11]. To overcome this problem, we introduced a classification system and unified response, BBB_{in}. Four different BBB influx response types, for which at least three quantitative data were available, were used. These influx responses were obtained using different techniques, have different units and are not directly inter-comparable. Based on their distribution, visualized using a box-and-whisker plot, each response type was classified into five BBB influx classes ranging from very low to very high BBB influx. Next to this classification, a more quantitative approach is useful, for example when the same peptide was investigated using different

techniques and an overall but simple BBB influx measure is required. Therefore, the resulting classes were converted to a BBB_{in}-response, which is a scaled value ranging between zero (no influx) to ten (very high influx), allowing to calculate an overall brain influx response independent from the influx response type from which it was derived.

Our approach was verified by demonstrating a 75% correspondence between our classification and the qualitative appreciation by the authors who performed the experiments. Figure 2 shows that the correspondence between our classification method and the estimation by the authors is high for class 2 and 3. However, the predictive power is much poorer for the other three BBB influx classes, explained by the fact that a negative correspondence was mostly attributed when the authors did not estimate the brain influx properties of the investigated peptides, which we ourselves interpreted that as class 2 or 3 without allowing any class difference. Therefore, we estimate this cross-verification method, although being rather qualitative and to some extent subjective, valuable. The obtained correspondence indicates that our conclusions are in line with the opinion of the authors, based on their scientific experience. For two-thirds of the peptides for which quantitative data were available for more than one BBB influx response type, the classification corresponded well, *i.e.* only one class difference. For other peptides, the deviating classification could be explained by differences in experimental factors, illustrating the use of the BBB_{in}-response during the evaluation of quantitative data for BBB influx of peptides.

Inherent to any data reduction technique, the use of this classification and the unified BBB_{in}-response includes a loss of details on the BBB transport, *e.g.* clearance versus permeability or peptide serum stability, serum protein binding or the presence of an efflux out of the brain, all influencing the net brain influx [26]. The overall BBB_{in}-response also misses the interpretational aspects which are included in the individual BBB influx responses. However, our brain influx classification and BBB_{in}-response permit direct comparison of the overall BBB influx characteristics of peptides, despite different methods being used. Moreover, it is the first time that a ready-to-use response is proposed: researchers can classify and calculate the BBB_{in}-response for newly investigated peptides by fitting their results in Table 1. This approach can be applied to other techniques and related BBB transport responses if sufficient data are available. For example, future recalculation of the classification system might be beneficial for the $P_{in\ vivo}$ response, for which only six data were available during this study. Seen the availability of a considerable amount of data for the other three selected influx response types ($n \geq 21$), we consider them more robust in time. The current awareness of the value of publishing negative research outcomes will also prevent the evolution to positively biased quantitative data for BBB influx of peptides, ultimately influencing the BBB_{in} classification study of peptides [27].

The BBB_{in}-response offers a framework to discuss and benchmark the brain influx the BBB transport results of peptides in a broader perspective. For example, for PACAP 38, a 30% faster influx into the brain was demonstrated than for PACAP 27 [28]. These conclusions can be nuanced by our classification system, which indicates that both peptides show a very high influx into the brain.

The scope of this study was not to provide new insights in the mechanisms that influence the BBB influx properties of peptides. However, the BBB influx class, a categorical value, and the BBB_{in}-response, a continuous value, can be used to further explore the brain influx of peptide. For example, seven different biological functionalities were identified for the investigated peptides. We observed differences in median BBB_{in}-response between these functionally different groups of peptides. The high median BBB_{in}-response of the PACAP/glucagon/VIP/secretin family indicates that the peripherally synthetized peptides can reach the brain, while the low median BBB_{in}-response of the opioid peptides indicates that structural modifications are needed to ensure efficient pain therapy. However, poor BBB penetration does not necessarily means no biological effect, as was demonstrated for cyclo(His-Pro). This peptide showed a very low brain influx rate, but a sufficient amount of the peptide reached the brain parenchyma, *i.e.* 0.01% of the injected dose per gram tissue, to reverse alcohol-induced narcosis [19,29]. No difference was observed in distribution of BBB_{in}-responses between peptides using a saturable or non-saturable transport system. This was unexpected as peptides using a saturable transport system generally show a higher net transfer across the BBB compared to those that cross the BBB by passive diffusion [22]. However, to draw substantiated conclusions on the BBB_{in} distribution of peptides having different biological functions, a larger data set is needed. Still, the comparison of the BBB_{in} for functionally different peptides is an illustrative example for the application of our classification method within the constraints of the current limited data set.

5. CONCLUSIONS

Currently, data on BBB influx properties of peptides suffer from inconsistencies with regards to used techniques and influx response types, making it difficult to directly and objectively compare the BBB influx properties of peptides. The introduced BBB influx classification system and derived BBB_{in}-response, a scaled value ranging between zero and ten, allow ranking of peptides based on their BBB influx characteristics despite differences in experimental set-up. This unified response opens perspectives to further unravel the transport mechanism and to determine required structural features for BBB transport of peptides.

6. REFERENCES

[1] Craik DJ, Fairlie DP, Liras S, Price D. The Future of Peptide-based Drugs. *Chem. Biol. Drug Des.* 2013, **81**: 136-147.

[2] Sato AK, Viswanathan M, Kent RB, Wood CR. Therapeutic peptides: technological advances driving peptides into development. *Curr. Opin. Biotech.* 2006; **17**: 638-642.

[3] Antosova Z, Mackova M, Kral V, Macek T. Therapeutic application of peptides and proteins: parenteral forever? *Trends Biotechnol.* 2009; **27**: 628-635.

[4] McGonigle P. Peptide therapeutics for CNS indications. *Biochem. Pharmacol.* 2012; **83**: 559-566.

[5] Alavijeh MS, Chishty M, Qaiser MS, Palmer AM. Drug Metabolism and Pharmacokinetics, the Blood-Brain Barrier, and Central Nervous System Drug Discovery. *Neurotherapeutics* 2005; **2**: 554-571.

[6] Wegener G, Rujescu D. The current development of CNS drug research. *Int. J. Neuropsychopharmacol.* 2013; **16**: 1687-1693.

[7] Chandler DJ. Something's got to give: psychiatric disease on the rise and novel drug development on the decline. *Drug Discov. Today* 2013; **18**: 202-206.

[8] Banks WA, Kastin AJ. Permeability of the blood-brain barrier to neuropeptides: the case for penetration. *Psychoneuroendocrino.* 1985; **10**: 385-399.

[9] Banks WA, Kastin AJ. Saturable transport of peptides across the blood-brain barrier. *Life Sci.* 1987; **41**: 1319-1338.

[10] Kastin AJ, Pan W. In *Progress in Drug Research* (Eds: Prokai L, Prokai-Tatrai K), Birkhäuser Verlag, **2003**, pp. 79-100.

[11] Van Dorpe S, Bronselaer A, Nielandt J, Stalmans S, Wynendaele E, Audenaert K, Van De Wiele C, Peremans K, Hsuchou H, De Tré G, De Spiegeleer B. Brainpeps: the blood-brain barrier peptide database. *Brain Struct. Funct.* 2012; **217**: 687-718.

[12] Smith QR. In *The Blood-Brain Barrier – Biology and Research Protocols* (Eds: Nag S), Humana Press, **2003**, pp. 193-247.

[13] Van Dorpe S, Adriaens A, Polis I, Peremans K, Van Bocxlaer, De Spiegeleer B. Analytical characterization and comparison of the blood-brain barrier permeability of eight opioid peptides. *Peptides* 2010; **31**: 1390-1399.

[14] Dogrukol-Ak D, Tore F, Tuncel N. Passage of VIP/PACAP/Secretin Family Across the Blood-Brain Barrier: Therapeutic Effects. *Curr. Pharm. Design* 2004; **10**: 1325-1340.

[15] Stalmans S, Wynendaele E, Bracke N, Gevaert B, D'Hondt M, Peremans K, Burvenich C, De Spiegeleer B. Chemical-Functional Diversity in Cell-Penetrating Peptides. *PLOS ONE* 2013; **8**: e71752.

[16] Stalmans S, Wynendaele E, Bracke N, Knappe D, Hoffmann R, Peremans K, Polis I, Burvenich C, De Spiegeleer B. Blood-Brain Barrier Transport of Short Proline-Rich Antimicrobial Peptides. *Protein Peptide Lett.* 2014; **21**: 399-406.

[17] Deguchi Y, Terasaki T. Transport of Basic Peptides at the Blood-Brain Barrier. In *Handbook of Biologically Active Peptides* (Ed: Kastin AJ), Elsevier Academic Press, **2006**, pp. 1443-1448.

[18] Egleton RD, Witt KA, Davis TP. Opiate Peptides and the Blood-Brain Barrier. In *Handbook of Biologically Active Peptides* (Ed: Kastin AJ), Elsevier Academic Press, **2006**, pp. 1429-1434.

[19] Kastin AJ, Pan W. Blood-Brain Barrier and Feeding: Regulatory Roles of Saturable Transport Systems for Ingestive Peptides. *Curr. Pharm. Des.* 2008; **14**: 1615-1619.

[20] Banks WA, Schally AV, Barrera CM, Fasold MB, Durham DA, Csernus VJ, Groot K, Kastin AJ. Permeability of the murine blood-brain barrier to some octapeptide analogs of somatostatin. *Proc. Natl. Acad. Sci. USA* 1990; **87**: 6762-6766.

[21] Banks WA, Kastin AJ. Bidirectional passage of peptides across the blood-brain barrier, In *Progress in Brain Research* (Eds: Ermisch A, Landgraf R, Rühle H-J), Elsevier Science, **1992**, pp. 139-147.

[22] Pan W, Kastin AJ. Why study transport of peptides and proteins at the neurovascular interface. *Brain Res. Rev.* 2004; **46**: 32-43.

[23] Egleton RD, Davis TP. Bioavailability and Transport of Peptides and Peptide Drugs into the Brain. *Peptides* 1997; **18**: 1431-1439.

[24] Smith MW, Gumbleton M. Endocytosis at the blood-brain barrier: From basic understanding to drug delivery strategies. *J. Drug Target.* 2006; **14**: 191-214.

[25] Tamai I, Tsuji A. Transporter-Mediated Permeation of Drugs Across the Blood-Brain Barrier. *J. Pharm. Sci*. 2000; **89**: 1371-1388.

[26] Kastin AJ, Pan W, Maness LM, Banks WA. Peptides crossing the blood-brain barrier: some unusual observations. *Brain Res.* 1999; **848**: 96-100.

[27] Matosin N, Frank E, Engel M, Lum JS, Newell KA. Negativity towards negative results: a discussion of the disconnect between scientific worth and scientific culture. *Dis. Model Mech.* 2014; **7**: 171-173.

[28] Banks WA, Kastin AJ, Komaki G, Arimura A. Passage of Pituitary Adenylate Cyclase Activating Polypeptide$_{1-27}$ and Pituitary Adenylate Cyclase Activating Polypeptide$_{1-38}$ Across the Blood-Brain Barrier. *J. Pharmacol. Exp. Ther.* 1993; **267**: 690-696.

[29] Banks WA, Kastin AJ, Akerstrom V, Jaspan JB. Radioactively iodinated cyclo(His-Pro) crosses the blood-brain barrier and reverses ethanol-induced narcosis. *Am. J. Physiol.-Endoc. M.* 1993; **264**: E723-E729.

SUPPLEMENTARY INFORMATION

Table S1: Classification K_{in} (MTR) data.

	Lower limit (ml/(g × min))	Upper limit (ml/(g × min))		BBB influx response
Class 1	0.00E+00	1.83E-04	*included*	**1**
Class 2	1.83E-04	3.78E-04	*included*	**3**
Class 3	3.78E-04	9.37E-04	*included*	**5**
Class 4	9.37E-04	2.10E-03	*included*	**7**
Class 5	2.10E-03	∞		**9**

ID	Peptide Name	K_{in} (MTR) (ml/(g × min))	BBB influx class	BBB influx response	PubID (Brainpeps)	Comment author	Correspond ?
6	Vapreotide; RC-160	9.23E-05	1	1	11	The entry rates were generally low.	+
7	CRH	2.24E-04	2	3	24	Influx into brain was slower than UCN II, which crossed the BBB at a moderate rate.	+
8	PACAP 27	2.13E-03	5	9	30	Enters brain at a modest rate.	-
9	PACAP 38	2.86E-03	5	9	30	Faster than PACAP-27 which enters at modest rate.	-
10	VIP	4.00E-04	3	5	22	Moderate rate of uptake.	+
11	Neuropeptide Y	1.94E-04	2	3	33	NPY entered brain significantly higher than the albumin control; slightly higher influx than cHP.	+
14	Orexin A	3.09E-04	2	3	35	Rapidly enters the brain.	-
16	Exendin-4	4.62E-04	3	5	39	Entry at a fast rate.	+
17	F^{13},Y^{19}-MCH	5.20E-05	1	1	34	P-T-MCH does not significantly cross the BBB, probably because of its binding to serum proteins.	+
21	Adrenomedullin	5.83E-04	3	5	37	Much faster than albumin (vascular control).	+
22	Urocortin-I	1.68E-04	1	1	38, 18	Urocortin I does not significantly penetrate the BBB.	+
22	Urocortin-I	0.00E+00	1	1	113	Adult mice did not transport urocortin across BBB.	+
23	Insulin	3.46E-04	2	3	32	Slow influx.	+
23	Insulin	8.66E-04	3	5	129	Insulin crosses the BBB.	+
23	Insulin	6.88E-04	3	5	129	Insulin crosses the BBB.	+
25	Ghrelin	3.24E-04	2	3	31	Influx, but not estimated.	+
27	Amylin	9.54E-04	4	7	32	Crosses BBB.	-
27	Amylin	8.99E-04	3	5	126	Amylin crosses the BBB.	+
28	[Tyr^{10}] Secretin-27	9.49E-04	4	7	77	SA was taken up by brain at a modest rate of 0.9-1.5 µl/(g x min).	+
31	Endomorphin-1	1.06E-03	4	7	97	High influx constant rates.	+
32	Endomorphin-2	1.14E-03	4	7	97	High influx constant rates.	+

ID	Peptide Name	K_{in} (MTR) (ml/(g × min))	BBB influx class	BBB influx response	PubID (Brainpeps)	Comment author	Correspond?
47	Pancreatic Polypeptide	1.15E-03	4	7	47	Able to cross BBB.	-
55	Epidermal Growth Factor	2.02E-03	4	7	54	EGF crosses the BBB rapidly.	+
57	[Met(O)67]CART-(55-102)	5.10E-04	3	5	58	Rapid rate of entry.	+
58	Mahogany (1377-1428)	5.53E-04	3	5	60	Crosses BBB.	+
59	Urocortin II	5.91E-04	3	5	24	Moderate rate of uptake.	+
66	Peptide YY (3-36)	4.90E-04	3	5	41	Similar rate to leptin. Based on our classification method, leptin and PYY belong to the same class (data leptin not included in this study).	+
74	CTAP	0.00E+00	1	1	97	Very low to no influx.	+
83	cHP	1.80E-04	1	1	58	cHP has the slowest K_i of a group of peptides involved in food ingestion.	+
83	cHP	1.79E-04	1	1	104	The rate of entry of cHP was low in comparison with other peptides.	+
93	DAMGO	4.00E-04	3	5	97	Very low to no influx.	-
100	TAPA	2.65E-04	2	3	95	Influx similar to sucrose which is slightly permeable for normal BBB.	+
104	TAPS	1.80E-04	1	1	97	Very low to no influx.	+
105	TAPP	1.12E-03	4	7	97	High influx constant rates.	+
106	CTOP	2.40E-04	2	3	97	Very low to no influx.	+
110	Dermorphin	2.18E-03	5	9	97	Very high influx into brain.	+
110	Dermorphin	1.90E-04	2	3	114	Positive control, shows influx.	+
110	Dermorphin	3.50E-04	2	3	120	Positive control, shows influx.	+
110	Dermorphin	1.60E-04	1	1	120	Positive control, shows influx.	-
110	Dermorphin	3.56E-04	2	3	120	Positive control, shows influx.	+
113	Obestatin (mouse)	1.86E-03	4	7	8	Extremely fast influx into the brain.	+
114	P41	3.68E-04	2	3	102	Slower influx properties (based in initial K_{in} data).	+
115	P42	2.49E-04	2	3	102	Slower influx properties (based in initial K_{in} data).	+
116	P43	0.00E+00	1	1	102	Rapid and high influx (based on initial K_{in} data, here $K_{in,ss}$ reported).	-
117	Sb-Aba	4.46E-04	3	5	102	Rapid and high influx (based on initial K_{in} data, here $K_{in,ss}$ reported).	+
121	Api88	3.70E-04	2	3	98	Small but significant influx.	+
122	Apidaecin Api137	7.30E-04	3	5	114	Influx, no estimation.	-
130	Agouti-Related Protein (83-132)	5.70E-05	1	1	64	AgRP(83-132) crosses BBB very slowly.	+

ID	Peptide Name	K_{in} (MTR) (ml/(g × min))	BBB influx class	BBB influx response	PubID (Brainpeps)	Comment author	Correspond?
131	RC-121	4.01E-05	1	1	11	The entry rates were generally low; entry rate was near the value generally found for albumin.	+
132	RC-161	2.32E-04	2	3	11	The entry rates were generally low.	+
134	(3-methyl-His^2) Thyrotropin-releasing hormone	1.15E-03	4	7	89	Significantly higher than sucrose and similar to previously reported small peptides (medium to high influx).	-
135	SKB P5	1.46E-04	1	1	102	Rapid and high influx (based on initial K_{in} data, here $K_{in,SS}$ reported).	-
136	AN110	3.43E-04	2	3	102	Rapid and high influx (based on initial K_{in} data, here $K_{in,SS}$ reported).	-
139	ADAB	5.15E-05	1	1	105	Slower rate of influx than TAPA (class 2), slow onset of antinociceptive effect.	+
140	ADAMB	2.90E-05	1	1	105	Slower rate of influx than TAPA (class 2), slow onset of antinociceptive effect.	+
141	cationic AVP_{4-9}	3.10E-04	2	3	106	$cAVP_{4-9}$ is effectively transported across BBB.	+
154	Oncocin	4.40E-04	3	5	114	Influx, no estimation.	+
155	Drosocin	8.60E-04	3	5	114	Influx, no estimation.	-
156	Drosocin Pro5Hyp	3.70E-04	2	3	114	Influx, no estimation.	+
157	LinS	4.50E-04	3	5	115	Have favorable initial brain influx rates.	+
158	LinNMe	1.70E-04	1	1	115	Have favorable initial brain influx rates.	-
159	CycS	1.10E-04	1	1	115	Have favorable initial brain influx rates.	-
160	CycNMe	3.10E-04	2	3	115	Have favorable initial brain influx rates.	+
168	SynB3	8.20E-04	3	5	120	High influx into brain.	+
169	Tat 47-57	1.13E-03	4	7	120	High influx into brain.	+
170	pVEC	6.05E-03	5	9	120	Very high influx into brain.	+
171	Transportan 10	1.14E-04	1	1	120	Low influx rate.	+
172	TP10-2	3.59E-04	2	3	120	Low influx rate.	+
173	D-[Ala^1]-peptide T-amide	1.13E-03	4	7	121	Crosses the BBB to a significantly greater extent than albumin.	-
173	D-[Ala^1]-peptide T-amide	2.50E-03	5	9	121	Crosses the BBB to a significantly greater extent than albumin.	-
173	D-[Ala^1]-peptide T-amide	2.92E-03	5	9	121	Crosses the BBB to a significantly greater extent than albumin.	-
173	D-[Ala^1]-peptide T-amide	2.50E-03	5	9	121	Crosses the BBB to a significantly greater extent than albumin.	-
174	$Neurotensin_{8-13}$ analog	5.12E-04	3	5	122	NT1 crosses the BBB. K_{in} in lower half of the range of K_{in}'s of other peptides.	+

ID	Peptide Name	K_{in} (MTR) (ml/(g × min))	BBB influx class	BBB influx response	PubID (Brainpeps)	Comment author	Correspond?
186	MIF-1	2.37E-02	5	9	125	One of the highest blood to brain rate of influx found for a peptide.	+
187	β-Amyloid$_{1-28}$	3.86E-04	3	5	130	β-Amyloid$_{1-28}$ entered brain slowly.	+
216	Insulin detemir	0.00E+00	1	1	137	Insulin detemir not transported across BBB.	+

Table S2: Classification K_{in} (Perfusion) data.

	Lower limit (ml/(g × min))	Upper limit (ml/(g × min))		BBB influx response
Class 1	0.00E+00	9.30E-04	*included*	**1**
Class 2	9.30E-04	2.34E-03	*included*	**3**
Class 3	2.34E-03	4.32E-03	*included*	**5**
Class 4	4.32E-03	1.25E-02	*included*	**7**
Class 5	1.25E-02	∞		**9**

ID	Peptide Name	K_{in} (Perfusion) (ml/(g × min))	BBB influx class	BBB influx response	PubID (Brainpeps)	Comment author	Correspond?
9	PACAP 38	1.53E-02	5	9	30	Fast influx.	+
10	VIP	2.16E-03	2	3	22	Moderate rate of uptake.	+
16	Exendin-4	1.90E-02	5	9	39	Exendin-4 crossed directly the BBB at fast rate.	+
17	F^{13}, Y^{19}-MCH	5.94E-04	1	1	34	P-T-MCH does not significantly cross the BBB probably because of its binding to serum proteins.	+
21	Adrenomedullin	6.76E-04	1	1	37	Much faster than albumin (vascular control).	-
22	Urocortin-I	8.60E-04	1	1	18	Urocortin I does not significantly penetrate the BBB.	+
28	[Tyr^{10}] Secretin-27	2.73E-03	3	5	77	SA was taken up by brain at a modest rate of 0.9-1.5 µl/(g x min).	+
37	Biphalin	2.34E-03	2	3	91	Influx significantly greater than sucrose.	+
38	DPDPE	1.46E-03	2	3	87	Brain uptake of DPDPE was significantly greater than sucrose, a vascular marker.	+
40	SAM 995	1.00E-03	2	3	26	Enters brain.	+
41	SAM 1095	2.20E-03	2	3	26	Enters brain (x faster than peptide 40).	+
59	Urocortin II	2.02E-02	5	9	24	High influx rate.	+
61	LHRH	1.25E-02	4	7	66	The results indicate that there is a bidirectional transport across the BBB.	-
64	Des-Octanoyl Ghrelin	5.73E-04	1	1	31	Influx, but not estimated.	-
66	Peptide YY (3-36)	2.34E-03	2	3	41	Similar rate to leptin (no data available). Thus influx into the brain.	+
69	p-[Cl-$Phe^{4'4'}$] biphalin	3.39E-03	3	5	91	Influx significantly greater than sucrose.	+
74	CTAP	1.61E-03	2	3	69	Greater amounts of radioactivity were detected in the brain for CTAP than inulin.	+

ID	Peptide Name	K_{in} (Perfusion) (ml/(g × min))	BBB influx class	BBB influx response	PubID (Brainpeps)	Comment author	Correspond?
177	Arginine Vasopressin	2.37E-03	3	5	127	Transfer rate 10 times higher than sucrose.	+
185	N-Tyr-MIF-1	4.44E-03	4	7	139	Entry rate significantly higher than the vascular marker albumin.	-
216	Insulin detemir	0.00E+00	1	1	137	Insulin detemir not transported across BBB.	+
217	Ziconotide	4.20E-03	3	5	138	Brain uptake statistically greater than inulin. Brain amounts of Ziconotide are low.	+

Table S3: Classification $P_{in\ vitro}$ data.

	Lower limit (cm/s)	Upper limit (cm/s)		BBB influx response
Class 1	0.00E+00	1.74E-05	*included*	**1**
Class 2	1.74E-05	3.44E-05	*included*	**3**
Class 3	3.44E-05	8.21E-05	*included*	**5**
Class 4	8.21E-05	1.53E-04	*included*	**7**
Class 5	1.53E-04	∞		**9**

ID	Peptide Name	P (cm/s)	BBB influx class	BBB influx response	PubID (Brainpeps)	Comment author	Correspond?
18	Deltorphin I	3.79E-05	3	5	132	Able to cross the *in vitro* BBB. Deltorphin I has higher permeability compared to majority of analogues.	**+**
19	Deltorphin II	3.92E-05	3	5	132	Able to cross the *in vitro* BBB. Deltorphin I has higher permeability compared to majority of analogues.	**+**
29	[Met^5] Enkephalin	2.00E-05	2	3	27	Rapidly degradated in plasma. Inhibition of endothelial cell peptidases increased significantly the permeability.	+
29	[Met^5] Enkephalin	7.74E-05	3	5	29	Rapidly degraded in plasma, inhibition of endothelial cell peptidases allows calculation of P. Influx not estimated.	+
32	Endomorphin-2	7.84E-06	1	1	101	Influx of EM-2 and analogs into brain is low but significantly higher than sodium fluorescein.	+
32	Endomorphin-2	5.32E-05	3	5	135	Endomorphin traverses the *in vitro* BBB.	+
37	Biphalin	9.17E-05	4	7	91, 29	Significant influx into brain.	+
38	DPDPE	8.21E-05	3	5	29	Crosses BBB.	+
38	DPDPE	8.21E-05	3	5	136	Shows *in vitro* BBB permeability.	+
39	[Glu^4]Deltorphin	6.33E-05	3	5	29	Crosses BBB to a lower extent than other tested compounds.	+
69	p-[Cl-Phe$^{4',4''}$] biphalin	1.53E-04	4	7	91, 29	Significant influx into brain, but higher than biphalin.	-
72	[p-ClPhe^4] DPDPE	1.38E-04	4	7	29	Crosses BBB to a higher extent than DPDPE and other tested compounds.	-
137	Dmt^1-Endomorphin 2	1.49E-05	1	1	101	Influx of EM-2 and analogs into brain is low but significantly higher than sodium fluorescein.	+
147	[(1S,2R)-Acpc]^2-Endomorphin 2	1.48E-05	1	1	101	Relatively low BBB permeability.	+
148	[(1S,2R)-Achc]^2-Endomorphin 2	1.51E-05	1	1	101	Relatively low BBB permeability.	+

ID	Peptide Name	P (cm/s)	BBB influx class	BBB influx response	PubID (Brainpeps)	Comment author	Correspond?
189	[D-Ala^{2},Ser^{4},D-Val^{5}]deltorphin	1.95E-05	2	3	132	Able to cross the *in vitro* BBB. Have lower permeability compared to parent peptide.	+
190	[D-Ala^{2},Ser^{4},D-Ala^{5}]deltorphin	2.35E-05	2	3	132	Able to cross the *in vitro* BBB. Have lower permeability compared to parent peptide.	+
191	[D-Ala^{2},Gln^{4},D-Val^{5}]deltorphin	1.12E-05	1	1	132	Able to cross the *in vitro* BBB. Have lower permeability compared to parent peptide.	-
192	[D-Ala^{2},Gln^{4},D-Ala^{5}]deltorphin	1.30E-05	1	1	132	Able to cross the *in vitro* BBB. Have lower permeability compared to parent peptide.	-
193	[Arg^{-1},Arg^{0},D-Ala^{2}]deltorphin II	2.69E-05	2	3	132	Able to cross the *in vitro* BBB. Decreased ability to cross the *in vitro* BBB compared to parent peptide.	+
194	[Arg^{0},D-Ala^{2}]deltorphin II	3.18E-05	2	3	132	Able to cross the *in vitro* BBB.	+
195	[Lys^{-1},Lys^{0},D-Ala^{2}]deltorphin II	2.35E-05	2	3	132	Able to cross the *in vitro* BBB. Decreased ability to cross the *in vitro* BBB compared to parent peptide.	+
196	[Lys^{0},D-Ala^{2}]deltorphin II	1.42E-05	1	1	132	Able to cross the *in vitro* BBB. Decreased ability to cross the *in vitro* BBB compared to parent peptide.	-
197	[Ala^{-1},Pro^{0},D-Ala^{2}]deltorphin II	2.90E-05	2	3	132	Able to cross the *in vitro* BBB. Similar ability to cross the *in vitro* BBB compared to parent peptide.	+
198	[Pro^{-1},Pro^{0},D-Ala^{2}]deltorphin II	3.70E-05	3	5	132	Able to cross the *in vitro* BBB. Similar ability to cross the *in vitro* BBB compared to parent peptide.	+
199	[Abu^{-1},Abu^{0},D-Ala^{2}]deltorphin II	4.88E-05	3	5	132	Able to cross the *in vitro* BBB. Similar ability to cross the *in vitro* BBB compared to parent peptide.	+
201	DPLPE-Phe-NH_2	2.78E-05	2	3	134	Shows passage across BBMEC monolayers.	+
202	DPLPE-Phe-OH	1.95E-05	2	3	134	Shows passage across BBMEC monolayers.	+
203	p-[Cl-Phe^{4}]DPLPE-Phe	8.33E-05	4	7	134	Show enhanced *in vitro* BBB permeability compared to the parent peptides, which shows passage across BBMEC monolayers.	+
204	p-[Br-Phe^{4}]DPLPE-Phe	5.56E-05	3	5	134	Shows enhanced *in vitro* BBB permeability compared to the parent peptides, which shows passage across BBMEC monolayers.	+

ID	Peptide Name	P (cm/s)	BBB influx class	BBB influx response	PubID (Brainpeps)	Comment author	Correspond?
205	p-[F-Phe^4]DPLPE-Phe	2.08E-05	2	3	134	No significantly different *in vitro* BBB permeability compared to the parent peptide which shows passage across BBMEC monolayers.	+
206	p-[I-Phe^4]DPLPE-Phe	1.67E-05	1	1	134	No significantly different *in vitro* BBB permeability compared to the parent peptide which shows passage across BBMEC monolayers.	-
207	Guanidino-Endomorphin II	5.42E-05	3	5	135	Shows similar permeability compared to Endomorphin II, which traverses the *in vitro* BBB.	+
208	Morphiceptin	3.06E-05	2	3	135	Morphiceptin showed no significant difference in permeability compared to Endomorphin II, which traverses the *in vitro* BBB.	+
209	Guanidino-Morphiceptin	6.70E-05	3	5	135	Shows increased permeability compared to Morphiceptin, which traverses the *in vitro* BBB.	+
210	Phe0-DPDPE	9.66E-05	4	7	136	Shows higher BBB permeability coefficient than the parent peptide DPDPE (or DPLCE), which shows *in vitro* BBB permeability.	+
211	DPDPE-Phe	8.61E-05	4	7	136	Shows higher BBB permeability coefficient than the parent peptide DPDPE (or DPLCE), which shows *in vitro* BBB permeability.	+
212	DPDPE-Arg-Gly	1.01E-04	4	7	136	Shows higher BBB permeability coefficient than the parent peptide DPDPE (or DPLCE), which shows *in vitro* BBB permeability.	+
213	DPDPE-Phe-Ala-NH-$(CH_2)_5$-CONH2	8.33E-05	4	7	136	Shows higher BBB permeability coefficient than the parent peptide DPDPE (or DPLCE), which shows *in vitro* BBB permeability.	+
214	DPLCE	9.39E-05	4	7	136	Shows higher BBB permeability coefficient than the parent peptide DPDPE (or DPLCE), which shows *in vitro* BBB permeability.	+
215	DPLCE-Arg-Pro-Ala	9.14E-05	4	7	136	Shows higher BBB permeability coefficient than the parent peptide DPDPE (or DPLCE), which shows *in vitro* BBB permeability.	+

ID	Peptide Name	P (cm/s)	BBB influx class	BBB influx response	PubID (Brainpeps)	Comment author	Correspond?
218	SNX-194	1.08E-05	1	1	138	Structural analogs of Ziconotide show permeation.	-
219	SNX-231	1.32E-05	1	1	138	Structural analogs of Ziconotide show permeation.	-
220	SNX-185	1.45E-05	1	1	138	Structural analogs of Ziconotide show permeation.	-

Table S4: Classification $P_{in\ vivo}$ data.

	Lower Limit (cm/s)	Upper limit (cm/s)		BBB_{in} response
Class 1	0.00E+00	4.75E-08	*included*	**1**
Class 2	4.75E-08	9.50E-08	*included*	**3**
Class 3	9.50E-08	4.34E-07	*included*	**5**
Class 4	4.34E-07	5.65E-07	*included*	**7**
Class 5	5.65E-07	∝		**9**

ID	Peptide name	$P_{in\ vivo}$ (cm/s)	BBB influx class	BBB_{in} response	PubID (Brainpeps)	Comment author	Correspond?
37	Biphalin	3.90E-07	3	5	91	Significant influx into brain.	+
69	p-[Cl-Phe$^{4'4'}$] biphalin	5.65E-07	4	7	91	Significant influx into brain, but higher than biphalin.	-
90	DADLE	5.00E-08	2	3	107, 108	P_{app} across BBB was very low.	+
142	AOA-DADLE	1.20E-07	3	5	107, 108	Poor permeation.	+
143	CA-DADLE	4.00E-08	1	1	107, 108	Poor permeation.	+
144	OMCA-DADLE	7.00E-08	2	3	107, 108	Poor permeation.	+

Table S5: Calculation median BBB_{in} response.

ID	Name	BBB influx response				
		K_{in} (MTR)	K_{in} (Perfusion)	$P_{in\ vitro}$	$P_{in\ vivo}$	Median BBB_{in} response[1]
6	Vapreotide; RC-160	1	-	-	-	1
7	CRH	3	-	-	-	3
8	PACAP 27	9	-	-	-	9
9	PACAP 38	9	9	-	-	9
10	VIP	5	3	-	-	4
11	Neuropeptide Y	3	-	-	-	3
14	Orexin A	3	-	-	-	3
16	Exendin-4	5	9	-	-	7
17	F^{13}, Y^{19}-MCH	1	1	-	-	1
18	Deltorphin I	-	-	5	-	5
19	Deltorphin II	-	-	5	-	5
21	Adrenomedullin	5	1	-	-	3
22	Urocortin-I	1	1	-	-	1
23	Insulin	5	-	-	-	5
25	Ghrelin	3	-	-	-	3
27	Amylin	6	-	-	-	6
28	[Tyr^{10}] Secretin-27	7	5	-	-	6
29	[Met^{5}] Enkephalin	-	-	4	-	4
31	Endomorphin-1	7	-	-	-	7
32	Endomorphin-2	7	-	3	-	5
37	Biphalin	-	3	7	5	5
38	DPDPE	-	3	5	-	4
39	[Glu^{4}]Deltorphin	-	-	5	-	5
40	SAM 995	-	3	-	-	3
41	SAM 1095	-	3	-	-	3
47	Pancreatic Polypeptide	7	-	-	-	7
55	Epidermal Growth Factor	7	-	-	-	7
57	[Met(O)67]CART-(55-102)	5	-	-	-	5
58	Mahogany (1377-1428)	5	-	-	-	5
59	Urocortin II	5	9	-	-	7
61	LHRH	-	7	-	-	7
64	Des-Octanoyl Ghrelin	-	1	-	-	1
66	Peptide YY (3-36)	5	3	-	-	4
69	p-[Cl-$Phe^{4'4'}$] biphalin	-	5	7	7	7
72	[p-ClPhe^{4}] DPDPE	-	-	7	-	7
74	CTAP	1	3	-	-	2
83	cHP	1	-	-	-	1
90	DADLE	-	-	-	3	3
93	DAMGO	5	-	-	-	5
100	TAPA	3	-	-	-	3

ID	Name	BBB influx response				
		K_{in} (MTR)	K_{in} (Perfusion)	$P_{in\ vitro}$	$P_{in\ vivo}$	Median BBB_{in} response[1]
104	TAPS	1	-	-	-	1
105	TAPP	7	-	-	-	7
106	CTOP	3	-	-	-	3
110	Dermorphin	3	-	-	-	3
113	Obestatin (mouse)	7	-	-	-	7
114	P41	3	-	-	-	3
115	P42	3	-	-	-	3
116	P43	1	-	-	-	1
117	Sb-Aba	5	-	-	-	5
121	Api88	3	-	-	-	3
122	Apidaecin Api137	5	-	-	-	5
130	Agouti-Related Protein (83-132)	1	-	-	-	1
131	RC-121	1	-	-	-	1
132	RC-161	3	-	-	-	3
134	(3-methyl-His^2)Thyrotropin-releasing Hormone	7	-	-	-	7
135	SKB P5	1	-	-	-	1
136	AN110	3	-	-	-	3
137	Dmt^1-Endomorphin 2	-	-	1	-	1
139	ADAB	1	-	-	-	1
140	ADAMB	1	-	-	-	1
141	cationic AVP_{4-9}	3	-	-	-	3
142	AOA-DADLE	-	-	-	5	5
143	CA-DADLE	-	-	-	1	1
144	OMCA-DADLE	-	-	-	3	3
147	$[(1S,2R)\text{-Acpc}]^2$-Endomorphin 2	-	-	1	-	1
148	$[(1S,2R)\text{-Achc}]^2$-Endomorphin 2	-	-	1	-	1
154	Oncocin	5	-	-	-	5
155	Drosocin	5	-	-	-	5
156	Drosocin Pro5Hyp	3	-	-	-	3
157	LinS	5	-	-	-	5
158	LinNMe	1	-	-	-	1
159	CycS	1	-	-	-	1
160	CycNMe	3	-	-	-	3
168	SynB3	5	-	-	-	5
169	Tat 47-57	7	-	-	-	7
170	pVEC	9	-	-	-	9
171	Transportan 10	1	-	-	-	1
172	TP10-2	3	-	-	-	3
173	D-[Ala^1]-peptide T-amide	9	-	-	-	9
174	$Neurotensin_{8-13}$ analog	5	-	-	-	5

ID	Name	BBB influx response				
		K_{in} (MTR)	K_{in} (Perfusion)	$P_{in\ vitro}$	$P_{in\ vivo}$	Median BBB_{in} response[1]
177	Arginine Vasopressin	-	5	-	-	5
185	N-Tyr-MIF-1	-	7	-	-	7
186	MIF-1	9	-	-	-	9
187	β-Amyloid$_{1-28}$	5	-	-	-	5
189	[D-Ala^2,Ser^4,D-Val^5]deltorphin	-	-	3	-	3
190	[D-Ala^2,Ser^4,D-Ala^5]deltorphin	-	-	3	-	3
191	[D-Ala^2,Gln^4,D-Val^5]deltorphin	-	-	1	-	1
192	[D-Ala^2,Gln^4,D-Ala^5]deltorphin	-	-	1	-	1
193	[Arg^{-1},Arg^0,D-Ala^2]deltorphin II	-	-	3	-	3
194	[Arg^0,D-Ala^2]deltorphin II	-	-	3	-	3
195	[Lys^{-1},Lys^0,D-Ala^2]deltorphin II	-	-	3	-	3
196	[Lys^0,D-Ala^2]deltorphin II	-	-	1	-	1
197	[Ala^{-1},Pro^0,D-Ala^2]deltorphin II	-	-	3	-	3
198	[Pro^{-1},Pro^0,D-Ala^2]deltorphin II	-	-	5	-	5
199	[Abu^{-1},Abu^0,D-Ala^2]deltorphin II	-	-	5	-	5
201	DPLPE-Phe-NH_2	-	-	3	-	3
202	DPLPE-Phe-OH	-	-	3	-	3
203	p-[Cl-Phe^4]DPLPE-Phe	-	-	7	-	7
204	p-[Br-Phe^4]DPLPE-Phe	-	-	5	-	5
205	p-[F-Phe^4]DPLPE-Phe	-	-	3	-	3
206	p-[I-Phe^4]DPLPE-Phe	-	-	1	-	1
207	Guanidino-Endomorphin II	-	-	5	-	5
208	Morphiceptin	-	-	3	-	3
209	Guanidino-Morphiceptin	-	-	5	-	5
210	Phe^0-DPDPE	-	-	7	-	7
211	DPDPE-Phe	-	-	7	-	7
212	DPDPE-Arg-Gly	-	-	7	-	7
213	DPDPE-Phe-Ala-NH-$(CH_2)_5$-$CONH_2$	-	-	7	-	7
214	DPLCE	-	-	7	-	7
215	DPLCE-Arg-Pro-Ala	-	-	7	-	7
216	Insulin detemir	1	1		-	1
217	Ziconotide	-	5		-	5
218	SNX-194	-	-	1	-	1
219	SNX-231	-	-	1	-	1
220	SNX-185	-	-	1	-	1

[1] Example of calculation of median BBB_{in} response, see below.

Example calculation median BBB_{in} response of Urocortin I (ID 22):

- K_{in} (MTR): more than one value available: $K_{in} = 1.68 \cdot 10^{-4}$ ml/(g × min) and $K_{in} = 0$ ml/(g × min). Both results correspond with class 1, thus a BBB_{in}-response of 1. The median BBB_{in}-response of Urocortin I for the K_{in} (MTR) response type equals 1.
- K_{in} (Perfusion): one result available: $K_{in} = 8.60 \cdot 10^{-4}$ ml/(g × min), which corresponds with a BBB_{in}-response of 1.
- No data available for Urocortin I for $P_{in\ vitro}$ and $P_{in\ vivo}$ responses.

⇨ The median BBB_{in}-response of Urocortin equals the median of the BBB_{in}-response of the K_{in} (MTR) response (calculated to be 1) and of the K_{in} (Perfusion) response (calculated to be 1) and is 1.

CHAPTER IV

QUALITY CONTROL OF CATIONIC CELL-PENETRATING PEPTIDES

"Quality is never an accident,
it is always the result of intelligent effort."

John Ruskin
(°1819 - †1900, English writer and critic of art and architecture)

Parts of this chapter were published:

Stalmans S, Gevaert B, Verbeke F, D'Hondt M, Bracke N, Wynendaele E, De Spiegeleer B. Quality control of cationic cell-penetrating peptides. *J. Pharmaceut. Biomed.* 2016; **117**: 289-297.

ABSTRACT

During fundamental research, it is recommended to evaluate the test compound identity and purity in order to obtain reliable study outcomes. For peptides, quality control (QC) analyses are routinely performed using reversed-phase liquid chromatography coupled to an ultraviolet (UV) detector system. These traditional QC methods, using a C_{18} column and a linear gradient with formic acid (FA) as acidic modifier in the mobile phase, might not result in optimal chromatographic performance for basic peptides due to their cationic nature and hence may lead to erroneous results. Therefore, the influence of the used chromatographic system on the final QC results of basic peptides was evaluated using five cationic cell-penetrating peptides and five C_{18}-chromatographic systems, differing in the column particle size (high performance liquid chromatography (HPLC) versus ultra-high performance liquid chromatography (UHPLC)), the acidic modifier (FA versus trifluoroacetic acid (TFA)), and the column temperature (30°C versus 60°C). Our results indicated that a UHPLC system with the C_{18} column thermostated at 30°C and a mobile phase containing TFA, was the most suitable routine QC analysis method for cationic peptides, outperforming the other systems in sensitivity and resolution. We also demonstrated the applicability of a single quad mass spectrometry (MS) detector system during QC analysis of (cationic) peptides, allowing identification of the peptide and its impurities, as well as the evaluation of the peak purity.

CHAPTER IV

QUALITY CONTROL OF CATIONIC CELL-PENETRATING PEPTIDES

Main focus in this chapter:

- To find a suitable reversed-phase C_{18} chromatographic analysis method for identification and purity profiling of cationic cell-penetrating peptides that are used for the evaluation of their BBB transport characteristics.
- To illustrate that the used chromatographic system determines the quality control conclusions.
- To demonstrate the use of a single quad mass spectrometry detector during routine quality control of (cationic) peptides.

1. RELEVANCE OF QUALITY CONTROL OF PEPTIDES DURING BIOCHEMICAL RESEARCH

During fundamental research, pharmaceutical regulatory guidelines do not (yet) apply. However, in order to obtain reliable research outcomes, quality assurance practices should already be employed during the early research phase [1,2]. In a later stage, when following Good Laboratory Practices (GLP), proper characterization of the test compound is mandatory prior to perform studies [3]. During quality control (QC) of peptides, the identity is verified and the presence of impurities is evaluated in order to quantify and qualify the peptide purity. For ligand binding assays, *in vitro* bioassays and *in vivo* studies, the total amount of peptide impurities is recommended to be lower than 5% [4]. Synthetic peptides can be chemically synthesized using Solid-Phase Peptide Synthesis (SPPS), in which amino acids are linked during individual, consecutive coupling steps, ultimately resulting in the desired peptide sequence [5]. During the synthesis process, the C-terminus of the peptide is covalently linked to a solid support matrix. The N-terminus of the attached amino acid reacts with incoming amino acids, which are N-α-protected, to form a covalent peptide bond. The N-α-protection group, of which the 9-fluorenylmethoxycarbonyl group (Fmoc) is the most widely used, avoids undesired reactions during peptide synthesis [5]. Structurally related synthesis impurities encompass amino acid deletion or insertion, incomplete removal of protection groups, oxidation or

reduction of amino acid residues, diastereoisomerization, dimers and oligomers, as well as side and end chain impurities [5]. In literature, several examples are available in which the presence of related peptide impurities complicate the interpretation of study results or cause erroneous study conclusions [6-9]. Moreover, the major peak found during QC analysis of peptide batches was not always the ordered peptide as already demonstrated for the quorum sensing peptide CVFSLFKKCN and obestatin, emphasizing the importance of thorough identification and purity evaluation of the test compound prior to performing biomedical experiments [4,10].

In this study, the quality aspects of a set of five cell-penetrating peptides (CPPs) will be evaluated. Cell-penetrating peptides are a particular group of peptides, being able to cross cellular barriers without causing significant membrane damage [11]. In **Chapter II**, it was already demonstrated that these peptides are a chemically diverse group of peptides, but are mostly characterized by a cationic nature, like for the selected peptides of this study, *i.e.* SynB3, Tat 47-57, pVEC, TP10 and TP10-2 (Table 1) [12]. The evaluation of the purity of CPPs used during cellular uptake studies is often ignored throughout literature, which can be an explanation for the discrepancy in study results. Analytical systems for quantification of CPPs described in literature comprise high performance liquid chromatographic (HPLC) analysis of fluorescently labeled or chemically modified CPPs [13,14] or the matrix-assisted laser desorption-time of flight mass spectrometry (MALDI-TOF MS) for which no chromatographic separation is required [15]. Thus, analytical separation systems for analysis of unmodified CPPs are hardly described up till now.

Table 1: Peptide information.

Peptide	Sequence	MW (Da)	pI[1]
SynB3	RRLSYSRRRF-NH_2	1395.7	11.5
Tat 47-57	YGRKKRRQRRR-NH_2	1558.9	11.7
pVEC	LLIILRRRIRKQAHAHSK-NH_2	2208.8	11.6
TP10	AGYLLGKINLKALAALAKKIL-NH_2	2181.8	10.4
TP10-2	AGYLLGKINLKPLAALAKKIL-NH_2	2207.8	10.4
R9	RRRRRRRRR-NH_2	1422.7	12.0

[1]Iso-electric point as calculated using MarvinSketch 5.10.3 (ChemAxon, Budapest, Hungary).

Standard in-house QC evaluation of the peptides traditionally includes a chromatographic system using a C_{18} column on which a linear gradient is run using a mobile phase containing 0.1% (m/V) formic acid (FA) in water and acetonitrile. Formic acid is preferred as acidic modifier as it is more directly compatible with MS detection systems. However, for cationic peptides, it is known that detrimental interactions with the surface silanols of reversed-phase columns occur, resulting in peak tailing and poor efficiency. The positive peptide charge, present in the acidified mobile phase, causes a low retention and poor resolution as well. Therefore, trifluoroacetic acid (TFA), a highly acidic strong ion-pairing agent, is preferred to adjust the retention and efficiency of cationic peptide

analysis [16-18]. During QC analysis of peptides, differences between the peptide purity reported by the supplier on the certificate of analysis and the results obtained by the biomedical laboratory are often observed, which are attributed to different analytical methods for example the use of HPLC versus UHPLC columns [4,19]. The latter are packed with sub 2 µm particles and outperform HPLC columns in separation efficiency and sensitivity due to sharper and higher peaks, which might explain the deviating purity results [19]. To evaluate the influence of the used chromatographic system on the conclusions made during routine peptide QC analysis, five different chromatographic systems were compared with regards to their QC result conclusions (Figure 1).

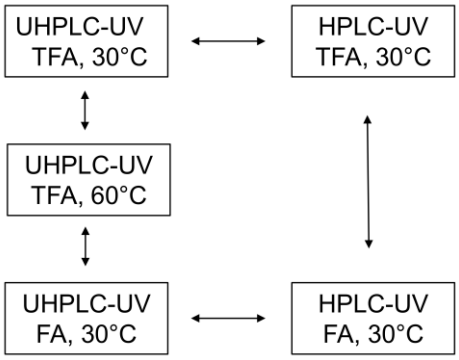

Figure 1: Overview of the five chromatographic systems for QC analysis of CPPs.

The chromatographic systems, all coupled to BEH C_{18} columns, differed in the particle size (HPLC versus UHPLC), the used acidic modifier (FA versus TFA), as well as in the column temperature (30°C versus 60°C). The results indicate that the used chromatographic system influences the (cationic) peptide purity results and affects the apparent impurity profile. The applicability of a GLP/GMP (good manufacturing practices)-compliant single quad MS detection system for routine QC analysis of (cationic) peptides is also demonstrated.

2. CHROMATOGRAPHIC SYSTEMS USED FOR QUALITY CONTROL OF CELL-PENETRATING PEPTIDES

Chemicals and reagents

The “traditional” CPPs were obtained from different suppliers: SynB3, Tat 47-57, pVEC and nona-arginine (R9) were ordered at LifeTein LLC (Somerset, USA) and TP10 and TP10-2 at Caslo ApS (Lyngby, Denmark) with a minimal requested purity of 95%. The sequences of the peptides are given in Table 1. The short, proline-rich antimicrobial peptides (PrAMPs, Prof. Ralf Hoffmann), *i.e.* apidaecin Api137, oncocin, drosocin and drosocin Pro5Hyp, and disulfide-rich (cyclic) peptides (Prof. David Craik), *i.e.* MCoTI-II, cVc1.1 and chlorotoxin, were provided by a collaborating research group.

Peptides were synthesized using a standard Fmoc-SPPS method. For chromatographic analysis, ultrapure water (18.2 MΩ × cm and TOC < 5 ppb) was produced using an Arium Pro VF TOC water purification system (Sartorius, Vilvoorde, Belgium). The UHPLC-MS grade reagents, *i.e.* acetonitrile, 2-propanol, TFA and FA, were purchased at Biosolve (Valkenswaard, The Netherlands), HPLC gradient grade acetonitrile at Fisher Chemical (Erembodegem, Belgium), and FA (LC-MS grade), TFA (LC-MS grade) and propionic acid at Sigma-Aldrich (Diegem, Belgium). HPLC/UHPLC glass vials and inserts were bought at Waters (Zellik, Belgium).

QC purity profiling of "traditional" cell-penetrating peptides

The HPLC chromatographic system consisted of a Waters Alliance 2695 separations module and Waters 2996 photodiode array (PDA) detector equipped with Empower 2 software for data acquisition. The UHPLC analyses were conducted on a Waters Acquity H-class UPLC® apparatus consisting of a quaternary solvent manager, an automatic sample injection system, combined with a flow through needle, a column heater and a UPLC®-PDA detector, with Empower 3 FR 2 software for data acquisition. A BEH C_{18} 130 Å column (XBridge (HPLC, 4.6 × 250 mm, 5 µm) or Acquity (UHPLC, 2.1 mm × 100 mm, 1.7 µm) both from Waters) was selected and the ratio of the column length and particle diameter (L/d_p) was the same for the HPLC and UHPLC column. A linear gradient separation was performed using a mobile phase consisting of 0.1% (m/V) of FA or 0.1% (V/V) TFA in water (A) and acetonitrile (B) running from 5% B to 60% B in 15 column volumes. Acetonitrile is used as organic modifier, being the generally preferred "solvent B" for peptides showing a lower viscosity and higher elution strength than methanol [20,21]. The gradient was preceded by an isocratic hold of three times the dwell volume of the chromatographic system. After running the gradient, the column was allowed to re-equilibrate during 10 column volumes. The sample compartment was thermostated at 5°C and the column temperature was maintained at 30°C or 60°C. For HPLC, the injection volume was 20 µl and the flow rate was 1.0 ml/min, while for UHPLC, the injection volume was 2 µl and the flow rate 0.6 ml/min, as determined following Guillarme *et al.* in order to obtain similar retention factors and resolution for both chromatographic systems [22]. UV detection was performed from 190-400 nm, with quantification at 215 nm. Lyophilized peptides were dissolved in an acidified (0.1% FA (m/V)) mixture of water and acetonitrile (95:5, V/V) to obtain a 1 mg/ml solution. The used solvent was analyzed as blank as well. During each sample set, one CPP was analyzed in duplicate, *i.e.* as first and last sample, to evaluate the performance of the chromatographic system. Impurities were quantified using the normalization procedure: the percentage ratio of the peak area of the impurity and the area of the highest peak was calculated. For calculation of the peptide purity, the ratio of the peak area of the peptide and the total area of observed peaks, corrected for solvent and system

peaks present in the blank chromatogram as well as impurities below the reporting threshold of 0.1% according to the European Pharmacopoeia (Ph. Eur.) [23], was calculated and multiplied by 100. In total, five chromatographic systems were evaluated as shown in Figure 1.

Evaluation of the chromatographic performance

To compare quantitatively the performance of the chromatographic systems, the limit of detection (LOD), equivalent to a signal-to-noise ratio of three, and the peak capacity were calculated. The peak capacity is a measure for the performance of a gradient separation, representing the number of peaks that can be resolved per unit of time [24]. The used formulas are given in Table 2.

Table 2: Response factors used to quantitatively evaluate the chromatographic performance of the (U)HPLC-UV systems.

Response factor	Formula[1]
Limit of detection (LOD) (ng)	$\frac{3 \times \text{concentrat ion} \times \text{injection volume}}{S/N}$
Peak capacity (n_p)	$1 + \frac{t_g}{1/n \times \sum_1^n w_h}$
Number of impurity peaks above reporting threshold	number > RT (0.1%)

[1]S/N = signal-to-noise ratio = 2H/h according to Ph. Eur. [25], with H = height of the peptide peak, measured from the peak maximum to the extrapolated baseline and h = height of the noise in a chromatogram obtained after injection of a blank sample, *i.e.* without peptide; t_g = gradient run time; n = number of peaks selected for calculation (*i.e.* 3: one at the beginning and the end of the gradient and the native peptide peak); w_h = peak width at half peak height and RT = reporting threshold of 0.1% (Ph. Eur.).

Both the peptide concentration, 1 mg/ml, as well as the injection volume, *i.e.* 2 µl for the UHPLC system and 20 µl for the HPLC system, were taken into account to calculate the LOD (Table 2). Beside these chromatographic response factors, the number of impurity peaks above the reporting threshold of 0.1% (Ph. Eur.) were counted as well to evaluate the chromatographic performance.

Identification of the main peak and impurities of cell-penetrating peptides

Mass spectrometric identification of the observed main peak and the impurities was performed using a HPLC-UV/MS system consisting of a Spectra System SN4000 interface, a Spectra System SCM1000 degasser, a Spectra System P1000XR pump, a Spectra System AS3000 autosampler, a Finnigan LCQ Classic ion trap mass spectrometer in positive ion mode (all Thermo, San José, CA, USA) and Waters 2487 dual wavelength UV detector, equipped with XCalibur 2.0 software (Thermo). Electrospray ionization (ESI) was conducted using a needle voltage of 4.5 kV. Nitrogen was used as the sheath and auxiliary gas with the heated capillary temperature set at 250°C. Peptide identification was performed based on *m/z* values with an abundance higher than 30% in the MS^1 spectra (*m/z* 100-2000) using the data dependent MS^2 spectra, *i.e.* from high abundant *m/z* in MS^1. The

ProteinProspector software (University of California, San Francisco, USA) was used to calculate the theoretical MS^2 fragmentation pattern according to Roepstorff and Fohlman [26], which is used to confirm peptide and/or impurity identification. The same HPLC method was used as described earlier, with FA as acidic modifier in the mobile phase. As Tat 47-57 did not show retention using this chromatographic system, a Prevail Organic Acid (Grace (Lokeren, Belgium), 4.6 × 250 mm, 5 µm) column was used instead, allowing to start the linear gradient at 100% A, which was also lowered to 40% using a linear gradient in 15 column volumes. All other parameters remained the same.

The UHPLC system using TFA as acidic modifier in the mobile phase, was coupled to a single quad MS detection system, consisting of a Waters Acquity isocratic solvent manager and a Waters Acquity QDa detector equipped with an ESI interface. The eluting mobile phase was split towards both the PDA and QDa detection system (ratio 10/1). The portion going to the QDa was diluted with 40:10:50 water:propionic acid:propanol (V/V/V) at a flow rate of 0.35 ml/min to obtain sufficient flow to the detector and allowing a post-column TFA displacement from the peptide resolving the TFA ion suppression effect, also referred to as TFA-fix method [27,28]. The QDa detector was operated in positive ion mode with the ESI capillary voltage set at +0.8 kV and the cone voltage at 15 V. The probe temperature was 600°C. A full mass spectrum between *m/z* 100 and 1250 was acquired at a sampling rate of 2.0 points/s.

3. QUALITY OF CELL-PENETRATING PEPTIDES

Purity of the "traditional" cell-penetrating peptides

The purity of the five CPPs was calculated based on the chromatograms obtained using the five chromatographic systems differing in the BEH C_{18} column particle size (HPLC versus UHPLC), the used acidic modifier in the mobile phase (FA versus TFA) and column temperature (30°C versus 60°C) (Table 3). Standard deviations of duplicated injections ranged between 0.12% and 0.42%.

Table 3: QC purity results of the CPPs obtained using five different chromatographic systems (UV detection at 215 nm).

Chromatographic system	Peptide purity				
	SynB3	**Tat 47-57**	**pVEC**	**TP10**	**TP10-2**
CoA[1]	95.2%	95.9%	98.7%	96.7%	98.8%
UHPLC, TFA, 30°C	95.6%	99.9%	94.9%	94.6%	99.2%
UHPLC, TFA, 60°C	95.4%	99.8%	95.2%	89.0%	99.5%
UHPLC, FA, 30°C	95.4%	-[2]	97.1%	94.1%	99.5%
HPLC, TFA, 30°C	94.4%	99.2%	96.3%	90.9%	98.5%
HPLC, FA, 30°C	94.3%	-[2]	-[3]	96.7%	99.7%

[1]Purity provided by the supplier on the certificate of analysis (CoA).
[2]No retention observed in the concerned chromatographic system.
[3]Poor chromatography was obtained, not allowing to draw a substantiated conclusion on the purity of the peptide. If the automatic forced drop integration mode was used to integrate the obtained peptide peak, an erroneous purity result of 60.8% would have been calculated.

The results presented in Table 3 indicate that the same conclusions could be drawn regarding the peptide purity for TP10-2 independent of the used system. For SynB3, the calculated purity obtained using the five different chromatographic systems ranged between 94 and 95%. Based on the purity results of the HPLC chromatographic systems, the purity of the SynB3 peptide was below 95%. When pVEC was analyzed using the HPLC-FA (30°C) system, poor chromatographic performance was obtained, which did not allow to quantify its purity. Based on the other chromatographic systems, the purity of pVEC ranged between 95% and 97%, hence fulfilling its purity requirements. For TP10, two chromatographic systems resulted in a purity of approximately 90%, while the other three results gave a purity of approximately 95%. Overall, for some of the cationic CPPs, different QC conclusions could be drawn depending on the used chromatographic system. Therefore, the general adagium that (peptide) purity results should always be specified by the used chromatographic method, clearly also strongly applies to cationic CPPs.

The peptides were positively identified using the MS^1 and MS^2 spectra using ESI-ion trap MS, based on their molecular mass and the presence of typical b- and y-fragments. The annotated MS spectra of the investigated CPPs can be retrieved in the Supporting Information (Figure S1).

Purity of the short, proline-rich antimicrobial and disulfide-rich (cyclic) peptides

The PrAMPs, *i.e.* apidaecin Api137, oncocin, drosocin and drosocin Pro5Hyp and the disulfide-rich (cyclic) peptides, *i.e.* MCoTI-II, cVc1.1 and chlorotoxin, were investigated as part of collaboration project with external research groups. The QC of these peptides, which also possess cell-penetrating properties, was performed by the collaborating lab. Raw chromatographic data and the used methods were provided and critically reviewed at arrival. For all peptides, the main peaks present in the HPLC chromatograms were identified as the intended peptide and the purity was above the required 95%. These peptides are hence not further analyzed.

Impurity profile of the cell-penetrating peptides

The experimentally obtained impurity profiles of the “traditional” CPPs remarkably differed between the different chromatographic systems. As an example, the obtained chromatograms of SynB3 are shown in Figure 2; the chromatograms of the other investigated CPPs can be found in the Supporting Information (Figure S2). Based on these chromatograms, TFA seems to be preferred over FA as acidic modifier, resulting in better peak resolution between the peptide and its impurities. In order to evaluate the chromatographic performance more objectively and quantitatively, the LOD, the peak

capacity, as well as the number of peaks above the reporting threshold of 0.1% were calculated (Table 4).

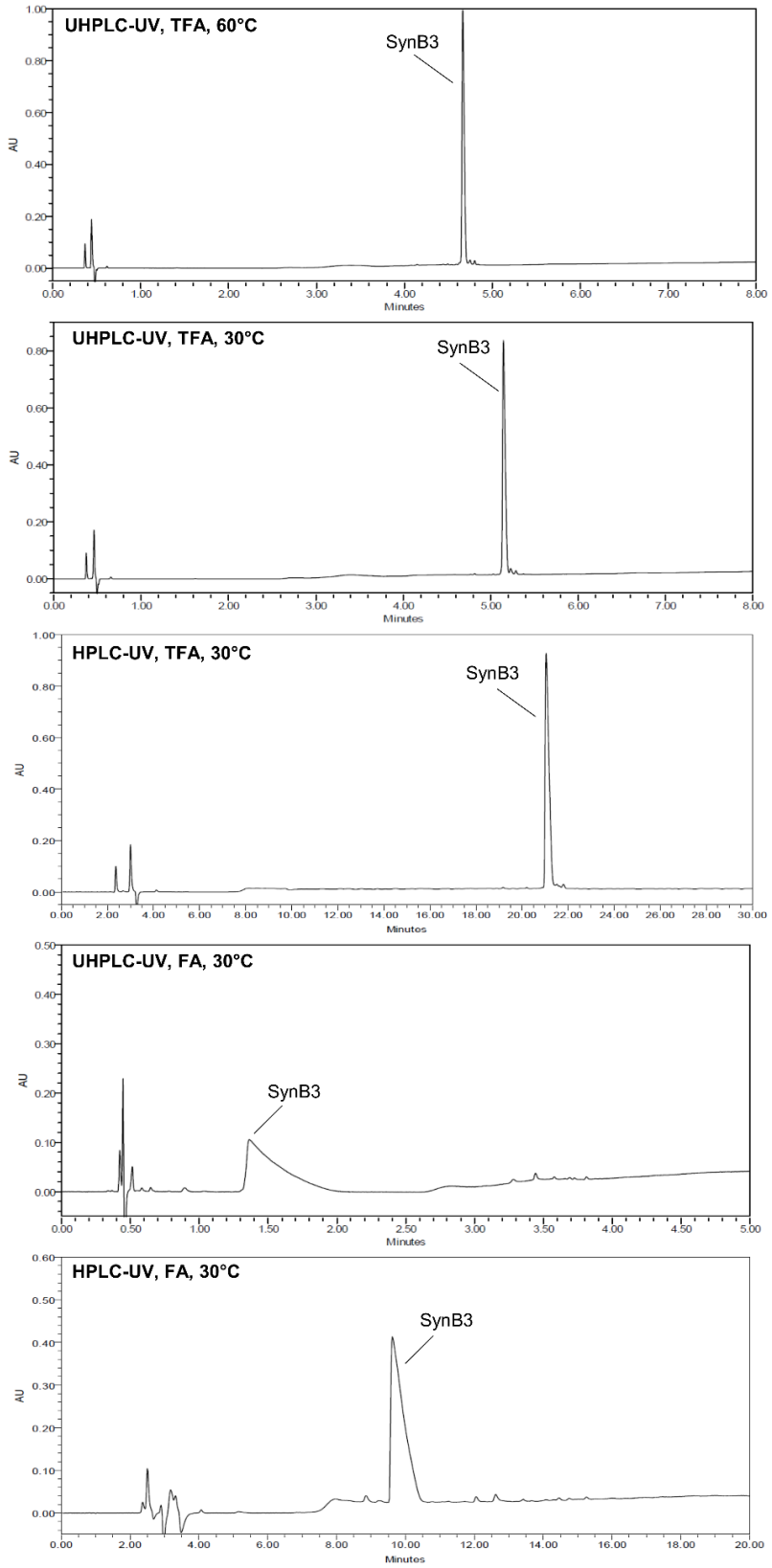

Figure 2: Impurity profile of SynB3 obtained by analyzing the peptide using five different chromatographic systems (all UV detection at 215 nm). Only the part of the chromatogram containing the peptide and impurity peaks is shown.

Table 4: Chromatographic performance of the five different chromatographic systems for the analysis of SynB3 quantitatively expressed using the limit of detection (LOD), the peak capacity and the number of peaks above the reporting threshold of 0.1% (Ph. Eur.).

Chromatographic system	LOD (ng)	Peak capacity (n_p)	Number of peaks > RT[1]
UHPLC, TFA, 30°C	1.1	430	6
UHPLC, TFA, 60°C	0.6	376	9
UHPLC, FA, 30°C	22.9	104	9
HPLC, TFA, 30°C	42.9	351	11
HPLC, FA, 30°C	498.7	278	11

[1]RT = reporting threshold (0.1% (Ph. Eur.)).

Generally, use of TFA as acidic modifier resulted in sharper peaks, with UHPLC being superior to HPLC and consequently an improved LOD. A similar conclusion can be drawn from the peak capacity or the number of peaks that can be resolved under the experimental chromatographic conditions [24]. Except for SynB3, use of TFA as acidic modifier resulted in a higher number of peaks above the reporting threshold of 0.1% compared to FA, without a significant difference between HPLC and UHPLC systems (data shown in the Supplementary Information Table S1). However, for SynB3, the number of peaks above the reporting threshold of 0.1% was significantly higher for the HPLC system compared to the UHPLC systems despite a worse LOD associated with HPLC (Table 4). A plausible explanation is the higher separation capacity of UHPLC, leading to the separation of small peaks, which individually are below the reporting threshold. When these peaks are not separated in the traditional HPLC system, they sum up, resulting in a peak above the reporting threshold, taken into account for the number of observed peaks.

UHPLC systems and TFA as acidic modifier resulted in chromatograms characterized by a better peak separation and consequently, more impurities can be distinguished. Moreover, Tat 47-57 is even not retained when FA is used in the mobile phase. Increasing the column temperature to 60°C did not result in a significant increase of the peak capacity and the LOD slightly improved. The effect of the column temperature on the retention varies among the different peptides, but can be used to optimize the selectivity of the chromatographic method [29]: increasing the column temperature results in a decrease in peptide retention due to an increased solubility in the mobile phase, a decrease in the viscosity of the mobile phase, increasing the peptide's diffusion coefficient, as well as an increase in the mass transfer between the mobile phase and the stationary phase [30,31]. For α-helical peptides heating the mobile phase also disrupts the amphipathicity of the peptides and consequently the affinity for the C_{18} stationary phase, resulting in shorter retention times [30]. Increasing the column temperature ultimately improves the kinetic efficiency and thus the separation of peptides [29,31]. However, for peptides, especially for the highly charged ones, the effect of increasing the temperature on the retention is difficult to predict as also the pK_a changes

with temperature, hence influencing charge interactions and inherently the selectivity [29,31]. Moreover, TFA shows poorer adsorption to the C_{18} stationary phase at elevated temperatures leading to less efficient ion-pairing with cationic peptides and a decrease in their retention [18]. Therefore, standard QC analysis of peptides can be operated at 30°C, but column temperature can be increased to enhance selectivity on a case-by-case evaluation. The investigated cationic CPPs did not benefit from a temperature increase.

Overall, the evaluation of the chromatographic performance of the five C_{18} chromatographic systems indicated that the UHPLC-TFA (30°C) system was the most suitable chromatographic system to perform the QC analysis of the selected cationic CPPs.

Identification of related impurities of the cell-penetrating peptides

Formic acid is routinely preferred over TFA to perform QC analysis as it is directly compatible with MS detection systems. However, we demonstrated that TFA is superior to FA during impurity profiling of the cationic CPPs being characterized by a better chromatographic performance. Recently developed GLP/GMP-compliant single quad MS detection systems are equipped to perform a post-column addition, with isopropanol and propionic acid are used to displace the ion suppressing TFA during the TFA-fix method [28]. Therefore, SynB3, having the second lowest peptide purity and a high number of impurities above the reporting threshold compared to the other CPPs, was analyzed using the UHPLC system (30°C) with TFA as acidic modifier, with the eluting mobile phase split to both the PDA detection system and the MS detection system. In Figure 3A, peak 1 corresponds with the SynB3 peptide based on obtained MS^1 spectrum. Peak 2 and 3 are the impurity peaks above the identification threshold of 0.5% (Ph. Eur.). Based on the MS^1 spectrum, peak 2 corresponds to an impurity with a mass difference of -87.22 Da compared to SynB3, indicating a deletion of one serine residue, while the mass difference of -156.26 Da of the impurity of peak 3 indicates a deletion of an arginine residue. These findings were corroborated by the MS^1 and MS^2 spectra obtained using the HPLC-UV/MS system: peak 2 corresponds to the Ser^4-deleted SynB3 peptide, while both the deletion of an arginine residue at the N- and C-terminus of SynB3 was identified. In Figure 3B, the typical b- and y-fragments of this arginine-deleted impurity are indicated.

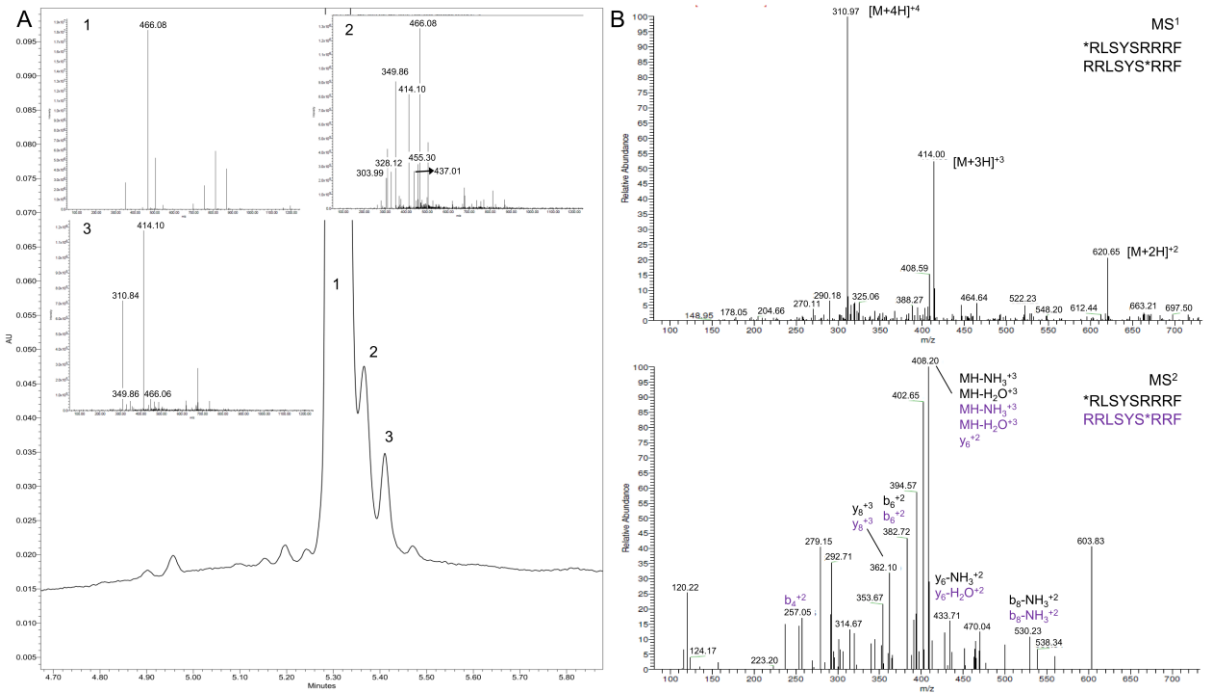

Figure 3: Application of a single quad MS detection system during routine QC analysis. (A) Obtained UV-chromatogram (215 nm) and MS^1 spectra of the peaks above the identification threshold (0.5%) after analyzing SynB3 using an UHPLC-UV/MS system. (B) MS^1 and MS^2 annotated mass spectra of the impurity of SynB3 corresponding to the arginine-deleted peptide obtained using an HPLC-UV/MS system.

Validation of the proposed QC method

In biomedical research, the highly cationic oligo-arginines are widely used CPPs. Therefore, as a validation of our proposed method for QC analysis of cationic CPPs, nona-arginine (R9) was analyzed using the UHPLC-UV/MS system with TFA as acidic modifier and the column thermostated at 30°C (Figure 4). Figure 4A demonstrates that the proposed QC method for cationic CPPs is able to separate the deletion analog(s) of R9: peak 1, the major impurity peak observed in the UV-chromatogram, was identified by this analytical system as octa-arginine (R8). The purity of the R9 sample, based on the UV (215 nm) peak areas and assuming relative response factors of 1 [32], could be quantified and estimated 92.7%.

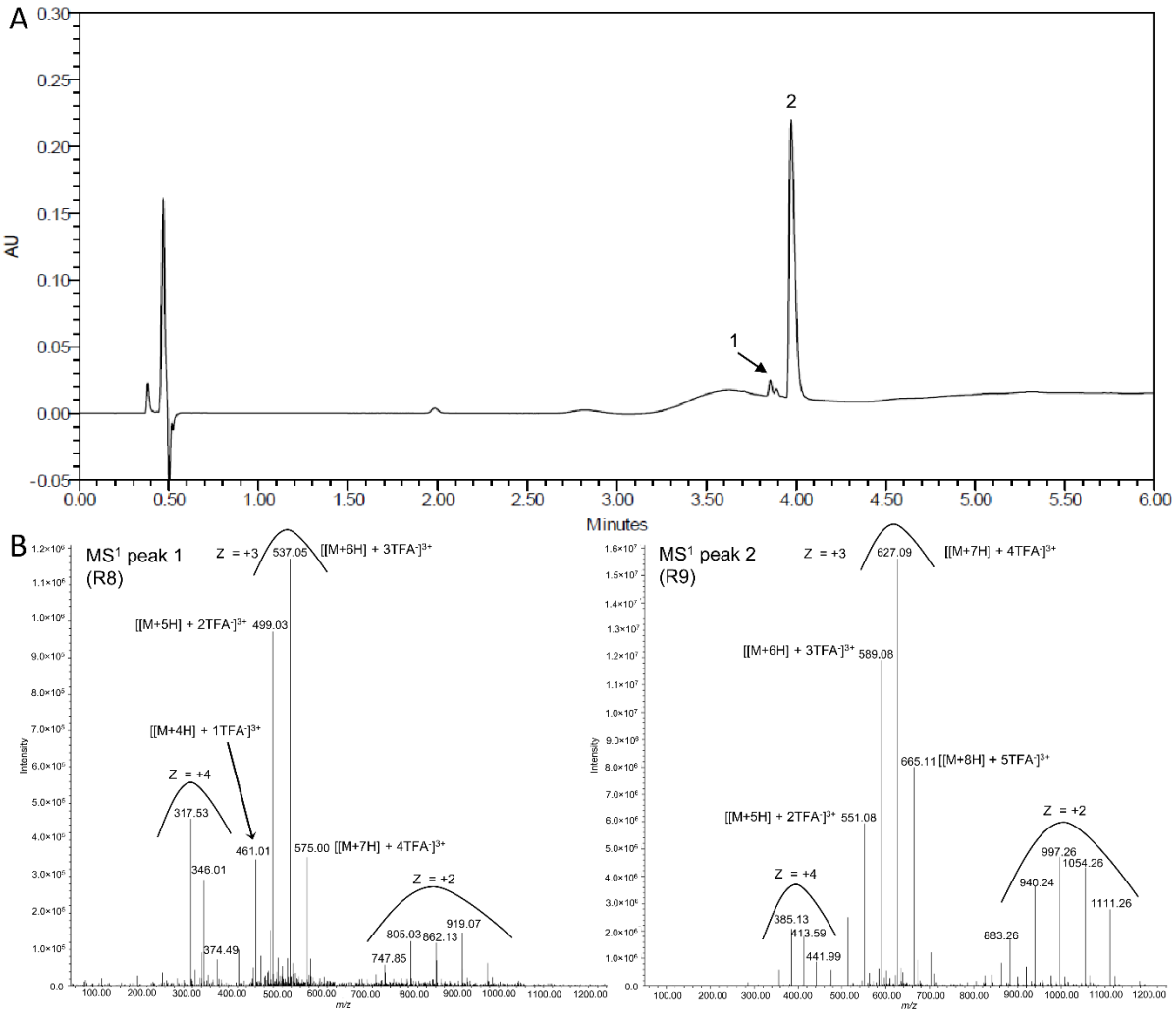

Figure 4: Quality control of R9 using an UHPLC-UV/MS system with TFA as acidic modifier in the mobile phase (30°C). (A) Chromatogram obtained using UV-detection at 215 nm. Peak 1 represents the major impurity peak; peak 2 corresponds with R9. (B) MS^1 spectra of peak 1 and 2 obtained using a single quad MS detection system. Peak 1 was identified as R8 and peak 2 as R9. The clusters of MS-observed ions represent ions in the same charge state (same z). Each cluster consists of ions with the same charge but differing in the number of attached protons and number of trifluoroacetate (TFA^-) anions forming ion pairs.

The MS^1 spectra of both R8 and R9 show an interesting pattern. Further investigation of these MS spectra revealed that each distribution of *m/z* peaks represented different charge states of ions, as indicated in the MS^1 spectrum of R9 (Figure 4B). For each charge state, multiple *m/z* peaks were present which represented the peptide in different charge states, *i.e.* $[M+nH]^{n+}$, forming ion pairs with trifluoroacetate ions (TFA^-) of the mobile phase resulting in charged ion pairs of the form $[[M+nH]^{n+} + mTFA^-]^{(n-m)+}$, with n-m representing the charge of the MS-observed ions (z). So, for each cluster of MS-observed ions with the same charge state, the difference between n (the number of protons linked to the peptide) and m (the number of TFA^- forming the ion pair) remains constant, *e.g.* for z = +2, n-m is +2. In the z = +2 cluster of de MS^1 spectrum of R9 (Figure 4B), the ion with *m/z* equal to 883.26 corresponds to the ion $[[M+5H] + 3TFA^-]^{2+}$, which is one proton and one TFA^- less than the

next ion, *i.e. m/z* equal to 940.24 representing the ion $[[M+6H] + 4TFA^-]^{2+}$. Likewise, the ions with *m/z* 997.26, 1054.26 and 1111.21 represent the ions $[[M+7H] + 5TFA^-]^{2+}$, $[[M+8H] + 6TFA^-]^{2+}$ and $[[M+9H] + 7TFA^-]^{2+}$, respectively. A similar observation was reported for proteins in the presence of non-volatile salts (*e.g.* NaCl) [33,34].

When evaluating the MS^1 spectra of SynB3 and Tat 47-57, the same pattern of distributions of ions for the different charge states was observed (see Supporting Information Figure S3). However, for these CPPs, being less cationic than R9, the non-TFA^- adducts were also present, which was absent for the R8 and R9 peptides. Thus, for the cationic CPPs, the MS spectra consist of different levels of MS-based ion distributions: apart from the isotopic envelopes, there are the mass clusters with identical charge states and finally, the different overall charge states can be observed. For the cationic CPPs, the concentration of propionic acid combined with isopropanol used during this method was not high enough to displace all TFA^- anions of the ion pair with differences observed between the different cationic CPPs.

4. DISCUSSION OF THE OBTAINED QUALITY CONTROL RESULTS

The comparison of the five C_{18}-chromatographic systems used to analyze five selected cationic CPPs, indicated that the UHPLC-TFA (30°C) system was the most suitable method for performing the QC analysis of cationic CPPs. This was validated by analyzing the highly cationic R9 peptide using the proposed QC method, which was able to separate R9 from its deletion analog R8. UHPLC chromatographic systems with TFA as acidic modifier resulted in the analytical method with the highest peak capacity and lowest LOD, which is the lowest compound concentration that can be reliably distinguished from the analytical noise and represents the sensitivity of the chromatographic method [35]. The International Conference on Harmonization (ICH) guideline on impurities in new drug products states that during impurity profiling, the used analytical method should commensurate with the level at which the impurities should be controlled [36]. For routine QC analysis of peptides, this means that the LOD is required to be lower than the reporting threshold of 0.1% when applying the Ph. Eur. Moreover, if there is only a small difference between the LOD and the reporting threshold, this can result in false negative responses as analytical data show some variability. This phenomenon also explains the observed differences in impurity profile between the evaluated chromatographic systems in this study: depending on the LOD of the method, an impurity is detected or not. These findings illustrate the need for general guidelines on developing methods for analytical characterization of peptide (drug) products as these compounds are currently excluded from most ICH guidelines because of their complex nature [37,38]. In these guidelines, the use of MS

detection systems, like single quad MS detectors, should also be encouraged. We demonstrated for SynB3 that the obtained MS^1 spectra can provide information on the identity of the observed peaks, but can also be used to evaluate the purity of the peaks, which might be a problem when analyzing cationic peptides due to poor separation [37]. For SynB3, it was suggested that impurity peaks coincide when analyzed using a HPLC system: non-separated impurity peaks sum up forming a peak above the reporting threshold of 0.1%. This has dual consequences: first, concurring peaks imply loss of information on the impurity profile of the peptide and secondly, in a pharmaceutical context, this can determine the decision on batch release or rejection. We thus demonstrated the use of single quad MS detection systems during routine QC analysis of (cationic) peptides, which are more accessible and affordable than the advanced MS detectors [39]. A major advantage is that these systems are compatible with TFA, which we demonstrated to be superior over FA-containing mobile phases for QC analysis of cationic CPPs. We demonstrated that the MS^1 spectra of cationic CPPs, obtained using this single quad MS detection system combined with a post-column TFA displacement, should be carefully interpreted, as TFA^- adducts can be present, especially in case of highly cationic peptides. We believe these GLP/GMP-compliant single quad MS detectors deserve to be a standard detection system in addition to UV detectors during QC analysis of peptides before being used in biomedical research as well as in pharmacopoeias and ICH guidelines [40].

5. CONCLUSIONS

From the comparison of five chromatographic systems, it can be concluded that for routine QC analysis of cationic CPPs, the use of an UHPLC system, equipped with BEH C_{18} column thermostated at 30°C, and TFA as acidic modifier is preferred. This chromatographic system is characterized by higher sensitivity and resolution, allowing an accurate evaluation of the purity and impurity profile of these peptides, which is essential for obtaining reliable study results in biomedical research. We demonstrated the use of a single quad MS detection system, which is compatible with a TFA-containing mobile phase, providing information on the peptide and impurity identity, as well as on the purity of the different observed peaks. Therefore, the routine use of these MS detectors during QC analysis of peptides should be encouraged by pharmacopoeias and international guidelines.

The purity of the five investigated CPPs, as well as of the four PrAMPs and three disulfide-rich (cyclic) peptides, provided and evaluated by a collaborating research group, was estimated to be above 95% as required to perform the *in vivo* BBB transport studies. The main peaks of the resulting chromatograms were identified as the intended peptides.

6. REFERENCES

[1] Stalmans S, Willems M, Adriaens E, Remon JP, De Spiegeleer B. Flatworm models in pharmacological research: The importance of compound stability testing. *Regul. Toxicol. Pharm.* 2014; **70**: 149-154.

[2] World Health Organization (WHO). Handbook: Quality Practices in Basic Biomedical Research. 2006; http://www.who.int/tdr/publications/documents/quality_practices.pdf.

[3] World Health Organization (WHO). Good Laboratory Practice (GLP) - Quality practices for regulated non-clinical research and development, second edition. 2009; http://www.who.int/tdr/publications/documents/glp-handbook.pdf.

[4] De Spiegeleer B, Vergote V, Pezeshki A, Peremans K, Burvenich C. Impurity profiling quality control testing of synthetic peptides using liquid chromatography-photodiode array-fluorescence and liquid chromatography-electrospray ionization-mass spectrometry: The obestatin case. *Anal. Biochem.* 2008; **376**: 229-234.

[5] D'Hondt M, Bracke N, Taevernier L, Gevaert B, Verbeke F, Wynendaele E, De Spiegeleer B. Related impurities in peptide medicines. *J. Pharm. Biomed. Anal.* 2014; **101**: 2-30.

[6] Verbeken M, Wynendaele E, Lefebvre RA, Goossens E, De Spiegeleer B. The influence of peptide impurity profiles on functional tissue-organ bath response: The 11-mer peptide INSL6[151-161] case. *Anal. Biochem.* 2012; **421**: 547-555.

[7] de Beukelaar J, Gratama J, Smitt PAS, Verjans GM, Kraan J, Luider TM, Burgers PC. The impact of impurities in synthetic peptides on the outcome of T-cell stimulation assays. *Rapid Commun. Mass Spectrom.* 2007; **21**: 1282-1288.

[8] Currier JR, Galley LM, Wenschuh H, Morafo V, Ratto-Kim S, Gray CM, Maboko L, Hoelscher M, Marovich MA, Cox JH. Peptide Impurities in Commercial Synthetic Peptides and Their Implications for Vaccine Trial Assessment. *Clin. Vaccine Immunol.* 2008; **15**: 267-276.

[9] Zhang JV, Ren P-G, Avsian-Kretchmer O, Luo C-W, Rauch R, Klein C, Hsueh AJW. Obestatin, a Peptide Encoded by the Ghrelin Gene, Opposes Ghrelin's Effects on Food Intake. *Science* 2007; **315**: 766d.

[10] Verbeke F, Wynendaele E, Braet S, D'Hondt M, De Spiegeleer B. Quality evaluation of synthetic quorum sensing peptides used in R&D. *J. Pharm. Anal.* 2015; doi:10.1016/j.jpha.2014.12.002.

[11] Madani F, Lindberg S, Langel Ü, Futaki S, Gräslund A. Mechanism of Uptake of Cell-Penetrating Peptides. *J. Biophys.* 2011; **2011**: 414729.

[12] Stalmans S, Wynendaele E, Bracke N, Gevaert B, D'Hondt M, Peremans K, Burvenich C, De Spiegeleer B. Chemical-Functional Diversity in Cell-Penetrating Peptides. *PLOS ONE* 2013; **8**: e71752.

[13] Oehlke J, Scheller A, Wiesner B, Krause E, Beyermann M, Klauschenz E, Melzig M, Bienert M. Cellular uptake of an α-helical amphipathic model peptide with the potential to deliver polar compounds into the cell interior non-endocytically. *Biochym. Biophys. Acta* 1998; **1414**: 127-139.

[14] Holm T, Netzereab S, Hansen M, Langel Ü, Hällbrink M. Uptake of cell-penetrating peptides in yeasts. *FEBS Lett.* 2005; **579**: 5217-5222.

[15] Aubry S, Aussedat B, Delaroche D, Jiao C-Y, Bolbach G, Lavielle S, Chassaing G, Sagan S, Burlina F. MALDI-TOF mass spectrometry: A powerful tool to study the internalization of cell-penetrating peptides. *Biochim. Biophys. Acta* 2010; **1798**: 2182-2189.

[16] Houbart V, Rozet E, Matagne A, Crommen J, Servais A-C, Fillet M. Influence of sample and mobile phase composition on peptide retention behaviour and sensitivity in reversed-phase liquid chromatography/mass spectrometry. *J. Chromatogr. A* 2013; **1314**: 199-207.

[17] Wang X, Carr PW. An unexpected observation concerning the effect of anionic additives on the retention behavior of basic drugs and peptides in reversed-phase liquid chromatography. *J. Chromatogr. A* 2007; **1154**: 165-173.

[18] Gilar M, Xie H, Jaworski A. Utility of Retention Prediction Model for Investigation of Peptide Separation Selectivity in Reversed-Phase Liquid Chromatography: Impact of Concentration of Trifluoroacetic Acid, Column Temperature, Gradient Slope and Type of Stationary Phase. *Anal. Chem.* 2010; **82**: 265-275.

[19] Gumustas M, Kurbanoglu S, Uslu B, Ozkan SA. UPLC versus HPLC on Drug Analysis: Advantageous Application and Their Validation Parameters. *Chromatographia* 2013; **76**: 1365-1427.

[20] Gilar M, Jaworski A, McDonald TS. Solvent selectivity and strength in reversed-phase liquid chromatography separation of peptides. *J. Chromatogr. A* 2014; **1337**: 140-146.

[21] Snyder LR, Dolan JW. High-Performance Gradient Elution: The Practical Application of the Linear-Solvent Strength Model. John Wiley & Sons, Inc., **2007**, pp. 252.

[22] Guillarme D, Nguyen DTT, Rudaz S, Veuthey J-L. Method transfer for fast liquid chromatography in pharmaceutical analysis: Application to short columns packed with small particle. Part II: Gradient experiments. *Eur. J. Pharm. Biopharm.* 2008; **68**: 430-440.

[23] European Pharmacopoeia 8.0. Substances for pharmaceutical use (04/02013: 2034).

[24] Neue UD. Theory of peak capacity in gradient elution. *J. Chromatogr. A* 2005; **1079**: 153-161.

[25] European Pharmacopoeia 8.0. 2.2.46. Chromatographic separation techniques (04/2009:20246).

[26] Roepstorff P, Fohlman J. Proposal for a common nomenclature for sequence ions in mass spectra of peptides. *Biomed. Mass Spectrom.* 1984; **11**: 601.

[27] Kuhlmann FE, Apffel A, Fischer SM, Goldberg G, Goodley PC. Signal Enhancement for Gradient Reverse-Phase High-Performance Liquid Chromatography-Electrospray Ionization Mass Spectrometry Analysis with Trifluoroacetic and Other Strong Acid Modifiers by Postcolumn Addition of Propionic Acid and Isopropanol. *J. Am. Soc. Mass Spectrom.* 1995; **6**: 1221-1225.

[28] Apffel A, Fischer S, Goldberg G, Goodley PC, Kuhlmann FE. Enhanced sensitivity for peptide mapping with electrospray liquid chromatography-mass spectrometry in the presence of signal suppression due to trifluoroacetic acid-containing mobile phases. *J. Chrom. A* 1995; **712**: 177-190.

[29] Fekete S, Veuthey J-L, Guillarme D. New trends in reversed-phase liquid chromatographic separations of therapeutic peptides and proteins: Theory and applications. *J. Pharmaceut. Biomed.* 2012; **69**: 9-27.

[30] Chen Y, Mant CT, Hodges RS. Temperature selectivity effects in reversed-phase liquid chromatography due to conformation differences between helical and non-helical peptides. *J. Chromatogr. A* 2003; **1010**: 45-61.

[31] Dolan JW. Temperature selectivity in reversed-phase high performance liquid chromatography. *J. Chromatogr. A* 2002; **965**: 195-205.

[32] De Spiegeleer BMJ, D'Hondt M, Vangheluwe E, Vandercruyssen K, De Spiegeleer BVI, Jansen H, Koijen I, Van Gompel J. Relative response factor determination of β-arthemeter degradants by a dry heat stress approach. *J. Pharmaceut. Biomed.* 2012; **70**: 111-116.

[33] Verkerk UH, Kebarle P. Ion-Ion and Ion-Molecule Reactions at the Surface of Proteins Produced by Nanospray. Information on the Number of Acidic Residues and Control of the Number of Ionized Acidic and Basic Residues. *J. Am. Soc. Mass Spectrom.* 2005; **16**: 1325-1341.

[34] S. Banerjee, Mazumdar S. Electrospray Ionization Mass Spectrometry: A Technique to Access the Information beyond the Molecular Weight of the Analyte. *Int. J. Anal. Chem.* 2012; **2012**: ID 282574.

[35] Armbruster DA, Pry T. Limit of Blank, Limit of Detection and Limit of Quantitation. *Clin. Biochem. Rev.* 2008; **29**: S49-S52.

[36] International Conference on Harmonisation of Technical Requirements for Registration of Pharmaceuticals for Human Use (ICH). Q3B(R2) Impurities in New Drug Products. 2006; http://www.ich.org/fileadmin/Public_Web_Site/ICH_Products/Guidelines/Quality/Q3B_R2/Step4/Q3B_R2__Guideline.pdf (accessed 22 May 2015).

[37] Gucinski AC, Boyne II MT. Identification of site-specific heterogeneity in peptide drugs using intact mass spectrometry with electron transfer dissociation. *Rapid Commun. Mass Spectrom.* 2014; **28**: 1757-1763.

[38] Vergote V, Burvenich C, Van de Wiele C, De Spiegeleer B. Quality specifications for peptide drugs: a regulatory-pharmaceutical approach. *J. Pept. Sci.* 2009; **15**: 697-710.

[39] Hamilton SE, Mattrey F, Bu X, Murray D, McCullough B, Welch CJ. Use of Miniature Mass Spectometer To Support Pharmaceutical Process Chemistry. *Org. Process Res. Dev.* 2014; **18**: 103-108.

[40] D'Hondt M, Gevaert B, Wynendaele E, De Spiegeleer B. Implementation of a single quad MS detector in routine QC analysis of peptide drugs. **Submitted**.

SUPPLEMENTARY INFORMATION

Figure S1: MS^1 and MS^2 spectra of the cationic CPPs obtained by analyzing the peptides using an HPLC-UV/MS system. In the MS^1 spectrum, the framed ion represents the ion of which the MS^2 spectrum was obtained.

SynB3:

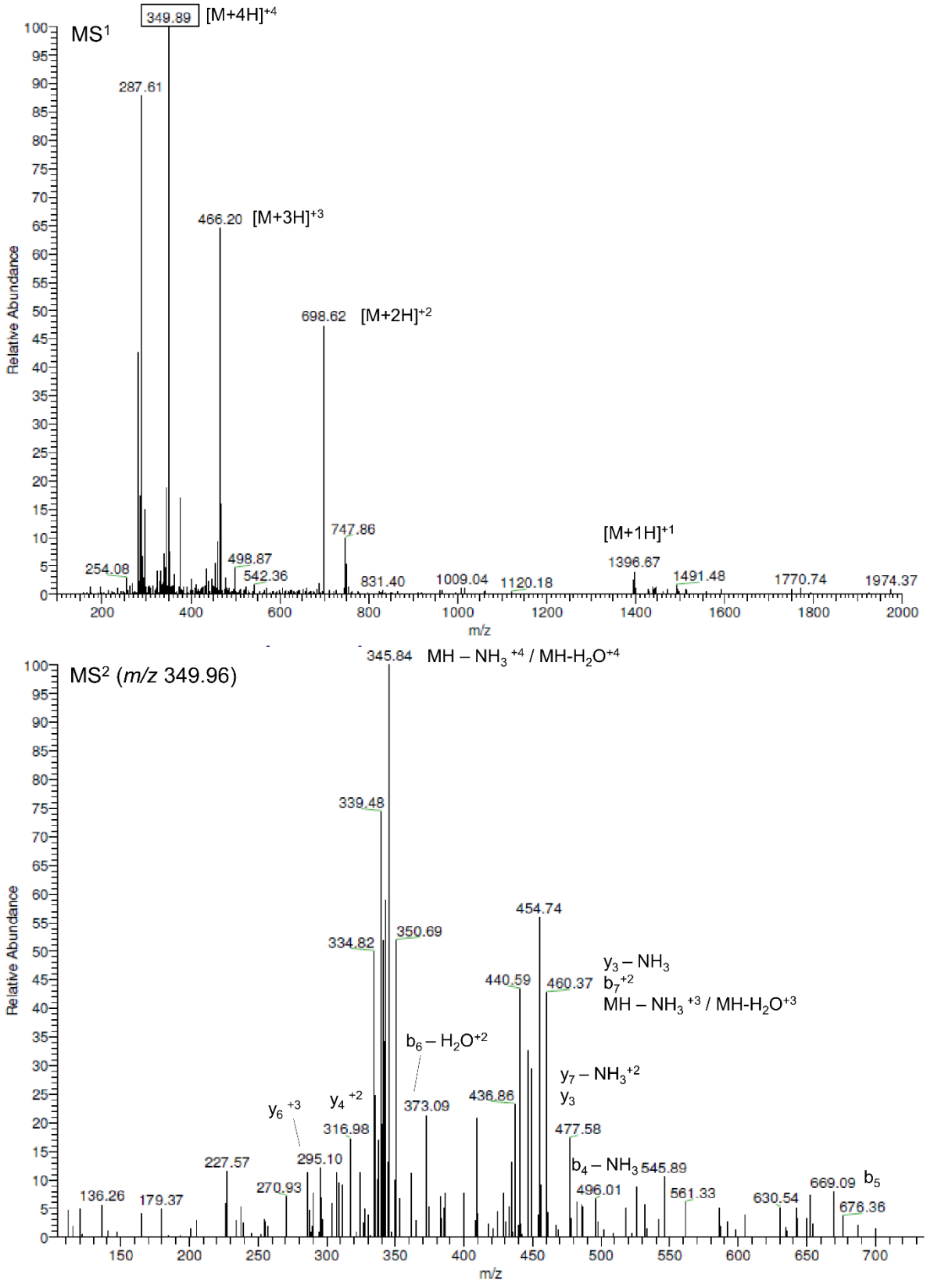

Tat 47-57:

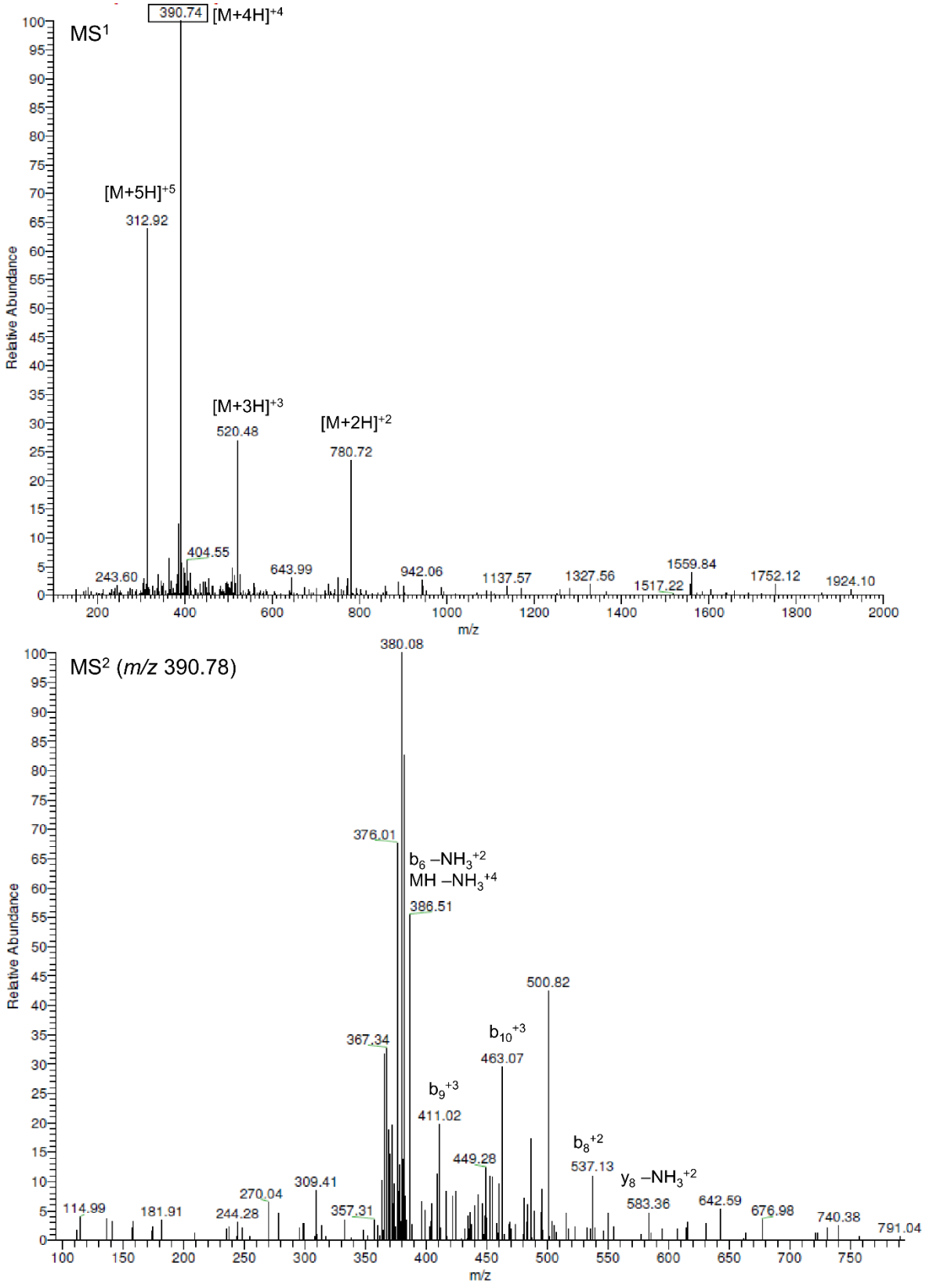
MS1
390.74 [M+4H]+4
[M+5H]+5
312.92
[M+3H]+3
520.48
[M+2H]+2
780.72
404.55
243.60
643.99
942.06
1137.57
1327.56
1517.22
1559.84
1752.12
1924.10
Relative Abundance
m/z
MS2 (m/z 390.78)
380.08
376.01
b6 –NH3+2
MH –NH3+4
386.51
500.82
367.34
b10+3
463.07
b9+3
411.02
b8+2
537.13
449.28
y8 –NH3+2
309.41
270.04
114.99
181.91
244.28
357.31
583.36
642.59
676.98
740.38
791.04
Relative Abundance
m/z

pVEC:

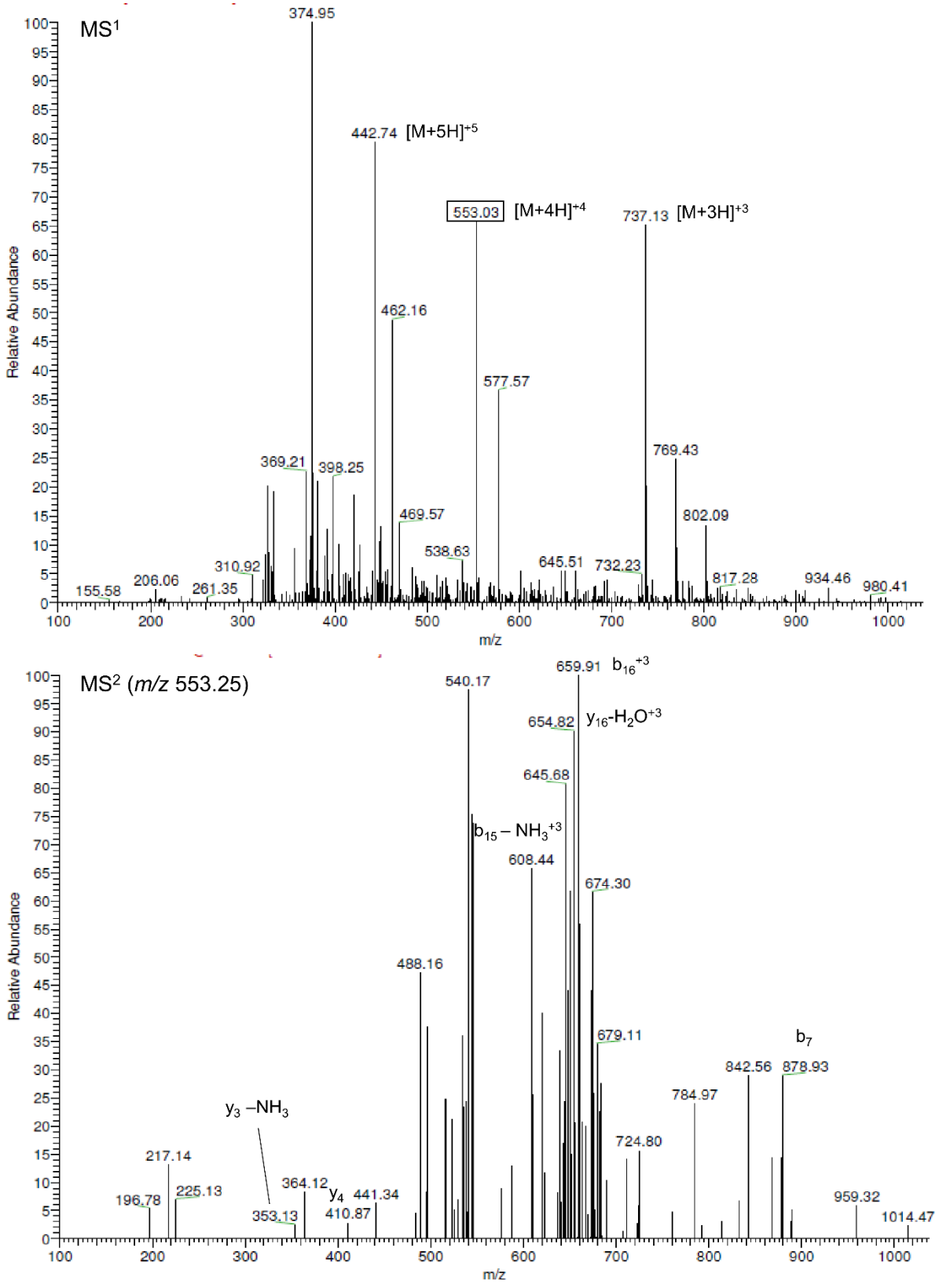
MS1
374.95
442.74 [M+5H]+5
553.03 [M+4H]+4
737.13 [M+3H]+3
462.16
577.57
769.43
369.21
398.25
469.57
802.09
538.63
645.51
732.23
817.28
934.46
980.41
310.92
206.06
261.35
155.58
Relative Abundance
m/z
MS2 (m/z 553.25)
659.91 b16+3
540.17
654.82 y16-H2O+3
645.68
b15 – NH3+3
608.44
674.30
488.16
679.11
b7
842.56
878.93
784.97
y3 –NH3
724.80
217.14
364.12
y4
441.34
225.13
196.78
353.13
410.87
959.32
1014.47
Relative Abundance
m/z

TP10:

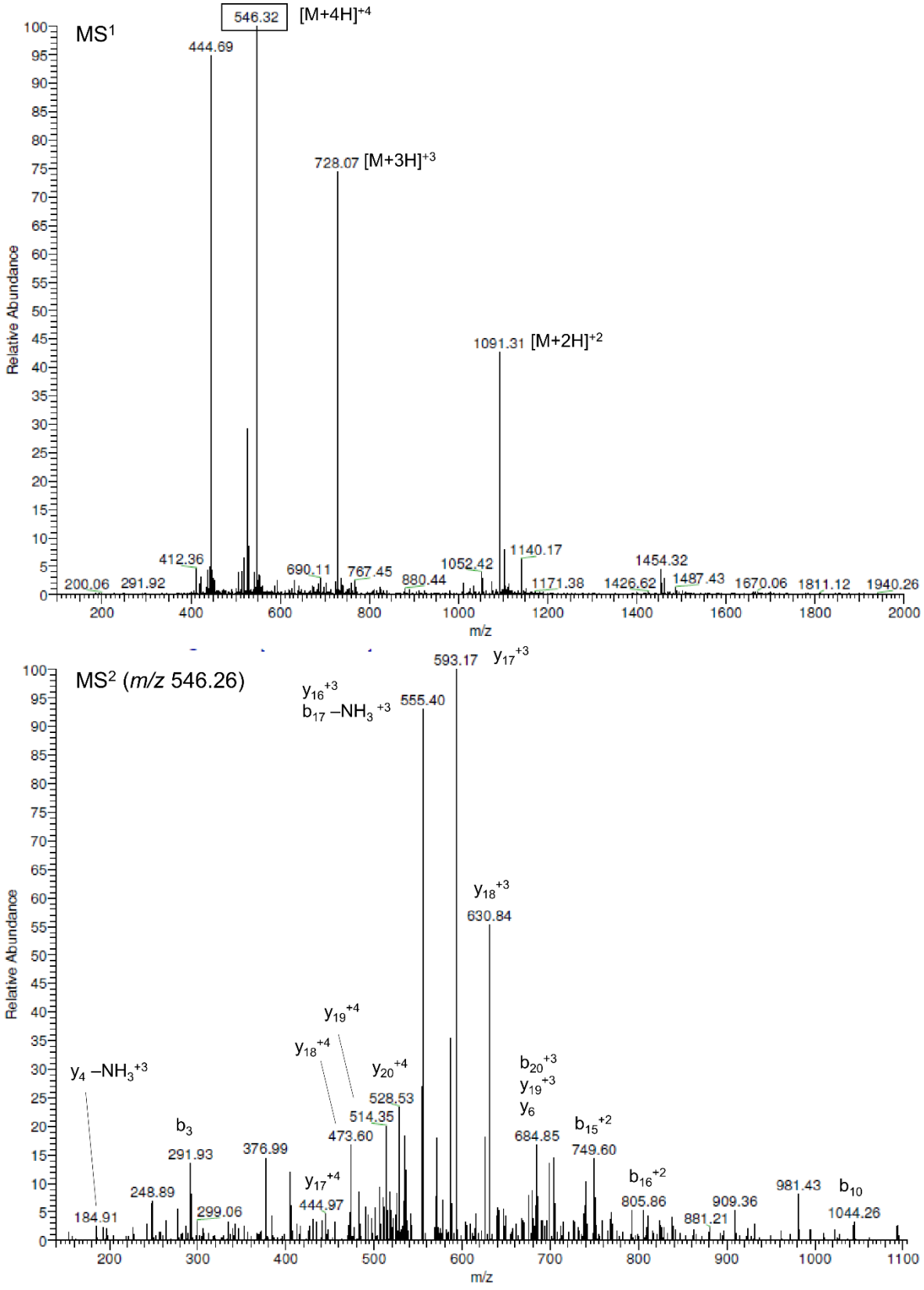
MS1
546.32 [M+4H]+4
444.69
728.07 [M+3H]+3
1091.31 [M+2H]+2
412.36
690.11
767.45
1052.42
1140.17
1454.32
200.06
291.92
880.44
1171.38
1426.62
1487.43
1670.06
1811.12
1940.26
Relative Abundance
m/z
MS2 (m/z 546.26)
593.17 y17+3
y16+3
b17 –NH3 +3
555.40
y18+3
630.84
y19+4
y18+4
y20+4
528.53
514.35
473.60
y4 –NH3+3
b3
291.93
376.99
248.89
299.06
184.91
y17+4
444.97
b20+3
y19+3
y6
684.85
b15+2
749.60
b16+2
805.86
909.36
881.21
981.43
b10
1044.26
Relative Abundance
m/z

TP10-2:

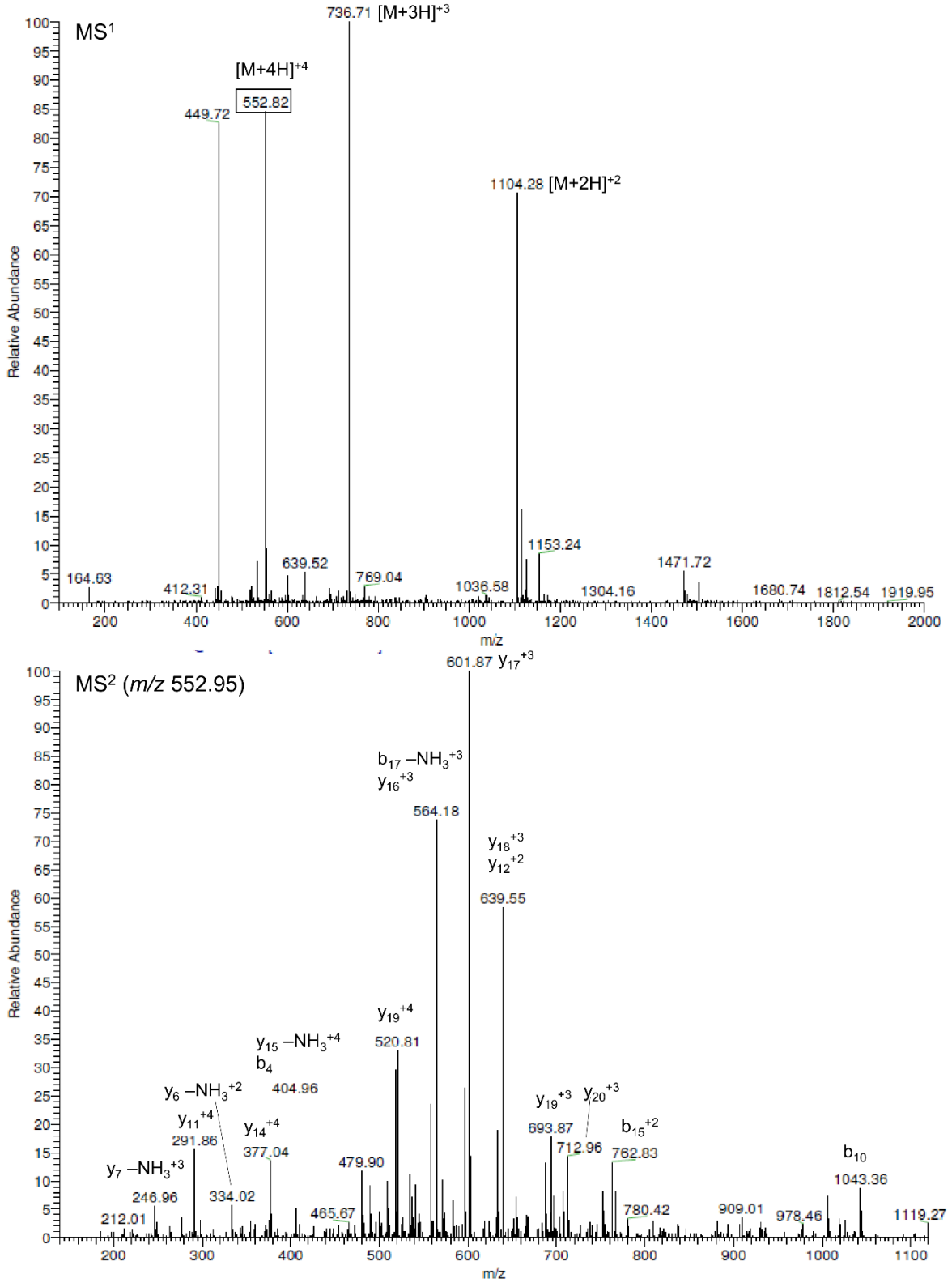
MS1
736.71 [M+3H]+3
[M+4H]+4
552.82
449.72
1104.28 [M+2H]+2
1153.24
1471.72
639.52
769.04
164.63
412.31
1036.58
1304.16
1680.74
1812.54
1919.95
Relative Abundance
m/z
MS2 (m/z 552.95)
601.87 y17+3
b17 –NH3+3
y16+3
564.18
y18+3
y12+2
639.55
y19+4
520.81
y15 –NH3+4
b4
404.96
y6 –NH3+2
y11+4
291.86
y14+4
377.04
y19+3
y20+3
693.87
712.96
b15+2
762.83
b10
1043.36
y7 –NH3+3
246.96
212.01
334.02
479.90
465.67
780.42
909.01
978.46
1119.27
Relative Abundance
m/z

Figure S2: Chromatograms of pVEC, Tat 47-57, TP10 and TP10-2 obtained after analyzing the peptides using the five different chromatographic systems. Only the part of the chromatogram containing the peptide and impurity peaks are shown.

pVEC:

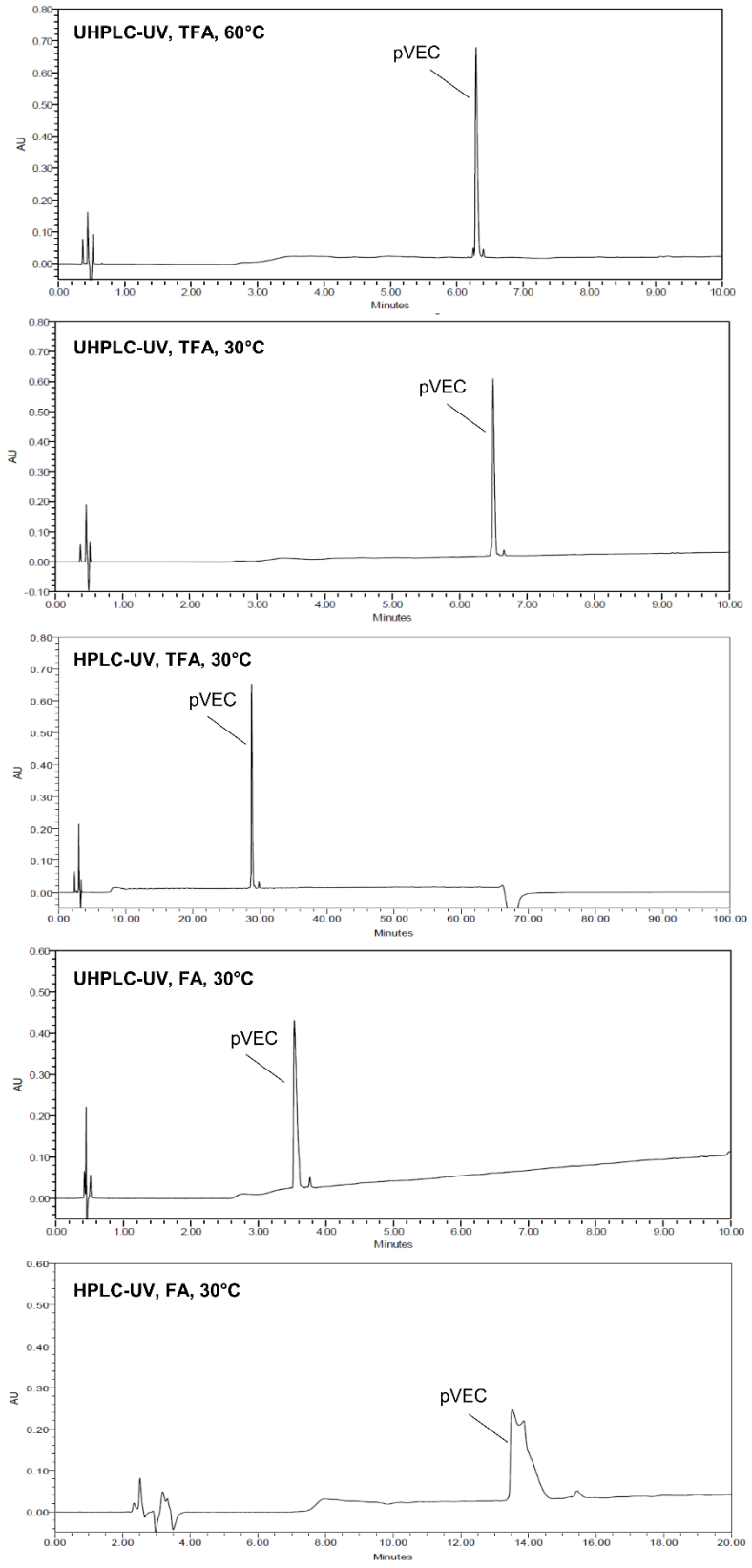

Tat 47-57:

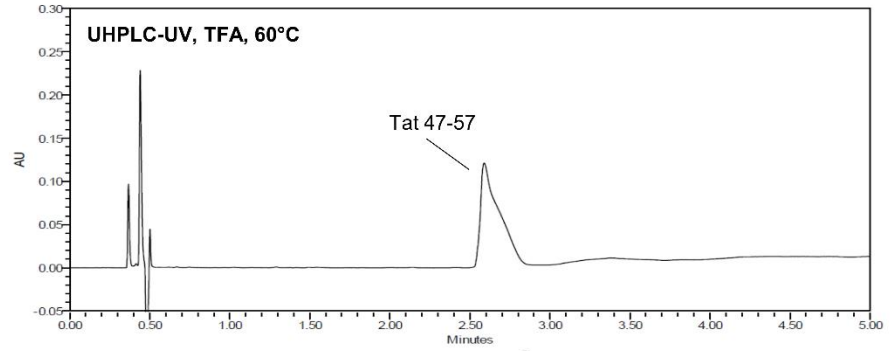
UHPLC-UV, TFA, 60°C
Tat 47-57
AU
Minutes

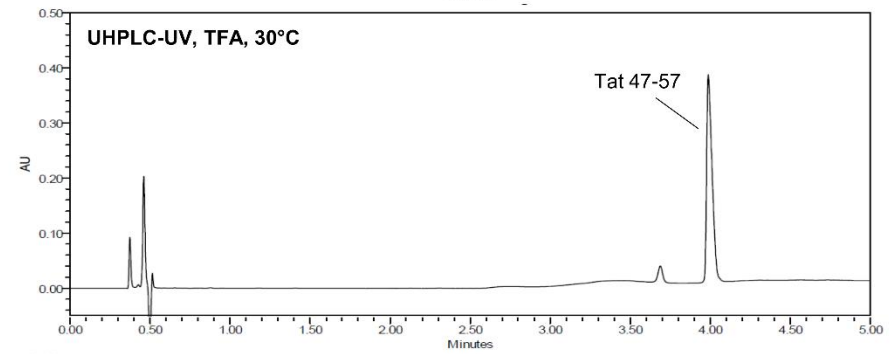
UHPLC-UV, TFA, 30°C
Tat 47-57
AU
Minutes

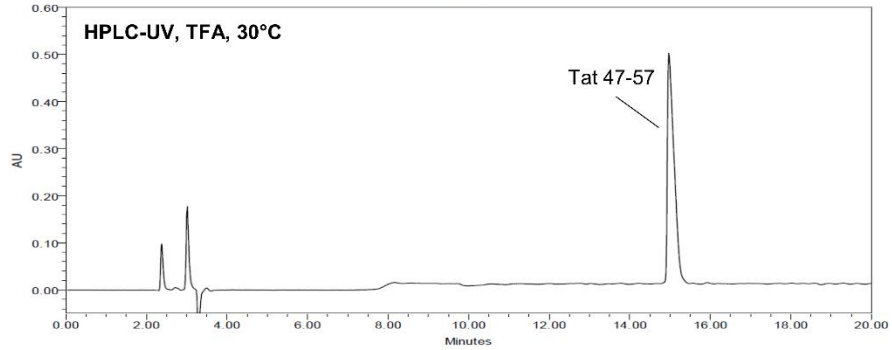
HPLC-UV, TFA, 30°C
Tat 47-57
AU
Minutes

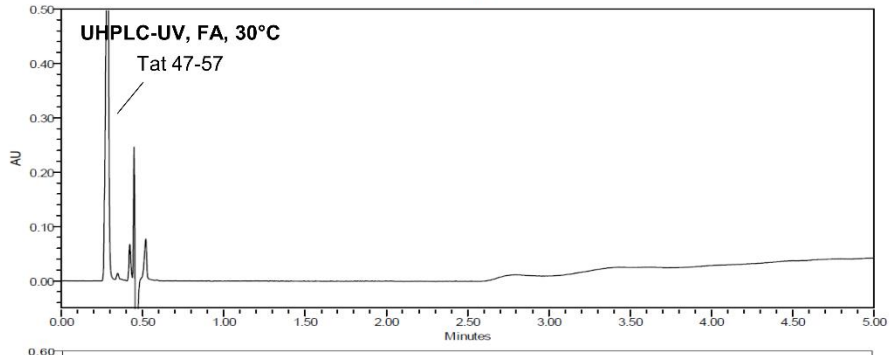
UHPLC-UV, FA, 30°C
Tat 47-57
AU
Minutes

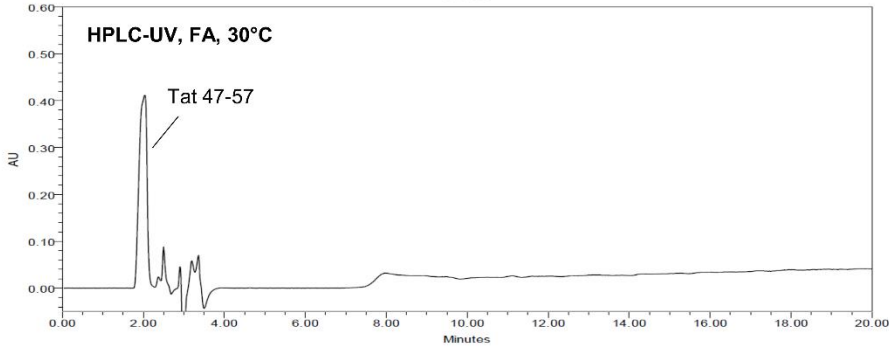
HPLC-UV, FA, 30°C
Tat 47-57
AU
Minutes

TP10:

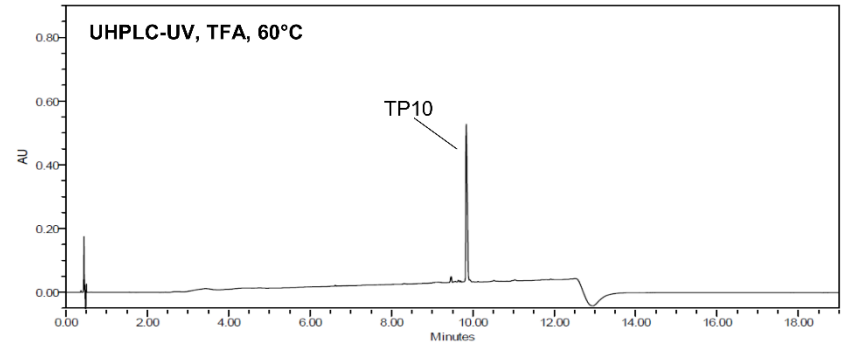
UHPLC-UV, TFA, 60°C
TP10
AU
Minutes

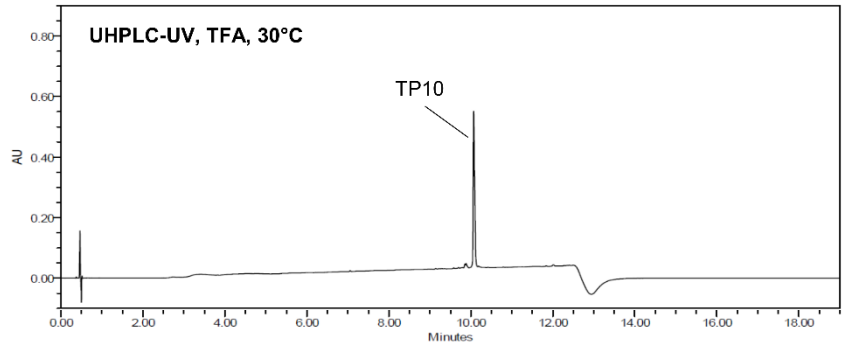
UHPLC-UV, TFA, 30°C
TP10
AU
Minutes

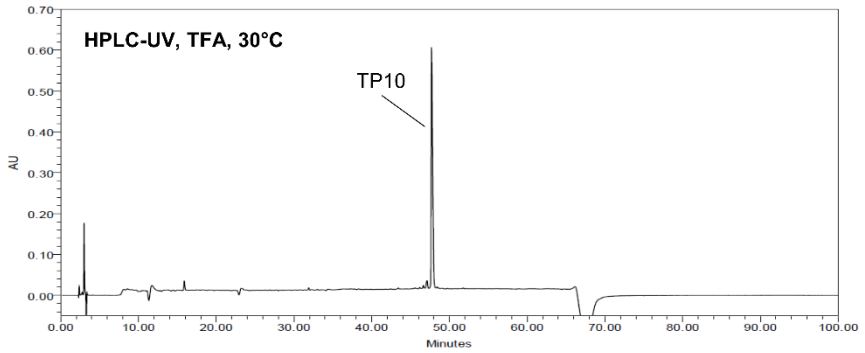
HPLC-UV, TFA, 30°C
TP10
AU
Minutes

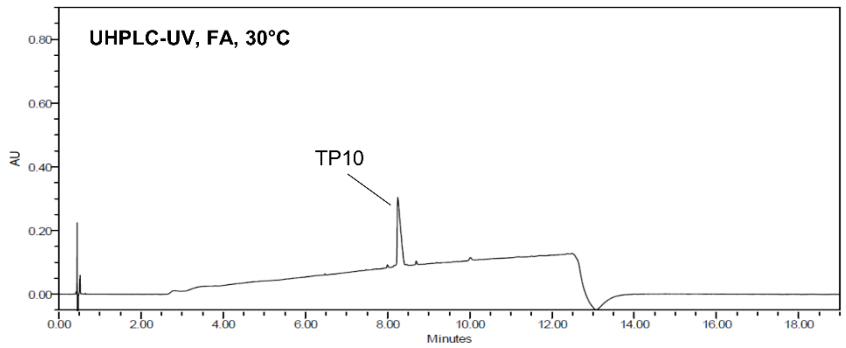
UHPLC-UV, FA, 30°C
TP10
AU
Minutes

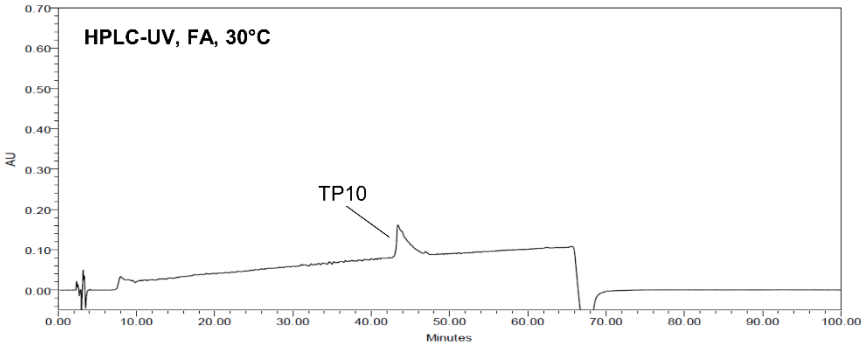
HPLC-UV, FA, 30°C
TP10
AU
Minutes

TP10-2:

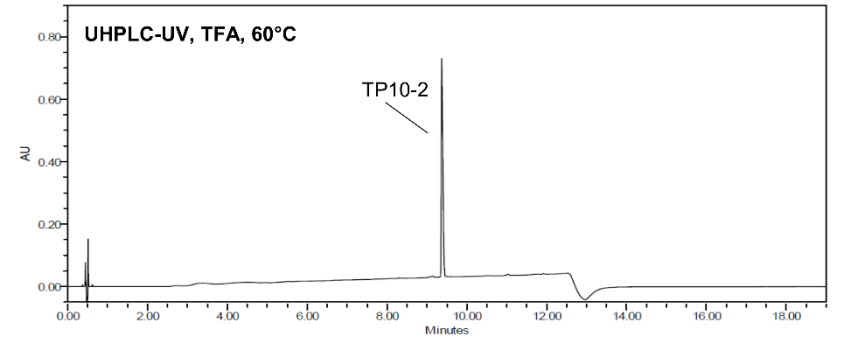
UHPLC-UV, TFA, 60°C
TP10-2
AU
Minutes

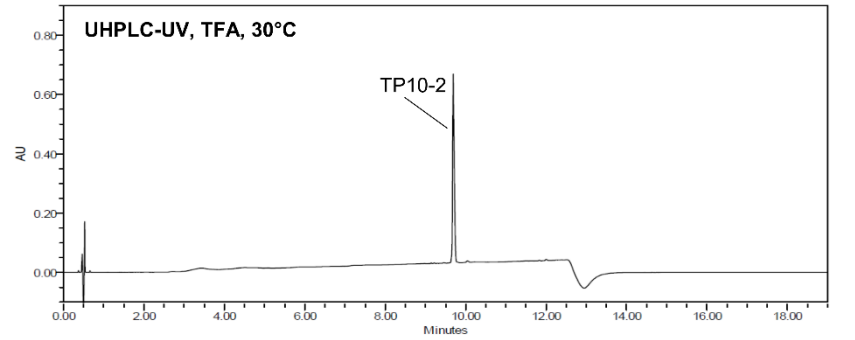
UHPLC-UV, TFA, 30°C
TP10-2
AU
Minutes

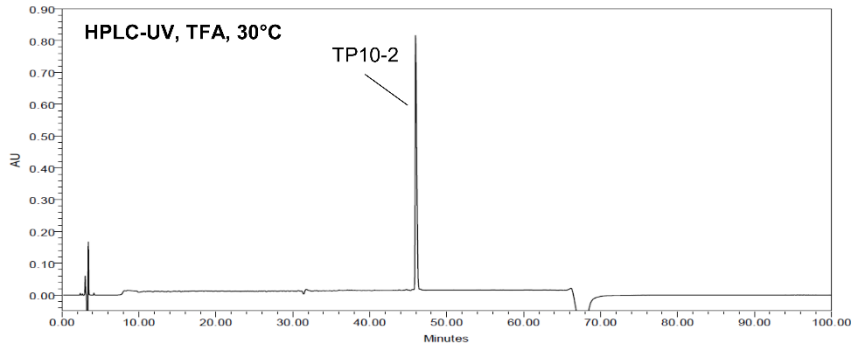
HPLC-UV, TFA, 30°C
TP10-2
AU
Minutes

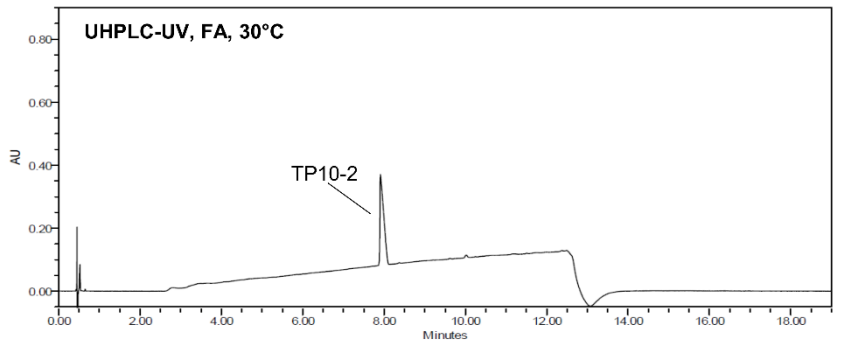
UHPLC-UV, FA, 30°C
TP10-2
AU
Minutes

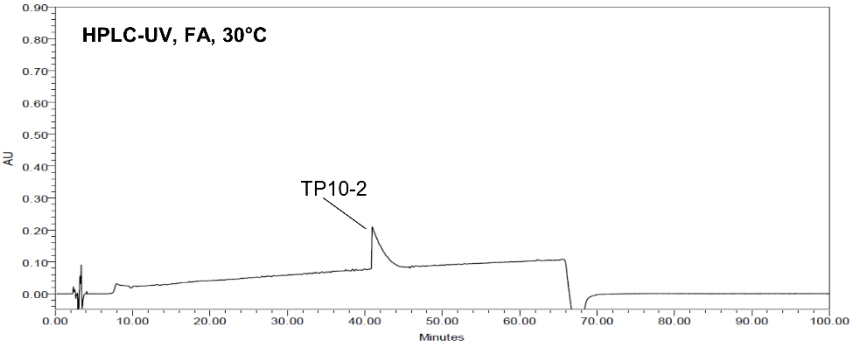
HPLC-UV, FA, 30°C
TP10-2
AU
Minutes

Figure 2: MS^1 spectra of SynB3 and Tat 47-57 obtained using the UHPLC-UV/MS chromatographic system with TFA as acidic modifier in the mobile phase (30°C). The clusters of MS-observed ions represent ions in the same charge state (same z). Each cluster consists of ions with the same charge but differing in the number of attached protons and number of trifluoroacetate (TFA^-) anions forming ion pairs.

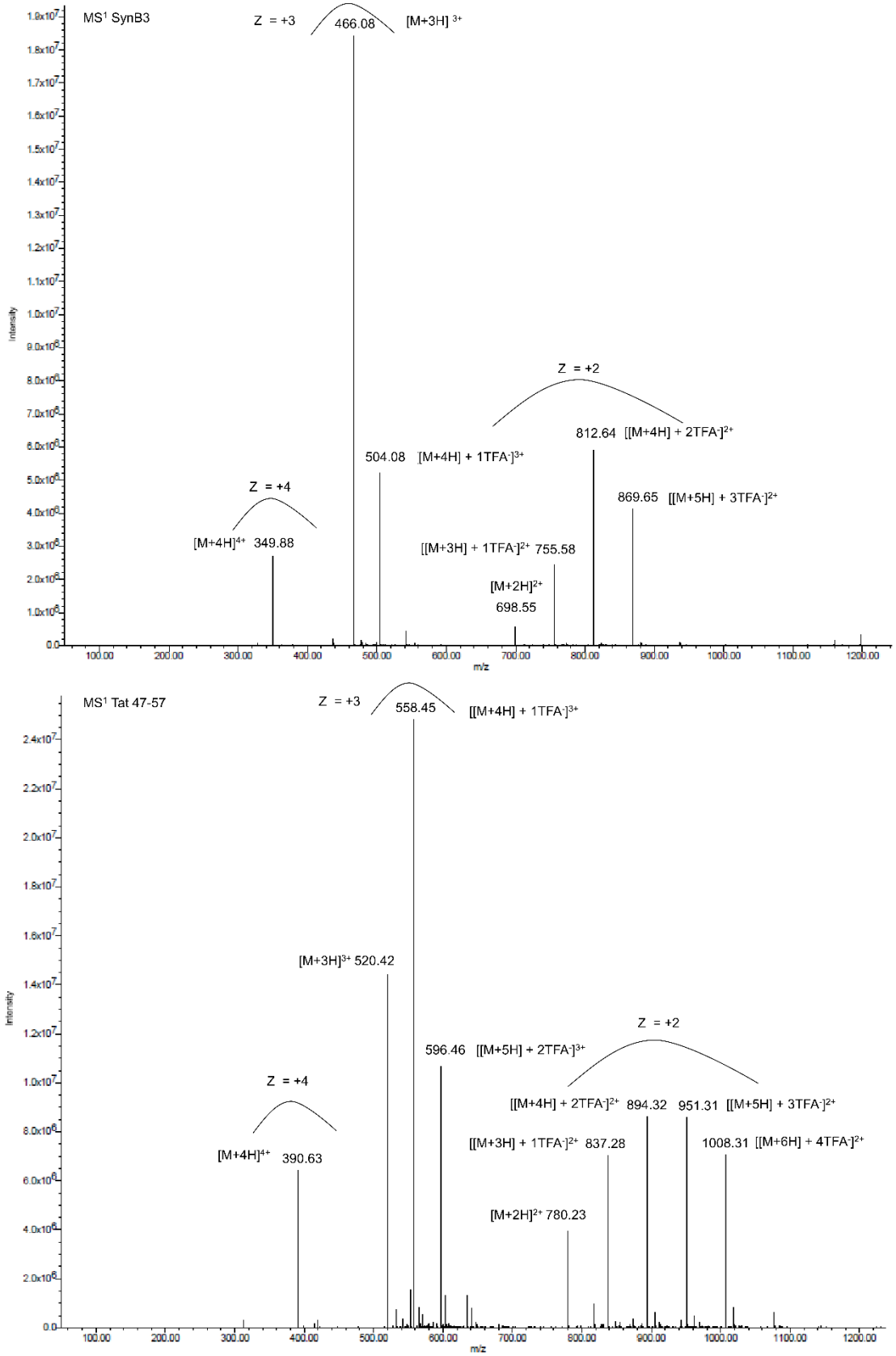

Table S1: Number of peaks above the reporting threshold of 0.1% (Ph. Eur.) for the five C_{18}-chromatographic systems used for the analysis of pVEC, Tat 47-57, TP10 and TP10-2.

Chromatographic system	Number of peaks > reporting threshold (0.1%)			
	pVEC	Tat 47-57	TP10	TP10-2
UHPLC, TFA, 30°C	4	1	9	3
UHPLC, TFA, 60°C	3	1	18	2
UHPLC, FA, 30°C	2	-[1]	8	2
HPLC, TFA, 30°C	3	2	14	5
HPLC, FA, 30°C	2	-[1]	1	1

[1]No retention observed in the concerned chromatographic system.

CHAPTER V

CELL-PENETRATING PEPTIDES SELECTIVELY CROSS THE BLOOD-BRAIN BARRIER *IN VIVO*

"Courage and perseverance have a magical talisman,
which difficulties disappear and obstacles vanish into the air"

John Quincy Adams
(°1767- †1848, Former president of the USA)

Parts of this chapter were published:

Stalmans S, Wynendaele E, Bracke N, Knappe D, Hoffmann R, Peremans K, Polis I, Burvenich C, De Spiegeleer B. Blood-Brain Barrier Transport of Short Proline-Rich Antimicrobial Peptides. *Protein Peptide Lett.* 2014; **21**: 399-406.

Stalmans S, Bracke N, Gevaert B, Peremans K, Burvenich C, Polis I, De Spiegeleer B. Cell-Penetrating Peptides Selectively Cross the Blood-Brain Barrier *In Vivo*. *PLOS ONE* 2015; **Accepted for publication**.

ABSTRACT

Cell-penetrating peptides (CPPs) are a group of peptides, which have the ability to cross cell membrane bilayers. Moreover, cell-penetrating properties have also been attributed to other biofunctional peptides, like antimicrobial peptides (AMPs) and disulfide-rich (cyclic) peptides. Fragmentary studies demonstrate the ability of CPPs to enhance transport of different cargoes across the blood-brain barrier (BBB). However, comparative, quantitative data on the BBB permeability of different CPPs are currently lacking. Therefore, the *in vivo* BBB transport characteristics were determined of five "traditional" CPPs, *i.e.* pVEC, SynB3, Tat 47-57, TP10 and TP10-2, selected based on the different subgroups observed in the chemical space of the CPPs, extended with the study of the BBB transport of "new" CPPs being four short, proline-rich AMPs (PrAMPs), *i.e.* apidaecin Api137, oncocin, drosocin and drosocin Pro5Hyp, and three disulfide-rich (cyclic) peptides, *i.e.* MCoTI-II, cVc1.1 and chlorotoxin. The results indicated that the investigated peptides showed divergent BBB transport characteristics, ranging from very high to no brain influx as determined using multiple time regression analysis and from high parenchymal distribution to entrapment in capillary endothelial cells, which was demonstrated using the capillary depletion method. Some peptides showed efflux out of the brain. Co-injection of pVEC with radioiodinated bovine serum albumin (BSA) did not enhance the brain influx of BSA, indicating that pVEC itself did not significantly alter the BBB properties. A saturable mechanism could not be demonstrated by co-injecting an excess dose of non-radiolabeled CPP. No significant regional differences in brain influx of the CPPs were observed, with the exception of pVEC, for which the regional variations were only marginal. The observed BBB influx transport properties cannot be correlated with their cell-penetrating ability, and therefore, good CPP properties do not imply efficient brain influx.

CHAPTER V

CELL-PENETRATING PEPTIDES SELECTIVELY CROSS THE BLOOD-BRAIN BARRIER *IN VIVO*

Main focus in this chapter:

- To characterize the blood-brain barrier transport of "traditional" cell-penetrating peptides as well as "new" cell-penetrating peptides, being biofunctional peptides with cell-penetrating properties.
- To determine whether cell-penetrating properties and blood-brain barrier transport are related for peptides.

1. WHY STUDY BLOOD-BRAIN BARRIER TRANSPORT OF CELL-PENETRATING PEPTIDES?

Cell-penetrating peptides are a particular group of peptides that have the ability to cross cell membranes without causing a significant lethal membrane damage [1]. The exact mechanism of cellular entry remains controversial, but a consensus exists that endocytosis and a direct penetration mechanism are involved [2,3]. Drawing conclusions on the cellular uptake mechanism of CPPs is impeded by different factors as already outlined in **Chapter I** and **II** of this thesis. Firstly, a variety of techniques and experimental protocols are used to investigate these peptides. Furthermore, multiple mechanisms can simultaneously be active and the employed mechanisms depend not only on the peptide studied but also on the cell type used, the peptide concentration and the attached cargo or label [2,3].

Since their discovery 20 years ago, hundreds of CPPs have already been described and can roughly be classified into three chemical groups: the cationic, amphipathic and hydrophobic CPPs [4]. The cationic CPPs contain a stretch of positive charges derived from arginine and lysine residues in their sequence, while the amphipathic peptides are characterized by a hydrophilic and hydrophobic part, mostly by adopting a helix structure. The hydrophobic CPPs are rich in apolar amino acids and have a low net charge. However, a clear overlap exists between these chemical groups, emphasizing that CPPs represent a chemically diverse group of peptides [**Chapter II**]. Moreover, cell-penetrating

properties have also been attributed to other classes of peptides, which are not investigated as CPPs per se, like AMPs, *e.g.* short, proline-rich AMPs (PrAMPs) and disulfide-rich (cyclic) peptides characterized by multiple disulfide bonds in the peptide structure of which the backbone can be cyclized [5-9]. With their amphipathic and cationic nature, due to the high proportion of arginines in their sequence, these AMPs are structurally related with the CPPs and are also able to translocate cells [10].

The majority of the CPPs are derived from naturally occurring proteins and peptides like heparin-binding proteins, DNA and/or RNA-binding proteins, homeoproteins, signal peptides, AMPs and viral proteins [4,11]. For some CPPs, their cell-penetrating properties are linked to the function of the parent peptide or protein, but for other peptides, the function of the CPP sequence in the full-length parent protein is still unclear [4]. Traditionally, CPPs are considered to be inert molecules, but actually these peptides can exert a biological activity themselves [12,13]. Moreover, for some CPPs, the biological function of the parent peptide or protein is conserved in the cell-penetrating sequence, a feature that can be therapeutically exploited [14-23]. However, up till now, only a limited number of studies have described the biological activity of CPPs although this information is indicative for potential side effects and relevant for future clinical applications [12,13]. The knowledge on the bioactivity of CPPs is particularly interesting for peptides having an endogenous [*e.g.* 14-18,20-22,24-28] and viral or bacterial origin [*e.g.* 19,29-37].

As CPPs are able to cross cellular membranes, the question arises whether this means that they can also pass the BBB, which protects the brain. The barrier function of the BBB is established by physical, transport as well as metabolic means, explaining its selective permeability for ions, solutes and (macro)molecules [38]. Only some fragmentary studies are describing the ability of CPPs to reach the brain parenchyma both *in vivo* and *in vitro* [39]. However, almost all studies investigate the brain delivery of a CPP attached to a cargo, which is known to influence the cell-penetrating, as well as the BBB transport properties. Moreover, different techniques are hereby used: measuring the pharmacological effect of the attached cargo or following the fluorescently labeled construct using *in vivo* imaging or fluorescence microscopy techniques. A detailed overview of the currently available brain influx studies of CPPs can be found in Table S1 of the Supplementary Information. Comparable, quantitative data on the BBB transport of CPPs are still lacking. Moreover, there is only limited knowledge on the BBB transport mechanism of CPPs. Only for the SynB vectors, which are cationic CPPs, an adsorptive-mediated translocation mechanism was proposed [40,41].

To evaluate whether different CPPs cross the BBB to the same extent, the BBB transport of five chemically diverse “traditional” CPPs with different cell-penetrating ability was quantitatively investigated. TP10, TP10-2, pVEC, SynB3 and Tat 47-57 were selected based on the different

subgroups of CPPs determined during the exploration of the chemical space, as indicated in Figure 1. The chemical diversity of the investigated peptides was extended with "new" peptides with cell-penetrating properties: four PrAMPs, *i.e.* apidaecin Api137, oncocin, drosocin and drosocin Pro5Hyp, and three disulfide-rich (cyclic) peptides, *i.e.* MCoTI-II, cVc1.1 and chlorotoxin. In Figure 1 is demonstrated how these peptides fit in the chemical space of the CPPs and in Table 1, an overview of the selected peptides is provided. In this study, their BBB influx transport rate, the parenchyma/capillary, as well as the efflux properties were investigated using an *in vivo* mouse model. Moreover, the influence of pVEC itself on the BBB permeability was also verified. Finally, the intra-brain regional distribution after brain uptake and the saturability of the brain influx mechanism of pVEC, TP10 and SynB3 was evaluated. Our results prove that CPPs selectively pass the BBB as not all CPPs cross the BBB to the same extent.

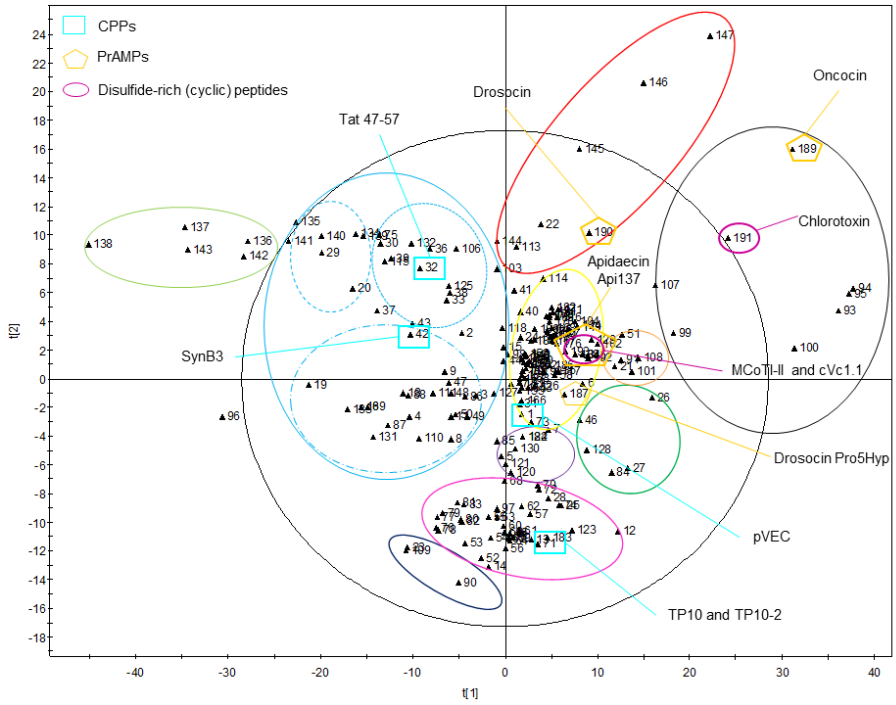

Figure 1: Chemical diversity of the peptides with cell-penetrating properties investigated for their BBB transport characteristics.

Table 1: Overview of the characteristics of the peptides investigated for their BBB transport properties (blue = "traditional" CPPs, orange = PrAMPs, purple = disulfide-rich (cyclic) peptides).

Peptide	Sequence	Molecular weight (Da)[1]	CP-response[2]	Log P[3]	pI[4]	% basic residues[5]
pVEC	LLIILRRRIRKQAHAHSK-NH_2	2208.8	1.318	-7.2	11.6	44%
TP10	AGYLLGKINLKALAALAKKIL-NH_2	2181.8	1.641	-3.7	10.4	19%
TP10-2	AGYLLGKINLKPLAALAKKIL-NH_2	2207.8	0.749	-3.5	10.4	19%
SynB3	RRLSYSRRRF-NH_2	1395.7	0.126	-4.7	11.5	50%
Tat 47-57	YGRKKRRQRRR-NH_2	1558.9	0.309	-9.2	11.7	73%
Apidaecin Api137	Gu-ONNRPVYIPRPRPPHPRL-OH[6]	2294.1	-[9]	-8.0	11.3	28%
Oncocin	VDKPPYLPRPRPPRRIYNR-NH_2	2390.2	-[9]	-7.9	11.2	32%
Drosocin[7]	GKPRPYSPRPTSHPRPIRV-OH	2198.9	-[9]	-10.0	11.4	32%
Drosocin Pro5Hyp	GKPR-4t-Hyp-YSPRPTSHPRPIRV-OH[8]	2214.9	-[9]	-10.9	11.3	32%
MCoTI-II	GGVCPKILKKCRRDSDCPGACICRGNGYCGSGSD (Cyclic backbone; disulfide briges: Cys4-Cys21; Cys11-Cys23; Cys17-Cys29)	3452.9	0.103[10]	-23.0	10.3	18%
cVc1.1	GCCSDPRCNYDHPEICGGAAGG (Cyclic backbone; disulfide bridges: Cys2-Cys8; Cys3-Cys16)	2160.3	-[9]	-16.0	4.2	9%
Chlorotoxin	MCMPCFTTDHQMARKCDDCCGGKGRGKCYGPQCLCR (Disulfide bridges: Cys2-Cys19; Cys5-Cys28; Cys16-Cys33; Cys20-Cys35)	3996.7	-[9]	-24.6	9.9	20%

[1]Obtained from the certificate of analysis provided by the supplier; [2]As described in Chapter II; [3]Log P calculated using Hyperchem 8.0 (Hypercube, Gainesville, FL, USA); [4]Iso-electric point as calculated using MarvinSketch 5.10.3 (ChemAxon, Budapest, Hungary); [5]Calculated as the ratio of the number of basic amino acids (arginine, lysine or histidine) and the total number of amino acid residues multiplied by 100; [6]Gu = N,N,N',N'-tetramethylguanidino and O = L-ornithine; [7]The unglycosylated drosocin analog was investigated; [8]Pro5Hyp = 4-trans hydroxyl L-proline (=4t-Hyp); [9]CP-response could not be calculated as currently, no quantitative data for cellular uptake were already published; [10]CP-response calculated based on quantitative data for cellular uptake described in [42].

2. MATERIALS AND METHODS

Peptides

TP10 and TP10-2 were purchased at Caslo ApS (Lyngby, Danmark); pVEC, SynB3 and Tat 47-57 at LifeTein LLC (Somerset, USA) and the positive control dermorphin at Bachem (Bubendorf, Switzerland) and Hanhong group (Shanghai, China). The PrAMPs, *i.e.* apidaecin Api137, oncocin, drosocin and drosocin Pro5Hyp, and the disulfide-rich (cyclic) peptides, *i.e.* MCoTI-II, cVc1.1 and chlorotoxin, were investigated as part of a collaborating project and were provided by prof. Ralf Hoffmann and prof. David Craik, respectively.

The QC of the peptides is described in **Chapter IV**: the main peak present in the chromatograms was identified as the intended peptide and the chromatographic purity of the peptides was above 95%.

Radioiodination and purification of peptides and BSA

A carrier-added (CA) protocol was used for radioiodination of the peptides. SynB3, Tat 47-57, the four PrAMPs, chlorotoxin, dermorphin and BSA (Merck KGaA, Darmstadt, Germany) were radiolabeled using the Iodo-Gen method [43]. After rinsing the Iodo-Gen tube using 1 ml of 130 mM phosphate buffer (pH 7.4), 50 µl of a 1 µmol/ml sodium iodide carrier dissolved in 0.1% (m/V) aqueous FA (2 µmol/ml for PrAMPs and BSA) was mixed with a volume containing 1 mCi of $Na^{125}I$ (Perkin Elmer, Zaventem, Belgium) and allowed to react for 6 min at room temperature. The peptides were iodinated by transfer of the iodonium solution to 50 µl of a 1 µmol/ml peptide solution dissolved in phosphate buffer (SynB3, Tat 47-57, PrAMPs, dermorphin, BSA) or 0.1% (m/V) FA in 95:5 (V/V) water:acetonitrile (chlorotoxin). The reaction was allowed to proceed during 6 min at room temperature while regularly mixing. TP10, TP10-2, pVEC, MCoTI-II and cVc1.1 were radiolabeled using the chloramine-T method [43]. Briefly, to 50 µl of a 1 µmol/ml peptide solution (TP10, TP10-2, MCoTI-II and cVc1.1) or 110 µl of a 1 mg/ml pVEC solution, dissolved in 0.1% FA in 95:5 water:acetonitrile, 20 µl of a 3.75 µmol/ml sodium iodide in aqueous 0.1% (m/V) FA (TP10, TP10-2, MCoTI-II and cVc1.1) solution or 20 µl of a 2.5 µmol/ml sodium iodide in 25 mM phosphate buffer (pH 8.5 (pVEC)) was added. Then, a volume containing 1 mCi of $Na^{125}I$ was transferred to this solution, followed by 30 µl of a 0.5 mg/ml (or 1 mg/ml for MCoTI-II) chloramine-T solution in 25 mM phosphate buffer (pH 7.4 (TP10, TP10-2, MCoTI-II and cVc1.1) or pH 8.5 (pVEC)). The iodination reaction proceeded during 40 s, followed by the addition of 30 µl of a 1 mg/ml (or 2 mg/ml for MCoTI-II) sodium metabisulfite in 25 mM phosphate buffer (pH 7.4 (TP10, TP10-2, MCoTI-II and cVc1.1) or pH 8.5 (pVEC)) to stop the iodination reaction. For evaluation of the influx mechanism,

pVEC, SynB3 and TP10 were radiolabeled using a no-carrier-added (NCA) protocol, in which the non-radioactive sodium iodide solution was replaced by its solvent.

After radiolabeling, the iodinated peptides were fractionated using an HPLC-UV apparatus (LaChrom Elite, Hitachi, Tokyo, Japan) equipped with a radioactivity detector (Berthold Technologies GmbH & Co. KG, Bad Wildbad, Germany) and fraction collector (Gilson International BV, Den Haag, The Netherlands), in line with the HPLC waste. For separation, a Vydac Everest C_{18} column (250 × 4.6 mm, 5 µm particle size; Grace, Lokeren, Belgium) was coupled to the HPLC system. Mixtures of water and acetonitrile acidified with 0.1% (m/V) FA or 0.1% (m/V) TFA (SynB3 and Tat 47-57) were used to create appropriate gradients for separation of peptides and their iodinated forms. After fractionation, the fractions containing the radiolabeled peptides were selected and evaporated using a N_2 flow. After radioiodination of BSA and the PrAMPs, 500 µl of phosphate buffer (130 mM, pH 7.4) was added to the reaction mixture and the solution was filtered over a silver filter (Sterlitech, Kent, USA), instead of being fractionated. Before each experiment, a QC of the iodinated peptide stock was performed using the same radio-HPLC-UV system as desribed above. The presence of the radiolabeled peptides was verified by comparing the retention time of the peaks of the iodinated peptides, both obtained using UV- and radiodetection, with the retention times observed during fractionation after radiolabeling. For all peptides, the QC results indicated the presence and identity of the radiolabeled peptides.

***In vivo* experiments in mice**

Female, ICR-CD-1 mice (Harlan Laboratories, Venray, The Netherlands), aged 7 to 10 weeks and weighing 28-36 g, were used during the *in vivo* BBB transport experiments. For the PrAMPs, being part of a separate research project, male mice were used. It is known that sex steroid hormones influence the BBB function; however, differences in permeability have only been demonstrated in aged and diseased animal models [44,45]. All animal experiments were performed in accordance with the Ethical Committee principles of laboratory animal welfare as approved by our institute (Ghent University, Faculty of Veterinary Medicine, no. 2009-052 and 2014-128). Prior to experiments, mice were anesthetized by intraperitoneal injection of a 40% urethane solution (3 g/kg) (Sigma-Aldrich, Diegem, Belgium).

Evaluation of blood-brain barrier influx

For evaluation of the blood-to-brain BBB transport of peptides, the multiple time regression (MTR) analysis technique was used. In brief, after anesthetization of the ICR CD-1 mice, the right jugular externalis vein and left carotid artery were isolated. Then, 200 µl of a 30000 cpm/µl peptide solution

(MTR stock solution), obtained by diluting the radiolabeled peptide stock using lactated Ringer's buffer containing 1% (m/V) BSA (LR/BSA), was injected into right jugular externalis vein of the mouse. At 1, 3, 5, 10, 12.5 and 15 min post intravenous (IV) injection, with first and last time points performed in duplicate, mice were decapitated, brains were collected, weighed and measured for radioactivity ($A_m(T)$) using a gamma counter (Wallac Wizard 1470, Perkin Elmer). Shortly before decapitation, blood was collected from the isolated left carotid artery, which was then centrifuged (10000 *g*, 15 min at 21°C) in order to measure the radioactivity of blood and serum ($C_p(T)$). Dermorphin and radioiodinated BSA were used as positive and negative control, respectively. The blood-to-brain entry during the experimental period of 15 min was evaluated by plotting the ratio of total brain radioactivity ($A_m(T)$) and arterial serum radioactivity ($C_p(T)$), corrected for the brain weight and serum volume, respectively, versus the exposure time (Θ), expressing the theoretical steady state serum level of the iodinated peptide at a given serum concentration [46,47]. The exposure time is calculated as the integral of the arterial serum radioactivity over time divided by the radioactivity at time t. The integral is calculated through the trapezoidal rule of the log-transformed data [47]. In the linear part of the curve, assuming a two-compartmental BBB model, data can be fitted using a linear model from which the unidirectional brain influx rate (K_{in}), also referred to as unidirectional blood-to-brain clearance K_1 [48], and the initial (vascular) brain distribution volume (V_i) can be determined using the following equation according to Gjedde and Patlak [46, 49-51]:

$$\frac{A_m(T)}{C_p(T)} = \frac{A_{brain}(T)}{A_{serum}(T)} = K_{in} \cdot \Theta + V_i \text{ with } \Theta = \int_0^T \frac{C_p(t) \cdot dt}{C_p(T)} \quad (1)$$

If during the experimental time frame the curve deviates from linearity due to a significant efflux out of the brain resulting in a transition from unidirectional to net transfer, the following expansion of the Gjedde-Patlak plot, a model of biphasic blood-brain transfer as derived from Wong *et al.* [52], was used to fit the uptake:

$$\frac{A_m(T)}{C_p(T)} = \frac{A_{brain}(T)}{A_{serum}(T)} = K \cdot \Theta + V_g\left(1 - e^{\left(-\Theta\left(\frac{K_1 - K}{V_g}\right)\right)}\right) + V_0 \overset{K=0}{\cong} V_g\left(1 - e^{\left(-\Theta\left(\frac{K_1}{V_g}\right)\right)}\right) + V_0 \quad (2)$$

with K_1 is the unidirectional clearance, K is the net clearance, V_g the brain tissue distribution volume, and V_0 the initial vascular brain distribution volume, experimentally determined as the vascular brain distribution volume of radioiodinated BSA [48,53]. If K equals to K_1, the model is linear. The meaning of the constants and parameters of the linear and biphasic model is illustrated in Figure 2.

To evaluate whether the BBB remains intact after intravenous injection of the CPPs, a MTR experiment was performed for radioiodinated BSA with and without an excess dose of 20 µg of pVEC, which is the estimated injected dose of pVEC if the peptide was radiolabeled using the CA protocol. A

MTR experiment with and without co-injection of an excess dose of 10 µg of unlabeled peptide was used to investigate whether the CPPs use a saturable or non-saturable transport mechanism to cross the BBB. During this experiment, peptides were radiolabeled using a NCA method.

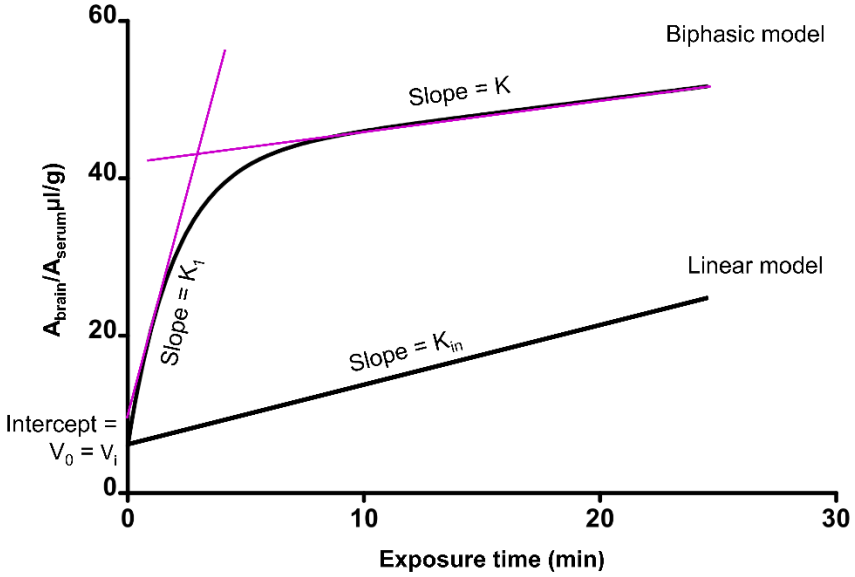

Figure 2: Meaning of constants and parameters of the linear and biphasic model.

Tissue distribution after IV injection

At the 15 min time points of the MTR experiment, six tissues, *i.e.* spleen, kidneys, lungs, heart and liver, were collected immediately after decapitation, weighed and measured in a gamma counter. The percentage of the injected dose for each isolated tissue was calculated as follows:

$$\%\text{injected dose} = \frac{A_{tissue}/w_{tissue}}{A_{IV\ injected}/w_{mouse}} \quad (3)$$

with A_{tissue} and $A_{IV\ injected}$ the measured radioactivity of the isolated tissue and the radioactivity of 200 µl of MTR stock solution, respectively, and w_{tissue} and w_{mouse} the weight of the considered tissue and injected mouse, respectively.

Regional variation in brain influx between different brain regions

For the CPPs, the regional variation in brain influx was evaluated. Therefore, after weighing and measuring the whole brain radioactivity, the brains collected during the MTR experiment of pVEC, SynB3 and TP10, as well as of the controls dermorphin and radiodiodinated BSA, were dissected into eight brain regions: (1) cerebellum, (2) medulla oblongata, (3) frontal cortex, (4) striatum, (5) hippocampus, (6) thalamus + hypothalamus, (7) midbrain and (8) occipital + parietal cortex, including

"rest of brain". Different dissected brain regions were weighed and measured in the gamma counter. The unidirectional influx rate and initial (vascular) brain distribution volume of the iodinated peptides for the different brain regions are determined using equation (1).

Peptide distribution to brain parenchyma and capillaries

The capillary depletion (CD) method was used to evaluate the distribution of the peptide between the brain parenchyma and capillaries [54,55]. In summary, the jugular internalis vein of two anesthetized ICR CD-1 mice were isolated. Then, 200 µl of a 10000 cpm/µl radiolabeled peptide solution (CD stock solution), obtained by diluting the radiolabeled peptide stock solution using LR/BSA buffer, was IV injected. Ten minutes after IV injection, mice were decapitated and brains were collected, weighed and measured for radioactivity. Prior to decapitation, blood was collected from the abdominal aorta followed by intracardial perfusion of the brain using 20 ml of LR buffer after clamping the aorta and severing the jugular veins. Then, brain was homogenized with 0.7 ml of ice-cold capillary buffer (10 mM HEPES, 141 mM NaCl, 4 mM KCl, 2.8 mM $CaCl_2$, 1 mM $MgSO_4$, 1mM NaH_2PO_4 and 10 mM D-glucose adjusted to pH 7.4) and 1.7 ml of 26% ice-cold dextran solution in capillary buffer. The resulting homogenate was weighed and centrifuged in a swinging bucket rotor at 5400 *g* for 30 min at 4°C, resulting in a pellet, *i.e.* capillaries, and supernatant, *i.e.* parenchyma and fat tissue, which were weighed and measured in the gamma counter. The radioactivity of blood and serum, obtained by centrifuging blood at 10000 *g*, 15 min at 21°C, were measured as well. Compartmental distribution was calculated as follows:

$$\text{Fraction}_{\text{capillaries or parenchyma}}(\%) = \frac{\frac{A_{\text{capillaries or parenchyma}}}{A_{\text{serum}}}}{\frac{A_{\text{capillaries}}}{A_{\text{serum}}} + \frac{A_{\text{parenchyma}}}{A_{\text{serum}}}} \times 100 \qquad (4)$$

Brain-to-blood transport

For evaluation of the efflux of the peptides out of the brain, ICR CD-1 mice were intraperitoneally anesthetized and the skin of the skull was removed. A puncture was made into the lateral ventricle using a 22 G needle marked with tape at 2 mm at the following coordinates: 1 mm lateral and 0.34 mm posterior with respect to the bregma. Then, 1 µl of a 25000 cpm/µl radiolabeled peptide solution (efflux stock solution), obtained by diluting the radiolabeled peptide stock solution using LR/BSA buffer, was injected in the lateral ventricle at a speed of 360 µl/h for 10 s using a syringe pump (KDS100, KR analytical, Cheshire, UK). At 1, 3, 5, 10, 12.5 and 15 min post injection, mice were decapitated and the brains were isolated, weighed and measured in the gamma counter. Prior to decapitation, blood was collected from the abdominal aorta, which was subsequently centrifuged

(10000 *g,* 15 min at 21°C) to obtain serum of which the radioactivity was measured. The brain half-time disappearance, $t_{1/2,brain}$, was calculated from the linear regression of the natural logarithm of the residual radioactivity in brain versus the experimental time as follows:

$$t_{1/2,brain} = \frac{\ln(2)}{k_{out}} \quad (5)$$

with k_{out} defined as the efflux rate constant calculated as the absolute value of the slope of the linear regression, applying first order kinetics [56].

***In vitro* metabolic stability**

The *in vitro* metabolic stability of CPPs and PrAMPs was determined in mouse serum, or plasma in case of the PrAMPs, and mouse brain homogenate according to pre-established protocols [57,58]. For the CPPs, the *in vitro* metabolic stability was also evaluated in liver and kidney homogenates. Prior to use, the protein content of each homogenate was determined using the Pierce Modified Lowry Protein Assay method (Thermo Scientific) to generate a stock solution with a protein concentration of 0.6 mg/ml by dilution with Krebs-Henseleit buffer (pH 7.4, Sigma-Aldrich). In brief, 100 µl of a 1 mg/ml peptide solution, dissolved in Krebs-Henseleit buffer (pH 7.4) was added to 900 µl of tissue extract or serum/plasma (500 µl of tissue homogenate or serum/plasma + 400 µl of Krebs-Henseleit buffer (pH 7.4) = 300 µg of protein in total) and incubated at 37°C while shaking at 750 rpm. Aliquots of 100 µl were sampled after 0, 15, 30, 60, 90 and 120 min of incubation into tubes containing an equal volume of aqueous TFA (1% V/V). For the serum samples of SynB3 and Tat 47-57, aliquots were taken as well at 2, 4, 6, 8, 10 and 12 min (in a separate experiment) and for TP10 and TP10-2 at 2, 5 and 10 min. Time points for sampling during the *in vitro* metabolic stability of the PrAMPs were 0, 5, 10, 20, 40 and 60 min.

After sampling, enzymatic activity was terminated by additional heat inactivation at 95°C for 5 min, followed by cooling the samples in an ice bath for 30 min. Centrifugation at 20000 *g* for 5 min at 5°C yielded a clear supernatant ready for HPLC-UV analysis. For the analysis of the serum samples of TP10 and TP10-2, a more extensive sample preparation was required to remove interfering compounds. Therefore, a solid-phase extraction (SPE) protocol using an Oasis® WCX µelution plate (Waters, Zellik, Belgium) was used prior to HPLC-UV analysis: at the specified time points, 100 µl aliquots were transferred to tubes containing 100 µl of a 4% (V/V) phosphoric acid solution and were consequently heated at 95°C during 5 min. After cooling the samples on an ice batch, interfering compounds were removed by SPE using a positive pressure-96 processor (Waters). Before application of the acidified sample on the Oasis® WCX µelution plate, which was conditioned with 200 µl of methanol and equilibrated with 200 µl of ultrapure water, the internal standard was added (TP10 for TP10-2 and vice versa). After loading the samples, the Oasis® WCX µelution plate was

washed using successively 200 µl of a 5% ammoniumhydroxide and 200 µl of a 70% acetonitrile solution. The peptides were eluted using four times 25 µL of a 1% TFA (V/V) in 10:90 water:acetonitrile. The resulting eluate was analyzed by HPLC-UV. Blank control solutions (placebo samples) were prepared as described above, but without adding the peptide. To confirm chemical stability and mass balance, control reference solutions without tissue homogenate or with a prior heat inactivation were analyzed as well. The HPLC-UV system consisted of a Waters Alliance 2695 separation module and a Waters 2996 PDA detector (detection from 190-400 nm, quantification at 215 nm), fitted with Empower 2 software for data handling (Waters). For each sample, 20 µl was injected and separated on an Vydac Everest C_{18} column (SynB3, Tat 47-57 and PrAMPs) or Prevail Organic Acid (pVEC, TP10 and TP10-2) column (250 × 4.6 mm, 5 µm particle size) both from Grace at 1 ml/min in an oven set at 30°C. Appropriate gradients for separation of the peptides and their metabolites were created by mixtures of 0.1% TFA (V/V) in water and 0.1% TFA (V/V) in acetonitrile. For analysis of the PrAMP *in vitro* metabolic stability samples, FA was used as acidic modifier in the mobile phase. The half-life was determined as:

$$t_{1/2} = -\frac{\ln(2)}{\text{slope}} \qquad (6)$$

with the slope derived from the curve of the natural logarithm of the percentage of the amount at the start of the incubation, *i.e.* t = 0 min, versus time.

For identification of the formed metabolites during incubation of pVEC in mouse serum, serum samples obtained at 0 min and 15 min post injection were injected into an Acquity H-class UPLC® apparatus consisting of a quaternary solvent manager, an automatic sample injection system, combined with a flow through needle, a column heater and an UPLC® PDA detector, with Empower 3 FR 2 software for data acquisition (all from Waters). An Acquity BEH C18 300 Å column (2.1 mm × 100 mm, 1.7 µm, Waters), thermostated at 30°C, was selected for separation using the same mobile phase as above. The eluting mobile phase was split towards both the PDA and a QDa detection system (ratio 10/1), consisting of an Acquity isocratic solvent manager and an Acquity QDa detector (both from Waters), equipped with an ESI interface. The fraction going to the QDa was diluted with 40:10:50 (V/V/V) water:propionic acid:2-propanol at a flow rate of 0.35 ml/min. The QDa detector was operated in positive ion mode with the ESI capillary voltage set at +0.8 kV and the cone voltage at 15 V. The probe temperature was 600°C. A full mass spectrum between *m/z* 100 and 1250 was acquired at a sampling rate of 2.0 points/s.

Statistics

Regression lines were computed using the least squares method. For fitting the MTR data using the biphasic model, Prism 6 software (GraphPad, La Jolla, USA) was used. The slopes of the regression lines of the ratio of the brain-to-serum radioactivity versus the exposure time were compared using the Prism 6 software. If the calculated P-value was greater than 0.05, the slopes were not statistically significantly different.

3. CHARACTERIZATION OF BLOOD-BRAIN BARRIER TRANSPORT OF CELL-PENETRATING PEPTIDES

The result section is subdivided into three subsections: in the first section, the BBB transport results of the five "traditional" CPPs, *i.e.* pVEC, TP10, TP10-2, SynB3 and Tat 47-57, will be presented, followed by the BBB transport data of the "new" CPPs: four PrAMPs, *i.e.* apidaecin Api137, oncocin, drosocin and drosocin Pro5Hyp, and three disulfide-rich (cyclic) peptides, *i.e.* MCoTI-II, cVc1.1 and chlorotoxin. In the third subsection, the results of the tissue distribution of the investigated peptides and the *in vitro* metabolic stability are given.

3.1. BLOOD-BRAIN BARRIER TRANSPORT OF "TRADITIONAL" CELL-PENETRATING PEPTIDES

Blood-to-brain transport kinetics

The results of the MTR analysis indicated that the five investigated CPPs crossed the BBB to a different extent. In Figure 3, the ratio of the brain and serum radioactivity is plotted versus the exposure time and the linear part of the curve was fitted using the Gjedde-Patlak model [46,49-51]. The unidirectional brain influx rates (K_{in}) and initial (vascular) brain distribution volumes (V_i) are summarized in Table 2. For pVEC, SynB3 and TP10, the MTR experiments were performed twice and their K_{in} and V_i were calculated by fitting all obtained data points. pVEC showed the highest brain influx rate of 6.02 µl/(g × min), followed by SynB3 and Tat 47-57 having a K_{in} of 5.63 µl/(g × min) and 4.73 µl/(g × min), respectively. In contrast, the transportan analogs showed a limited brain influx, especially TP10 having a K_{in} close to zero (0.05 µl/(g × min)); the K_{in} of TP10-2 was 0.36 µl/(g × min). The calculated unidirectional blood-to-brain influx rate of dermorphin (K_{in} = 0.63 µl/(g × min)) corresponds to the brain influx results previously obtained data for this positive control at our lab [48]. The radioiodinated vascular marker BSA shows a significant influx into the brain (K_{in} = 0.16 µl/(g × min)). Bovine serum albumin has been demonstrated to show non-specific binding to cerebral

capillaries of which the extent was much greater for radioiodinated than tritiated BSA, explaining its significant K_{in}-value [59].

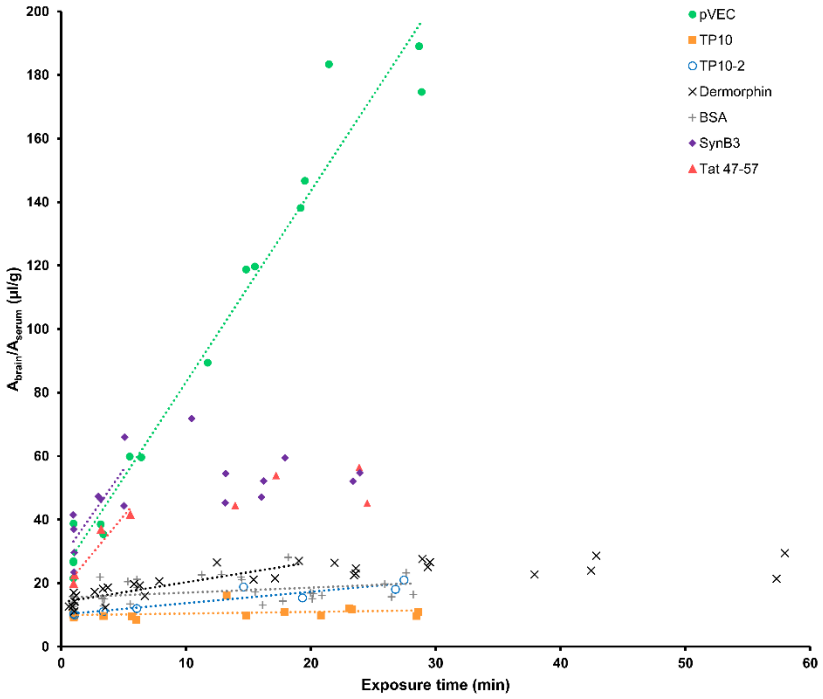

Figure 3: Results of the MTR analysis experiment of the five CPP using the linear model.
The ratio of the brain-to-serum radioactivity is plotted versus the exposure time and fitted using the linear Gjedde-Patlak model. For SynB3, Tat 47-57 and dermorphin, only the linear part of the curve is fitted using the linear model.

Table 2: Overview of the quantitative influx characteristics (± 65% confidence limits) of the five investigated CPPs based on linear and biphasic modeling of the MTR analysis data.

Influx parameter	pVEC	TP10	TP10-2	SynB3	Tat 47-57	Dermorphin	BSA
Linear Gjedde-Patlak model							
K_{in} (µl/(g× min))	6.02 ± 0.29	0.05 ± 0.04	0.36 ± 0.06	5.63 ± 1.83	4.73 ± 1.23	0.63 ± 0.10	0.16 ± 0.07
V_i (µl/g)	23.13 ± 4.33	9.88 ± 0.66	10.07 ± 1.00	27.62 ± 5.58	17.43 ± 4.04	13.98 ± 0.79	15.42 ± 1.11
Biphasic model							
V_0 (vascular) (µl/g)	-	-	-	10.27	10.27	10.27	-
V_g (tissue) (µl/g)	-	-	-	44.47 ± 7.75	34.38 ± 9.32	13.72 ± 2.17	-
K_1 (µl/(g × min))	-	-	-	29.84 ± 8.42	13.50 ± 3.88	2.54 ± 0.50	-
K (µl/(g × min))	-	-	-	≈ $1.92 \cdot 10^{-16}$	0.27 ± 0.46	0.03 ± 0.06	-

K_{in} = Unidirectional brain influx rate.
V_i = Initial (vacular) brain distribution volume.
V_0 = Vascular brain distribution volume, experimentally determined as the brain distribution volume of radioiodinated BSA (10.27 µl/g).
V_g = Tissue brain distribution volume.
K_1 = Unidirectional clearance or slope of the initial phase of the brain influx curve.
K = Net clearance or slope of the plateau phase of the brain influx curve.

The curves of the ratio of the brain and serum radioactivity versus the exposure time of SynB3 and Tat 47-57 reached a plateau-phase after about 5 min. In Figure 4, the MTR data of these peptides were fitted using a biphasic model and is summarized in Table 2 [52]. K_1 represents the unidirectional influx of the initial phase of curve and for SynB3 the K_1 (29.84 µl/(g × min)) is more than twice as high

as that of Tat 47-57 (13.50 µl/(g × min)). After reaching the plateau-phase, which can be explained by efflux of the peptide out of the brain and/or distribution and elimination of the peptide, the ratio of the brain and serum radioactivity did no longer increase for these peptides: K is about 0 µl/(g × min) for SynB3 and is 0.27 ± 0.46 µl/(g × min) for Tat 47-57, which is not statistically significantly different from zero. Thus, after the initial phase characterized by high brain influx rates, the BBB transport of SynB3 and Tat 47-57 reached a plateau of no net brain clearance.

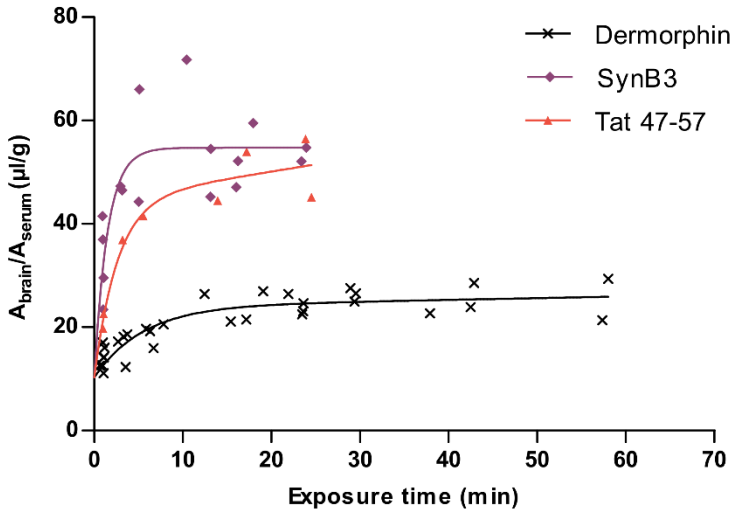

Figure 4: Result of the MTR analysis experiment of SynB3, Tat 47-57 and dermorphin using the biphasic model. The ratio of the brain-to-serum radioactivity is plotted versus the exposure time and fitted using the biphasic model.

The MTR curve of pVEC did not show a plateau-phase in the 15 min time range of the performed MTR experiments. Moreover, the amount of pVEC reaching the brain, represented by the ratio of the brain-to-serum radioactivity, greatly transcends that of the other investigated CPPs. For this CPP, the initial (vascular) brain distribution volume, representing the effective vascular space of the peptide, was higher than that of the vascular marker radioiodinated BSA which was about 15 µl/g. This was also observed for SynB3 for which the V_i was 27.62 µl/g. For the other CPPs, the V_i was of the same magnitude as of radioiodinated BSA (Tat 47-57) or was significantly smaller (transportan analogs).

The capillary depletion method was used to evaluate the brain parenchymal and capillary distribution of the radiolabeled peptides after perfusion of the brain in order to remove capillary bound peptides. The parenchymal fraction was 80% for pVEC, 77% for SynB3, 79% for Tat 47-57, 85% for TP10 and 84% for TP10-2. Thus, the measured radioactivity of the brain during the MTR experiment mainly originated from peptides present in the brain parenchyma. Only about 15 to 25% of the CPPs remained trapped by the endothelial cells.

Brain-to-blood transport kinetics

The efflux properties of the CPPs out of the brain were investigated by measuring the residual brain radioactivity after intracerebroventricular injection of the radiolabeled peptides. The efflux transfer constant k_{out} was derived from the absolute value of the slope of the natural logarithm of the brain radioactivity versus the experimental time curve (Figure 5). The k_{out} of pVEC (0.10 ± 0.11 min^{-1}) was not statistically significantly different from zero. The efflux data of pVEC showed a larger variability compared to the other investigated CPPs. However, the analysis of the radioactivity of the control samples of efflux stock solution, used to evaluate of the performance of the experimental set-up of the efflux study, did not provide any reason to reject the data. All other investigated CPPs showed a statistically significant efflux out of the brain. The k_{out} calculated for SynB3 was 0.05 ± 0.01 min^{-1}, for TP10 k_{out} was 0.09 ± 0.02 min^{-1}, and for TP10-2 k_{out} was 0.06 ± 0.01 min^{-1}. These efflux rate constants equal a half-time disappearance ($t_{1/2,brain}$) of 15 min, 8 min and 11 min, respectively. The highest efflux rate was observed for Tat 47-57, having a k_{out} of 0.21 ± 0.08 min^{-1} or $t_{1/2,brain}$ of 3 min. These brain half-time disappearances of less than 15 min suggest the existence of an active efflux transport system for the investigated peptides [60]. The observed efflux of SynB3 and Tat 47-57 is also consistent with the observed plateau-phase during the MTR experiment.

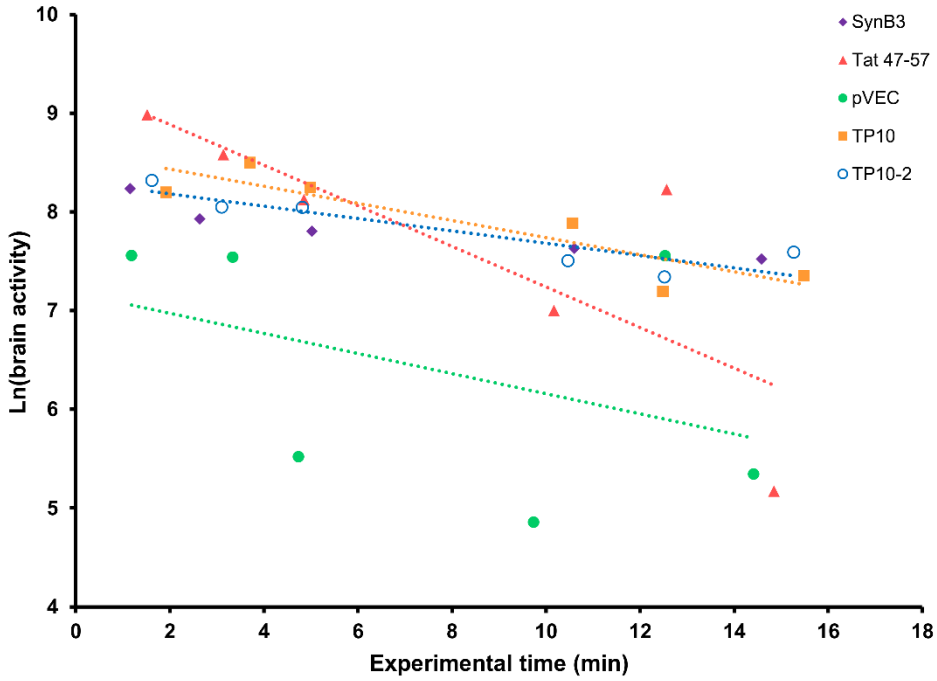

Figure 5: Brain-to-blood kinetics of the CPPs. The natural logarithm of the residual brain radioactivity is plotted versus the experimental time. The slope of the curve represents the efflux rate constant, k_{out}.

Evaluation of the influx mechanism

As pVEC showed an extraordinary high brain influx, the BBB transport of this peptide was further explored. We hypothesized that pVEC itself (transiently) could increase the BBB permeability. To evaluate this hypothesis, a MTR experiment was performed with the radioiodinated vascular marker BSA, with and without co-injection of 20 µg of pVEC. The slopes of the curves of radioiodinated BSA and radioiodinated BSA with an excess dose of pVEC were not statistically different ($P > 0.05$, Figure 6A). Thus, under the experimental conditions of this study, the BBB did not show an increased permeability for radioiodinated BSA after IV injection of pVEC, indicating the BBB integrity was not significantly influenced by pVEC.

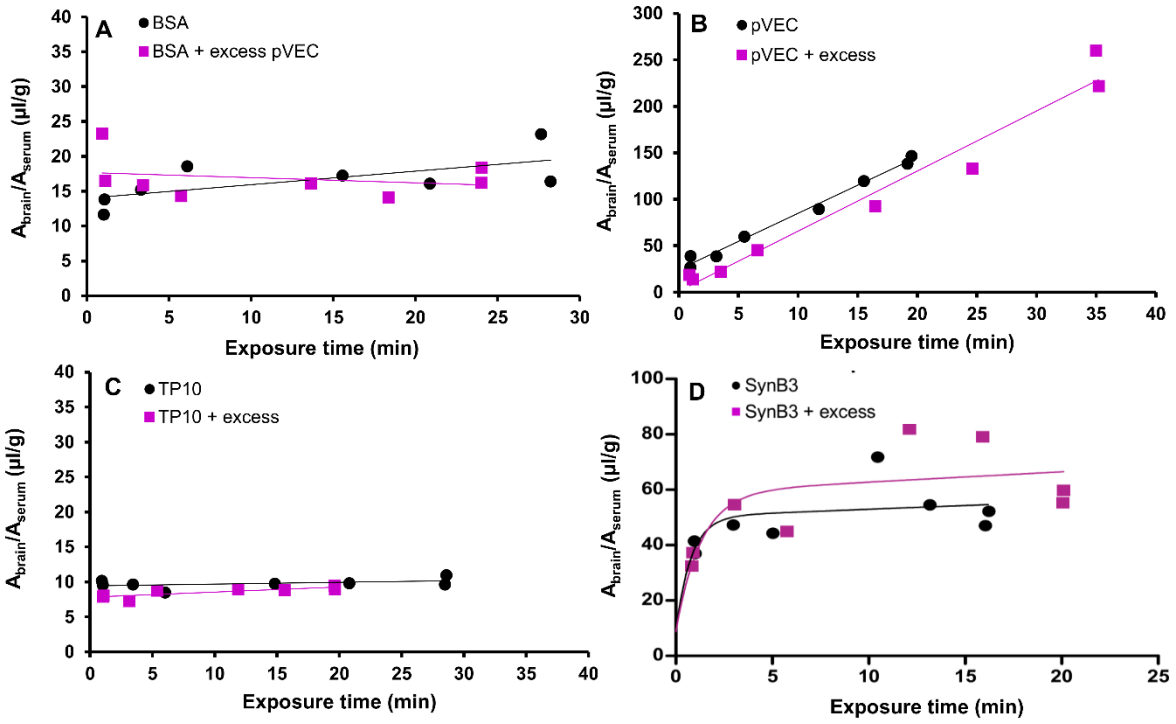

Figure 6: Evaluation of the BBB permeability after injection of pVEC and used brain influx mechanism of pVEC, TP10 and SynB3. Data were fitted using the linear Gjedde-Patlak model, except for the data of SynB3, which were fitted using the biphasic model. (A) Evaluation of the BBB permeability after IV injection of pVEC: ratio of brain-to-serum radioactivity versus exposure time of radioiodinated BSA with (purple squares) and without (black dots) an excess dose of pVEC (20 µg). (B-D) Evaluation of the saturability of influx of pVEC, TP10 and SynB3, respectively across the BBB: ratio of brain-to-serum radioactivity versus exposure time with (purple squares) and without (black dots) an excess dose of the CPP (10 µg).

Next, the saturability of the brain influx mechanism of pVEC, SynB3 and TP10, being representatives of the three different groups of CPPs observed during the BBB transport studies, was evaluated. Therefore, a MTR experiment was performed for these peptides, radiolabeled using a NCA method, with and without an excess dose of 10 µg of the unlabeled peptide. The results are shown in Figure 6B-D: there was no statistically significant difference in unidirectional brain influx rate between the experiment of the peptides alone or when co-injected with an excess dose ($P > 0.05$). For SynB3, the

the slopes of the initial, linear part of the curves fitted using the linear Gjedde-Patlak model, were not statistically significantly different ($P > 0.05$). Thus, during the performed experiments, the brain influx mechanism of pVEC, SynB3 and TP10 was not saturable. Although the K_{in} was unaffected, the excess dose of unlabeled pVEC caused a significant decrease of V_i from 24 µl/g to 1 µl/g, suggesting saturable binding sites on the brain endothelium, a phenomenon which was similarly observed for glucagon [61].

Regional intra-brain distribution

For pVEC, SynB3 and TP10, the regional differences in brain influx were investigated. Therefore, during the MTR experiments of these peptides, brains were dissected into eight different brain regions and their regional unidirectional influx rate K_{in} was determined using the Gjedde-Patlak model. For SynB3, TP10, as well as the controls radioiodinated BSA and dermorphin, no statistically significant difference in brain influx rates were observed between the different dissected brain regions ($P > 0.05$, Figure 7). The slopes, *i.e.* K_{in}, of the initial, linear part of the curves fitted using the linear Gjedde-Patlak model were compared for SynB3 and dermorphin.

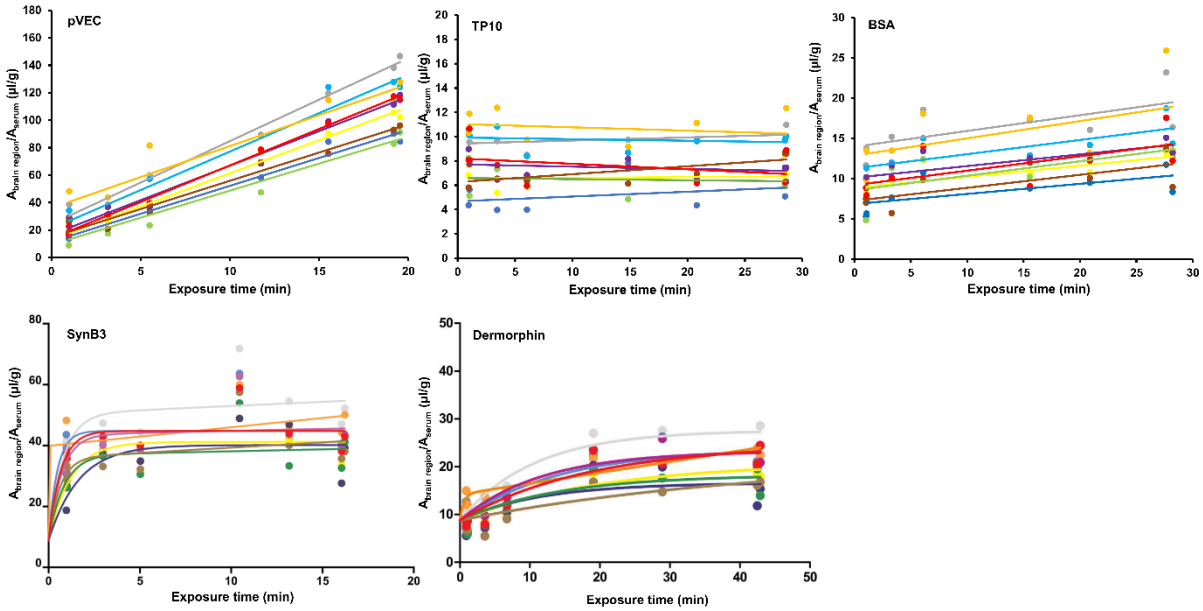

Figure 7: Regional variations in BBB influx of pVEC, TP10, SynB3, dermorphin and radioiodinated BSA. The data of pVEC, TP10 and radioiodinated BSA are fitted using the linear Gjedde-Patlak model; the data of SynB3 and dermorphin were fitted using the biphasic model. Grey = whole brain, yellow = frontal cortex, purple = occipital + parietal cortex, light blue = cerebellum, dark blue = striatum, brown = thalamus + hypothalamus, orange = pons medulla, green = hippocampus and red = midbrain.

For pVEC, the slopes of the curves of the ratio of the brain-to-serum radioactivity versus the exposure time differed significantly ($P < 0.05$). In Table 3, the individual K_{in} and V_i values of the whole brain and brain regions after IV injection of pVEC are summarized. Nevertheless, the difference in

unidirectional brain influx rates is not pronounced: the influx of pVEC was only slightly higher in the cerebellum, cortex and midbrain compared to the pons medulla, hippocampus, thalamus and hypothalamus and striatum.

Table 3: K_{in} and V_i values of the whole brain and eight brain regions of pVEC (between brackets the 65% confidence interval is indicated).

Brain region	K_{in} (µl/(g × min))	V_i (µl/g)
Whole brain	6.04 [5.78, 6.30]	24.37 [21.23, 27.51]
Cerebellum	5.61 [5.12, 6.10]	21.02 [15.09, 26.95]
Pons medulla	4.51 [3.87, 5.15]	36.06 [28.34, 43.78]
Frontal cortex	4.84 [4.66, 5.02]	12.93 [10.77, 15.09]
Striatum	4.07 [3.77, 4.37]	11.47 [7.81, 15.13]
Hippocampus	3.94 [3.51, 4.37]	9.33 [4.13, 14.54]
Occipital and parietal cortex	5.03 [4.73, 5.32]	16.61 [13.02, 20.19]
Thalamus and hypothalamus	4.12 [3.86, 4.38]	17.72 [11.58, 17.86]
Midbrain	5.32 [5.17, 5.46]	13.88 [12.15, 15.62]

3.2. BLOOD-BRAIN BARRIER TRANSPORT OF "NEW" CELL-PENETRATING PEPTIDES

Blood-to-brain transport kinetics

In Figure 8, the results of the MTR analysis of the four investigated PrAMPs and three disulfide-rich (cyclic) peptides are shown. Clearly, the two classes of peptides differed in the extent of BBB influx.

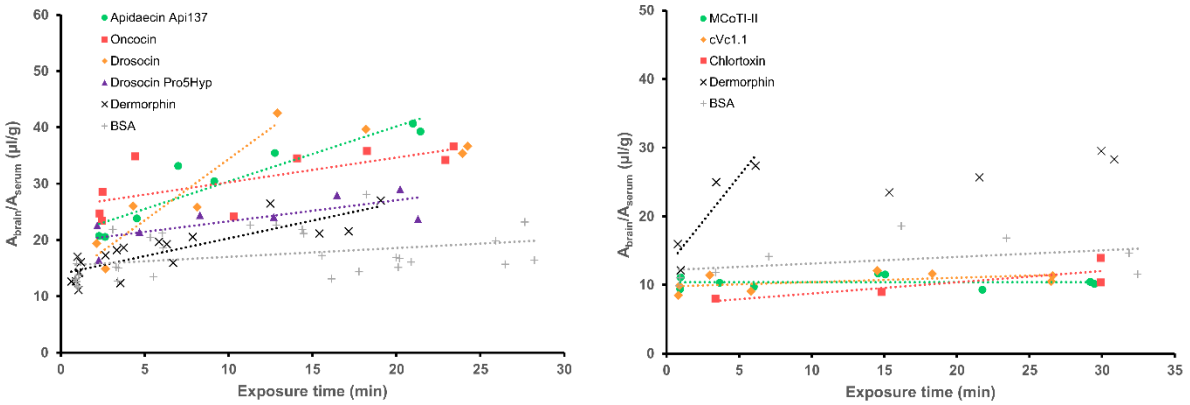

Figure 8: Results of the multiple time regression analysis experiment of four PrAMPs (left) and three disulfide-rich (cyclic) peptides, fitted using the linear Gjedde-Patlak model. For drosocin and dermorphin, only the linear part of the curve was fitted by the linear model.

The unidirectional brain influx rates and initial (vascular) brain distribution volumes are summarized in Table 4 and 5. The PrAMPs showed a significant brain influx: drosocin showed the highest K_{in} of 2.18 µl/(g × min), followed by apidaecin Api137, with an estimated K_{in} of 0.77 µl/(g × min). Similar unidirectional brain influx rates were observed for oncocin and drosocin Pro5Hyp having a K_{in} of 0.44 µl/(g × min) and 0.37 µl/(g × min), respectively. On the other hand, the disulfide-rich (cyclic) peptides did not show a significant brain influx: only a very low K_{in} was observed for cVc1.1 and chlorotoxin

and a non-significant value for MCoTI-II (Table 5). The K_{in} of these peptides was not significantly different from radioiodinated vascular marker BSA ($P > 0.05$).

Table 4: Overview of the quantitative influx characteristics (± 65% confidence limits) of the four investigated PrAMPs peptides based on linear and biphasic modeling of the MTR analysis data.

Influx parameter	Apidaecin Api137	Oncocin	Drosocin	Drosocin Pro5Hyp
Linear Gjedde-Patlak model				
K_{in} (µl/(g× min))	0.73 ± 0.13	0.44 ± 0.17	2.18 ± 0.53	0.37 ± 0.14
V_i (µl/g)	23.43 ± 1.70	25.84 ± 2.32	12.59 ± 3.87	19.57 ± 1.79
Biphasic model				
V_0 (vascular) (µl/g)	-	-	10.27[1]	-
V_g (tissue) (µl/g)	-	-	29.1 ± 37.41	-
K_1 (µl/(g × min))	-	-	4.29 ± 1.93	-
K (µl/(g × min))	-	-	≈ $1.77 \cdot 10^{-16}$	-

[1]No data available for dermorphin and radioiodinated BSA for the BBB transport study of the PrAMPs. V_0 of radioiodinated BSA, obtained during BBB transport of CPPs was used (Table 2).
K_{in} = Unidirectional (brain) influx rate.
V_i = Initial (vascular) brain distribution volume.
V_0 = Vascular brain distribution volume, experimentally determined as the brain distribution volume of radioiodinated BSA.
V_g = Tissue brain distribution volume.
K_1 = Unidirectional clearance or slope of the initial phase of the brain influx curve.
K = Net clearance or slope of the plateau phase of the brain influx curve.

Table 5: Overview of the quantitative influx characteristics (± 65% confidence limits) of the three disulfide-rich (cyclic) peptides as well as dermorphin and radioiodinated BSA based on linear and biphasic modeling of the MTR analysis data.

Influx parameter	MCoTI-II	cVc1.1	Chlorotoxin	Dermorphin	BSA
Linear Gjedde-Patlak model					
K_{in} (µl/(g× min))	$9.37 \cdot 10^{-5}$ ± 0.03	0.06 ± 0.04	0.16 ± 0.10	2.65 ± 0.86	0.10 ± 0.08
V_i (µl/g)	10.39 ± 0.50	9.76 ± 0.65	7.10 ± 2.26	12.60 ± 3.44	12.15 ± 1.62
Biphasic model					
V_0 (vascular) (µl/g)	-	-	-	9.15	-
V_g (tissue) (µl/g)	-	-	-	16.23 ± 3.56	-
K_1 (µl/(g × min))	-	-	-	8.76 ± 3.32	-
K (µl/(g × min))	-	-	-	0.08 ± 0.15	-

K_{in} = Unidirectional (brain) influx rate.
V_i = Initial (vascular) brain distribution volume.
V_0 = Vascular brain distribution volume, experimentally determined as the brain distribution volume of radioiodinated BSA.
V_g = Tissue brain distribution volume.
K_1 = Unidirectional clearance or slope of the initial phase of the brain influx curve.
K = Net clearance or slope of the plateau phase of the brain influx curve.

Only for drosocin, a biphasic BBB influx behavior was observed, thus for this peptide the MTR results were also fitted using the biphasic model (Table 4). After an initial increase in the ratio of the brain and serum radioactivity (K_1 was 4.29 µl/(g × min)), a plateau is reached characterized by no net brain clearance (K not significantly different from zero).

For PrAMPs, showing a significant brain influx, the parenchymal and capillary distribution was investigated using the capillary depletion method. The observed parenchymal fractions ranged between 67% for drosocin and drosocin Pro5Hyp, and 77% for apidaecin Api137. The brain radioactivity of these PrAMPs are mainly derived from peptides distributed to the brain parenchyma.

In contrast, the parenchymal fraction of oncocin was only 18%, indicating the 82% of peptide remains trapped in the brain capillary endothelial cell.

Brain-to-blood transport kinetics

During the brain efflux study of the four PrAMPs, a clear efflux out of the brain was demonstrated for drosocin, the only peptide showing a biphasic brain influx behavior. The calculated k_{out} was 0.22 ± 0.10 min^{-1}, which corresponds with a brain half-time disappearance of 3 min. This low value of $t_{1/2,brain}$ suggests the use of an active efflux system [60]. The other three PrAMPs did not show a significant brain-to-blood transport. After intracerebroventricular injection of the disulfide-rich (cyclic) peptides, only MCoTI-II could reach the peripheral blood circulation with a k_{out} of 0.07 ± 0.04 min^{-1} ($t_{1/2,brain}$ = 9 min) also indicating the existence of an active efflux system for this peptide.

3.3. TISSUE DISTRIBUTION AND *IN VITRO* METABOLIC STABILITY

Tissue distribution after IV injection

The tissue distribution of the investigated peptides was evaluated at the 15 min time point of the MTR experiments. In Figure 9, the results of the CPPs, as well as the controls dermorphin and radioiodinated BSA are shown. pVEC and Tat 47-57 showed a high liver distribution compared to the other tissues. The transportan analogs did also show this high liver concentration, but an even higher serum distribution was observed. SynB3 was mainly distributed to the spleen and serum and to a lesser extent to the liver. This CPP also showed a significant heart distribution. The results of the controls dermorphin and radioiodinated BSA were similar as reported in previous studies, with high liver distributions for both controls and also high serum concentrations for radioiodinated BSA [48,62,63].

The tissue distribution pattern of the PrAMPs was analogous: the highest radioactivity was found in serum (Figure 10). Apidaecin Api137, drosocin and drosocin Pro5Hyp also distributed significantly to the kidneys, but to a lesser extent than serum. For oncocin, a significant distribution to the lungs is noted as well. For the disulfide-rich (cyclic) peptides, the tissue distribution was also similar within this group of peptides (Figure 10). MCoTI-II, cVc1.1 and chlorotoxin were extensively distributed to the kidneys and to a lesser extent to the serum compartment. Thus, the distribution to the different tissues varied among the different investigated peptides, which is also observed for other already investigated peptides [48,62,63].

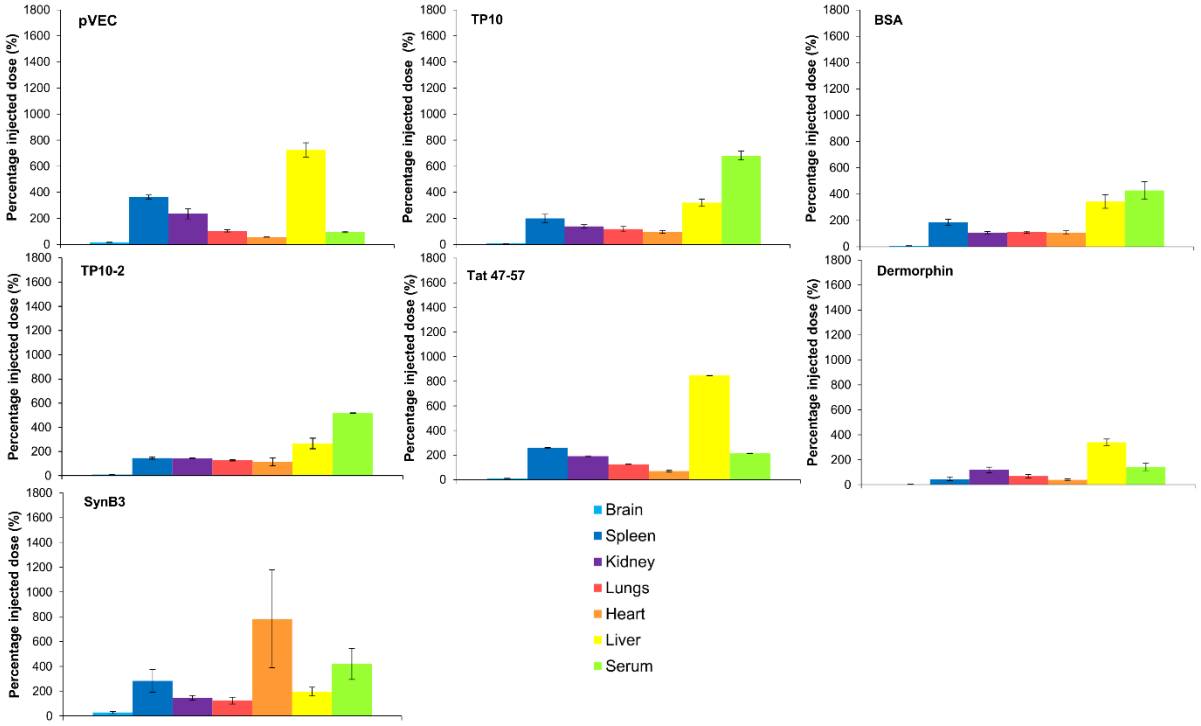

Figure 9: Relative tissue distribution of the radiolabeled CPPs and the controls dermorphin and radioiodinated BSA 15 min post IV injection expressed as the percentage of the injected dose, representing the ratio of the weight corrected radioactivity of the tissue and the injected radioactivity (± SEM, n = 2). From the left to the right: brain (light blue), spleen (dark blue), kidneys (purple), lungs (red), heart (orange), liver (yellow) and serum (light green).

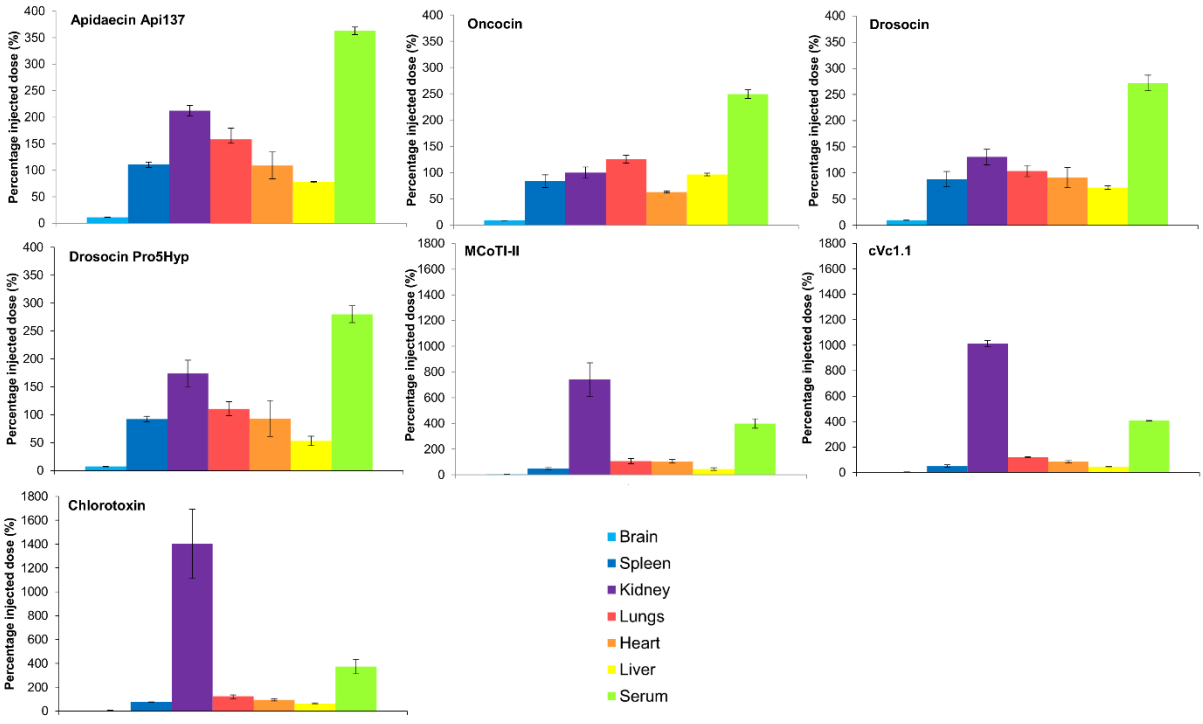

Figure 10: Relative tissue distribution of the radiolabeled PrAMPs and disulfide-rich (cyclic) peptides 15 min post IV injection expressed as the percentage of the injected dose, representing the ratio of the weight corrected radioactivity of the tissue and the injected radioactivity (± SEM, n = 2). From the left to the right: brain (light blue), spleen (dark blue), kidneys (purple), lungs (red), heart (orange), liver (yellow) and serum (light green).

In vitro peptide stability in mouse serum and brain, kidney and liver homogenates

Data on the metabolic stability of CPPs are scarce [42,64-66]. Therefore, the stability of the investigated CPPs was determined in mouse serum, as well as in mouse brain, liver and kidney homogenates. Also for the PrAMPs, the *in vitro* metabolic stability was evaluated in mouse plasma and brain tissue homogenate. The results are summarized in Table 5. The *in vitro* serum stability of MCoTI-II, cVc1.1 and chlorotoxin was investigated by prof. D. Craik and personally communicated to us.

Table 5: Overview of the *in vitro* metabolic stability results of the investigated peptides.

Peptide	$t_{1/2}$ serum (min)	$t_{1/2}$ brain (min)	$t_{1/2}$ kidneys (min)	$t_{1/2}$ liver (min)
pVEC	< 3	68	7	43
TP10	1316	176	34	139
TP10-2	229	102	11	118
SynB3	6	21	5	37
Tat 47-57	3	54	18	60
MCoTI-II[1]	> 13 000	-	-	-
cVc1.1[1]	> 13 000	-	-	-
Chlorotoxin[1]	> 13 000	-	-	-
Peptide	**$t_{1/2}$ plasma (min)**	**$t_{1/2}$ brain (min)**	**$t_{1/2}$ kidneys (min)**	**$t_{1/2}$ liver (min)**
Apidaecin Api137	220	637	-	-
Oncocin	47	142	-	-
Drosocin	81	363	-	-
Drosocin Pro5Hyp	157	409	-	-

[1]Data personally communicated by prof. D. Craik (e-mailed by Aaron Poth on 10 December 2014).

In the brain and liver homogenate, the stability varied among the CPPs: in mouse brain, the half-lives ranged between 21 min (SynB3) and 176 min (TP10) and in the liver homogenate between 37 min (SynB3) and 139 min (TP10). The transportan analogs showed high serum stability, with a half-life of 22 h for TP10 and 4 h for TP10-2. In contrast, Tat 47-57, SynB3 and pVEC were not so stable in serum, having a half-life of less than 5 min. Kidney enzymes also extensively metabolized the investigated CPPs: the half-lives ranged between 5.5 min (SynB3) and 34 min (TP10). For pVEC, showing an extraordinary brain influx, the formed metabolites during serum incubation were further investigated. One metabolite was determined and identified as the pVEC peptide with the first six hydrophobic N-terminal amino acids deleted, formed by cleavage of the first N-terminal arginine-arginine bond ($pVEC_{7-18}$), which is known to be unstable in serum (Figure 11) [64].

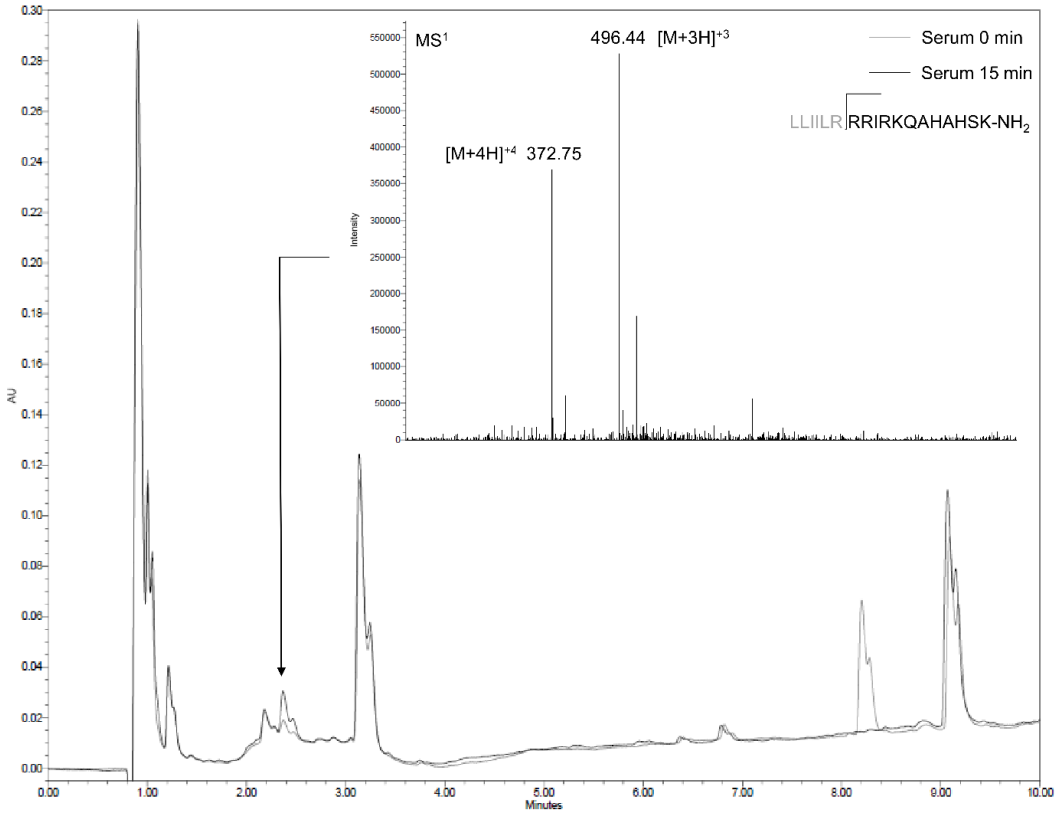

Figure 11: Identification of metabolite of pVEC formed during *in vitro* incubation in mouse serum.

The PrAMPs also showed a high *in vitro* brain stability with the lowest $t_{1/2}$ of 142 min observed for oncocin. The plasma half-lives ranged between 47 min and 81 min for oncocin and drosocin, respectively, and 157 min and 220 min for drosocin Pro5Hyp and apidaecin Api137, respectively. These results are in line with already published results, although established in serum using a different protocol [67-69]. MCoTI-II, cVc1.1 and chlorotoxin showed an extremely high serum stability, which is a particular feature of these peptides attributed to the cyclic backbone and/or the presence of multiple disulfide bonds in their structure [70,71].

4. EVALUATION OF BLOOD-BRAIN BARRIER TRANSPORT DATA OF CELL-PENETRATING PEPTIDES

Despite the ability of CPPs to enter mammalian cells, only a few studies have fragmentarily investigated their transcellular transport characteristics. Lindgren *et al.* demonstrated for TP10 its ability to cross a Caco-2 cell layer, while penetratin passed the cell layer to a lower extent due to rapid degradation [72]. For the Tat peptide, *in vitro* transcellular delivery studies could not demonstrate the capacity of the peptide to cross the cell layers [73-75]. *In vivo* evaluation of CPP-mediated delivery of cargoes resulted in divergent outcomes. Tat-mediated delivery of neuroprotective therapeutics across the BBB in ischemia and seizure models gave promising results,

but in these models the BBB is compromised [75]. For a limited set of CPPs, studies are available demonstrating their ability to mediate CNS delivery of different cargoes *in vivo* (Table S1 of the Supplementary Information) [39]. Currently, CPPs are investigated as possible carriers for BBB-impermeable cargoes. However, quantitative knowledge on the BBB transport characteristics of CPPs without a cargo is also needed as these peptides can be produced endogenously through metabolization of proteins and might exert biological activity. As this information is currently lacking, the *in vivo* BBB transport of five "traditional" CPPs was investigated to evaluate whether cell-penetrating properties of peptides inherently imply the ability to cross the BBB. The selected peptides constitute different clusters in the exploration of the chemical space of the CPPs and thus structurally disseminate (Figure 1). TP10-2 only differs one amino acid from TP10, but differentiates in α-helicity and extent of cellular uptake [76]. Beside this structural variability, the model peptides also differ in cell-penetrating ability, expressed as the CP-response, which was introduced in **Chapter II**: TP10 and pVEC have the highest cellular influx with a CP-response of 1.641 and 1.318, respectively, while SynB3 and Tat 47-57 show the lowest cellular penetration, having a CP-response of 0.126 and 0.309, respectively (Table 1). The chemical space of the investigated peptides was further extended with four PrAMPs and three disulfide-rich (cyclic) peptides. Cell-penetrating properties have already been attributed to these peptides, which are not specifically investigated as CPPs. Moreover, their chemical structures are positioned in the chemical space of the CPPs (Figure 1), justifying their inclusion in our study aiming to evaluate the correlation between cell-penetrating properties and the extent of BBB penetration.

In this study, the selected peptides showed quite different BBB transport properties. The CPPs Tat 47-57, pVEC and SynB3 showed relatively high unidirectional brain influx rates (K_{in}), of 4.73 µl/(g × min), 6.02 µl/(g × min) and 5.63 µl/(g × min), respectively, as obtained by fitting the MTR data using the linear Gjedde-Patlak model. On the other hand, the transportan analogs showed a very low to negligible brain influx. This was also observed for the disulfide-rich (cyclic) peptides, which was expected for chlorotoxin [77]. All PrAMPs significantly crossed the BBB with the unidirectional brain influx rates ranging between 0.37 µl/(g × min) for drosocin Pro5Hyp and 2.18 µl/(g × min) for drosocin. The brain influx kinetics of the controls dermorphin and radioiodinated BSA obtained during the different BBB transport studies were consistent as well as in line with previously performed experiments. The blood-to-brain transport of pVEC was extraordinary high: the amount of peptide reaching the brain was much higher compared to SynB3, Tat 47-57 and the PrAMPs, with a maximal ratio of brain-to-serum radioactivity of about 180 µl/g for pVEC versus about 70 µl/g for SynB3. This high brain influx was not caused by an apparent increase in BBB permeability, as co-injection of radioiodinated BSA with pVEC did not result in an increased brain entry of the vascular

marker. Using the capillary depletion method, it was demonstrated that the peptides effectively crossed the BBB with a parenchymal fraction of about 80% for all CPPs and 67% (drosocin and its analog) to 77% (apidaecin Api137) for the PrAMPs. The capillary depletion experiment indicated that oncocin remained trapped in the capillary endothelial cells as its parenchymal fraction was only 18%. In contrast to pVEC, both SynB3 and Tat 47-57 showed a biphasic BBB influx behavior, which was also observed for drosocin: after an initial sharp increase, the MTR-curve reached a plateau-phase, resulting in a non-significant net brain clearance of these peptides. This plateau-phase can at least partly be explained by the significant efflux out of the brain for these peptides with k_{out} of 0.05 min^{-1} for SynB3, of 0.21 min^{-1} for Tat 47-57 and of 0.22 min^{-1} for drosocin. Also TP10 (k_{out} = 0.09 min^{-1}), TP10-2 (k_{out} = 0.06 min^{-1}) and MCoTI-II (0.07 min^{-1}) showed a significant efflux out of the brain. The brain half-time disappearances suggest the existence of an active efflux transport system for these peptides [60]. For SynB3, TP10 and the controls dermorphin and radioiodinated BSA, no differences in influx between the eight dissected brain regions were observed. For pVEC, the K_{in} values of the dissected brain regions statistically differed, but the observed regional difference was not pronounced compared to other peptides such as amylin and insulin showing clear regional variations in brain influx [78]. It is unlikely that alterations in cerebral blood flow due to the changing local metabolic demand explain the observed differences in regional brain uptake, as this only affects the uptake of compounds showing a very rapid brain influx, *i.e.* those of which the brain influx can be determined using the brain uptake index (BUI) method [78-80]. The BBB influx (K_{in}) of pVEC, TP10 and SynB3 was not saturated when peptides were co-injected with an excess dose of 10 µg of unlabeled peptide. For pVEC, the V_i significantly decreased suggesting the presence of saturable binding sites, similarly as observed for glucagon. These saturable binding sites may include receptors or enzymes located at the brain capillary endothelium [61].

All investigated CPPs were mainly distributed to the liver and serum, which was also previously demonstrated for pVEC and TP10 [64]. For pVEC and Tat 47-57, a very high liver concentration was observed compared to the other tissues, which can indicate metabolization, but also uptake of the peptides and their metabolites in hepatocytes. The disulfide-rich (cyclic) peptides were extensively distributed to the kidneys, also pointing to metabolization and/or uptake in nephrocytes, as well as to renal excretion of these peptides. The transportan analogs, SynB3 and the four PrAMPs, showed a high serum distribution, that can be explained either by protein binding or high serum stability and the latter was confirmed during the *in vitro* metabolic stability study of the transportan analogs and PrAMPs where a serum half-life of 22 h was calculated for TP10 and of 4 h for TP10-2, while the plasma half-lives of the PrAMPs were higher than or equal to 47 min. SynB3, pVEC and Tat 47-57 were not stable in serum, having half-lives of less than 6 min. Thereby, it cannot be excluded that

radiolabeled metabolites of these CPPs contribute to the observed brain radioactivity during the evaluation of the blood-to-brain transport. During *in vivo* metabolic stability studies, metabolites present in serum, as well as in brain tissue can be identified, providing the full picture of which peptides do actually cross the BBB. This information is valuable during structure-property relationship studies for BBB transport of CPPs, or peptides in general. The low serum stability originates from the presence of arginine-arginine bonds, which are absent in the sequence of the transportan analogues [64]. The low stability was already reported for Tat 47-57 [65], as well as for pVEC, for which a rapid C-terminal lysine (Lys^{18}) cleavage was demonstrated when incubated in human serum [66]. In contrast, Sarko *et al.* demonstrated a (human) serum half-life of a few hours by evaluating the activity of the ^{68}Ga-DOTA labeled pVEC [64]. During this *in vitro* study, we could not demonstrate the formation of this Lys^{18}-cleaved pVEC metabolite when incubated in mouse serum. Instead, we identified a metabolite being pVEC from which the first six hydrophobic N-terminal amino acid residues were cleaved off ($pVEC_{7-18}$). A structure-activity relationship study revealed that these cleaved-off N-terminal hydrophobic residues are crucial for the cellular uptake properties, suggesting that the found metabolite $pVEC_{7-18}$ is not cell-penetrating [81]. Thus, both pVEC and $pVEC_{7-18}$, having similar cationic nature, could contribute to the measured brain radioactivity during the MTR experiment of pVEC as both contain a radiolabeled tyrosine residue. Once the brain tissue was reached, the mouse brain half-life indicates the peptides remain sufficiently stable to allow further distribution in the brain parenchyma.

The investigated “traditional” CPPs differ in the used cellular influx mechanism and adopted secondary structure at the membrane interface. For SynB3, an endocytosis-dependent mechanism is described, which is initiated after an electrostatic interaction [82]. The uptake of Tat 47-57 is endocytosis-driven as well, but starting from a certain threshold concentration, the peptide directly penetrates into the cell [2,82-84]. The use of endocytosis-dependent and -independent mechanisms has been demonstrated for pVEC [2,81,85,86]. This peptide is derived from the murine vascular endothelial cadherin, located in the adherens junctions between the vascular endothelial cells, and constitutes the 13 cytosolic amino acids closest to the membrane and five amino acids from the C-terminus of the transmembrane region (615-632) [24]. As already mentioned, these five hydrophobic residues, located at the N-terminus of the pVEC sequence, appear to be crucial for cellular uptake and directly interact with the plasma membrane [81]. The cellular interaction of pVEC, SynB3 or Tat 47-57 does not cause any membrane disturbances [81,82]. This corroborates with our results where we could not demonstrate that pVEC increased the BBB permeability, as the influx of radioiodinated BSA did not augment after co-injection with pVEC. For TP10, the used cell-penetrating mechanism remains controversial: Padari *et al.* described an endocytosis-driven mechanism, while more recent

studies ascribe a pore-forming mechanism [87-89]. The investigated peptides also have a different secondary structure at the membrane interface: when in solution, all peptides have a random coil structure, but at the membrane interface, pVEC adopts a β-sheet structure and TP10 becomes α-helical, while SynB3 and Tat 47-57 remain random coiled [76,90]. Overall, the investigated CPPs differ essentially in the presence or absence of arginine residues, thus their cationic nature (chemical properties), in their secondary structure at the membrane interface (physicochemical properties) and inherently, in the cellular uptake mechanism (biological properties).

Based on the BBB transport results, three groups of CPPs can be distinguished. The cationic-amphipathic peptide pVEC constitutes the first group, which shows a rapid brain influx, resulting finally in a relatively high ratio of brain-to-serum radioactivity. SynB3 and Tat 47-57, both short cationic CPPs, form the second group and have relatively high initial brain influx rates, but their brain influx shows a biphasic behavior. The third group consists of the transportan analogs, TP10 and TP10-2, which show no to slow brain influx, respectively. The first two groups are composed of arginine-rich peptides, while the transportans only contain lysine-residues in their sequences and have a much lower charge density of 19% versus 44%, 50% and 73% of pVEC, SynB3 and Tat 47-57, respectively (Table 1). Thus, arginine-rich CPPs seem to more effectively and rapidly influx the BBB in the investigated experimental time period. These findings are affirmed by the BBB transport results of the PrAMPs, which are also arginine-rich but have a lower charge-density compared to pVEC, SynB3 and Tat 47-57. The disulfide-rich (cyclic) peptides are characterized by a very low charge-density (Table 1). The BBB influx properties of pVEC, SynB3 and Tat 47-57 are also superior to other peptides already investigated for their BBB transport characteristics: using the proposed classification method described in **Chapter III** of this thesis, these peptides show a very high brain influx (class 5), while TP10 and TP10-2 have a very low (class 1) and low (class 2) brain influx, respectively. These findings were not expected based on the cell-penetrating properties of these CPPs, quantitatively expressed as the CP-response. TP10 had the highest CP-response (1.641), but the poorest BBB influx characteristics. In contrast, medium cell-penetrating properties were attributed to SynB3 and Tat 47-57, but high BBB influx was concluded. Moreover, cell-penetrating properties were attributed to the disulfide-rich (cyclic) peptides with a CP-response of 0.103 for MCoTI-II indicating a rather low cellular influx, but no significant BBB influx was observed. Our data indicate that CPPs selectively cross the BBB and that their brain influx behavior cannot be directly positively correlated with their cell-penetrating properties (Figure 12).

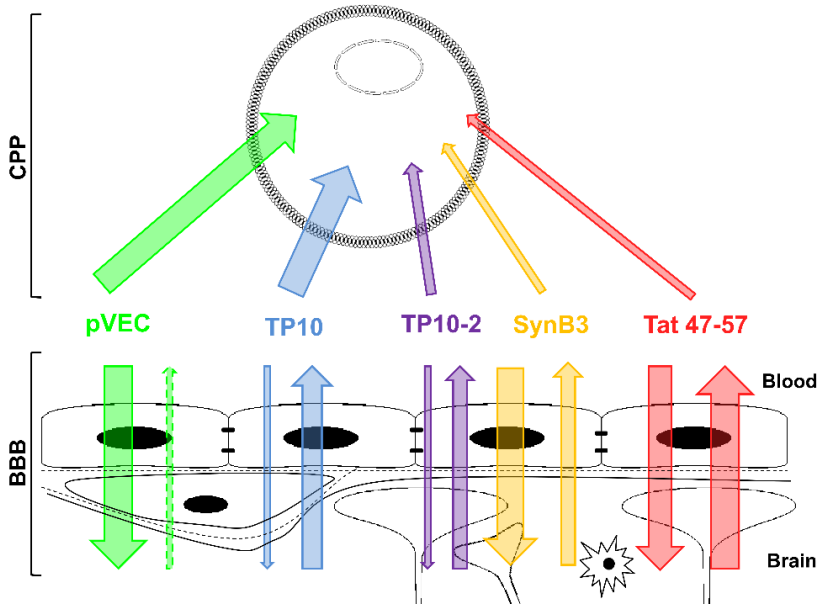

Figure 12: Schematic overview of the relationship between cell-penetrating (upper part of the figure) and BBB-penetrating properties of the five investigated CPPs (lower part of the figure). The thickness of the arrows indicates the extent of influx and/or efflux. The non-significant efflux of pVEC is indicated by a dashed line.

As described in **Chapter I** of this thesis, crossing the BBB comprises multiple steps, which can explain why the cell-penetrating properties of peptides are not related to the BBB influx properties of CPPs. The first step includes the passage of the luminal membrane at the blood-brain interface of which the extent can be related to the cell-penetrating properties of the peptides, unless a specific interaction with a transporter or receptor is involved. Next the peptide enters the cytosol of the capillary endothelial cell, where the CPP can be metabolized or can remain in tact and finally reach the abluminal membrane. If exocytosed out of the capillary endothelial cell, the peptide has crossed the BBB. It is expected that the CPPs, their formed radiolabeled metabolites in case of cytosolic metabolization, or both can cross the abluminal membrane as the capillary fraction obtained during capillary depletion experiment was only about 20%, except for oncocin. Because of the cationic nature of the CPPs, it was expected that the CPPs would cross the BBB using the adsorptive-mediated transcytosis mechanism, which was already demonstrated to be the influx mechanism of SynB3 [41]. However under the applied experimental conditions, the BBB influx of the CPPs was not saturable. Only for pVEC, a decrease of V_i was observed when the peptide was co-injected with an excess dose, suggesting the saturable binding sites for this peptides, including receptor(s), enzymes or a charge interaction. Taken our data together, it is assumed that the BBB transport of CPPs involves an initial charge interaction with the negatively charged glycocalyx and phospholipid head groups as a high charge density derived from arginine residues seems to favor BBB influx. This charge interaction triggers the uptake into the capillary endothelial cell, presumably by passive diffusion as the BBB influx mechanism is not saturable. Clearly, the mechanism of transport of the CPPs, or peptides in

general, is unresolved. Also knowledge on the intracellular fate of these peptides in the capillary endothelial cell is helpful for understanding the transport acrosss the BBB. Nevertheless, the results of this study provide several pieces of the puzzle of this complex, but highly relevant research topic.

5. CELL-PENETRATING PEPTIDES SELECTIVELY CROSS THE BLOOD-BRAIN BARRIER *IN VIVO*

The BBB transport properties of five structurally different model CPPs, showing a variable extent of cellular penetration, were investigated. SynB3, Tat 47-57 and pVEC showed relatively high (initial) brain influx rates, while the influx of TP10 and TP10-2 was low. The CPPs use a non-saturable influx mechanism and do not cause a (transient) increase in BBB permeability, as demonstrated for pVEC. Except for pVEC, all peptides showed a significant efflux out of the brain, which partly explains the biphasic behavior of SynB3 and Tat 47-57. Our BBB transport results indicate that CPPs selectively cross the BBB and thus cell-penetrating properties of peptides do not imply BBB-penetrating ability. These findings were corroborated by the BBB transport data of the PrAMPs and disulfide-rich (cyclic) peptides.

6. REFERENCES

[1] Madani F, Lindberg S, Langel Ü, Futaki S, Gräslund A. Mechanisms of Cellular Uptake of Cell-Penetrating Peptides. *J. Biophys.* 2011; **2011**: 414729.

[2] Copolovici DM, Langel K, Eriste E, Langel Ü. Cell-Penetrating Peptides: Design, Synthesis, and Applications. *ACS Nano* 2014; **8**: 1972-1994.

[3] Bechara C, Sagan S. Cell-penetrating peptides: 20 years later, where do we stand? *FEBS Lett.* 2013; **587**: 1693-1702.

[4] Milletti F. Cell-penetrating peptides: classes, origin, and current landscape. *Drug Discov. Today* 2012; **17**: 850-860.

[5] Hansen A, Schäfer I, Knappe D, Seibel P, Hoffmann R. Intracellular Toxicity of Proline-Rich Antimicrobial Peptides Shuttled into Mammalian Cells by the Cell-Penetrating Peptide Penetratin. *Antimicrob. Agents Chemother.* 2012; **56**: 5194-5201.

[6] Tomasinsig L, Skerlavaj B, Papo N, Giabbai B, Shai Y, Zanetti M. Mechanistic and Functional Studies of the Interaction of a Proline-rich Antimicrobial Peptide with Mammalian Cells. *J. Biol. Chem.* 2006; **281**: 383-391.

[7] Otvos L Jr, Cudic M, Chua BY, Deliyannis G, Jackson DC. An Insect Antibacterial Peptide-Based Drug Delivery System. *Mol. Pharm.* 2004; **1**: 220-232.

[8] Kragol G, Hoffmann R, Chattergoon MA, Lovas S, Cudic M, Bulet P, Condie BA, Rosengren KJ, Montaner LJ, Otvos L Jr. Identification of crucial residues for the antibacterial activity of the proline-rich peptide, pyrrhocoricin. *Eur. J. Biochem.* 2002; **269**: 4226-4237.

[9] Greenwood KP, Daly NL, Brown DL, Stow JL, Craik DJ. The cyclic cysteine knot miniprotein MCoTI-II is internalized into cells by macropinocytosis. *Int. J. Biochem. Cell B.* 2007; **39**: 2252-2264.

[10] Splith K, Neundorf I. Antimicrobial peptides with cell-penetrating properties and vice versa. *Eur. Biophys. J.* 2011; **40**: 387-397.

[11] Lindgren M, Langel Ü. Classes and Prediction of Cell-Penetrating Peptides. In *Cell-Penetrating Peptides: Methods and Protocols* (Ed: Langel Ü), Human Press Inc., **2011**, pp. 3-19.

[12] Brugnano J, Ward BC, Panitch A. Cell penetrating peptides can exert biological activity: a review. *Biomol. Concepts* 2010; **1**: 109-116.

[13] Verdurmen WPR, Brock R. Biological responses towards cationic peptides and drug carriers. *Trends Pharmacol. Sci.* 2010; **32**: 116-124.

[14] Suhorutsenko J, Eriste E, Copolovici D-M, Langel Ü. Human Protein 53-Derived Cell-Penetrating Peptides. *Int. J. Res. Ther.* 2012; **18**: 291-297.

[15] Johansson HJ, El-Andaloussi S, Holm T, Mäe M, Jänes J, Maimets T, et al. Characterization of a Novel Cytotoxic Cell-penetrating Peptide Derived From p14ARF Protein. *Mol. Ther.* 2008; **16**: 115-123.

[16] Jones S, Holm T, Mäger I, Langel Ü, Howl J. Characterization of Bioactive Cell Penetrating Peptides from Human Cytochrome c: Protein Mimicry and the Development of a Novel Apoptogenic Agent. *Chem. Biol.* 2010; **17**: 735-744.

[17] Sandgren S, Wittrup A, Cheng F, Jönsson M, Eklund E, Busch S, Belting M. The Human Antimicrobial Peptide LL-37 Transfers Extracellular DNA Plasmid to the Nuclear Compartment of Mammalian Cells via Lipid Rafts and Proteoglycan-dependent Endocytosis. *J. Biol. Chem.* 2004; **279**: 17951-17956.

[18] Howl J, Matou-Nasri S, West DC, Farquhar M, Slaninova J, Östenson C-G, Zorko M, Östlund P, Kumar S, Langel Ü, McKeating J, Jones S. Bioportide: an emergent concept of bioactive cell-penetrating peptides. *Cell. Mol. Life Sci.* 2012; **69**: 2951-2966.

[19] Taylor BN, Mehta RR, Yamada T, Lekmine F, Christov K, Chakrabarty AM, Green A, Bratescu L, Shilkaitis A, Beattie CW, Das Gupta TK. Noncationic Peptides Obtained From Azurin Preferentially Enter Cancer Cells. *Cancer Res.* 2009; **69**: 537-546.

[20] Löfgren K, Wahlström A, Lundberg P, Langel Ü, Gräslund A, Bedecs K. Antiprion properties of prion protein-derived cell-penetrating peptides. *FASEB J.* 2008; **22**: 2177-2184.

[21] Li Y, Yokota T, Gama V, Yoshida T, Gomez JA, Ishikawa K, Sasaguri H, Cohen HY, Sinclair DA, Mizusawa H, Matsuyama S. Bax-inhibiting peptide protects cells from polyglutamine toxicity caused by Ku70 acetylation. *Cell Death Differ.* 2007; **14**: 2058-2067.

[22] Östlund P, Kilk K, Lindgren M, Hällbrink M, Jiang Y, Budihna M, Cerne K, Bavec A, Östenson C-G, Zorko M, Langel Ü. Cell-Penetrating Mimics of Agonist-Activated G-Protein Coupled Receptors. *Int. J. Pept. Res. Ther.* 2005; **11**: 237-247.

[23] Jones S, Martel C, Belzacq-Casagrande A-S, Brenner C, Howl J. Mitoparan and target-selective chimeric analogues: Membrane translocation and intracellular redistribution induces mitochondrial apoptosis. *Biochim. Biophys. Acta* 2008; **1783**: 849-863.

[24] Elmquist A, Lindgren M, Bartfai T, Langel Ü. VE-Cadherin-Derived Cell-Penetrating Peptide, pVEC, with Carrier Functions. *Exp. Cell Res.* 2001; **269**: 237-244.

[25] Duchardt F, Ruttekolk IR, Verdurmen WPR, Lortat-Jacob H, Bürck J, Hufnagel H, Fischer R, van den Heuvel M, Löwik DWPM, Vuister GW, Ulrich A, de Waard M, Brock R. A Cell-penetrating Peptide Derived from Human Lactoferrin with Conformation-dependent Uptake Efficiency. *J. Biol. Chem.* 2009; **284**: 36099-36108.

[26] Niarchos DK, Perez SA, Papamichail M. Characterization of a novel cell penetrating peptide derived from Bag-1 protein. *Peptides* 2006; **27**: 2661-2669.

[27] Doan N-D, Létourneau M, Vaudry D, Doucet N, Folch B, Vaudry H, Fournier A, Chatenet D. Design and characterization of novel cell-penetrating peptides from pituitary adenylate cyclase-activating polypeptide. *J. Control. Release* 2012; **163**: 256-265.

[28] Brugnano JL, Chan BK, Seal BL, Panitch A. Cell-penetrating peptides can confer biological function: Regulation of inflammatory cytokines in human monocytes by MK2 inhibitor peptides. *J. Control. Release* 2011; **155**: 128-133.

[29] Nakase I, Hirose H, Tanaka G, Tadokoro A, Kobayashi S, Takeuchi T, Futaki S. Cell-surface Accumulation of Flock House Virus-derived Peptides Leads to Efficient Internalization via Macropinocytosis. *Mol. Ther.* 2009; **17**: 1868-1876.

[30] Manosroi J, Lohcharoenkal W, Götz F, Werner RG, Manosroi W, Manosroi A. Polioviral receptor binding ligand: A novel and safe peptide drug carrier from polioviral capsid. *Drug Deliv.* 2012; **19**: 21-27.

[31] Lee J-E, Lim HJ. LDP12, a novel cell-permeable peptide derived from L1 capsid protein of the human papillomavirus. *Mol. Biol. Rep.* 2012; **39**: 1079-1086.

[32] Langedijk JPM. Tranlocation activity of C-terminal Domain of Pestivirus Erns and Ribotoxin L3 Loop. *J. Biol. Chem.* 2002; **277**: 5308-5314.

[33] Lu S, Tager LA, Chitale S, Riley LW. A cell-penetrating peptide derived from mammalian cell uptake protein of *Mycobacterium tuberculosis*. *Anal. Biochem.* 2006; **353**: 7-14.

[34] Vivès E, Brodin P, Lebleu B. A Truncated HIV-1 Tat Protein Basic Domain Rapidly Translocates through the Plasma Membrane and Accumulates in the Cell Nucleus. *J. Biol. Chem.* 1997; **272**: 16010-16017.

[35] Montrose K, Yang Y, Sun X, Wiles S, Krissansen GW. Xentry, a new class of cell-penetrating peptide uniquely equipped for delivery of drugs. *Sci. Rep.* 2013; **3**: 1661.

[36] Freire JM, Veiga AS, Rego de Figueiredo I, de la Torre BG, Santos NC, Andreu D, Da Poian AT, Castanho MARB. Nucleic acid delivery by cell penetrating peptides derived from dengue virus capsid protein: design and mechanism of action. *FEBS J.* 2014; **281**: 191-215.

[37] Oess S, Hildt E. Novel cell permeable motif derived from the PreS2-domain of hepatitis-B virus surface antigens. *Gene Ther.* 2000; **7**: 750-758.

[38] Abbott NJ, Patabendige AAK, Dolman DEM, Yusof SR, Begley DJ. Structure and function of the blood-brain barrier. *Neurobiol. Dis.* 2010; **17**: 13-25.

[39] Zou L-L, Ma J-L, Wang T, Yang T-B, Liu C-B. Cell-Penetrating Peptide-Mediated Therapeutic Molecule Delivery into the Central Nervous System. *Curr. Neuropharmacol.* 2013; **1**: 197-208.

[40] Hervé F, Ghinea N, Scherrmann J-M. CNS Delivery Via Adsorptive Transcytosis. *AAPS J.* 2008; **10**: 455-472.

[41] Rousselle C, Smirnova M, Clair P, Lefauconnier J-M, Chavanieu A, Calas B, Scherrmann JM, Temsamani J. Enhanced Delivery of Doxorubicin into the Brain via a Peptide-Vector-Mediated Strategy: Saturation Kinetics and Specificity. *J. Pharmacol. Exp. Ther.* 2001; **296**: 124-131.

[42] Cascales L, Henriques ST, Kerr MC, Huang Y-H, Sweet MJ, Daly NL, Craik DJ. Identification and Characterization of a New Family of Cell-penetrating Peptides – Cyclic Cell-penetrating peptides. *J. Biol. Chem.* 2011; **286**: 36932-36943.

[43] Vergote V, Baert B, Vandermeulen E, Peremans K, van Bree H, Slegers G, Burvenich C, De Spiegeleer B. LC-UV/MS characterization and DOE optimization of the iodinated peptide obestatin. *J. Pharmaceut. Biomed.* 2008; **46**: 127-136.

[44] Ötzas B, Küçük M, Kaya M. Sex-dependent changes in blood-brain barrier permeability in epileptic rats following acute hyperosmotic exposure. *Pharmacol. Res.* 2001; **43**: 469-472.

[45] Krause DN, Duckles SP, Pelligrino DA. Influence of sex steroid hormones on cerebrovascular functions. *J. Appl. Physiol.* 2006; **101**: 1252-1261.

[46] Gjedde A. High- and low-affinity transport of D-glucose from blood to brain. *J. Neurochem.* 1981; **36**: 1463-1471.

[47] Kastin AJ, Akerstrom V, Pan W. Validity of multiple-time regression analysis in measurement of tritiated and iodinated leptin crossing the blood-brain barrier: meaningful controls. *Peptides* 2001; **22**: 2127-2136.

[48] Verbeken M, Wynendaele E, Mauchauffée E, Bracke N, Stalmans S, Bojnik E, Benyhe S, Peremans K, Polis I, Burvenich C, Gjedde A, Hernandez J-F, De Spiegeleer B. Blood-brain transfer and antinociception of linear and cyclic N-methyl-guanidine and thiourea-enkephalins. *Peptides* 2015; **63**: 10-21.

[49] Pan WH, Banks WA, Fasold MB, Bluth J, Kastin AJ. Transport of brain-derived neurotrophic factor across the blood-brain barrier. *Neuropharmacology* 1998; **37**: 1553-1561.

[50] Patlak CS, Blasberg RG, Fenstermacher JD. Graphical evaluation of blood-to-brain transfer constants from multiple-time uptake data. *J. Cerebr. Blood F. Met.* 1983; **3**: 1-7.

[51] Gjedde A. Calculation of cerebral glucose phosphorylation from brain uptake of glucose analogs in vivo: a re-examination. *Brain Res.* 1982; **257**: 237-274.

[52] Wong DF, Gjedde A, Wagner HN Jr. Quantification of neuroreceptors in the living human brain. I. Irreversible binding of ligands. *J. Cerebr. Blood F. Met.* 1986; **6**: 137-46.

[53] Gjedde A, Bauer WR, Wong D. Neurokinetics: The dynamics of neurobiology in vivo. Springer US, **2011**, doi: 10.1007/978-1-4419-7409-9.

[54] Triguero D, Buciak J, Pardridge WM. Capillary depletion method for quantification of blood-brain-barrier transport circulating peptides and plasma-proteins. *J. Neurochem.* 1990; **54**: 1882-1888.

[55] Gutierrez EG, Banks WA, Kastin AJ. Murine tumor-necrosis-factor-alpha is transported from blood to brain in the mouse. *J. Neuroimmunol.* 1993; **47**: 169-176.

[56] Banks WA, Kastin AJ. Quantifying carrier-mediated transport of peptides from brain to the blood. *Method Enzymol.* 1989; **168:** 652-660.

[57] Vergote V, Van Dorpe S, Peremans K, Burvenich C, De Spiegeleer B. In vitro metabolic stability of obestatin: Kinetics and identification of cleavage products. *Peptides* 2008; **29**: 1740-1748.

[58] Svenson J, Vergote V, Karstad R, Burvenich C, Svendsen JS, De Spiegeleer B. Metabolic Fate of Lactoferricin-Based Antimicrobial Peptides: Effect of Truncation and Incorporation of Amino Acid Analogs on the In Vitro Metabolic Stability. *J. Pharmacol. Exp. Ther.* 2010; **332**: 1032-1039.

[59] Pardridge WM, Eisenberg J, Cefalu WT. Absence of albumin receptor on brain capillaries in vivo or in vitro. *Am. J. Physiol.* 1985; **249**: E264-E267.

[60] Banks WA, Fasold MB, Kastin AJ. Measurement of Efflux Rates from Brain to Blood. In *Methods in Molecular Biology, Neuropeptide Protocols* (Eds: Irvine GB, William CH), Humana Press Inc., **1997**, pp. 353-360.

[61] Banks WA, Jaspan JB, Huang W, Kastin AJ. Transport of Insulin Across the Blood-Brain Barrier: Saturability at Euglycemic Doses of Insulin. *Peptides* 1997; **18**: 1423-1429.

[62] Novoa A, Van Dorpe S, Wynendaele E, Spetea M, Bracke N, Stalmans S, Betti C, Chung NN, Lemieux C, Zuegg J, Cooper MA, Tourwé D, De Spiegeleer B, Schiller PW, Ballet S. Variation of the Net Charge, Lipophilicity, and Side Chain Flexibility in Dmt^{1}-DALDA: Effect on Opioid Activity and Biodistribution. *J. Med. Chem.* 2012; **55**: 9549-9561.

[63] Czihal P, Knappe D, Fritsche S, Zahn M, Berthold N, Piantavigna S, Müller U, Van Dorpe S, Herth N, Binas A, Köhler G, De Spiegeleer B, Martin LL, Nolte O, Sträter N, Alber G, Hoffmann R. Api88 Is a Novel Antibacterial Designer Peptide To Treat Systemic Infections with Multidrug-Resistant Gram-Negative Pathogens. *ACS Chem. Biol.* 2012; **7**: 1281-1291.

[64] Sarko D, Beijer B, Boy RG, Nothelfer E-M, Leotta K, Eisenhut, Altmann A, Haberkorn U, Mier W. The Pharmacokinetics of Cell-Penetrating Peptides. *Mol. Pharm.* 2010; **7**: 2224-2231.

[65] Grunwald J, Rejtar T, Sawant R, Wang Z, Torchilin VP. TAT Peptide and Its Conjugates: Proteolytic Stability. *Bioconjugate Chem.* 2009; **20**: 1531-1537.

[66] Elmquist A, Langel Ü. *In Vitro* Uptake and Stability Study of *p*VEC and Its All-D analog. *Biol. Chem.* 2003; **384**: 387-393.

[67] Hoffmann R, Bulet P, Urge L, Otvös L Jr. Range of activity and metabolic stability of synthetic antibacterial glycopeptides from insects. *Biochim. Biophys. Acta* 1999; **1426**: 459-467.

[68] Berthold N, Czihal P, Fritsche S, Sauer U, Schiffer G, Knappe D, Alber G, Hoffmann R. Novel Apidaecin 1b Analogs with Superior Serum Stabilities for Treatment of Infections by Gram-Negative Pathogens. *Antimicrob. Agents Ch.* 2013; **57**: 402-409.

[69] Knappe D, Piantavigna S, Hansen A, Mechler A, Binas A, Nolte O, Martin LL, Hoffmann R. Oncocin (VDKPPYLPRPRPPRRIYNR-NH2): A Novel Antibacterial Peptide Optimized against Gram-Negative Human Pathogens. *J. Med. Chem.* 2010; **53**: 5240-5247.

[70] Craik DJ. Plant cyclotides: circular, knotted peptide toxins. *Toxicon* 2001; **39**: 1809-1813.

[71] Clark RJ, Jensen J, Nevin ST, Callaghan BP, Adams DJ, Craik DJ. The Engineering of an Orally Active Conotoxin for the Treatment of Neuropathic Pain. *Angew. Chem. Int. Ed.* 2010; **49**: 6545-6548.

[72] Lindgren ME, Hällbrink MM, Elmquist AM, Langel Ü. Passage of cell-penetrating peptides across a human epithelial cell layer in vitro. *Biochem. J.* 2004; **377**: 69-76.

[73] Violini S, Sharma V, Prior JL, Dyszlewski M, Worms-Piwnica D. Evidence for a Plasma Membrane-Mediated Permeability Barrier to Tat Basic Domain in Well-Differentiated Epithelial Cells: Lack of Correlation with Heparan Sulfate. *Biochemistry-US* 2002; **41**: 12652-12661.

[74] Tréhin R, Krauss U, Beck-Sickinger AG, Merkle HP, Nielsen HM. Cellular Uptake but Low Permeation of Human Calcitonin-Derived Cell-Penetrating Peptides and Tat (47-57) Through Well-Differentiated Epithelial Models. *Pharm. Res.* 2004; **21**: 1248-1256.

[75] Simon MJ, Kang WH, Gao S, Banta S, Morrisson B III. TAT Is Not Capable of Transcellular Delivery Across an Intact Endothelial Monolayer In Vitro. *Ann. Biomed. Eng.* 2011; **39**: 394-401.

[76] Song J, Kai M, Zhang W, Zhang J, Liu L, Zhang B, Liu X, Wang R. Cellular uptake of transportan 10 and its analogs in live cells: Selectivity and structure-activity relationship studies. *Peptides* 2011; **32**: 1934-1941.

[77] Dardevet L, Rani D, El Aziz TA, Bazin I, Sabatier J-M, Fadl M, Brambilla E, De Waard M. Chlorotoxin: A Helpful Natural Scorpion Peptide to Diagnose Glioma and Fight Tumor Invastion. *Toxins* 2015; **7**: 1079-1101.

[78] Banks WA, Kastin AJ. Differential Permability of the Blood-Brain Barrier to Two Pancreatic Peptides: Insulin and Amylin. *Peptides* 1998; **19**: 883-889.

[79] Jay TM, Lucignani G, Crain AM, Jehle J, Sokoloff L. Measurement of Local Cerebral Blood Flow with [^{14}C]Iodoantipyrine in the Mouse. *J. Cerebr. Blood F. Met.* 1988; **8**: 121-129.

[80] Kastin AJ, Pan W. Peptide transport across the blood-brain barrier. In *Progress in Drug Research* (Eds: Prokai L, Prokai-Tatrai K), Birkhauser Verlag, **2003**, pp. 79-100.

[81] Elmquist A, Hansen M, Langel Ü. Structure-activity relationship study of the cell-penetrating peptide pVEC. *BBA-Biomembranes* 2006; **1758**: 721-729.

[82] Drin G, Cottin S, Blanc E, Rees AR, Temsamani J. Studies on the Internalization Mechanism of Cationic Cell-Penetrating Peptides. *J. Biol. Chem.* 2003; **278**: 31192-31201.

[83] Futaki S, Nakase I, Tadokoro A, Takeuchi T, Jones AT. Arginine-rich peptides and their internalization mechanisms. *Biochem. Soc. T.* 2007; **35**: 784-787.

[84] Brock R. The Uptake of Arginine-Rich Cell-Penetrating Peptides: Putting the Puzzle Together. *Bioconjugate Chem.* 2014; **25**: 863-868.

[85] Herbig ME, Assi F, Textor M, Merkle HP. The Cell Penetrating Peptides pVEC and W2-pVEC Induce Transformation of Gel Phase Domains in Phospholipid Bilayers without Affecting Their Integrity. *Biochemistry-US* 2006; **45**: 3598-3609.

[86] Akdag IO, Ozkirimli E. The Uptake Mechanism of the Cell-Penetrating pVEC Peptide. *J. Chem.* 2013; **2013**: 851915.

[87] Padari K, Säälik P, Hansen M, Koppel K, Raid R, Langel Ü, Pooga M. Cell Transduction Pathways of Transportans. *Bioconjugate Chem.* 2005; **16**: 1399-1410.

[88] Yandek LE, Pokorny A, Florén A, Knoelke K, Langel Ü, Almeida PFF. Mechanism of the Cell-Penetrating Peptide Transportan 10 Permeation of Lipid Bilayers. *Biophys. J.* 2007; **92**: 2434-2444.

[89] Islam MZ, Ariyama H, Alam JM, Yamazaki M. Entry of Cell-Penetrating Peptide Transportan 10 into a Single Vesicle by Translocating Across Lipid Membrane and Its Induced Pores. *Biochemistry* 2014; **53**: 386-396.

[90] Éiríksdóttir E, Konate K, Langel Ü, Divita G, Deshayes S. Secondary structure of cell-penetrating peptides controls membrane interaction and insertion. *Biochem. Biophys. Acta* 2010; **1798**: 1119-1128.

SUPPLEMENTARY INFORMATION

Table S1: Overview literature studies describing brain delivery by CPPs.

CPP	Cargo	Technique	*In vivo/ in vitro*	(Quantitative) result[1]	Reference
SynB1	Benzylpenicillin	*In situ* brain perfusion in rats (single time) + capillary depletion	*In vivo*	Q: Without SynB1: K_{in} = 0.15 µl/s/g ↔ coupled to SynB1: K_{in} = 1.14 µl/s/g. 80% synB1 coupled benzylpenicillin in parenchyma.	[1]
SynB1	Dalargin	*In situ* brain perfusion (single time) in rats + antinociceptive test	*In vivo*	Q: Without CPP: V_d = 16.7 µl/g↔ coupled to SynB1: V_d = 309 µl/g. Enhancement of analgesic activity.	[2]
SynB1	Doxorubicin	*In situ* brain perfusion in rats (single time) + capillary depletion	*In vivo*	Q: Without CPP: K_{in} = 0.25 µl/s/g ↔ coupled to SynB1: K_{in} = 1.50 µl/s/g. 70% SynB1 coupled benzylpenicillin in parenchyma.	[3]
SynB1	Doxorubicin	*In situ* brain perfusion in mice (single time) + capillary depletion	*In vivo*	Q: Without CPP: V_d = < 100 µl/g↔ coupled to SynB1: V_d = 776.4 µl/g. 60% SynB1 coupled doxorubicin in parenchyma.	[4]
SynB1	PEG-gelatin-siloxane nanoparticles	Determination transcellular transport across co-culture BBB model and determination of PG-GS-SynB particles in brain after IV injection of mice using *in vivo* imaging.	*In vitro/ In vivo*	D: Vectorizing the nanoparticles with the SynB peptide enhances the transport across the BBB *in vitro* as well as *in vivo*.	[18]
SynB3	Dalargin	*In situ* brain perfusion (single time) in rats + antinociceptive test	*In vivo*	Q: Without CPP: V_d = 16.7 µl/g↔ coupled to SynB3: V_d = 240 µl/g. Enhancement of analgesic activity.	[2]
(L- en D-) SynB3	Doxorubicin	*In situ* brain perfusion in mice (single time) + capillary depletion	*In vivo*	Q: Without CPP: V_d = < 100 µl/g↔ coupled to (L-en D-)SynB3: V_d = 961.8 (L) en 788.4 (D) µl/g. 50% SynB1 coupled doxorubicin in parenchyma.	[4]
SynB3	Paclitaxel	*In situ* brain perfusion in mice	*In vivo*	D: Vectorized paclitaxel bypasses P-gp at luminal side of BBB.	[5]
SynB3	Morphine-6-glucuronide	*In situ* brain perfusion in mice + antinociceptive tests	*In vivo*	Q: Without CPP: K_{in} = 0.024 µl/s/g ↔ coupled to SynB3: K_{in} = 1.27 µl/s/g. Improvement of pharmacological activity.	[6]
SynB3	Endomorphin-1 (linked by disulfide linkage)	Tail flick antinociceptive test	*In vivo*	Q: Five-fold increase in antinociception compared to EM-1 alone.	[39]
D-Penetratin	Doxorubicin	*In situ* brain perfusion in rats (single time) + capillary depletion.	*In vivo*	Q: Without CPP: K_{in} = 0.25 µl/s/g ↔ coupled to D-Penetratin: K_{in} = 2.14 µl/s/g. 70% SynB1 coupled benzylpenicillin in parenchyma.	[3]
Penetratin	-	IV injection → stained with fluorescent tag.	*In vivo*	D: no staining → no brain influx.	[7]
Penetratin	scFvs	Mice were IV injected with scFv-CPP construct. Then the presence of scFv-CPP in brain cryosections was evaluated after fluorescent labeling using a fluorescence microscope.	*In vivo*	D: scFv-CPP construct clearly appeared in brain cells after IV injection.	[26]
Penetratin	Doxorubicin loaded transferrin liposomes	The amount of doxorubicin in brain homogenate was evaluated using HPLC at different time points after IV injection in rats.	*In vivo*	Q: Tf-Penetratin liposomes showed maximal brain penetration after 24h (about 3.67% ID/g).	[27]
Penetratin	PEG-PLA nanoparticles loaded with coumarin-6	*In vivo* imaging and pharmacokinetic and biodistribution studies using LC-MS/MS analysis of coumarin-6 in brain homogenate.	*In vivo*	D: Fluorescence in rat brain was higher for penetratin-NP treated rats than for NP-treated ones. Brain uptake was enhanced when NP was coupled to penetratin.	[28]
Tat 47-57	NEP1-40	Focal ischemia model in rats → evaluate outcome after ischemia + detect presence of vectorized NEP1-40.	*In vivo*	B: Improvement of neurologic outcomes. D: Tat-NEP1-40 detected in brain using Western blot and immunofluorescence.	[8]
Tat 47-57	NR2B9c	Measuring effect of vectorized NR2B9c in a rat stroke model.	*In vivo*	Q: Treatment with Tat-NR2B9c reduced the volume of cerebral infarction with 67% and 87% in cortical infarction volume.	[10]

CPP	Cargo	Technique	*In vivo/ in vitro*	(Quantitative) result[1]	Reference
Tat 47-57	β-galactosidase	Fluorescence confocal microscopy: tissues were dissected from mice 20 min after i.p. injection	*In vivo*	D: - Tat-FITC: strong signals in all areas of brain (not with control FITC). - Tat-β-Gal: brain sections from mice analyzed: 2h post injection, strong activity around capillaries, not in parenchyma, starting from 4h after injection all brain regions showed strong β-Gal activity. - BBB remained intact (Evan's blue albumin complexes not in brain sections).	[11]
Tat 47-57	Green fluorescent protein (GFP)	Evaluation of transcellular transport of Tat-GFP across bEnd-3-astrocyte coculture layer.	*In vitro*	D: Tat-GFP was able to translocate bEnd-3 cell layer but not astrocyte layer. No influence on barrier integrity observed.	[12]
Tat 47-57	PEG-b-Chol nanoparticles (loaded with ciprofloxacine, quantum dots or FITC)	Confocal microscopy of rat brain sections 4h after IV injection in the tail vein.	*In vivo*	D: Tat-conjugated nanoparticles loaded with FITC or quantum dots crossed the BBB, while FITC and quantum dots alone did not and were localized around blood vessels in the brain.	[13]
Tat 47-57	PEG decorated gelatin-siloxane nanoparticles	*In vivo* imaging (mice) and TEM.	*In vivo*	Q: Tat-modification of the nanoparticles resulted in a quantitatively higher fluorescent signal in the brain than no-Tat nanoparticles (total signal counts of 708.69 ± 4.8 counts/ (sc × s) versus 670.47 ± 8.96 counts/ (sc × s)). TEM analysis revealed that the BBB remained intact.	[14]
Tat 47-57	δ-V1-1 (isozyme specific inhibitor of δ-PKC)	Two *in vivo* models of vascular stress: transient focal ischemia in normotensive rats and chronic hypertension.	*In vivo*	B: δ-V1-1-Tat increased the number of patent microvessels by 92% compared to control (Tat) treated animals and increased cerebral blood flow by 26% following acute focal ischemia (not with Tat peptide alone). In chronic hypertension model, the cerebral blood flow increased by 12%.	[15]
Tat 47-57	PACAP-38	Six hours after i.p. injection of FITC-labeled peptides, the fluorescence intensity of isolated brains was determined.	*In vivo*	B: PACAP-Tat showed a 2.5 fold higher efficiency to traverse the BBB than PACAP.	[16]
Tat 47-57	GDNF	Evaluation of cryosections of mouse brain 4h post i.p. injection using fluorescence microscopy.	*In vivo*	D: The fusion proteins crossed the BBB and transduced the brain parenchyma.	[17]
Tat 47-57	PEG-cholesterol (PEG-b-Col) nanoparticles	Evaluation of presence of FITC loaded PEG-b-Col-Tat nanoparticles in brain cryosections using confocal microscope 4h after IV injection of rats.	*In vivo*	D: PEG-b-Col-Tat particles crossed the BBB.	[19]
Tat 47-57	Bcl-X_L	Evaluation of infarct volume and neurological deficit in ischemic insult mice model.	*In vivo*	D: Tat- Bcl-X_L reduces the infarct volume and neurological deficits when administered before and after ischemic insult.	[22]
Tat 47-57	GDNF	Evaluation whether IV administration of Tat-GDNF prevent brain injury after transient focal ischemia.	*In vivo*	D: After IV administration, the Tat-GDNF protein reaches the ischemic zone and reduced the brain injury and infarction zone.	[23]
Tat 47-57	Ritonavir loaded nanoparticles	Measuring radioactivity of ritonavir in brain tissue digest after decapitation of mice at different time points.	*In vivo*	Q: The brain drug level was 800-fold higher than that with drug in solution at two weeks (0.1 µg/g (solution) versus 80.3 µg/g (Tat-nanoparticles)).	[25]
Tat	Doxorubicine loaded transferrin ligated liposomes	The amount of doxorubicine in brain homogenate was evaluated using HPLC at different time points after IV injection in rats.	*In vivo*	Q: Tf-Penetratin liposomes showed max brain penetration after 24h (about 2.89% ID/g).	[27]
Tat	Quantum dots	Rats were infused intra-arterially and after euthanizing the rat, the brain was isolated and quantum dot fluorescence was evaluated.	*In vivo*	D: If quantum dots are conjugated to Tat, the brain tissue was labeled. Histological data confirm the passage across the endothelial cell line of the blood-brain barrier.	[31]

CPP	Cargo	Technique	*In vivo/ in vitro*	(Quantitative) result[1]	Reference
D-Tat	^{99m}Tc-Tricarbonyl and fluorescein-5-maleimide	Biodistribution was evaluated in mice. At several time points after IV injection, tissues were evaluated by fluorescence microscopy and radiometric analysis.	*In vivo*	D: Little brain permeation was determined.	[32]
Tat	G_3R_6-cholesterol (conjugated to Tat and forms nanoparticles)	4h after i.v. injection of the nanoparticles, rabbit brain sections were evaluated for FITC-loaded nanoparticles using a confocal microscope.	*In vivo*	D: FITC was detected in the brain sections when coupled to CG_3R_6TAT nanoparticles (not if not coupled to nanoparticles), indicating the nanoparticles cross the BBB.	[34]
Tat 47-57	Cholesterol liposomes loaded with coumarin-6	After i.v. injection of the coumarin-6 loaded TAT-liposomes in mice, the coumarin-6 concentration was determined in brain tissue.	*In vivo*	D: The AUC (0-t) for TAT-liposomes was 1.79 to 2.54 times higher than non-conjugated liposomes.	[35]
(D-)Tat 47-57	Liposomes	*In vivo* biodistribution study in mice of (D-)Tat-coupled liposomes loaded with coumarin-6. At different time points after IV injection, the concentration of coumarin-6 was determined *i.a.* in brain tissue. Capillary depletion study was used to demonstrate distribution to brain parenchyma.	*In vivo*	Q: The concentration of coumarin-6 delivered using (D-)Tat-coupled liposomes was 2 to 2.5 times higher than liposomes coupled to a Tat analogue with basic residues replaced by glycine and glutamic acid residues.	[36]
Tat 48-57	FITC doped silica nanoparticles (FSNPs)	The Tat-FSNPs were intra-arterially injected into rats. After completing the procedure, the rats were decapitated and the brain was sliced into 4 pieces and imaged using a fluorescence microscope.	*In vivo*	D: The images confirm labeling of branches of the right middle cerebral artery. Thus, not the nanoparticles crossed the blood-brain barrier.	[37]
Tat 46-57	Doxorubicin loaded nanoparticles (and co-modified with T7 ligand)	*In vivo* imaging and evaluation of survival time of tumor bearing mice.	*In vivo*	D/B: Compared to control liposomes, the TAT-T7 co-modified doxorubicin-loaded liposomes markedly accumulated in the glioma brain tumor. Also the survival time of these mice significantly increased.	[40]
Tat 47-57	VIP	Efficiency assay of traversing the BBB by fluorimetry; food intake assay and evaluation of effect on scopolamine induced amnesia.	*In vivo*	Q: After i.p. injection, the brain uptake efficiency of VIP-TAT (1.81) was twice as high as that of VIP (0.78). B: VIP-TAT had a significantly stronger anorexigenic effect than VIP. Q/B: Administration of VIP-TAT significantly inhibited stronger than VIP alone the reduction of the latent time induced by scopolamine.	[41]
Tat 47-57	BRBP1 (and linked to the proapoptotic peptide KLA as well)	IV injection of fluorescently labeled BRBP1-TAT-KLA in mice with breast cancer brain metastasis.	*In vivo*	D: Compared to TAT-KLA, BRBP1-TAT-KLA showed higher fluorescence intensity in the brain metastasis lesions.	[44]
R7-myristoylated	-	NIR fluorescence imaging after IV injection + immunohistochemical staining.	*In vivo*	D: Presence of fluorescently labeled vector demonstrated.	[9]
rR9	RVG29-cargo (plasmid DNA)	Evaluation of luciferase activity of in several tissues after injection of rR9-RVG29-pGL3 (gene) construct in the tail vein of mice.	*In vivo*	B: At 72h, the luciferase expression was 3-fold higher than for the control group.	[21]
R8	RGD	Translocation across an *in vitro* BBB model AND *in vivo* imaging in C6 glioma bearing mouse model.	*In vitro/ In vivo*	D: R8-RGD reached the brain and accumulated in the glioma foci. Also *in vitro*, R8-RGD crossed the BBB.	[24]

CPP	Cargo	Technique	*In vivo/ in vitro*	(Quantitative) result[1]	Reference
R8	Liposomes	*In vivo* biodistribution study of R8-coupled liposomes loaded with coumarin-6. At different time points after IV injection, the concentration of coumarin-6 was determined *i.a.* in brain tissue. Capillary depletion study was used to demonstrate distribution to brain parenchyma.	*In vivo*	Q: The concentration of coumarin-6 delivered using R8-coupled liposomes was 3.5 times higher than liposomes coupled to a Tat analogue with basic residues replaced by glycine and glutamic acid residues.	[36]
R2-R5	EM-1 analogs	Antinociceptive test	*In vivo*	D: Unless the decreased affinity for the opioid receptor, the vectorized analogs showed potent antinociceptive effect, partly caused by the improved bioavailability.	[29]
Oligoarginine	Transferrin ligated liposomes	Rat were IV injected with vectorized liposomes and at different time points, brain was isolated and evaluated using NIR imaging.	*In vivo*	D: The brain penetration of Tf-PR-liposomes was 8-fold greater than plain liposomes.	[30]
R11	No cargo, but FITC labeled.	Evaluation of immunoreactivity (using goat anti-FITC antibodies) in mouse brain sections after systemic administration of 11R-FITC.	*In vivo*	D: Strong immunoreactivity was observed in vessels and surrounding cells of cortex, striatum and thalamus, which was not seen when systemically injecting 11E-FITC.	[43]
pVEC	pVEC covalently attached to gHo (glioma homing sequence) = gHoPe2	Evaluation of presence of FAM-labeled gHoPe2, IV injected in mice, in cryosections of the brain.	*In vivo*	D: In intracranial brain tumor model, the gHoPe2-FAM peptides were present in the intracranial tumors, not in healthy brain tissue. Thus the construct crossed the BBB.	[20]
Mastoparan	Doxorubicin loaded transferrin liposomes	The amount of doxorubicin in brain homogenate was evaluated using HPLC at different time points after IV injection in rats.	*In vivo*	D: Accumulation of Tf-Mastoparan liposomes was lower compared to Tf-Tat and Tf-Penetratin liposomes.	[27]
(RXRRBR)2XB	AMO (antisense morpholino oligonucleotides)	IV injection to mice (single time and multiple time injection) and evaluation of presence of fluorescence in different brain areas using fluorescence microscopy.	*In vivo*	D: Fluorescence was widely detected throughout the brain and increased when multiple injections were given.	[33]
PepFect 32 (PepFect 14-Angiopep-2 construct)	pDNA	*In vitro* Transwell experiment. Transport across the bEnd.3 layer was demonstrated by measuring plasmid transfection in U87 cells.	*In vitro*	Q: PepFect 32 showed the most efficient transfection of the luciferase-expressing plasmid in U87 cells.	[38]
LNP	pDNA	Evaluation of *in vitro* transport of LNP-modified pDNA nanoparticles across the BMEC layer.	*In vitro*	Q: P_{app} of LNP-modified pDNA nanoparticles was 92.43×10^{-6} cm/s, while if not LNP-modified, the P_{app} was $\leq 65 \times 10^{-6}$ cm/s.	[42]

[1]Q: Quantitative result; B: biological effect; D: effect described.

References

[1] Rousselle C, Clair P, Temsamani J, Scherrmann J-M. Improved Brain Delivery of Benzylpenicillin with a Peptide-vector-mediated Strategy. *J. Drug Target.* 2002; **10**: 309-315.

[2] Rousselle C, Clair P, Smirnova M, Kolesnikov Y, Pasternak GW, Gac-Breton S, Rees AR, Scherrmann J-M, Temsamani J. Improved Brain Uptake and Pharmacological Activity of Dalargin Using a Peptide-Vector-Mediated Strategy. *J. Pharmacol. Exp. Ther.* 2003; **306**: 371-376.

[3] Rousselle C, Clair P, Lefauconnier J-M, Kaczorek M, Scherrmann J-M, Temsamani J. New Advances in the Transport of Doxorubicine through the Blood-brain barrier by a Peptide Vector-Mediated Strategy. *Mol. Pharmacol.* 2000; **57**: 679-686.

[4] Rousselle C, Smirnova M, Clair P, Lefauconnier J-M, Chavanieu A, Calas B, Scherrmann J-M, Temsamani J. Enhanced Delivery of Doxorubicin into the Brain via a Peptide-Vector-Mediated Strategy: Saturation Kinetics and Specificity. *J. Pharmacol. Exp. Ther.* 2001; **296**: 124-131.

[5] Blanc E, Bonnafous C, Merida P, Cisternino S, Clair P, Scherrmann J-M, Temsamani J. Peptide-vector strategy bypasses P-glycoprotein efflux, and enhances brain transport and solubility of paclitaxel. *Anti-cancer drug.* 2004; **15**: 947-954.

[6] Temsamani J, Bonnafous C, Rousselle C, Fraisse Y, Clair P, Granier L-A, Rees AR, Kaczorek M, Scherrmann J-M. Improved Brain Uptake and Pharmacological Activity Profile of Morphine-6-Glucuronide Using a Peptide Vector-Mediated Strategy. *J. Pharmacol. Exp. Ther.* 2005; **313**: 712-719.

[7] Bolton SJ, Jones DNC, Darker JG, Eggleston DS, Hunter AJ, Walsh FS. Cellular uptake and spread of the cell-permeable peptide penetratin in adult rat brain. *Eur. J. Neurosci.* 2000; **12:** 2847-2855.

[8] Wang Q, Gou X, Xiong L, Jin W, Chen S, Hou L, Xu L. Trans-activator of Transcription-mediated Delivery of NEP1-40 Protein into the Brain Has a Neuroprotective Effect against Focal Cerebral Ischemic Injury via Inhibition of Neuronal Apoptosis. *Anesthesiology* 2008; **108**: 1071-1080.

[9] Pham W, Zhao B-Q, Lo EH, Medarova Z, Rosen B, Moore A. Crossing the blood-brain barrier: A potential application of myristoylated polyarginine for in vivo neuroimaging. *NeuroImage* 2005; **28:** 287-292.

[10] Aarts M, Liu Y, Liu L, Besshoh S, Arundine M, Gurd JW, Wang Y-T, Salter MW, Tymianski M. Treatment of Ischemic Brain Damage by Perturbing NMDA Receptor-PSD-95 Protein Interactions. *Science* 2002; **298**: 846-850.

[11] Schwarze SR, Ho A, Vocero-Akbani A, Dowdy SF. In Vivo Protein Transduction: Delivery of a Biologically Active Protein into the Mouse. *Science* 1999; **285:** 1569-1572.

[12] Simon MJ, Kang WH, Gao S, Banta S, Morrison III B. TAT Is Not Capable of Transcellular Delivery Across an Intact Endothelial Monolayer *In Vitro*. *Ann. Biomed Eng.* 2010; **39**: 394-401.

[13] Liu L, Guo K, Lu J, Venkatraman SS, Lu D, Ng KC, Ling E-A, Moochhala S, Yang Y-Y. Biologically active core/shell nanoparticles self-assembled from cholesterol-terminated PEG-TAT for drug delivery across the blood-brain barrier. *Biomaterials* 2008; **29**: 1509-1517.

[14] Tian X-h, Wei F, Wang T-x, Wang D, Wang J, Lin X-n, Wang P, Ren L. Blood-brain barrier transport of Tat peptide and polyethylene glycol decorated gelatin-siloxane nanoparticle. *Mater. Lett.* 2012; **68**: 94-96.

[15] Bright R, Steinberg GK, Mochly-Rosen D. δPKG mediates microcerebrovascular dysfunction in acute ischemia and in chronic hypertensive stress in vivo. *Brain Res.* 2007; **1144**: 146-155.

[16] Yu R, Guo X, Huang L, Zeng Z, Zhang H. The novel peptide PACAP-TAT with enhanced traversing ability attenuates the severe injury induced by repeated smoke inhalation. *Peptides* 2012; **38**: 142-149.

[17] Dietz GPH, Valbuena PC, Dietz B, Meuer K, Müller P, Weishaupt JH, Bähr M. Application of a blood-brain-barrier-penetrating form of GDNF in a mouse model for Parkinson's disease. *Brain Res.* 2006; **1082**: 61-66.

[18] Tian X-h, Wei F, Wang T-x, Wang P, Lin X-n, Wang J, Wang D, Ren L. In vitro and in vivo studies on gelatin-siloxane nanoparticles conjugated with SynB peptide to increase drug delivery to the brain. *Int. J. Nanomed.* 2012; **7**: 1031-1041.

[19] Liu L, Venkatraman SS, Yang Y-Y, Guo K, Lu J, He B, Moochhala S, Kan L. Polymeric Micelles Anchored With TAT for Delivery of Antibiotics Across the Blood-Brain Barrier. *Biopolymers* 2008; **90**: 617-623.

[20] Eriste E, Kurrikoff K, Suhorutsenko J, Oskolkov N, Copolovici DM, Jones S, Laakkonen P, Howl J, Langel Ü. Peptide-Based Glioma-Targeted Drug Delivery Vector gHoPe2. *Bioconjugate Chem.* 2013; **24**: 305-313.

[21] Gong C, Li X, Xu L, Zhang Y-H. Target delivery of a gene into the brain using the RVG29-oligoarginine peptide. *Biomaterials* 2012; **33**: 3456-3463.

[22] Kilic E, Dietz GPH, Hermann DM, Bähr M. Intravenous TAT-Bcl-XL Is Protective after Middle Cerebral Artery Occlusion in Mice. *Ann. Neurol.* 2002; **52**: 617-622.

[23] Kilic Ü, Kilic E, Dietz GPH, Bähr M. Intravenous TAT-GDNF Is Protective After Focal Cerebral Ischemia in Mice. *Stroke* 2003; **34**: 1304-1310.

[24] Liu Y, Ran R, Chen J, Kuang Q, Tang J, Mei L, Zhang Q, Gao H, Zhang Z, He Q. Paclitaxel loaded liposomes decorated with a multifunctional tandem peptide for glioma targeting. *Biomaterials* 2014; **35**: 4835-4847.

[25] Rao KS, Reddy MK, Horning JL, Labhasetwar V. TAT-conjugated nanoparticles for the CNS delivery of anti-HIV drugs. *Biomaterials* 2008; **29**: 4429-4438.

[26] Skrlj N, Drevensek G, Hudoklin S, Romih R, Curin Serbec V, Dolinar M. Recombinant Single-Chain Antibody with the Trojan Peptide Penetratin Positioned in the Linker Region Enables Cargo Transfer Across the Blood-Brain Barrier. *Appl. Biochem. Biotech.* 2013; **169**: 159-169.

[27] Sharma G, Modgil A, Zhong T, Sun C, Singh J. Influence of Short-Chain Cell-Penetrating Peptides on Transport of Doxorubicin Encapsulating Receptor-Targeted Liposomes Across Brain-Endothelial Barrier. *Pharm. Res.* 2014; **31**: 1194-1209.

[28] Xia H, Gao X, Gu G, Liu Z, Hu Q, Tu Y, Song Q, Yao L, Pang Z, Jiang X, Chen J, Chen H. Penetratin-functionalized PEG-PLA nanoparticles for brain drug delivery. *Int. J. Pharm.* 2012; **436**: 840-850.

[29] Wang C-l, Guo C, Wang Y-q, Zhou Y, Li Q, Ni L-m, Wang R. Synthesis and antinociceptive effects of endomorphin-1 analogs with C-terminal linked by oligoarginine. *Peptides* 2011; **32**: 293-299.

[30] Sharma G, Modgil A, Layek B, Arora K, Sun C, Law B, Singh J. Cell penetrating peptide tethered bi-ligand liposomes for delivery to brain *in vivo*: Biodistribution and transfection. *J. Control. Rel.* 2013; **167**: 1-10.

[31] Santra S, Yang H, Stanley JT, Holloway PH, Moudgil BM, Walter G, Mericle RA. Rapid and effective labeling of brain tissue using TAT-conjugated CdS:Mn/ZnS quantum dots. *Chem. Comm.* 2005; **25**: 3144-3146.

[32] Bullock KE, Dyszlewski M, Prior JL, Pica CM, Sharma V, Piwnica-Worms D. Characterization of Novel Histidine-Tagged Tat-Peptide Complexes Dual-Labeled with ^{99m}Tc-Tricarbonyl and Fluorescein for Scintigraphy and Fluorescence Microscopy. *Bioconjugate Chem.* 2002; **13**: 1226-1237.

[33] Du L, Kayali R, Bertoni C, Fike F, Hu H, Iversen PL, Gatti RA. Arginine-rich cell-penetrating peptide dramatically enhances AMO-mediated ATM aberrant splicing correction and enables delivery to brain and cerebellum. *Hum. Mol. Genet.* 2011; **20**: 3151-3160.

[34] Wang H, Xu K, Liu L, Tan JPK, Chen Y, Li Y, Fan W, Wei Z, Sheng J, Yang Y-Y, Li L. The efficacy of self-assembled cationic antimicrobial peptide nanoparticles against *Cryptococcus neoformans* for the treatment of meningitis. *Biomaterials* 2010; **31**: 2874-2881.

[35] Qin Y, Chen H, Yuan W, Kuai R, Zhang Q, Xie F, Zhang L, Zhang Z, Liu J, He Q. Liposome formulated with TAT-modified cholesterol for enhancing the brain delivery. *Int. J. Pharm.* 2011; **419**: 85-95.

[36] Qin Y, Zhang Q, Chen H, Yuan W, Kuai R, Xie F, Zhang L, Wang X, Zhang Z, Liu J, He Q. Comparison of four different peptides to enhance accumulation of liposomes into the brain. *J. Drug Target.* 2012; **20**: 235-245.

[37] Santra S, Yang H, Dutta D, Stanley JT, Holloway PH, Tan W, Moudgil BM, Mericle RA. TAT conjugated, FITC doped silica nanoparticles for bioimaging applications. *Chem. Commun.* 2004; **2004**: 2810-2811.

[38] Srimanee A, Regberg J, Hallbrink M, Kurrikoff K, Veiman K-L, Vajragupta O, Langel U.Peptide-Based Delivery of Oligonucleotides Across Blood-Brain Barrier Model. Int. *J. Pept. Res. Ther.* 2014; **20**: 169-178.

[39] Liu H, Zhang W, Ma L, Fan L, Gao F, Ni J, Wang R. The improved blood-brain barrier permeability of endomorphin-1 using the cell-penetrating peptide synB3 with three different linkages. *Int. J. Pharm.* 2014; **476**: 1-8.

[40] Zong T, Mei L, Gao H, Cai W, Zhu P, Shi K, Chen J, Wang Y, Gao F, He Q. Synergistic Dual-Ligand Doxorubicin Liposomes Improve Targeting and Therapeutic Efficacy of Brain Glioma in Animals. *Mol. Pharm.* 2014; **11**: 2346-2357.

[41] Yu R, Yang Y, Cui Z, Zheng L, Zeng Z, Zhang H. Novel peptide VIP-TAT with higher affinity for PAC1 inhibited scopolamine induced amnesia. *Peptides* 2014; **60**: 41-50.

[42] Yao H, Wang K, Wang Y, Wang S, Li J, Lou J, Ye L, Yan X, Lu W, Huang R. Enhanced blood-brain barrier penetration and glioma therapy mediated by a new peptide modified gene delivery system. *Biomaterials* 2015; **37**: 345-352.

[43] Gotanda Y, Wei F-Y, Haranda H, Ohta K, Nakamura K-i, Tomizawa K, Ushijima K. Efficient Transduction of 11 Poly-arginine Peptide in an Ischemic Lesion of Mouse Brain. *J. Stroke Cerebrovasc.* 2014; **23**: 2023-2030.

[44] Fu B, Long W, Zhang Y, Zhang A, Miao F, Shen Y, Pan N, Gan G, Nie F, He Y, Zhang J, Teng G. Enhanced antitumor effects of the BRBP1 compound peptide BRBP1-TAT-KLA on human brain metastatic breast cancer. *Sci. Rep.* 2015; **5**: 8029.

CHAPTER VI

REGULATORY DEVELOPMENT OF GERIATRIC MEDICINES: TO GIP OR NOT TO GIP?

"An old man is twice a child"

William Shakespeare
(°1564 - †1616, English poet, playwright and actor)

Parts of this chapter were published:

De Spiegeleer B, Wynendaele E, Bracke E, Veryser L, Taevernier L, Degroote A, Stalmans S. Development of geriatric medicines: To GIP or not to GIP? **Submitted**.

ABSTRACT

Geriatric patients represent the main users of medicines, but were historically often minimally included in clinical trials, resulting in a gap in the knowledge of the benefit/risk balance of medicines in this heterogeneous population. As the worldwide population is aging, the need for safe and effective medicines for older patients is proportionally increasing. The aim of this review is to provide an overview of the current regulatory status of the development of geriatric medicines, the encountered challenges and the view of the involved stakeholders, coming to the conclusion, by analogy with pediatrics, whether to GIP or not to GIP (Geriatric Investigation Plan).

CHAPTER VI

REGULAGORY DEVELOPMENT OF GERIATRIC MEDICINES: TO GIP OR NOT TO GIP?

Main focus in this chapter:

- Regulatory status of the development of medicines for geriatric patients.
- Views of the different involved stakeholders.
- Identification and exploration of challenges in the development of geriatric medicines, with special emphasis on the alteration of the blood-brain barrier permeability during the aging process.

1. INTRODUCTION

Worldwide, the population aged 60 and over is the fastest growing group of persons. Due to the reduction in fertility, the population is globally aging. In developing countries, the population is still young as the percentage of children and young persons is high. In contrast, the number of older people has surpassed the number of children younger than age 15 in the more developed countries: the population aged 60 years and older is expected to rise from 287 million (23%) in 2013 to 417 million (32%) in 2050 [1]. As an example, the population pyramid of the European Union (EU) is shown in Figure 1: per sex, each bar corresponds to the proportion of the population at that age in the total population [2]. The baby boomer bulge is moving up, while the other age groups are narrowing by 2080 [2].

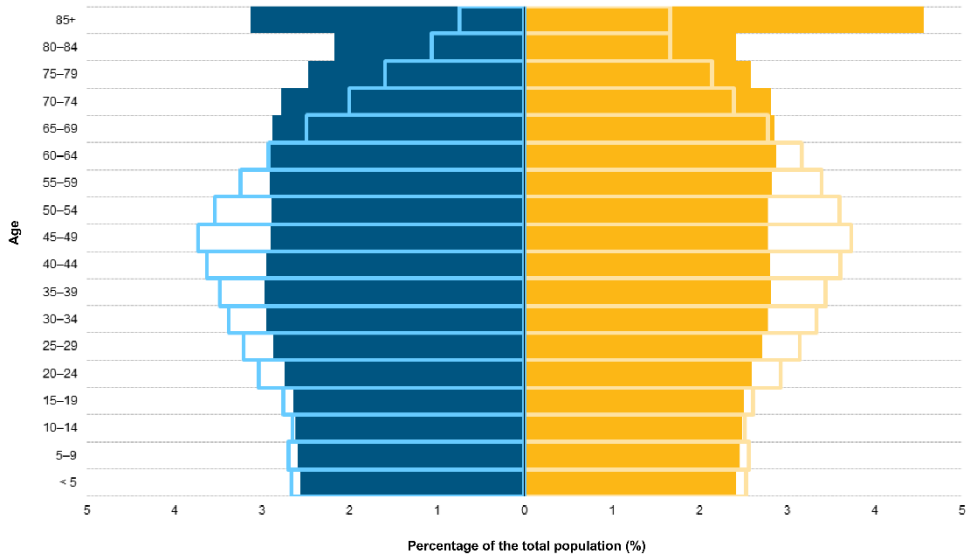

Figure 1: Population pyramid of European Union in 2014 (bordered) and 2080 (solid).The blue or left part represent men and the orange or right part women (Source: Eurostat).

Aging is commonly accepted to be a multifactorial process, but still, many theories on aging exist. Within the different theories on aging, three categories can be differentiated: the first category comprises the accumulation of damage to informational molecules, a second category concerns regulation of specific genes and the third category are theories claiming depletion of stem cells [3]. The age-associated changes are the result from a gradual loss in homeostatic mechanisms, which already starts in adulthood. When at later age a certain level is reached, this loss of functions will become apparent, especially when external stress is applied [3]. Thus, aging implies the gradual change of various physiological, biological, physical and social functions in the human being [4]. The geriatric syndrome includes all common problems the older population may encounter due to aging, like iatrogenesis (adverse drug reactions), immobility, immune deficiency and impairment of vision and hearing [3]. Frailty includes the most problematic uttering of aging and is a clinical condition characterized by an increased vulnerability to poor resolution of homeostasis after exposure to (minimal) stress, expressed as a disproportionate change in health status. The frailty condition is characterized by an increased risk of adverse outcomes like falls, delirium and disability, but frail geriatric patients also demonstrate non-specific clinical presentations like extreme fatigue, weight loss and frequent infections [5]. Thus, geriatric patients can be stratified by numerical age or based on the frailty status.

In Figure 2, age-related physiological and functional changes are summarized [6-10]. The resulting alterations in body composition and organ functions cause changes in the pharmacokinetics and pharmacodynamics (PK/PD) of drugs [7,8].

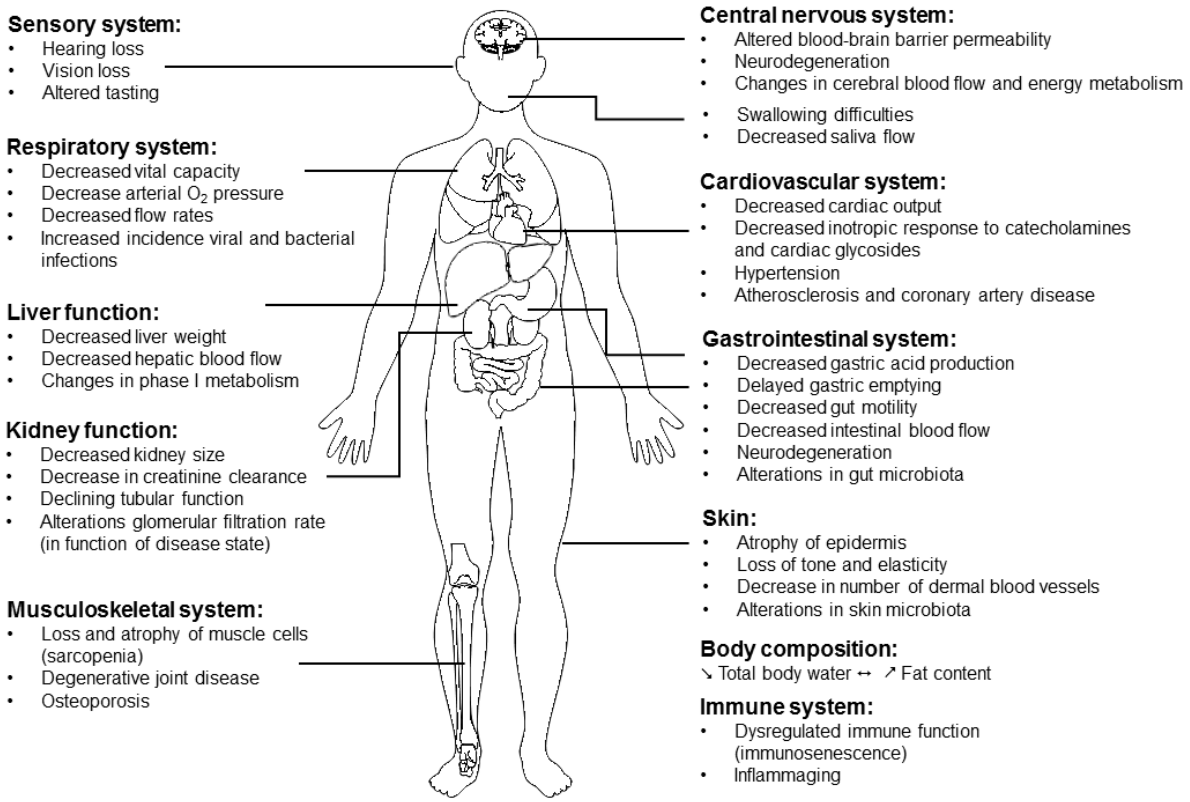

Figure 2: Selection of relevant age-related physical and functional changes [6-12].

Table 1 contains the pharmacokinetic consequences of relevant age-related functional changes.

Table 1: Pharmacokinetic consequences of age-related physiological and functional changes [6,7].

Process	Age-related change	Pharmacokinetic consequence
Absorption	Increased gastric pH	Slightly decreased absorption
	Delayed gastric emptying	
	Reduced splanchnic blood flow	
	Decreased absorption surface	
	Decreased gastrointestinal motility	
	Decreased hepatic blood flow	Reduced fist pass metabolism
Distribution	Increased body fat	Increased distribution volume and half-life of lipophilic drugs
	Decreased total body water	Increased plasma concentration of hydrophilic drugs
	Decreased serum albumin	Increased of free fraction in plasma of highly protein-bound acidic drugs
	Increased α1-acid glycoprotein	Decreased free fraction of basic drugs
	Increased blood-brain barrier (BBB) permeability	Increased brain distribution
Metabolism	Decreased hepatic mass	Phase I metabolism may be impaired.
Elimination	Decreased renal blood flow	Impaired renal elimination
	Decreased glomerular filtration rate	

Pharmacodynamics are less researched in the elderly population. Several studies already indicated the increased sensitivity to cardiovascular medicines, anticoagulants, drugs acting via the central nervous system (CNS) and general anesthetics, which cannot only be ascribed to pharmacokinetic changes [8,13]. For example, use of neuroleptic drugs by the geriatric patient is associated with increased delirium, extrapyramidal symptoms and postural hypotension and increased body sway and exaggerated sedative effects are seen with geriatric use of benzodiazepines. Also drugs with anticholinergic actions affect cognition and orientation of the elderly patient [13].

The aging process is not a disease, but increases the vulnerability to it [14]. In the geriatric population, cardiovascular diseases (*i.a.* hypertension and heart failure), dementia (including Alzheimer's disease (AD)), Parkinson's disease, Chronic Obstructive Pulmonary Diseases (COPD), depression, diabetes, cancer and musculoskeletal disorders (*i.a.* rheumatoid arthritis, osteoarthritis and osteoporosis) are commonly reported chronic disease conditions [15,16]. Moreover, there exists a high rate of co-occurrence of chronic conditions, termed comorbidity [16]. The rate and manifestation of the aging process varies among individuals, explaining the more pronounced heterogeneity of the geriatric population [4].

The comorbid elderly population is characterized by polypharmacy, *i.e.* taking multiple medicines simultaneously, which complicates their drug regimen [8]. A Medline survey indicated that the average number of prescription drugs in people older than 65 years was two to nine and increases with age [4]. Beside increased drug costs, polypharmacy causes the geriatric patient to be at risk for adverse drug reactions, drug-drug interactions, non-adherence to drug therapy and functional decline [17]. Although older patients use 30 to 50% of all prescription drugs, they are to a large extent excluded from clinical trials, even from trials investigating drugs for highly age-associated diseases like heart failure and Parkinson's disease [4,18-20]. A systematic review indicated that in 38.5% of the randomized clinical trials, people aged above 65 years were excluded and in 81.3% of the trials, patients with comorbidities were absent [21]. The main reason for their historical exclusion is the heterogeneity of the geriatric population, which may cause dilution of the effect of the drug and the inability to demonstrate statistically sound results. The older patients are also at higher risk for adverse drug reactions and drug-drug interactions, as well as to become sick or die during the trial period, implying dropout. Finally, also personal, practical (*e.g.* transportation problems) and economic reasons are identified [18,19]. This minimal inclusion of elderly in clinical trials causes that for the majority of the available drugs, the safety and efficacy is not known for the geriatric patients, especially for the very old (> 80 years) and frail elderly, impeding evidence-based drug therapy and further augmenting the risk for adverse drug reactions [18]. Moreover, geriatric patients differ from the younger adults in their specific medication-related needs, *e.g.* with regards to the manageability of the drug product [4]. Therefore, this heterogeneous population requires an individual patient-

centered therapeutic approach instead of treatment of a single disease or population, because the latter approach may have little efficacy in this comorbid and vulnerable patient group [4,22].

There also exists a gap in the knowledge of safety and efficacy of drugs in the pediatric population. However, both the USA, since 1997, and the EU, since 2007, have established a pediatric regulation, aiming to improve the health of children through improvements of research and to provide a regulatory framework for obtaining safe and effective pediatric medicines [23]. Upon compliance to the Written Request for the FDA and the Paediatric Investigation Plan (PIP) for the EMA, which contain the timings and description of pediatric studies, incentives can be obtained [23]. As there is also an urgent need for evidence-based drug therapies in the elderly, the current regulatory status of the development of geriatric medicines will be evaluated here, as well as the view of the different involved stakeholders. Finally, current challenges will be identified and analyzed, coming to the conclusion, whether to GIP or not to GIP (Geriatric Investigation Plan).

2. CURRENT REGULATORY STATUS OF GERIATRIC MEDICINE DEVELOPMENT

In this first section, it is evaluated whether the need for the development of safe and effective drugs of geriatric medicines is translated in the regulatory guidelines and/or regulations of the three main regulatory bodies: European Medicines Agency (EMA) for the European Union (EU), Food and Drug Administration for the United States of America (USA) and the Pharmaceutical and Medical Devices Agency (PMDA) for Japan. The guidelines of the International Conference on Harmonisation (ICH), which are adopted by these regulatory authorities, will be discussed in a separate section. Beside the evaluation of the current regulatory status, the availability of a strategy to anticipate on the aging population is investigated. A summary is given in Figure 3.

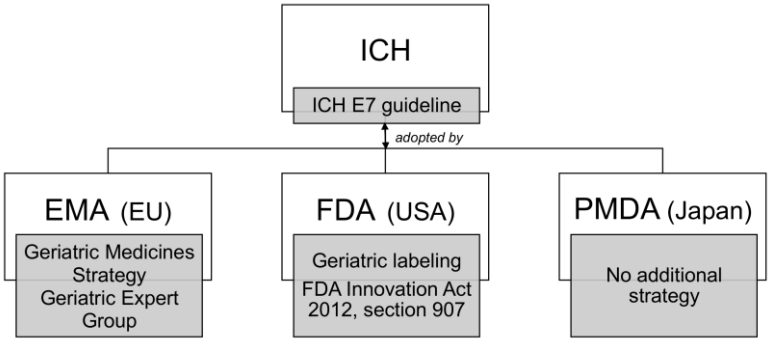

Figure 3: Summary of the current regulatory status of the development of geriatric medicines.

ICH guidelines

In 1993, the ICH published the ICH E7 guideline entitled "Studies in Support of Special Populations: Geriatrics E7". This E7 document was published as a harmonized tripartite guideline, established and adopted by the European, American and Japanese regulatory authorities [24]. In the late 1980s, these regulatory authorities recognized that the increasing elderly population requires special consideration in clinical trials and participants of these trials should represent the population that will be treated by the drug in clinical practice [24]. In 2006, on request of the EMA, the ICH E7 guideline was revised, resulting in a concept paper which was then translated into an addendum E7 Questions & Answers (Q&A) document in 2010 [25,26].

The E7 guideline defines the geriatric population arbitrarily as patients aged above 65 years [24]. However, in the Q&A document is encouraged to incorporate various age groups in the clinical database like for example 65-74, 75-84 and ≥ 85, with special emphasis on the very old (≥75 years) representing the fastest growing population group, as well as those with concomitant therapies and comorbidities and the frail elderly [25]. It is preferred that geriatric patients are represented in Phase 3 clinical trials in a sufficient number allowing to demonstrate the benefit-risk balance in this population and covering the entire age spectrum representative for the target population. These trials allow to determine age-related differences in drug response like adverse event rates, effectiveness and dose-response. During the clinical trials including older patients, it is also recommended to address specific adverse events occurring in the elderly and to include age-specific endpoints [24,25].

Age-related differences are often due to differences in the pharmacokinetics of the drug, related to the abnormal renal and hepatic function in the elderly and should be evaluated during pharmacokinetic studies. The guideline does not require routine dose-response or other pharmacodynamic studies in geriatric patients, except for drugs with CNS effects like hypnotic and sedative drugs, and if clinical trials indicate a potentially medically significant age-associated difference in the drug's effectiveness or adverse event profile, which cannot be explained by pharmacokinetic differences. Drug-drug interaction studies should only be performed if the therapeutic range of the drug or likely concomitant drugs is narrow [24,25].

Surprisingly, although the importance of adapted formulations and dosages was discussed in the concept paper of 2006 revising the E7 guideline, this aspect was not further elaborated in the Q&A document of the E7 guideline [25,26]. Other ICH documents that incorporate age-related aspects in a general way are the E4 and E5(R1) guidelines, in which it is stated that the influence of age on the dose and dose-response should be evaluated during drug development [27,28].

European Medicines Agency (EU)

In 2011, the EMA published the Geriatric Medicines Strategy, containing the efforts the Agency wants to undertake to ensure that the needs of older people are taken into account in the development and evaluation of new medicines. Their strategy is based on two principles: (1) ensuring that medicines used by geriatric patients are of high quality and appropriately researched in this population, both before and after authorization, and (2) improving availability of information on the use of medicines for older people, in order to allow informed prescription [29]. The EMA focusses on four key areas. First, gaps are being identified in the regulatory and scientific knowledge and appropriate measures are taken to tackle them, *i.a.* by seeking input from the Committee for Medicinal Products for Human Use (CHMP) and the Pharmacovigilance Risk Assessment Committee (PRAC, previously Pharmacovigilance Working Party (PhVWP)) and in the provision of scientific advice to the industry during drug development. Second, a Geriatric Expert Group (GEG) is established to provide the CHMP with advice on specific issues on the elderly [29]. This GEG is currently working on a proposal for the characterization of the frailty status of patients enrolled in clinical trials [30]. Third, to ensure the development of new medicines for the elderly is following the adopted ICH E7 guideline, the EMA provides scientific advice, comments on peer review applications and updates the assessment report templates to focus assessor's attention on geriatric data. Finally, the need for specific pharmacovigilance activities is under consideration [29].

In 2013, the implementation of the Geriatric Medicines Strategy with respect to product information of newly approved medicinal products was evaluated. Of the 81 peer reviewed applications, 75% received comments with regards to geriatric data and 84% of these applicants finally included these comments [31]. This specific review of applications for geriatric aspects was beneficial for the inclusion of data with regards to the safety and efficacy in the application and consequently in the Product Information Leaflet (PIL) and Summary of the Product Characteristics (SmPC) [31]. Simultaneously, scientific guidelines were also reviewed for compliance with the E7 guideline [32]. In 93% of the cases, the guidelines did not fully comply, especially with regards to the requirements for the type and amount of data on the efficacy and safety in the elderly population. It was concluded that input of GEG in the drafting phase of the scientific guidelines is recommended [32].

The EMA is also aware that in order to identify all quality aspects that are unique for the geriatric medicines, all stakeholders should be involved. Currently, EMA is working on a reflection paper on the quality aspects of medicines for older people, which should assist the industry in the development of geriatric medicines and in the regulatory review of these applications [33].

Food and Drug Administration (USA)

Before the adoption of the ICH E7 guideline in 1994, the FDA published already in 1989 a guideline for the study of drugs likely to be used in the elderly [34]. In 1997, the FDA established the Geriatric Use subsection of the Precautions section of the labeling for human prescription drugs and biological products. This section includes relevant information about the use of the drug product in the elderly. Guidance is provided to the industry on submitting geriatric labeling. Importantly, this measure was also retrospective, implying that for specified approved drug products, the application holders must submit a geriatric labeling supplement [35].

In 2014, the FDA published the "FDA action plan to enhance the collection and availability of demographic subgroup data" [36]. The main aim is to provide safe and effective medical products that must be available for a broad range of patients that need them. This action plan is part of Section 907 of the FDA Safety and Innovation Act of 2012, in which the FDA had to investigate to which extent clinical trial participation and inclusion of safety and effectiveness data of demographic subgroups, including age, sex, race and ethnicity, are included in the applications submitted to the Agency [36]. Following this study, in which different stakeholders were consulted, an action plan was established, which can be divided into three priorities. The first priority, quality, includes the improvement of the completeness and quality of demographic subgroup data collection, reporting and analysis. Therefore, relevant guidances, like the ICH E7 guideline, were revised and updated and FDA reviewers were trained on demographic inclusion, analysis and communication of clinical data and better standardization of data collection categories for age. For example, the Good Review Practice guidance was prepared to assist FDA staff in the clinical review of Investigational New Drug (IND) applications, stating *i.a.* to avoid the use of unjustified upper age limits [37].

The second priority, participation, is the identification of the barriers to subgroup enrollment in clinical trials and the employment of strategies to encourage greater participation, with special emphasis on the patients aged above 75 years. The FDA thus seeks to collaborate with the industry to help ensure appropriate use of enrollment criteria in clinical trial protocols in order to avoid the disproportional exclusion of the older patients [36]. Making demographic subgroup data more available, understandable and transparent covers the third priority, transparency. In the end, the FDA aims at improving data quality, encouraging greater participation in clinical trials and making the demographic subgroup information data more available and transparent, resulting in easy access of all stakeholders to meaningful clinical information and thus allowing informed decisions [36]. A survey of the digital Infuzion® database, which was established upon collaboration with the FDA to structure electronic clinical trial data, focused on the inclusion of patients with multiple chronic conditions in clinical trials during the fiscal year 2010. The survey covered 147 studies with in total

115342 study subjects of which only 19% was aged above 65 years [38]. Recently approved medicines like ivabradine for the treatment of congestive heart failure, a chronic condition with higher prevalence with older people, already show a higher proportion of geriatric patients aged above 65 years in their clinical trials (38%), of which 11% was older than 75 years [39].

Pharmaceutical and Medical Devices Agency (Japan)

To our knowledge, in contrast to the European and American regulatory authorities, no additional strategy with regards to the development of geriatric medicine is established by the Japanese regulatory authorities. However, in a recent article, PMDA employees expressed their concern about the underrepresentation of geriatric patients in clinical trials. Although the authors do not represent the formal view of the PMDA, there is an awareness that more efforts are needed to properly characterize the benefits and risks of drugs for older people [40].

Thus, in contrast to the pediatric medicines, there are only guidelines available on the development of geriatric medicines, which have no legislative power. Moreover, the available E7 guideline focusses on clinical trials, not on the full development of geriatric medicines. Within the framework of the Geriatric Medicines Strategy and the FDA action plan to enhance the collection and availability of demographic subgroup data, the EMA and the FDA have taken additional measures in order to more completely answer the medicinal needs of the elderly (Figure 3).

3. VIEWS OF DIFFERENT STAKEHOLDERS

The different stakeholders involved in the development of geriatric medicines are the pharmaceutical industry, developing and manufacturing medicines, the regulatory authorities, evaluating and approving medicines, the healthcare professionals, prescribing medicines and the patients, using medicines. Each involved party considers the development of geriatric medicines from a different perspective.

Pharmaceutical Industry

EFPIA, the European Federation of Pharmaceutical Industries and Associations, committed to collaborate with other stakeholders in order to promote the development of safe and effective medicines for the aging population [41]. In a position paper, EFPIA recommended the pharmaceutical industry to implement the ICH E7 guideline and its Q&A document. By improvement of patient recruitment in clinical trials, older patients with stable and common comorbidities should be included in order that drug efficacy, safety and tolerability can be characterized in this population.

EFPIA also recommends to address the medical needs of older patients through innovation. New innovative medicines should address current gaps in the prevention and treatment of specific geriatric conditions, like sarcopenia, and these medicines should be developed using new tools, models and study methodologies [41]. Also development of age-appropriate drug formulations will be a challenge [42]. Finally, the pre- and post-marketing safety evaluation in older patients should be optimized, aiming at the early detection of safety issues [41].

However, there is a concern that the inclusion of a geriatric group in clinical trials may increase the variability of endpoints, resulting in larger and more complex studies and delaying the development of new medicines. Therefore, the pharmaceutical industry also emphasizes more involvement of the regulatory bodies to provide specific scientific advices, for example on the inclusion of patients above 75 years with co-morbidities, loss of function or geriatric syndromes [43].

Regulatory authorities

Already in the late 1980s, the FDA published a guideline on studying drugs likely to be used in the elderly [34]. Later, in 1993, an internationally agreed ICH E7 guideline, Studies in Support of Special Populations: Geriatrics, was established by the FDA, EMA and PMDA representing an agreed guidance concerning the inclusion of geriatric patients in clinical trials [24]. Both FDA, through the FDA Innovation Act of 2012 Section 907, and EMA, through the Geriatric Medicines Strategy, took additional measures to ensure the availability of safe and effective drugs for the elderly and to address their specific needs [29,36]. Based on initial evaluations of new marketing authorizations, the view is that the situation is improving, despite that the geriatric patients aged >75, especially the frail and those with comorbidities, are still excluded from clinical trials [42-44]. Yet, the current opinion of the FDA, EMA and PMDA is that there is no need for specific regulations.

In the European Union, the opinion on the importance of addressing the specific needs of the elderly differs between the different member states. A first study gauging the views of health-related professionals from nine European countries, identified differences especially between the newer and older members of the EU [45]. Although this study represents the views of health-related professionals, the observed discrepancy in views may be the result of political differences in the decision making on clinical trial regulation and practice in older people in the different EU countries [45]. Another study indicated that 67% of the national agencies of 21 European countries felt that input from geriatric medicine would be useful in evaluating drugs in their country. However, 90% of these countries had neither committees, nor policies related to prescribing to older people, while 58% had such policies for children [46].

Healthcare providers

Both the European and American geriatric societies agree that the persistent exclusion of older people from clinical trials impede evidence-based medicine in the geriatric population. Inclusion of the elderly in clinical trials is needed in order to better understand benefits and the potential adverse effects in this population. This is in accordance with the general principle that the patients that will use the drug in clinical practice must be represented by the clinical trial participants [18]. Beers *et al.* evaluated the difference in view of clinical and non-clinical professionals on the information needed for rational drug prescription [47]. Clinical professionals (healthcare providers) indicated that they need more information on the safety aspects of medicines, such as sedative, cardiovascular, locomotor and anticholinergic effects, as well as information about the drug-disease interaction and dosing instructions for older patients [47]. These items are not yet included in the ICH E7 guideline nor in the Q&A document and therefore, the healthcare providers suggest to optimize the guideline. This contrasts the current opinion of the non-clinical professionals (regulators and industry) [46]. The same research group also investigated the availability of information necessary for appropriately prescribing in older patients in the SmPC of recently approved medicines [48]. It was concluded that the SmPCs do not sufficiently provide adequate information about efficacy and safety on the older people, especially the very old and frail. However, the European Public Assessment Reports (EPARs) presented this information sufficiently well [48]. Similar conclusions were drawn during an American study [49]. Thus, optimization of the ICH E7 guideline towards adoption in the SmPC of the clinical relevant information on the geriatric population is recommended. Moreover, after concluding a persistent exclusion of elderly from clinical trials regarding heart failure despite of existing regulatory recommendations, a group of geriatricians believed that analogous to the pediatric medicines, regulatory authorities should enforce in inclusion of elderly in (relevant) clinical trials in order to improve the current situation [19].

Patients

The developmental challenges related to the use of medicines reported by the older people and their caregivers could be classified into physical, cognitive and medicine-related difficulties. Physical difficulties are related to the age-related physiological and functional changes, for example inability to read the leaflet information and to open packaging or difficulties to swallow the drug. Cognitive difficulties cover confusion, memory problems, comprehension and stress due to disease symptoms, *e.g.* lack of immediate effect of slow release formulations. Medicine-related difficulties encompass the polypharmacy reality: concerns about mixing up tablets and confusion on names of medicines and generics [50].

Old patients indicate the need for practical information on the drug like what to do in case a dose was forgotten. Importantly, this information should be understandable, as currently the used language is often still too technical and medical. Using a quick response (QR) code on the packaging, the availability of drug-related information can be enhanced. Elderly also encounter problems with the identification of a medicine. Standardized symbols and colors for the packaging and tablets could be used to help to distinguish between the different types of drugs. Finally, older patients would like to choose from different formulations for one medicine like liquid or solid dosage forms [50].

4. CHALLENGES IN THE DEVELOPMENT OF GERIATRIC MEDICINES

Several challenges related to the development of geriatric medicines were identified and some further explored. A first challenge comprises the altered organ functions, which manifest heterogeneously in the geriatric population. The age-related changes of the immune system, skin physiology, gut microbiota composition, BBB and stem cells are given as an example, with special emphasis on the changes of the BBB permeability. Other selected challenges include the requirements of age-appropriate drug products, challenges with regards to clinical trials in the elderly population and the related ethical issues, pharmacovigilance activities in the older population, the applicability of personalized geriatric medicines and finally the pharmacoeconomic aspects of drug therapy for the elderly.

4.1. ALTERED ORGAN FUNCTIONS

With aging, different organ systems show functional and physical alterations as illustrated in Figure 2 [6-12]. These changes influence the pharmacokinetics, *i.e.* absorption, distribution, metabolization and elimination, as well as the pharmacodynamics of the drug. The pharmacokinetic alterations are mainly due to changes in the gastrointestinal system and body composition, as well as to hepatic and/or renal impairment (Table 1) [6-7]. The influence of alterations of these organ systems is extensively evaluated during pharmacokinetic studies as stated in the ICH E7 guideline [24]. However, other age-related organ changes can significantly affect the drug therapy in the elderly as well.

Immunosenescence and inflammaging

Aging is characterized by progressive changes of the immune system, also referred to as immunosenescence, causing higher susceptibility to infections, cancer and autoimmune diseases [51]. Immunosenescence affects the constituent cells of both the innate and adaptive immune

system and is due to prolonged antigenic stimulation [51,52]. A reduction of the thymus function causes a decrease in T-lymphocyte production and consequently a modification in cytokine secretion. This results in elevated levels of TNF-α, interleukin-6 and C-reactive protein, which are also produced by adipose tissue and due to a decline in the production of sex hormones and exposure to stress, and cause a low-grade chronic inflammatory status or so-called inflammaging [51-53]. Thus, many factors and molecules originating from different tissues, like adipose tissue and muscles, organs like liver and brain, the immune system and gut microbiota, contribute to inflammaging [53]. This state of low-grade inflammation is responsible for the decline and onset of several diseases like cancer, frailty and sarcopenia, osteoporosis, cardiovascular diseases, atherosclerosis, hypertension, obesity, type-2 diabetes and dementia [51,53]. Therefore, inflammaging is a promising therapeutic target for the treatment of several diseases in the elderly and deserves more research in order to unravel the underlying complex mechanisms causing this chronic inflammatory status [53].

Aged skin physiology

During aging, structural and functional changes occur at the skin, characterized by *i.a.* dryness of the stratum corneum, decrease in skin surface lipids, atrophy of the skin capillary network and altered cutaneous metabolism [54-56]. Currently, it is not clear how and if these factors influence the percutaneous penetration of drugs [56]. Studies investigating the difference in transdermal penetration of drugs between younger adults and elderly resulted in conflicting results. For marketed transdermal products, no age-related differences could be demonstrated [57,58]. Thus, because of the uncertainty on the effect of aging on the percutaneous absorption of drugs and the age-related PK/PD changes, it would be beneficial to determine if adapted doses of transdermal formulated drugs must be provided for the elderly population, certainly within the framework of the development of age-appropriate drug formulations. Indeed, transdermal drug delivery forms a suitable alternative for oral dosage forms, not only because it avoids gastrointestinal absorption and hepatic first-pass effect, but rather because it allows to minimize adverse drug reactions and inherently, to increase drug adherence [54,55,58].

Age-related changes in gut microbiota

Aging is also characterized by changes in the composition of the gut microbiota, the bacterial population present in the gastrointestinal tract [59]. Gut microbiota affect several physiological functions, like digestion, drug efficacy, being involved in the enterohepatic circulation, carcinogenesis and immune function [58-62]. Swallowing dysfunction, dentition problems, the increased gut transit time and environmental and nutritional changes associated with aging cause alterations in the

microbiotal composition. As already mentioned, these changes can contribute to the state of inflammaging [53,62-64]. The study of the age-associated changes of the gut microbiota is in an early phase and thus there are still some unresolved questions. For example, can these changes in microbiota affect the enterohepatic circulation of drugs and thus contribute to altered PK/PD of medicines in geriatric patients [60]? As frail patients appear to have specific changes in gut microbiota, can these changes be used as biomarkers for frailty or more in general for the health status of the elderly [64]? Can probiotics be used to balance the gut microbiota [62]?

Stem cell depletion

One of the theories on aging is the depletion of stem cells [3]. Indeed, stem cells undergo profound changes during the aging process, resulting in diminished responsiveness to tissue injury, dysregulation of proliferative activities and deterioration of functional activities [65]. This depletion of stem cells is driven by several cell-intrinsic, environmental and systemic factors like accumulation of toxic metabolites and DNA damage in stem cells, defects in proteostasis, which comprises the cellular processes responsible for synthesis, folding and turnover of proteins. Other factors are proliferative exhaustion of stem cells, characterized by a depletion in stem cell pool and disturbed cell-cycle activity, extracellular signaling, like inflammatory regulators and alterations in the microenvironment where stem cells reside or niches, and finally epigenetic remodeling [65]. The age-associated changes in stem cell function are especially of interest for Advanced Therapy Medicinal Products (ATMPs). Recently, the EMA recommended the approval in the EU of the first stem cell therapy for the treatment of moderate to severe limbal stem cell deficiency due to physical and chemical burns to the eye in adults for approval [66]. The question was explicitly raised during risk assessment whether this therapy is applicable for the elderly, awaiting clinical data will become available for application of this ATMP therapy in the geriatric population [67].

Blood-brain barrier dysfunction

During the aging process, important changes occur at the BBB, which ultimately result in an increased permeability [68-72]. Early research on the effect of aging on the BBB indicated subtle but significant histologic and physiologic changes of the BBB, as well as an increased vulnerability to external factors like hypertension and cerebrovascular ischemia [73-75]. However, these findings were mainly based on aged animal models and showed interspecies variability, undermining to draw general conclusions for humans. A systematic review of the literature data on the influence of aging on the human BBB function using imaging techniques and assessment of the cerebrospinal

fluid/serum ratio of albumin or immunoglobulin G (IgG), effectively indicated that the BBB permeability increases with normal aging [68].

Structural and functional changes in the aging BBB

Both structural and functional changes are observed at the BBB during the aging process. An overview is given in Figure 4.

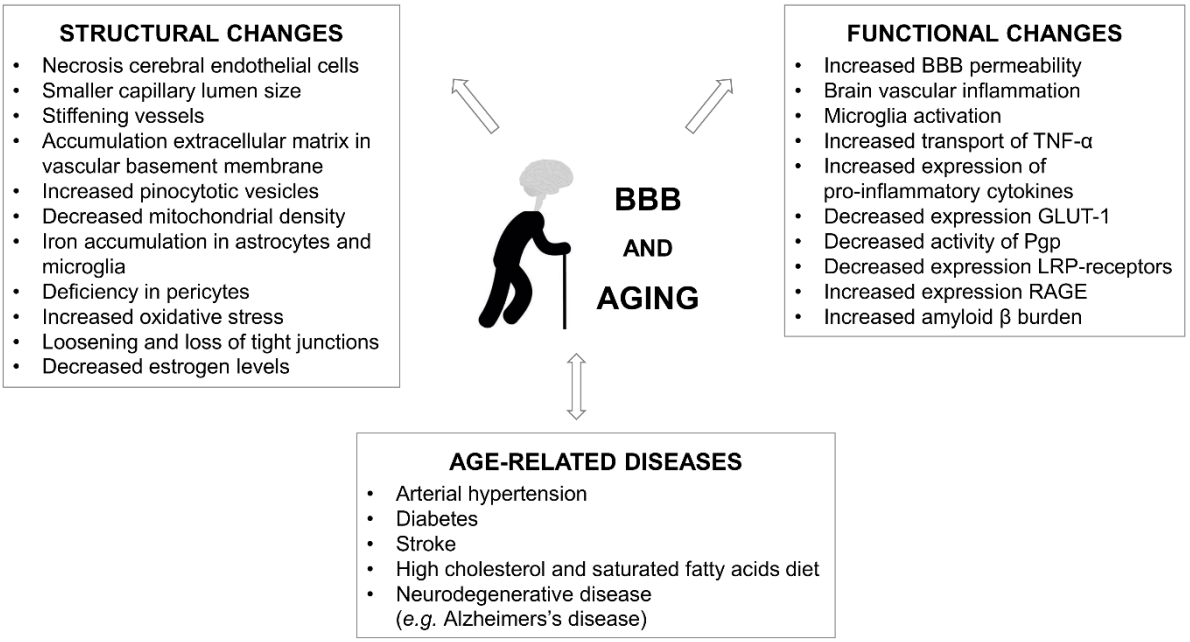

Figure 4: Overview of the age-related diseases and the structural and functional changes at the BBB [69-71].

Structural alterations in the neurovascular unit include focal necrosis of the cerebral endothelial cells, resulting in decreased cortical and white matter microvascular density, smaller capillary lumen size, stiffening of the vessels, accumulation of extracellular matrix components in the vascular basement membrane, increased pinocytotic vesicles, decreased mitochondrial density, implying that energy-dependent processes become impaired at the aging BBB. The cells of the neurovascular unit, *i.e.* astrocytes, microglial cells and neurons, play a key role in maintaining the brain iron homeostasis, necessary for normal physiological brain function. During aging, it is observed that iron accumulates both in the astrocytes and microglia in the brain regions associated with motor and cognitive functions. A suggested mechanism for this accumulation in astrocytes is the reduction of ceruloplasmin expression, a ferroxidase necessary for conversion to ferrous iron in order that it can be exported out of the cell [68,76]. This accumulated iron causes a dysregulation of the brain iron homeostasis and can have neurotoxic effects as this iron excess can generate free radicals [76]. Brain aging is also characterized by a loss in pericytes leading to brain vascular damage through reduction in the brain microcirculation as well as an increase in the BBB permeability due to a reduction in the

expression of tight junction proteins like ZO-1, occludin and claudin-5 [70-72,77]. This increase in BBB permeability allows the accumulation of vasculotoxic and neurotoxic macromolecules [77]. Due to this BBB dysfunction, aging is also associated with vascular inflammation [71,72]. Heightened peripheral inflammation causes increased levels of pro-inflammatory TNF-α in brain endothelial cells in geriatric persons, which in turn enhances the expression of pro-inflammatory cytokines at the BBB level. These cytokines, more specifically TNF-α, also suppress the expression of tight junction protein complexes like occludin-1 and ZO-1, resulting in a loosening of the BBB [57,60]. The vascular inflammation is also manifested at the microglia, the immunological part of the neurovascular unit, which alter their phenotype with age: they adopt an activated, pro-inflammatory phenotype in response to IFN-γ, which is produced by infiltrated immune cells that gained access to the BBB due to the age-related increase in permeability [69,72]. The activated microglia, together with the iron accumulation in these glial cells, form a source of oxidative damage to cells composing the BBB. More studies are needed to understand the relationship between the effects of reactive oxygen species (ROS) and the BBB impairment [69,76,79]. A decrease in estrogen levels associated with aging is also involved in the age-related malfunction of the BBB. Estrogen is known to have important protective effects on the cerebral endothelial cells, decreases the cerebral vascular tone and increases cerebral blood flow [69,80,81]. Thus, a combination of age-related changes at the BBB interface results in an increase of the BBB permeability, heightening the passage of pro-inflammatory compounds and cells as well as toxic agents, that in a vicious circle further enhance the increase in BBB disruption.

Several transporter functions at the BBB alter with aging. The expression of the glucose transporter, GLUT-1, is reduced, together with transporters for amino acids, choline and peptides, subverting the bioavailability of these essential compounds in the brain [69-71,75]. Also the Pgp function is decreased, causing accumulation of (potential) toxic compounds that reach the brain [68-71,82,83]. Other reported changes are the decrease of the low-density lipoprotein receptor-related protein (LRP)-receptors and the increased expression of the receptors for advanced glycation end products (RAGE). LRPs (LRP-1) as well as Pgp mediate the efflux of amyloid β (Aβ) from the brain, while RAGE is involved in the influx of Aβ in the brain. Thus, changes of these transporters at the BBB result in an increased amyloid burden in the aging brain [69].

Age-related diseases influencing the BBB

Age-associated diseases like arterial hypertension, diabetes and stroke are risk factors for alterations of the BBB permeability or aggravate it (Figure 4). Several studies also demonstrated a link between diet consumption and BBB function [84]. One study concluded that mid-life obesity was positively related to a decrease in integrity of the BBB at older age in women [85]. Another study suggested

that diets rich in saturated fatty acids accelerated the onset of BBB dysfunction with aging [86]. Obesity is also found to be associated with the heightened systemic state of inflammation in older mice, exacerbating the BBB dysfunction and contributing to the neuroinflammation process and oxidative stress in the brain [87]. The BBB breakdown associated with the aging process is found to initiate in the hippocampus, the brain region critical for memory and learning [88]. This was demonstrated by comparison of the regional BBB permeability between aged patients with no and mild cognitive impairment using an advanced dynamic contrast-enhanced MRI protocol [88]. Both groups showed BBB breakdown in the hippocampus but not in the other brain regions. The BBB dysfunction was more pronounced for the patient with mild cognitive impairment [88]. These results indicate that in the early aging stage, BBB disruption is initiated in the hippocampus and is associated with cognitive impairment [87-89]. This cognitive impairment is seen in Alzheimer's disease (AD), a type of dementia typically affecting geriatric persons and characterized by accumulation of Aβ and hyperphosphorylated tau [69,90].

Currently, a lot of research is performed to elucidate the role of BBB dysfunction in the etiology of neurodegenerative diseases, like Parkinson's disease and, especially, AD [91]. For both diseases, it is assumed that neuroinflammation and BBB disruption are involved in the pathogenesis of neurodegeneration, because of the increased permeability for neurotoxic agents. Most, but not all, studies concluded an increased BBB permeability in AD patients or animal models and that structural and functional changes occur at the BBB of these patients [91]. As previously indicated, changes in the transporter functions with aging result in accumulation of Aβ, forming an important link between aging and AD, characterized by senile plaques of Aβ in the brain [90,91]. Amyloid β alters several functions of the neurovascular unit, causing further BBB dysfunction and neurodegeneration. First, pericyte coverage of capillaries is reduced compared to non-demented persons, which is possibly caused by the neurotoxic effect of Aβ, as demonstrated *in vitro* [90]. Amyloid β also induces changes in the astrocyte function in AD brain: astrocytes found in the proximity of Aβ plaques lack the expression of scavenger receptors, which are needed for the internalization and degradation of Aβ, contributing to its accumulation. The mechanism how Aβ induces this altered function of astrocytes is still not clear. Finally, activated microglia surround the Aβ plaques in AD brains. As explained earlier, this activated phenotype results in neurotoxicity, but also induces phagocytosis of Aβ plaques. Amyloid β is normally phagocytosed by a specialized subset of macrophages, recruited from the peripheral circulation. In AD individuals, it was demonstrated that these macrophages inefficiently phagocytose Aβ compared to healthy individuals, also contributing to the accumulation of Aβ [90]. In contrast, other studies indicate that reduced Aβ metabolism causes its accumulation and plaque formation [91]. Moreover, beside the Aβ hypothesis, other Aβ-independent risk factors and pathologic conditions like inflammation, oxidative stress, diabetes, cardiovascular disease, are

associated with AD. These factors also affect the BBB, demonstrating again the link between BBB dysfunction and AD [69,91]. The question remains whether BBB dysfunction is the primary cause or is a secondary consequence of AD, but clearly the BBB plays a multifaceted role in the etiology of AD [71,90,91].

4.2. AGE-APPROPRIATE DRUG PRODUCTS

A drug should be formulated in a way that independent and safe management, handling and administration can be accomplished by the patient, which is stated in the ICH Q8(R2) guideline on pharmaceutical development [92-94]. To achieve this goal, a comprehensive understanding of the needs of the target population is required. In Table 2, exemplary specific needs of the elderly patients are listed, as well as the possible solutions to address them [4].

Table 2: Specific needs of geriatric patients and possible solutions to address these needs (partly adopted from Stegemann *et al.*) [4,95].

Requirements	Specific needs of elderly	Possible solution
Appropriate dose strength	Dose strengths covering declining metabolic capacity and drug-drug interactions in polymedication conditions	Lower dose strengths, allowing dose titration
Identification of drug product	Simplify drug product identification	Colored or specifically shaped dosage forms
	Simplified and readable medicines information through use of pictograms and adapted labeling	Larger font and simple wording in leaflet, product picture on the pill-box
	Potential medication errors in polypharmacy	Easy and clearly identifiable drug products
Manageability of drug product	Suitable age-adequate packaging to access the drug product with motoric capability limitations and diseases	*E.g.* low strength screw top, no child-resistant packaging
Swallowability of drug product	Easy to swallow oral dosage forms options (age-appropriate drug formulations)	Conversion into multiparticulates or sprinkle, prefilled oral liquid dosage form options
Complexity of drug therapy	Decrease pill burden	Modified release formulation, dual or multiple release formulations or combination products
	Complex medication schedules	Define implementation strategies and contextual cues
	Supportive device tools	Medication organizers with medication control or alert system
Safety of excipients	Excipients with low toxicological profile	Appropriately researched excipients for use in the elderly population

First, available dose strengths should cover all patients' needs, and provide the flexibility to clinicians to adapt the drug therapy in the elderly patient in function of the altered pharmacokinetic and pharmacodynamic profile, as well as in function of concomitant therapy. In other words, the

availability of appropriate doses will allow an individually tailored and optimal drug therapy in the elderly [92,95]. Manageability of the drug product is another important pillar, as the geriatric patient is often confronted with a decline in motoric functions, whether or not associated with disease. For these patients, the packaging and splitting of a drug product can be an important hindrance. Especially child-resistant packaging, which is a regulatory requirement, forms a serious hurdle [92]. A third requirement for the elderly is the ease of product identification [92,95]. Guidances are already available for the readability of the labeling and the package leaflet of medicinal products [96,97], however because of the decrease of vision in function of age, use of color or color combinations and shapes of solid dosage forms must be encouraged [92,95]. Another major concern is the swallowability of the drug product. To overcome swallowing issues of capsules and tablets, alternative solid dosage forms, like liquids, orally disintegrating tablets or small solid forms (*e.g.* multiparticulates), should be investigated resulting in age-appropriate drug formulations [4,42,55,95]. There is also a great need to find ways to cope with the complex drug schedules to which the elderly patients are often confronted. These solutions will also decrease the risk for adverse drug reactions due to drug interactions and poor adherence related with polypharmacy. Fixed-dose combination products and sustained release products form possible solutions to reduce the pill burden and frequency of dosing [4,42,92]. Finally, when developing age-appropriate drug formulations, attention should be paid to the safety of excipients in the geriatric population [95]. Especially excipients for liquid formulations are of toxicological risk, like propylene glycol which can pass an impaired BBB and cause neurological damage, like seen with neonates [95].

It is noted that during pediatric drug development, the pharmaceutical industry is confronted with similar problems, like swallowing difficulties. As still much research needs to be performed in both fields and as there are many parallels in needs between the geriatrics and pediatrics like the need for dose adaptation and age-appropriate drug formulations, the pharmaceutical industry should combine their efforts in order to develop optimal age-appropriate drug products, taking into account the differences between the two populations [4,21,42,55,92,95]. The needs of the pediatric population mainly depend on age, while the needs of the geriatric population are determined by the individual health status [95]. Regulatory challenges include the questions how to cope with child-resistant packaging of geriatric drug products and with combined drug therapies [92].

4.3. CLINICAL TRIALS AND ETHICAL ASPECTS OF GERIATRIC MEDICINES

Several guidance and opinion documents with regards to clinical trials and ethical aspects of geriatric medicines are yet available. The PREDICT (increasing the PaRticipation of the ElDerly In Clinical Trials) consortium, funded by the European Union, conducted a study aimed at identifying, addressing and

resolving the issues related to the exclusion of older people from clinical trials. Based on the study outcomes, a charter was established in order to put an end to the persistent exclusion of geriatric patients (Table 3) [98].

Table 3: Charter for the rights of older people in clinical trials (PREDICT consortium [98]).

1.	Older people have the right to access evidence-based treatments
2.	Promoting the inclusion of older people in clinical trials and preventing discrimination
3.	Clinical trials should be made as practicable as possible for older people
4.	The safety of clinical trials in older people
5.	Outcome measures should be relevant for older people
6.	The values of older people participating in clinical trials should be respected

In 2013, the Geriatric Medicines Working Party of the European Forum for Good Clinical Practice's (EFGCP), a non-profit organization by and for individuals conducting biomedical research, published guidelines on the medical research for and with older people [99,100]. The guidelines describe recommendations on the ethical aspects of clinical trials in older people within the legal framework of regulations and guidelines [99,100]. In the report of the annual meeting of the American Geriatrics Society in 2008, the European and American geriatric societies outlined the challenges for the inclusion of older adults in clinical trials [18]. Based on these three different documents, four main challenges regarding clinical trials of geriatric medicines can be distilled.

Clear justification of inclusion and exclusion criteria for participants of clinical trials

Industry-sponsored trials are aimed at obtaining approval of the investigated drug and demonstrating the drug's effectiveness and safety is of minor importance. Therefore, restrictive eligibility criteria exclude the older patient, often characterized by complex illnesses, from these trials and include patients that significantly differ from the population that will take the drug in clinical practice [18]. In order to overcome this problem of unrealistic clinical trials, every exclusion criterion should be clearly justified [18,99,100].

Recruitment and obtaining informed consent in the older population

Another challenging difficulty will be the recruitment and obtaining informed consent in the older participants, who can be cognitively impaired [18]. Maximizing effective and clear communication, with emphasis on readability and easy-to-understand information, involvement of caregivers, use of research networks and overcoming potential problems with access and transport, can improve recruitment and retention of older participants [99,101,102]. Careful attention should be given to screening of cognitive impairment and to the verification if the participant understood the given information and implications of participation. In case the participant fails to fully understand the

given information, a proxy decision-maker can be involved [18,99,100]. Older patients in a trial also should be hosted in a familiar environment appropriate for older care in order to minimize distress and fear [100].

Dealing with comorbidity and polypharmacy

The geriatric population is characterized by comorbidity and polypharmacy, which make them more susceptible to adverse drug reactions, causing selective attrition and missing data and thus complicating data evaluation. Although randomized controlled clinical trials are used to minimize the differences in comorbidities between the different participant groups, the heterogeneity of the elderly population raises the question whether this standard methodology of clinical trials should be refined [18]. The EMA's Modeling and Simulation Working Group was established to help in the development of standards for the design, conduct, analysis and reporting of modeling and simulation (M&S). PK/PD population M&S can help to evaluate PK/PD in older patients identifying covariates important for variability in drug response and quantifying age-related effects on safety and efficacy. Thus, PK/PD M&S is a promising tool to optimize clinical trial design and operation in the elderly population [43].

Definition of age-relevant outcomes

As recommended in the ICH E7 guideline, age-relevant outcomes or endpoints should be defined in clinical trials involving elderly patients [24,25]. Due to its comorbidity and/or frailty, a therapy can cause disease-specific improvements, but can have little impact on the day-to-day function of the geriatric patient. Therefore, functional outcomes should be considered during the clinical trials in the older population. An example of a functional outcome is gait speed, which has a predictive validity for adverse outcomes like mortality and onset of disability. However, more experience is needed to refine clinical trial methodology that uses functional outcomes [103]. Moreover, various diseases may have different clinical manifestations in the geriatric population, making the evaluation of clinical trials more complicated [104]. Quality of life is also an important outcome, especially for the very old patients at the end of life [100]. Currently, age-related conditions like frailty and sarcopenia are not labeled as diseases, but should be considered as targets for a clinical intervention [103]. As frailty is the most problematic expression of aging, affecting a quarter to half of the older population (aged above 85), research for a medicinal therapy for prevention and treatment of this condition is urgent [5].

Representation of geriatric expertise in the ethics committee reviewing geriatric trials will be crucial to assure these challenges will be taking into account. This ethics committee should always ward the balance between the levels of risk and the benefits for the geriatric patient [100].

4.4. PHARMACOVIGILANCE

According to the WHO, pharmacovigilance includes the science and activities aiming at detecting, assessing, understanding and preventing adverse effects or other drug related problems in the post-authorization phase of medicines [105]. A major cause for adverse drug reactions in the clinical practice is the inappropriate use of drugs due to inappropriate dose or duration of the therapy, drug interactions, off-label use or use in contraindicated circumstances [106]. These adverse drug reactions can be monitored during pharmacovigilance activities, which is especially of importance for the elderly population as they are frequently excluded from clinical trials and are at higher risk for adverse drug reactions than younger adults [106,107]. In 2012, the new pharmacovigilance legislation came into force in the EU, which is translated in practical terms in the Good Pharmacovigilance Practices (GVP). In the Geriatric Medicines Strategy of the EMA, the need for specific pharmacovigilance activities for the geriatric population was expressed [29]. However, only limited guidance concerning the elderly could be retrieved in the different modules (V, VI, VII, VIII and IX) of the GVP, like on the incorporation of the implications of drug use in the elderly in the Risk Management Plan if this patient group was not included in the clinical trials (module V) and the importance to pay special attention to safety information of the elderly (module VI) [108-112]. In contrast to the pediatrics, no specific guidance was found for the pharmacovigilance practices in the geriatric population [113]. FDA guidelines on pharmacovigilance also contained no or only limited guidance with regards to the elderly [114-116]. However, pharmacovigilance in the geriatric population is challenging and deserves special guidelines. The occurrence of adverse drug reactions is underestimated in this patient group, because they are often considered as age-related problems or manifest atypically and thereby not reported. Moreover, polypharmacy and the presence of multiple co-morbidities complicate the establishment of adverse drug reactions [117]. In older patients, the endpoints of the drug therapy deviate from those in younger adults [116]. This stresses the importance of obtaining sufficient data in the pre-authorization phase if medicines are intended to be used by geriatric patients, by inclusion of a representative group of elderly in clinical trials, in which age-related endpoints are evaluated [117,118]. If the older population was not included in the pre-authorization clinical trials and use by this population is probable, the Risk Management Plan should reflect this gap of benefit-risk information and post-authorization studies are required [118].

In the EU, these post-authorization safety studies (PASS) are legally binding when requested by the EMA both in the marketing authorization phase, as well as in the post-authorization phase [106,111].

4.5. PERSONALIZED MEDICINE

The geriatric population is recognized to be heterogeneous. However, because of the lack of sufficient knowledge on the efficacy and safety of medicines, the trial and error approach is currently used to medically treat the geriatric patients. This may result in patient dissatisfaction, adverse drug reactions and consequently poor adherence to the therapy [119]. This is especially of concern for therapies with a narrow therapeutic index, like chemotherapeutic agents [120]. A more suitable approach would be personalized or individualized medicine, in which the medical therapy is tailored to the individual characteristics of the patient [119]. Initially, personalized medicine was based on symptoms (*e.g.* angina) and phenotypical characteristics (*e.g.* LDL cholesterol), which resemble the approach used in daily practice. Since the completion of the human genome project, the personalization of medicine was boosted by progress of the pharmacogenomics, mainly applied in the oncology field [119,121]. Optimization of the drug therapy in the elderly can be accomplished by using biomarkers, which indicate the functional, disease and frailty status of the older patient, as well as the biological age [122-124]. Based on these biomarker values, the appropriate dose for the geriatric patient can be determined, as obtained during clinical trials in this population. Beside appropriate dosages, age-appropriate drug formulations are also required in order to provide optimal, individualized drug therapy for the elderly [125].

4.6. PHARMACOECONOMICS

The past decade, the research and development cost (R&D) has more than doubled from US$800 million to an estimated cost of US$2.6 billion in 2013. This increase can be attributed to the higher failure rates, as well as to the larger and more complex clinical trials [126]. Unless innovative clinical trial principles will be rapidly developed, inclusion of geriatric patients will contribute to this increase in R&D cost.

Partly due to the lack of benefit-risk balance data for the geriatric population, inappropriate drug use is common in this patient group, forming the main cause of adverse drug reactions [106,127]. In a national survey performed in the USA, 11.4-35.3% of the emergency department visits by the elderly was because of a drug-related reason. An European study indicated that 20% of the ambulatory patients are faced with adverse drug reactions and 10-20% of the geriatric hospital admissions was drug-related [106,127]. Adverse drug reactions also cause a prolonged hospital stay [106]. This has

economic consequences: in the USA, the annual costs related to the management of adverse drug reactions is estimated to be $US 30.1 billion; in the EU, the total economic burden to the social security or healthcare system is € 79 billion. Moreover, 32 to 69% of the drug related hospital admissions was considered to be (possibly) preventable [127]. These preventable adverse drug reactions are mostly more serious and life-threatening than the non-preventable events and are thus associated with higher costs [128]. There also exists a mutual causal correlation between adverse drug reactions and adherence to drug therapy, which is generally poor in the geriatric population faced with a complex drug regimen due to polypharmacy [127]. Thus, age-appropriate drug products with demonstrated efficacy and safety in the elderly population, taking into account their specific needs, will help to decrease the rate of adverse drug reactions in the geriatric population and thus lower the economic impact of geriatric drug therapy on the social security system [106,127]. Several drug classes like antibiotics, anticoagulants, medicines with narrow toxic-therapeutic range (*e.g.* digoxin and fenytoin), diuretics, hypoglycemic agents, antineoplastic agents and NSAIDS, are mainly responsible for hospitalization due to adverse drug reactions [127]. Based on these data, a priority list can be established to determine the medicines that need urgently to be appropriately researched in the elderly in the post-authorization phase.

In health economics, cost-utility (or cost-effectiveness) analyses are used to measure the cost-effectiveness of a medicinal therapy and is a good indication of the economic impact of a therapy on the social security or healthcare system [129,130]. This cost-utility analysis supports policy makers in determining the pricing and reimbursement of new medicines [129,130]. The aging population impacts and challenges the society and especially the social security systems. To optimally allocate health and social care resources within limited budgets, competing health and social services should be investigated for their relative value for money [130]. During cost-utility studies, Quality Adjusted Life Years (QALYs) are used as health-related utility measures and take into account the quality, *i.e.* health status, and quantity, *i.e.* mortality, of life generated by a healthcare intervention [130,131]. A cost-utility ratio expresses the cost of the therapy per QALY or the cost to gain a year of perfect health [130,131]. QALYs are obtained by categorizing the self-reported health status by the patient based on previous research which is used to value this health status in terms of quality of life [130]. For the measurement of the quality adjusted component of QALY, Health Related Quality of Life (HRQOL) measures are used, such as the generic quality of life instruments EQ-5D, WHOQoL or SF-6D [129,130,132-134]. Several issues are identified when assessing the health state in the elderly using these generic instruments. A first issue concerns the (poor) ability of older people to identify their health status, which is necessary to obtain QALYs. Another issue is that elderly value quality of life differently than younger adults and distinctly define health [130]. Therefore, more relevant quality of life scales specific for older people, with or without dementia, should be used when performing cost-

utility analyses in the elderly population such as CASP-19, PGC Morale scale or ICECAP-O [129,130,132-134].

The use of QALYs in the setting of geriatric medicines is criticized because of its focus on survival, which inevitably results in a lower value for an older person because of the reduced capacity for survival duration compared to a younger individual [129]. Moreover, the presence of co-morbidities in the elderly, limits the ability to benefit from a successful therapy as these comorbidities impede to return to the state of perfect health [130]. For geriatric patients, the aim of a healthcare intervention is not to improve the health status per se, but rather the broader wellbeing. Thus, only generic HRQOL instruments in this population may undervalue the range of services provided, biasing allocation decisions. Instruments covering dimensions "beyond health" can be labeled as wellbeing instruments in which two main conceptualizations can be identified: the first one focusses on wellbeing as an inherently subjective concept, not containing health dimensions [135]. In contrast, the second approach treats wellbeing as representing individuals' welfare, which is dependent of individuals' functionality and thus encompassing HRQOL dimensions [136]. Moreover, for frail older people, small improvements of health tend to be highly valued in the improvement of the quality of life. Not health alone determines the quality of life of an elderly person but also the presence of emotional support and empathy contributing to the general wellbeing [129,137]. Thus a broader approach, incorporating the attributes that highly determine the quality of life, should be used to economically evaluate the geriatric medicines and importantly taking into account the comorbidity and polypharmacy of the geriatric patients [129,138]. The number of instruments developed specifically to address and evaluate outcomes of healthcare services targeted at older people is growing. However, guidance is lacking on which instrument as golden standard can or should be used for cost-utility analysis for interventions aimed at older peoples and deserves more research. Finally, the quality of decisions during cost-utility analyses are as good as the evidence that supports it. This evidence is often poor due to the minimal inclusion of elderly in clinical trials and the measurement of different outcomes during trials in this population, impeding comparison with treatments researched in broader age groups. More research in the elderly population is needed to reduce the uncertainty of decisions during cost-utility analyses concerning older people [130].

5. TO GIP OR NOT TO GIP?

Currently, the ICH E7 and FDA's Geriatric Labeling guidelines encompass the available regulatory framework regarding the development of geriatric medicines. However, these guidelines could not achieve the systematic inclusion of the elderly in clinical trials, even when the older population will be the main user of the investigated drug [18,139]. Both the EMA and FDA are aware of this mostly minimal inclusion of older patients in clinical trials and have taken measures to address the specific needs of the elderly. The question is whether guidelines are enough to achieve safe and effective drug therapy for the elderly.

The ICH E7 guideline focusses only on clinical trials, but development of age-appropriate geriatric medicines needs to start before the clinical phase. For example, the development of appropriate dosage forms and the influence of the age-related physiological changes and disease on the PK/PD of the drug must already be studied prior to administration to the elderly. In the framework of the Paediatric Regulation published by the EMA, the pharmaceutical industry is obliged to submit a PIP, which contains the studies that will be performed in children and the measures that have been taken to develop child-appropriate dosage forms, covers the needs of all age groups of children and defines the timings of the studies compared to adults [23]. This PIP is reviewed by the Paediatric Committee (PDCO), which is composed of experts in the field and once agreed, it is binding and forms the basis for the development and authorization of drug products [23]. Currently, regulatory authorities are not yet prone to establish similar regulations or Geriatric Investigation Plan (GIP) for the geriatric medicines and want to improve the current framework of guidelines, assisted by the GEG of the EMA or trained reviewers by the FDA, who will check the applications for their compliance to these guidelines. However, the time span in which older people use medicines is longer than the time frame of the pediatrics, *i.e.* 0-18 years, especially now life-expectancy is increasing. This stresses the stringency to take measures to provide age-appropriate medicines for the elderly.

Currently, regulatory progress is limited as guidelines are delayed, like the points to consider to characterize the frailty status, which was drafted in 2013 [30]. Also healthcare providers feel the need for a more legally binding regulatory framework. Involvement of all stakeholders is needed to achieve that all aspects of geriatric medicines are covered, ranging from scientific advice and, eventually, incentives for the pharmaceutical industry to the availability of sufficient information both for the older patients and healthcare providers and age-appropriate drug formulations, allowing optimal therapy in the elderly (Figure 5).

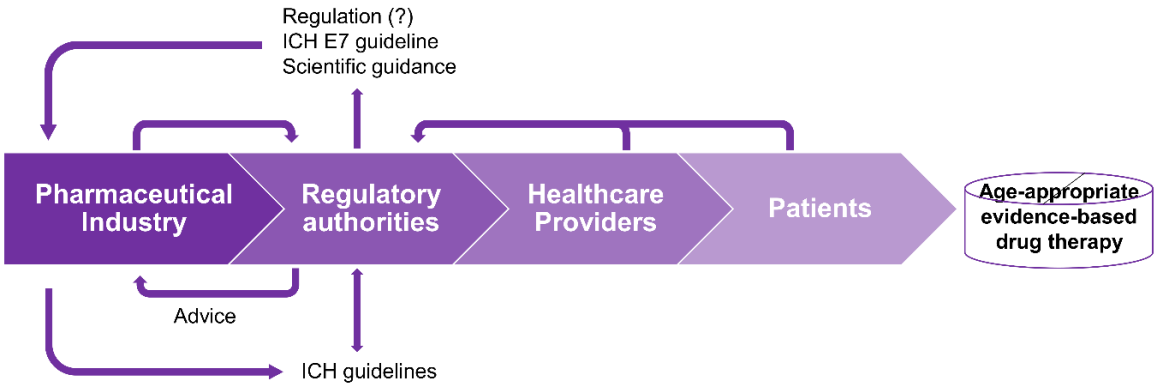

Figure 5: Different steps and stakeholders in the development of geriatric medicines.

We acknowledge that within the current regulatory framework on development of medicines, the utility of some regulations is questionable. However, we believe that GIP is not, and, even more, will have a high value for money being of benefit for all stakeholders. Lessons learned from the application of the pediatric legislation are valuable and should be taken into account when considering similar geriatric regulations. Importantly, a balance between the economic burden and benefit, *e.g.* in the form of extended market exclusivity or reduced regulatory fees, should be found to encourage the industry to apply these regulations.

Moreover, these proposed strategies concern only the newly developed drug products, but do not address already approved medicines. Are pharmacovigilance data enough to update the SmPCs with data on the geriatric patients? Should SmPCs be proactively updated using pharmacovigilance or clinical trial data, *e.g.* for priority medicines based on adverse drug reactions rates in the elderly?

So, whether we should GIP or not will depend on whether the current strategies to ensure safe and effective drugs for the elderly achieve their objectives. However, there is no time to waste.

6. REFERENCES

[1] United Nations (UN), Department of Economic and Social Affairs, Population Division. World Population Prospects - The 2012 Revision Key Findings and Advance Tables (Working paper no. ESA/P/WP.227). 2013; http://esa.un.org/wpp/Documentation/pdf/WPP2012_%20KEY%20FINDINGS.pdf (accessed 18 March 2015).

[2] Eurostat, Konstantinos Giannakouris. Ageing characterises the demographic perspectives of the European societies (Issue number 72/2008). 2008; http://ec.europa.eu/eurostat/documents/3433488/5583040/KS-SF-08-072-EN.PDF/1c8f668a-d1d9-42cb-80b1-eaf3dfc1b7df (accessed 18 March 2015).

[3] Kane RL, Ouslander JG, Abrass IB, Resnick B. Clinical Implications of the Aging Process. In *Essentials of Clinical Geriatrics*, 7th edition (Eds: Kane RL, Ouslander JG, Abrass IB, Resnick B), McGraw-Hill, **2013**, http://accessmedicine.mhmedical.com/content.aspx?bookid=678&Sectionid=44833878 (accessed 18 March 2015).

[4] Stegemann S, Ecker F, Maio M, Kraahs P, Wohlfart R, Breitkreutz J, Zimmer A, Bar-Shalom D, Hettrich P, Broegmann B. Geriatric drug therapy: Neglecting the inevitable majority. *Ageing Res. Rev.* 2010; **9**: 384-398.

[5] Clegg A, Young J, Iliffe S, Rikkert MO, Rockwood K. Frailty in elderly people. *Lancet* 2013; **381**: 752-762.

[6] Boss GR, Seegmiller JE. Age-Related Physiological Changes and Their Clinical Significance. *West J. Med.* 1981; **135**: 434-440.

[7] Klotz U. Pharmacokinetics and drug metabolism in the elderly. *Drug Met. Rev.* 2009; **41**: 67-76.

[8] Sera LC, McPherson ML. Pharmacokinetics and Pharmacodynamic Changes Associated with Aging and Implications for Drug Therapy. *Clin. Geriatr. Med.* 2012; **28**: 273-286.

[9] Castle SC. Clinical Relevance of Age-Related Immune Dysfunction. *Clin. Infect. Dis.* 2000; **31**: 578-585.

[10] Hung C-W, Chen Y-C, Hsieh W-L, Chiou S-H, Kao C-L. Ageing and neurodegenerative diseases. *Ageing Res. Rev.* 2010; **9S**: S36-S46.

[11] Aanerud J, Borghammer P, Chakravarty MM, Vang K, Rodell AB, Jónsdottir KY, Møller A, Ashkanian M, Vafaee MS, Iversen P, Johannsen P, Gjedde A. Brain energy metabolism and blood flow differences in healthy aging. *J. Cereb. Blood Flow Metab.* 2012; **32**: 1177-1187

[12] Johannsen P, Jakobsen J, Gjedde A. Statistical maps of cerebral blood flow deficits in Alzheimer's disease. *Eur. J. Neurol.* 2000; **7**: 385-392.

[13] Mukhtar O, Jackson SHD. Drug therapies in older adults (part 1). *Clin. Med.* 2015; **15**: 47-53.

[14] Hayflick L. Biological Aging Is No Longer an Unsolved Problem. *Ann. N.Y. Acad. Sci.* 2007; **1100**: 1-13.

[15] Willemen M, Jansen PAF, Leufkens HGM. Pharmaceuticals and the Elderly. In *Priority Medicines for Europe and the World "A Public Health Approach to Innovation", Chapter 7.2: Cross-Cutting Issues: Elderly* (Ed: World Health Organization (WHO)), **2004**.

[16] Guralnik JM, Ferrucci L. Demography and Epidemiology. In *Hazzard's Geriatric Medicine and Gerontology*, 6th edition (Eds: Halter JB, Ouslander JG, Tinetti ME, Studenski S, High KP, Asthana S), McGraw-Hill, **2009**, http://accessmedicine.mhmedical.com/content.aspx?bookid=371&Sectionid=41587608 (accessed 18 March 2015).

[17] Shah B, Hajjar ER. Polypharmacy, Adverse Drug Reactions, and Geriatric Syndromes. *Clin. Geriatr. Med.* 2012; **28**: 173-186.

[18] Cherubini A, Del Signore S, Ouslander J, Semla T, Michel JP. Fighting Against Age Discrimination in Clinical Trials. *J. Am. Ger. Soc.* 2010; **58**: 1791-1796.

[19] Cherubini A, Oristrell J, Pla X, Ruggiero C, Ferretti R, Diestre G, Clarfield M, Crome P, Hertogh C, Lesauskaite V, Prada G-I, Szczerbinska K, Topinkova E, Sinclair-Cohen J, Edbrooke D, Mills GH. The Persistent Exclusion of Older Patients From Ongoing Clinical Trials Regarding Heart Failure. *Arch. Intern. Med.* 2011; **171**: 550-556.

[20] Fitzsimmons PR, Blayney S, Mina-Corkill S, Scott GO. Older participants are frequently excluded from Parkinson's disease research. *Parkinsonism Relat. D.* 2012; **18**: 585-589.

[21] Kaplan W, Wittz VJ, Mantel-Teeuwisse A, Stolk P, Duthey B, Laing R. Priority Medicines for Europe and the World 2013 Update. *World Health Organization;* 2013: http://www.who.int/medicines/areas/priority_medicines/MasterDocJune28_FINAL_Web.pdf?ua=1 (accessed 18 March 2015).

[22] Evans WJ. Drug discovery and development for ageing: opportunities and challenges. *Philos. T. R. Soc. B* 2011; **366**: 113-119.

[23] Zisowsky J, Krause A, Dingemanse J. Drug Development for Pediatric Populations: Regulatory Aspects. *Pharmaceutics* 2010; **2**: 364-388.

[24] International Conference on Harmonisation of Technical Requirements for Registration of Pharmaceuticals for Human Use (ICH). ICH Harmonised Tripartite Guideline - Studies in Support of Special Populations: Geriatrics E7. 1993; http://www.ich.org/fileadmin/Public_Web_Site/ICH_Products/Guidelines/Efficacy/E7/Step4/E7_Guideline.pdf (accessed 18 March 2015).

[25] International Conference on Harmonisation of Technical Requirements for Registration of Pharmaceuticals for Human Use (ICH). E7 Studies in Support of Special Populations: Geriatrics – Questions & Answers. 2010; http://www.ich.org/fileadmin/Public_Web_Site/ICH_Products/Guidelines/Efficacy/E7/Q_As/E7_Q_As_step4.pdf (accessed 18 March 2015).

[26] International Conference on Harmonisation of Technical Requirements for Registration of Pharmaceuticals for Human Use (ICH). Final Concept Paper - E7(R1) Studies in Support of Special Populations: Geriatrics *(Revision of the ICH E7 guideline)*. 2008; http://www.ich.org/fileadmin/Public_Web_Site/ICH_Products/Guidelines/Efficacy/E7/Q_As/E7R1_Final_Concept_Paper.pdf (accessed 18 March 2015).

[27] International Conference on Harmonisation of Technical Requirements for Registration of Pharmaceuticals for Human Use (ICH). Dose-Response Information to Support Drug Registration E4. 1994; http://www.ich.org/fileadmin/Public_Web_Site/ICH_Products/Guidelines/Efficacy/E4/Step4/E4_Guideline.pdf (accessed 18 March 2015).

[28] International Conference on Harmonisation of Technical Requirements for Registration of Pharmaceuticals for Human Use (ICH). Ethnic Factors in the Acceptability of Foreign Clinical Data E5(R1). 1998; http://www.ich.org/fileadmin/Public_Web_Site/ICH_Products/Guidelines/Efficacy/E5_R1/Step4/E5_R1__Guideline.pdf (accessed 18 March 2015).

[29] European Medicines Agency (EMA). EMA geriatric medicines strategy (EMA/CHMP/137793/2011). 2011; http://www.ema.europa.eu/docs/en_GB/document_library/Other/2011/02/WC500102291.pdf (accessed 18 March 2015).

[30] European Medicines Agency (EMA). Proposal for the development of a points to consider for baseline characterization of frailty status (EMA/335158/2013). 2013; http://www.ema.europa.eu/docs/en_GB/document_library/Other/2013/06/WC500144373.pdf (accessed 18 March 2015).

[31] European Medicines Agency (EMA). EMA Geriatric Medicines Strategy – Report analysis on Product Information (EMA/352652/2013). 2013; http://www.ema.europa.eu/docs/en_GB/document_library/Report/2013/10/WC500152545.pdf (accessed 18 March 2015).

[32] European Medicines Agency (2013). EMA Geriatric Medicines Strategy – Report analysis of scientific guidelines (EMA/352591/2013). http://www.ema.europa.eu/docs/en_GB/document_library/Report/2013/10/WC500152544.pdf (accessed 18 March 2015).

[33] European Medicines Agency (EMA). Concept paper on the need for a reflection paper on quality aspects of medicines for older people (EMA/165974/2013). 2013; http://www.ema.europa.eu/docs/en_GB/document_library/Scientific_guideline/2013/04/WC500141560.pdf (accessed 18 March 2015).

[34] Food and Drug Administration (FDA). Guideline for the study of drugs likely to be used in the elderly. 1989; http://www.fda.gov/downloads/Drugs/GuidanceComplianceRegulatoryInformation/Guidances/ucm072048.pdf (accessed 18 March 2015).

[35] Food and Drug Administration (FDA). Guidance for Industry – Content and Format for Geriatric Labeling. 2001; http://www.fda.gov/downloads/Drugs/GuidanceComplianceRegulatoryInformation/Guidances/ucm075062.pdf (accessed 18 March 2015).

[36] Food and Drug Administration (FDA). FDA action plan to enhance the collection and availability of demographic subgroup data. 2014; http://www.fda.gov/downloads/RegulatoryInformation/Legislation/FederalFoodDrugandCosmeticActFDCAct/SignificantAmendmentstotheFDCAct/FDASIA/UCM410474.pdf (accessed 18 March 2015).

[37] Food and Drug Administration (FDA). Good Review Practice: Clinical Review of Investigational New Drug Applications. 2013; http://www.fda.gov/downloads/Drugs/GuidanceComplianceRegulatoryInformation/UCM377108.pdf (accessed 24 March 2015).

[38] Digital Infuzion, Inc. White Paper: U.S. Food and Drug Administration (FDA) Inventory of Clinical Trials Protocols and Clinical Study Data. 2011; http://www.fda.gov/downloads/Drugs/DevelopmentApprovalProcess/ConductingClinicalTrials/UCM309552.pdf (accessed 14 September 2015).

[39] Food and Drug Administration (FDA). Drug Trials Snapshot: CORLANOR. 2015; http://www.fda.gov/Drugs/InformationOnDrugs/ucm446899.htm (accessed 14 September 2015).

[40] Asahina Y, Sugano H, Sugiyama E, Uyama Y. Representation of older patients in clinical trials for drug approval in Japan. *J. Nutr. Health Aging* 2014; **18**: 520-523.

[41] European Federation of Pharmaceutical Industries and Associations (EFPIA). EFPIA Position on Drug Development for Older and Ageing Patients. 2013; http://www.efpia.eu/uploads/Modules/Documents/efpia-position-paper-geriatrics-11102013.pdf (accessed 18 March 2015).

[42] Wahlich J, Stegemann S, Orlu-Gul M. Meeting commentary – "Medicines for older adults: Learning from practice to develop patient centric drug products". *Int. J. Pharm.* 2013; **456**: 251-257.

[43] European Medicines Agency (EMA). Ensuring safe and effective medicines for an ageing population: Workshop Proceedings (EMA/425943/2012). 2012; http://www.ema.europa.eu/docs/en_GB/document_library/Report/2012/08/WC500131045.pdf (accessed 18 March 2015).

[44] Cerreta F, Temple R, Asahina Y, Connaire C. Regulatory activities to address the needs of older patients. *J. Nutr. Health Aging* 2015; **19**: 232-233.

[45] Crome P, Lally F, Cherubini A, Oristrell J, Beswick AD, Clarfield AM, Hertogh C, Lesaukaite V, Prada GI, Szczerbinska K, Topinkova E, Sinclair-Cohen J, Edbrooke D, Mills G. Exclusion of Older People from Clinical Trials – Professional Views from Nine European Countries Participating in the PREDICT Study. *Drug. Aging* 2011; **28**: 667-677.

[46] Martin R, Cherubini A, O'Neill D. Pharmacology applied to geriatric medicine – Medical licensing for older people. *Eur. Geriatr. Med.* 2011; **2**: 319-321.

[47] Beers E, Egberts TCG, Leufkens HGM, Jansen PAF. The Views of Healthcare Professionals, Drug Developers and Regulators on Information about Older People Needed for Rational Drug Prescription. *PLOS ONE* 2013; **8**: e72060.

[48] Beers E, Egberts TCG, Leufkens HGM, Jansen PAF. Information for Adequate Prescribing to Older Patients – An Evaluation of the Product Information of 53 Recently Approved Medicines. *Drug. Aging* 2013; **30**: 255-262.

[49] Steinmetz KL, Coley KC, Pollock BG. Assessement of geriatric information on the drug label for commonly prescribed drugs in older people. *J. Am. Geriatr. Soc.* 2005; **53**: 891-894.

[50] Orlu-Gul M, Raimi-Abraham B, Jamieson E, Wei L, Murray M, Stawarz K, Stegemann S, Tuleu C, Smith FJ. Public engagement workshop: How to improve medicines for older people? *Int. J. Pharm.* 2014; **459**: 65-69.

[51] Michaud M, Balardy L, Moulis G, Gaudin C, Peyrot C, Vellas B, Cesari M, Nourhashemi F. Proinflammatory Cytokines, Aging, and Age-Related Diseases. *JAMDA* 2013; **14**: 877-882.

[52] Müller L, Pawelec G. Aging and immunity – Impact of behavioral intervention. *Brain Behav. Immun.* 2014; **39**: 8-22.

[53] Cevenini E, Monti D, Franceschi C. Inflamm-aging. *Curr. Opin. Clin. Nutr.* 2013; **16**: 14-20.

[54] Jia Q, Nash JF. Pathology of Aging Skin. In *Textbook of Aging Skin* (Eds: Farage MA, Miller KW, Maibach HI), Springer-Verlag, **2010**.

[55] Perrie Y, Singh Badhan RK, Kirby DJ, Lowry D, Mohammed AR, Ouyang D. The impact of ageing on the barriers to drug delivery. *J. Control. Rel.* 2012; **161**: 389-398.

[56] Konda S, Meier-Davis SR, Cayme B, Shudo J, Maibach HI. Age-related Percutaneous Penetration Part 1: Skin Factors. *Skin Therapy Lett.* 2012; **17**: 1-5.

[57] Konda S, Meier-Davis SR, Cayme B, Shudo J, Maibach HI. Effect of Age on Dermatopharmacokinetics and Overview of Transdermal Products. *Skin Therapy Lett.* 2010; **17**: 5-7.

[58] Kaestli L-Z, Wisilewski-Rasca A-F, Bonnabry P, Vogt-Ferrier N. Use of Transdermal Drug Formulations in the Elderly. *Drug. Aging* 2008; **25**: 269-280.

[59] O'Toole PW, Claesson MJ. Gut microbiota: Changes throughout the lifespan from infancy to elderly. *Int. Dairy J.* 2010; **20**: 281-291.

[60] Roberts MS, Magnusson BM, Burczynski FJ, Weiss M. Enterohepatic Circulation. Physiological, Pharmacokinetic and Clinical Implications. *Clin. Pharmacokinet.* 2002; **41**: 751-790.

[61] Wynendaele E, Verbeke F, D'Hondt M, Hendrix A, Van De Wiele C, Burvenich C, Peremans K, De Wever O, Bracke M, De Spiegeleer B. Crosstalk between the microbiome and cancer cells by quorum sensing peptides. *Peptides* 2015; **64**: 40-48.

[62] Brüssow H. Microbiota and healthy ageing: observational and nutritional intervention studies. *Microb. Biotechnol.* 2013; **6**: 326-334.

[63] Woodmansey EJ. Intestinal bacteria and ageing. *J. Appl. Microbiol.* 2007; **102**: 1178-1186.

[64] O'Toole PW, Brigidi P. The Intestinal Microbiota and Aging. In *Probiotic Bacteria and Their Effect on Human Health and Well-Being* (Eds: Guarino A, Quigley EMM, Walker WA), Karger, **2013**, pp. 25-31.

[65] Oh J, Lee YD, Wagers AJ. Stem cell aging: mechanisms, regulators and therapeutic opportunities. *Nat. Med.* 2014; **20**: 870-880.

[66] European Medicines Agency (EMA). First stem cell therapy recommended for approval in EU – New treatment for rare condition caused by burns to the eye (EMA/786996/2014). 2014; http://www.ema.europa.eu/docs/en_GB/document_library/Press_release/2014/12/WC500179333.pdf (accessed 19 April 2015).

[67] European Medicines Agency (EMA). Summary of the risk management (RMP) for Holoclar (*ex vivo* expanded autologous human corneal epithelial cells containing stem cells (EMA/26006/2015). 2015;

http://www.ema.europa.eu/docs/en_GB/document_library/EPAR_-_Risk-management-plan_summary/human/002450/WC500179032.pdf (accessed 28 April 2015).

[68] Farrall AJ, Wardlaw JM. Blood-brain barrier: Ageing and microvascular disease – systematic review and meta-analysis. *Neurobiol. Aging* 2009; **30**: 337-352.

[69] Popescu BO, Toescu EC, Popescu LM, Bajenaru O, Muresanu DF, Schultzberg M, Bogdanovic N. Blood-brain barrier alterations in ageing and dementia. *J. Neurol. Sci.* 2009; **283**: 99-106.

[70] Zeevi N, Pachter J, McCullough LD, Wolfson L, Kuchel GA. The Blood-Brain Barrier: Geriatric Relevance of a Critical Brain-Body Interface. *J. Am. Geriatr. Soc.* 2010; **58**: 1749-1757.

[71] Marques F, Sousa JC, Sousa N, Palha JA. Blood-brain-barriers in aging and in Alzheimer's disease. *Molecular Degener.* 2013; **8**: 38.

[72] Elahy M, Jackaman C, Mamo JCL, Lam V, Dhaliwal SS, Giles C, Nelson D, Takechi R. Blood-brain barrier dysfunction developed during normal aging is associated with inflammation and loss of tight junctions but not with leukocyte recruitment. *Immun. Ageing* 2015; **12**: 2.

[73] Mooradian AD. Effect of Aging on the Blood-Brain Barrier. *Neurobiol. Aging* 1988; **9**: 31-39.

[74] Mooradian AD. Potential Mechanism of the Age-Related Changes in the Blood-Brain Barrier. *Neurobiol. Aging* 1994; **15**: 751-755.

[75] Shah GN, Mooradian AD. Age-related changes in the blood-brain barrier. *Exp. Gerontol.* 1997; **32**: 501-519.

[76] Ward RJ, Zucca FA, Duyn JH, Crichton RR, Zecca L. The role of iron in brain ageing and neurodegenerative disorders. *Lancet Neurol.* 2014; **13**: 1045-1060.

[77] Bell RD, Winkler FA, Sagare AP, Singh I, LaRue B, Deane R, Zlokovic BV. Pericytes control key neurovascular functions and neurological phenotype in adult brain and during brain aging. *Neuron* 2010; **68**: 409-427.

[78] Minogue AM, Jones RS, Kelly RJ, McDonald CL, Connor TJ, Lynch MA. Age-associated dysregulation of microglial activation is coupled with enhanced blood-brain barrier permeability and pathology in APP/PS1 mice. *Neurobiol. Aging* 2014; **35**: 1442-1452.

[79] Enciu A-M, Gherghiceanu M, Popescu BO. Triggers and Effectors of Oxidative Stress at Blood-Brain Barrier Level: Relevance for Brain Ageing and Neurodegeneration. *Oxid. Med. Cell. Longev.* 2013; **2013**: 297512.

[80] Ötzas B, Küçük M, Kaya M. Sex-dependent changes in blood-brain barrier permeability in epileptic rats following acute hyperosmotic exposure. *Pharmacol. Res.* 2001; **43**: 469-472.

[81] Krause DN, Duckles SP, Pelligrino DA. Influence of sex steroid hormones on cerebrovascular functions. *J. Appl. Physiol.* 2006; **101**: 1252-1261.

[82] Bartels AL, Kortekaas R, Bart J, Willemsen ATM, de Klerk OL, de Vries JJ, van Oostrom JCH, Leenders KL. Blood-brain barrier P-glycoprotein function decreases in specific brain regions with aging: A possible rol in progressive neurodegeneration. *Neurobiol. Aging* 2009; **30**: 1818-1824.

[83] Pekcec A, Schneider EL, Baumgärtner W, Stein VM, Tipold A, Potschka H. Age-dependent decline of blood-brain barrier P-glycoprotein expression in canine brain. *Neurobiol. Aging* 2011; **32**: 1477-1485.

[84] Hsu TM, Kanoski SE. Blood-brain barrier disruption: mechanistic links between Western diet consumption and dementia. *Front. Aging Neurosci.* 2014; **6**: 88.

[85] Gustafson DR, Karlsson C, Skoog I, Rosengren L, Lissner L, Blennow K. Mid-life adiposity factors relate to blood-brain barrier integrity in late life. *J. Intern Med.* 2007; **262**: 643-650.

[86] Takechi R, Pallebage-Gamarallage MM, Lam V, Giles C. Aging-Related Changes in Blood-Brain Barrier Integrity and the Effect of Dietary Fat. *Neurodegenerative Dis.* 2013; **12**: 125-135.

[87] Tucsek Z, Toth P, Sosnowska D, Gautam T, Mitschelen M, Koller A, Szalai G, Sonntag WE, Ungvari Z, Csiszar A. Obesity in Aging Exacerbates Blood-Brain Barrier Disruption, Neuroinflammation, and Oxidative Stress in the Mouse Hippocampus: Effects on Expression of Genes Involved in Beta-Amyloid Generation and Alzheimer's Disease. *J. Gerontol. A Biol. Sci. Med. Sci.* 2014; **69**: 1212-1226.

[88] Montagne A, Barnes SR, Sweeney MD, Halliday MR, Sagare AP, Zhao Z, Toga AW, Jacobs RE, Jacobs RE, Liu CY, Amezcua L, Harrington MG, Chui HC, Law M, Zlokovic BV. Blood-Brain Barrier Breakdown in the Aging Human Hippocampus. *Neuron* 2015; **85**: 296-302.

[89] Pelegri C, Canudas AM, del Valle J, Casadesus G, Smith MA, Camins A, Pallas M, Vilaplana J. Increased permeability of blood-brain barrier on the hippocampus of a murine model of senescence. *Mech. Ageing Dev.* 2007; **128**: 522-528.

[90] Erickson MA, Banks WA. Blood-brain barrier dysfunction as a cause and consequence of Alzheimer's disease. *J. Cerebr. Blood F. Met.* 2013; **33**: 1500-1513.

[91] Stolp HB, Dziegielewska KM. Review: Role of developmental inflammation and blood-brain barrier dysfunction in neurodevelopmental and neurodegenerative diseases. *Neuropath. Appl. Neuro.* 2009; **35**: 132-146.

[92] Stegemann S. Challenges and opportunities in the design of age-appropriate drug products. *Z. Gerontol. Geriatr.* 2012; **6**: 479-484.

[93] International Conference on Harmonisation of Technical Requirements for Registration of Pharmaceuticals for Human Use (ICH). ICH Harmonised Tripartite Guideline – Pharmaceutical Development Q8(R2). 2009; http://www.ich.org/fileadmin/Public_Web_Site/ICH_Products/Guidelines/Quality/Q8_R1/Step4/Q8_R2_Guideline.pdf (accessed 18 March 2015).

[94] Stegemann S, Baeyens J-P, Becker R, Maio M, Bresciani M, Shreeves T, Azadi C, Ecker F, Gogol M. Design of pharmaceutical products to meet future patient needs requires modification of current development paradigms and business models. *Z. Gerontol. Geriatr.* 2014; **4**: 285-287.

[95] Breitkreutz J, Boos J. Paediatric and geriatric drug delivery? *Expert Opin. Drug Deliv.* 2007; **4**: 37-45.

[96] European Commission – Enterprise and industry directorate-general, consumer goods – pharmaceuticals. Guideline on the readability of the labelling and package leaflet of medical products for human use. 2009; http://ec.europa.eu/health/files/eudralex/vol-2/c/2009_01_12_readability_guideline_final_en.pdf (accessed 25 March 2015).

[97] Food and Drug Administration (FDA). Guidance – Useful Written Consumer Medication Information. 2006; http://www.fda.gov/downloads/drugs/guidancecomplianceregulatoryinformation/guidances/ucm080602.pdf (accessed 25 March 2015).

[98] Cherubini A, Crome P. Increasing enrolment in Clinical Trials and the PREDICT Study. EMA Workshop: Ensuring safe and effective medicines for an ageing population, 22-23 March 2012, London. http://www.ema.europa.eu/docs/en_GB/document_library/Presentation/2012/04/WC500125146.pdf (accessed 18 March 2015).

[99] Diener L, Hugonot-Diener L, Alvino S, Baeyens JP, Bone MF, Chirita D, Husson JM, Maman M, Piette F, Tinker A, Von Raison F. Guidance synthesis. Medical research for and with older people in Europe: Proposed ethical guidance for good clinical practice: ethical considerations. *J. Nutr. Health Aging* 2013; **17**: 625-627.

[100] European Forum for Good Clinical Practice Geriatric Medicines Working Party (EFGCP-GMWP). Medical research for and with older people in Europe. 2013; https://www.kcl.ac.uk/sspp/departments/sshm/news/EFGCP-GMWP-Research-Guidelines-Final-edited-2013-05-27.pdf (accessed 18 March 2015).

[101] McMurdo MET, Robert H, Parker S, Wyatt N, May H, Goodman C, Jackson S, Gladman J, O'Mahony S, Ali K, Dickinson E, Edison P, Dyer C. Improving recruitment of older people to research through good practice. *Age Ageing* 2011; **40**: 659-665.

[102] Cusack S, O'Toole PW. Challenges and Implication of Biomedical Research and Intervention Studies in Older Populations: Insights from the ELDERMET Study. *Gerontology* 2013; **59**: 114-121.

[103] Working Group on Functional Outcome Measures for Clinical Trials. Functional Outcomes for Clinical Trials in Frail Older Persons: Time To Be Moving. *J. Gerontol. A Biol. Sci. Med. Sci.* 2008; **63**: 160-164.

[104] Wallace RB. Conducting Case-Control and Cohort Studies in Older Adults. In *The Epidemiology of Aging* (Eds: Newman AB, Cauley JA), Springer Science + Business Media, **2012**.

[105] World Health Organization (WHO). Essential Medicines and health products: pharmacovigilance. 2015; http://www.who.int/medicines/areas/quality_safety/safety_efficacy/pharmvigi/en/ (accessed 26 March 2015).

[106] Sultana J, Cutroneo P, Trifirò G. Clinial and economic burden of adverse drug reactions. *J. Pharmacol. Pharmacother.* 2013; **4**: S73-S77.

[107] European Medicines Agency (EMA). Medicines for older people. 2015; http://www.ema.europa.eu/ema/index.jsp?curl=pages/special_topics/general/general_content_000249.jsp (accessed 26 March 2015).

[108] European Medicines Agency (EMA). Guideline on good pharmacovigilance practices (GVP) – Module V – Risk management systems (Rev 1) (EMA/838713/2011 Rev 1). 2014; http://www.ema.europa.eu/docs/en_GB/document_library/Scientific_guideline/2012/06/WC500129134.pdf (accessed 26 March 2015).

[109] European Medicines Agency (EMA). Guideline on good pharmacovigilance practices (GVP) – Module VI – Management and reporting of adverse reactions to medicinal products (Rev 1) (EMA/873138/2011 Rev 1). 2014; http://www.ema.europa.eu/docs/en_GB/document_library/Scientific_guideline/2014/09/WC500172402.pdf (accessed 26 March 2015).

[110] European Medicines Agency (EMA). Guideline on good pharmacovigilance practices (GVP) – Module VII – Periodic safety update report (Rev 1) (EMA/816292/2011 Rev 1). 2013; http://www.ema.europa.eu/docs/en_GB/document_library/Scientific_guideline/2013/04/WC500142468.pdf (accessed 26 March 2015).

[111] European Medicines Agency (EMA). Guideline on good pharmacovigilance practices (GVP) – Module VIII – Post-authorisation safety studies (Rev 1) (EMA/813938/2011 Rev 1). 2013; http://www.ema.europa.eu/docs/en_GB/document_library/Scientific_guideline/2012/06/WC500129137.pdf (accessed 26 March 2015).

[112] European Medicines Agency (EMA). Guideline on good pharmacovigilance practices (GVP) – Module IX – Signal Management (EMA/827661/2011). 2012; http://www.ema.europa.eu/docs/en_GB/document_library/Scientific_guideline/2012/06/WC500129147.pdf (accessed 26 March 2015).

[113] European Medicines Agency (EMA). Guideline on conduct of pharmacovigilance for medicines used by the paediatric population. 2007; http://www.ema.europa.eu/docs/en_GB/document_library/Scientific_guideline/2009/09/WC500003764.pdf (accessed 26 March 2015).

[114] Food and Drug Administration (FDA). Guidance for Industry – Good Pharmacovigilance Practices and Pharmacoepidemiologic Assessment. 2005; http://www.fda.gov/downloads/RegulatoryInformation/Guidances/UCM126834.pdf (accessed 26 March 2015).

[115] Food and Drug Administration (FDA). Guidance for Industry – Premarketing Risk Assessment. 2005; http://www.fda.gov/downloads/RegulatoryInformation/Guidances/UCM126958.pdf (accessed 26 March 2015).

[116] Food and Drug Administration (FDA). Guidance for Industry – Development and Use of Risk Minimization Action Plans. 2005; http://www.fda.gov/downloads/RegulatoryInformation/guidances/ucm126830.pdf (accessed 26 March 2015).

[117] Baeyens JP. Geriatrician's perspective on implementation of the new pharmacovigilance legislation (presented at Seventh stakeholders' forum on the implementation of the new pharmacovigilance legislation (EMA)). 2013; http://www.ema.europa.eu/docs/en_GB/document_library/Presentation/2013/10/WC500151646.pdf (accessed 26 March 2015).

[118] Montero D. Pharmacovigilance and the elderly – Some proposals for improvement (presented at Ensuring safe and effective medicines for an aging population (EMA)). 2012; http://www.ema.europa.eu/docs/en_GB/document_library/Presentation/2012/04/WC500125152.pdf (accessed 26 March 2015).

[119] Food and Drug Administration (FDA). Paving the way for personalized medicine – FDA's Role in a New Era of Medical Product Development. 2013; http://www.fda.gov/downloads/ScienceResearch/SpecialTopics/PersonalizedMedicine/UCM372421.pdf (accessed 18 March 2015).

[120] Walko CM, McLeod HL. Personalizing Medicine in Geriatric Oncology. *J. Clin. Oncol.* 2014; **32**: 2581-2586.

[121] Prasad K, Breckenridge A. Pharmacogenomics: a new clinical or regulatory paradigm? European experiences of pharmacogenomics in drug regulation and regulatory initiatives. *Drug Discov. Today* 2011; **16**: 867-872.

[122] Crimmins E, Vasunilashorn S, Kim JK, Alley D. Biomarkers Related to Aging in Human Populations. In *Advances in Clinical Chemistry* (Ed: Makowski GS), Academic Press, **2008**, pp. 161-216.

[123] Jee H, Jeon BH, Kim YH, Kim H-K, Choe J, Park J, Jin Y. Development and Application of Biological Age Prediction Models with Physical Fitness and Physiological Components in Korean Adults. *Gerontology* 2012; **58**: 344-353.

[124] Salter H, Holland R. Biomarkers: refining diagnosis and expediting drug development – reality, aspiration and the role of open innovation. *J. Intern. Med.* 2014; **276**: 215-228.

[125] Stegemann S. Pharmacotherapy in Older Adults: An Approach towards Individualised Therapeutic Care Concepts. *International Pharmaceutical Industry – Regulatory & Marketplace* 2012; **3**: 8-12. http://ipimediaworld.com/wp-content/uploads/2012/04/Pages-from-IPI-V3I3-web.pdf (accessed 18 March 2015).

[126] Mullard A. New drugs cost US$2.6 billion to develop. *Nat. Rev. Drug Discov.* 2014; **13**: 87.

[127] Leporini C, De Sarro G, Russo E. Adherence to therapy and adverse drug reactions: is there a link? *Expert Opin. Drug Saf.* 2014; **13**: S41-S55.

[128] Field TS, Gilman BH, Subramanian S, Fuller JC, Bates DW, Gurwitz JH. The Costs Associated With Adverse Drug Events Among Older Adults in the Ambulatory Setting. *Med. Care* 2005; **43**: 1171-1176.

[129] Ratcliffe J, Laver K, Couzner L, Crotty M. Health Economics and Geriatrics: Challenges and Opportunities. In: *Geriatrics* (Ed: Atwood C), Intech, **2012**, http://www.intechopen.com/books/geriatrics/health-economic-evaluation-and-geriatrics-challenges-and-opportunities (accessed 18 March 2015).

[130] Edlin R. Assessing the cost-effectiveness of therapies for older people. In *International Handbook on Ageing and Public Policy* (Eds: Harper S, Hamblin K, Hoffman J, Leeson G), Edward Elgar Publishing Limited, **2014**, pp. 167-177.

[131] Prieto L, Sacristán JA. Problems and solutions in calculating quality-adjusted life years (QALYs). *Health Qual. Life Out.* 2003; **1**: 80.

[132] Courtney M, Edwards H, Stephan J, O'Reilly M, Duggan C. Quality of life measures for residents of aged care facilities: a literature review. *Australas. J. Ageing* 2003; **22**: 58-64.

[133] Coast J, Flynn TN, Natarajan L, Sproston K, Lewis J, Louviere JJ, Peters TJ. Valuing the ICECAP capability index for older people. *Soc. Sci. Med.* 2008; **67**: 874-882.
[134] Hoe J, Orrell M, Livingston G. Quality of Life Measures in Old Age. In *Principles and Practice of Geriatric Psychiatry,* 3rd edition (Eds: Abou-Saleh MT, Katona C, Kumar A), John Wiley & Sons, **2011**.
[135] Morgan S, Grootendorst P, Lexchin J, Cunningham C, Greyson D. The cost of drug development: A systematic review. *Health Policy* 2011; **100**: 4-17.
[136] Nussbaum M. The quality of life. Clarendon Press, **1993**.
[137] Vogt-Ferrier N. Older patients, multiple comorbidities, polymedication… should we treat everything? *Eur. Geriatr. Med.* 2011; **2**: 48-51.
[138] Nordin Olsson I, Runnamo R, Engfeldt P. Medication quality and quality of life in the elderly, a cohort study. *Health Qual. Life Out.* 2011; **9**: 95.
[139] Hinshaw T, Kapusnik-Uner J, Zarowitz B, Matuszewski K. Identifying Knowledge Gaps in the Labeling of Medications for Geriatric Patients. *P. T.* 2013; **38**: 535-540.

SUMMARY & GENERAL CONCLUSIONS

"The man who moves mountains begins by carrying away small stones"

Confucius
(°551 BC - †479 BC, Chinese politician and philosopher)

SUMMARY & GENERAL CONCLUSIONS

This research project aims to quantitatively evaluate the blood-brain barrier (BBB) transport of cell-penetrating peptides (CPPs). As described in **Chapter I**, CPPs are a structural diverse group of peptides that are able to cross cellular membranes. These peptides have a low toxicity profile, but might also exert biological activity. Cell-penetrating peptides are mainly investigated as possible vectors for cell-impermeable cargoes with already numerous success stories that have been reported, also when applied for brain-targeting purposes. The BBB, fundamentally composed of capillary endothelial cells sealed by tight junctions, strictly regulates the transport of ions, solutes, water, macromolecules and blood cells into the brain in order to maintain the brain homeostasis, which is essential for normal CNS function. This barrier is not static and can be regulated and modulated as illustrated by several studies demonstrating that peptides can cross the BBB. With aging, the BBB shows an increased permeability due to structural and functional alterations, which is further aggravated by age-related diseases.

In **Chapter II**, the chemical space of a set of 186 (non-)CPPs was explored using multivariate data analysis techniques, allowing to rationally select model peptides for this research. Based upon differences in the chemical structure, the selected peptides could be categorized into six groups, in which eight smaller subclusters were identified. Quantitative data for cellular influx available for the 186 selected peptides was used to calculate the CP-response, a unified response expressing the extent of cellular uptake. This CP-response was introduced to allow direct comparison of the cell-penetrating properties of peptides within the constraints of inconsistency in used experimental protocols. The CP-response was also used to perform a quantitative structure-property relationship (QSPR) study, which provided new insides into the structural features determining the cellular uptake of peptides, like the influence of the shape, structure complexity and compactness, but also confirmed the importance of cationic charge and amphipathicity.

A classification system for peptides based on their BBB influx properties was introduced in **Chapter III**. Like for the cellular uptake studies, a plethora of methods and experimental set-ups are used to characterize the BBB transport of peptides. During an exploration of the Brainpeps database, four different BBB influx response types were selected for which quantitative data were available. Based on the distribution of these data, five classes of BBB influx magnitude, *i.e.* ranging from very low to very high influx, were defined. These classes were converted to a BBB_{in}-response, a scaled value ranging from zero (very low influx) to ten (very high influx), which is independent of the BBB influx

response from which it is derived. The classification system and BBB_{in}-response allow an objective evaluation of obtained BBB influx data like evaluation of outliers, but also can be applied during QSPR studies.

The quality control (QC) of the peptides investigated during this research is described in **Chapter IV**. Five cationic CPPs were analyzed using five different C_{18}-chromatographic systems differing in column particle size (HPLC versus UHPLC), acidic modifier (FA versus TFA) and column temperature (30°C versus 60°C). The performance of the different systems for analysis of these peptides was compared. It was demonstrated that the used chromatographic system determined the final QC results, with the C_{18}-UHPLC system, operated at 30°C and using TFA as acidic modifier in the mobile phase was identified to be the most suitable method. Trifluoroacetic acid-containing mobile phases are compatible with single quad MS detector systems for which the use during routine QC of peptides was demonstrated, providing information on the identity and purity of the peaks observed during chromatographic analysis. It was concluded that the purity of all peptides evaluated for their BBB transport was above the requested 95% and their identity was confirmed using HPLC-UV/MS.

The main research question of this thesis is answered in **Chapter V**, in which the *in vivo* BBB transport of CPPs is described. The brain influx, parenchymal/capillary distribution and efflux out of the brain was quantitatively investigated of five “traditional” CPPs, *i.e.* pVEC, TP10, TP10-2, SynB3 and Tat 47-57, as well as of “new” CPPs, being four short, proline-rich AMPs (PrAMPs) *i.e.* apidaecin Api137, oncocin, drosocin and drosocin Pro5Hyp, and three disulfide-rich (cyclic) peptides, *i.e.* MCoTI-II, cVc1.1 and chlorotoxin, which also have cell-penetrating properties and are positioned in the chemical space of the CPPs. The results indicate that the investigated peptides showed divergent BBB transport properties characterized by the blood-to-brain transport ranging from very low or no influx to very high brain influx, by a mainly parenchymal distribution to entrapment in capillary endothelial cells and in some cases by efflux out of the brain. The tissue distribution, which varied among the investigated peptides, as well as the *in vitro* metabolic stability of the peptides was also described. From these results, it can be concluded that peptides with cell-penetrating properties selectively cross the BBB.

Finally, in line with the DruQuaR tradition, a regulatory aspect of this research is elaborated. The BBB is assumed to be intact during the BBB transport studies as a healthy and young mouse model is used. With aging, the BBB shows an increased permeability and thus BBB transport might be altered. Other organ systems also show functional changes during the aging process, which has consequences for the use of medicines in the elderly, a population group that is numerically expanding worldwide. Therefore, in **Chapter VI**, it is investigated how these age-related functional changes are taken into

account during the development of medicines for geriatric patients and which regulatory framework is currently provided. The views of the different involved stakeholders are analyzed and the encountered challenges are identified. It can be concluded that today, a gap exists in the knowledge on the benefit-risk ratio of medicines in the geriatric population due to mostly minimal inclusion in clinical trials. Non-binding guidelines are available, but regulatory authorities are aware of this knowledge gap. All stakeholders, each representing a different aspect of the development of geriatric medicines should be involved in the regulatory process, ultimately aiming to provide safe and efficacious drugs for this population.

Based on the obtained results, the main research question of this thesis being **"Do CPPs selectively cross the BBB?"**, could be answered: **YES**, CPPs cross the BBB to a different extent. The investigated model peptides differed chemically and showed a different extent in cellular influx, numerically expressed by the CP-response. However, for the investigated CPPs, the CP-response was not correlated with the extent of BBB influx, expressed by the BBB_{in}-response. Therefore, it is concluded that cell-penetrating properties of peptides do not automatically imply efficient brain influx.

While answering the main question of this Ph.D. project, new research opportunities were identified, which deserve further investigation. Another burning question is whether a **similar mechanism is used for cellular and BBB influx**. If this is the case, mechanistic information on the cellular influx can be used to predict the BBB uptake of CPPs and can help to unravel the BBB transport mechanism of peptides. Therefore, it is important to further characterize the peptides that can cross the BBB. Detailed information about the ***in vivo* serum and brain metabolization** is also required to obtain the full picture. For example, during *in vitro* incubation of pVEC in serum, the formation of a metabolite representing the pVEC peptide cleaved from the N-terminal hydrophobic amino acid residues was demonstrated. Based on a structure-activity relationship study of pVEC, this metabolite is assumed to be not cell-penetrating. If both peptides show brain influx, the BBB transport properties cannot be attributed solely to their cell-penetrating properties. This is valuable information for the study of the structural features determining the BBB transport of (cell-penetrating) peptides. For identification and quantification of the formed metabolites *in vivo*, new advanced sample preparation and MS detection systems, designed to quantify very small amounts of peptides, are required. Moreover, with the introduction of these very sensitive MS systems and suitable sample preparation methods, the use of radiotracers becomes superfluous.

During this research, an *in vivo* mouse model was used to study the BBB transport of CPPs as this still is the "golden standard". However, suitable ***in vitro* BBB models** have eminent advantages. The search for *in vitro* models showing good correlation with *in vivo* models is challenging because of the complex nature of the BBB and the interplay between the cells and other components of the neurovascular unit. A promising *in vitro* model is the triple co-culture of endothelial cells, pericytes and astrocytes. These *in vitro* models can be used to obtain a large data set of BBB transport data of (cell-penetrating) peptides, required for reliable QSPR study, but can also be applied to study the possible mechanism of BBB transport.

Chemo-molecular descriptors numerically expressing the peptide structure are also needed for performing QSPR studies. During this research, it was noted that **peptide-specific descriptors** are limited available, and if disposable, they show limited applicability mostly due to their restricted use for peptide structures only consisting of natural L-amino acids. New descriptors for the hydrophobicity, secondary structure and charge characteristics are urgently needed. Moreover, current commercially available descriptor calculation packages are developed for small molecules leading to difficulties in the interpretation of the descriptor meaning for larger peptide structures. Thus, use of peptide-specific descriptors, which can be calculated for all peptide and peptoid structures, will bring QSPR studies of peptides to a higher level and will allow to distract more relevant information.

Peptides are omnipresent in the human body being endogenously formed, *i.a.* through metabolization of proteins, or of exogenous origin. Peptide structures show a high specificity and potency, implying that small amounts of peptides can exert a prolonged effect. Therefore, it is of **general importance to know which peptides can gain access to the brain, which brain regions they reach, how long they reside in the CNS and what their possible pharmacodynamic effects are.** Models based on QSPR studies can be used to identify peptide structures that might be able to cross the BBB. This evaluation is of importance during the development of peptide medicines that gained increased interest from the pharmaceutical industry. BBB transport of peptides is expected to be a prerequisite in case of CNS therapeutics or the QSPR models can be used as a tool to evaluate the CNS toxicity profile of the new peptide medicine. These models can also be applied to scan protein and peptide libraries for sequences that possibly can cross the BBB. This information is highly relevant for peptide structures that can exert a biological effect and thus also can affect the CNS function. The proposed approach allows to identify peptide sequences hidden in the protein structure that can cross the BBB once formed after metabolization of the parent protein. For these hidden peptide structures, so-called cryptic peptides, it can be further investigated whether they can

affect and modulate the CNS function. Imaging MS is a relatively new technique allowing to evaluate the **temporal-spatial distribution of the peptide in the brain**. This information can be used to evaluate region-specific uptake in the brain, which can be of therapeutic interest or can help to unravel the potential role or function of the peptide in the CNS. The temporal distribution provides information of the time frame in which the peptide resides in that brain region.

Aging is known to be associated with increased BBB permeability. This is relevant for drug therapy in the elderly causing changes in the brain distribution and CNS (side) effects, which is currently neglected during the development of geriatric medicines. Availability of **biomarkers for BBB dysfunction or models for BBB permeability** can assist in dose adjustment of medicines in the elderly or can be used to evaluate potential risks of drug therapy in this patient population. Possible markers could be the pro-inflammatory cytokines of which the blood levels are increased with aging or the gut microbiota composition, which is known to influence the BBB function and shows alterations in composition with aging. Gender differences should also be taken into account as sex steroidal hormones are known to influence the BBB permeability. The role of BBB dysfunction is acknowledged for neurodegenerative diseases. Another important question is whether **BBB dysfunction is associated with the etiology of other CNS diseases** like epilepsy, autism, schizophrenia, depression or brain cancer, which might offer new therapeutic options.

By demonstrating the selective ability of CPPs to cross the BBB, we have laid the fundaments of further research. We demonstrated that current available studies evaluating both cellular influx and BBB transport of peptides are characterized by inconsistencies in experimental set-up and methodologies. Therefore, we introduced unified responses for the cellular uptake and BBB influx of peptides. **Harmonization and standardization** of these protocols, including consistent evaluation of positive and negative controls, would allow to more reliably compare peptides with regards their cell- and BBB-penetrating properties, helping to answer open questions like the used mechanism and required structural features both for cellular influx and BBB transport. Finally, the fact that CPPs can be formed endogenously, stresses the importance for the **characterization of possible biological (CNS) effects** of these peptides.

SAMENVATTING & ALGEMENE CONCLUSIES

"Samenkomen is een begin; samenblijven is vooruitgang; samenwerken is succes"

Henry Ford
(°1863 - †1947, Amerikaans industrieel)

SAMENVATTING & ALGEMENE CONCLUSIES

De doelstelling van dit onderzoeksproject is het kwantitief onderzoeken van het bloed-hersenbarrière (BBB-)transport van cel-penetrerende peptiden (CPPs). Zoals beschreven in **Hoofdstuk I**, zijn CPPs een groep van structureel verschillende peptiden, die celmembranen kunnen passeren. Deze peptiden zijn gekenmerkt door een laag toxiciteitsprofiel, maar kunnen ook een biologische activiteit vertonen. Cel-penetrerende peptiden worden voornamelijk onderzocht als mogelijke vectoren voor cel-ondoorlaatbare moleculen en er zijn reeds talrijk succesverhalen gerapporteerd, ook voor gerichte toediening in de hersenen. De BBB is samengesteld uit de endotheelcellen van de capillairen onderling verbonden via hechte netwerken van eiwitten ("tight junctions") en reguleert nauwgezet het transport van ionen, water, (macro)moleculen en bloedcellen van en naar de hersenen, opdat de hersenhomeostase kan gehandhaafd blijven, wat essentieel is voor een normale functie van het centraal zenuwstelsel. Deze barrière is niet statisch en kan gereguleerd en gewijzigd worden, zoals geïllustreerd door verschillende studies waarin de mogelijkheid van peptiden om de BBB te passeren wordt aangetoond. Tijdens het verouderingsproces vertoont de BBB een verhoogde doorlaatbaarheid als gevolg van structurele en functionele veranderingen, wat verder kan verergerd worden door ouderdomsziekten.

In **Hoofdstuk II** werden de modelpeptiden voor dit onderzoek geselecteerd op basis van de exploratie van de chemische diversiteit van een set van 186 (niet-)CPPs met behulp van multivariate data-analysetechnieken. Op basis van verschillen in de chemische structuur konden de geselecteerde peptiden onderverdeeld worden in zes groepen, waarbinnen nog acht kleinere subgroepen konden onderscheiden worden. De kwantitatieve data voor celopname die beschikbaar zijn voor deze 186 geselecteerde peptiden werden gebruikt om de CP-respons, een universele response die de mate van celopname uitdrukt, te berekenen. Deze CP-respons werd geïntroduceerd om een directe vergelijking van de cel-penetrerende eigenschappen van peptiden toe te laten, ondanks de inconsistentie in de gebruikte experimentele protocollen. De CP-respons werd ook gebruikt om een kwantitatieve structuur-eigenschapsrelatie-onderzoek (QSPR) uit te voeren. Deze studie bood nieuwe inzichten in de structurele eigenschappen van peptiden die bepalend zijn voor celopname, zoals het belang van de vorm, structuurcomplexiteit en -compactheid, en daarnaast werd het belang van de positieve lading en amfipaticiteit bevestigd.

In **Hoofdstuk III** werd een classificatiesysteem voor peptiden op basis van hun BBB-influx geïntroduceerd. Zoals vastgesteld voor de celopnamestudies, worden er ook een diversiteit aan methoden en experimentele protocollen gebruikt om het BBB-transport van peptiden te karakteriseren. Tijdens de exploratie van de Brainpeps database werden vier verschillende types van BBB-influxresponsen geselecteerd, waarvoor kwantitatieve data beschikbaar waren. Op basis van de verdeling van deze data werden vijf klassen van een bepaalde BBB-influx grootte-orde gedefinieerd, gaande van zeer lage tot zeer hoge influx. Deze klassen werden omgezet naar een BBB_{in}-respons, een getal van 0 (zeer lage influx) tot 10 (zeer hoge influx), dat onafhankelijk is van de BBB-influxrespons waarvan het afkomstig is. Dit classificatiesysteem en de BBB_{in}-respons laten een objectieve evaluatie toe van de BBB-influxresultaten, zoals de evaluatie van afwijkende resultaten, maar kunnen ook gebruikt worden tijdens het uitvoeren van QSPR-studies.

De kwaliteitscontrole van de onderzochte peptiden is beschreven in **Hoofdstuk IV**. Vijf kationische CPPs werden geanalyseerd met behulp van vijf verschillende C_{18}-chromatografische systemen die onderling verschilden in kolompartikelgrootte (HPLC versus UHPLC), zuurcomponent van de mobiele fase (mierenzuur (FA) versus trifluoro-azijnzuur (TFA)) en kolomtemperatuur (30°C versus 60°C). De prestatie van de verschillende chromatografische systemen, gebruikt voor de analyse van deze peptiden, werden vergeleken. Er werd aangetoond dat het gebruikte chromatografische systeem bepalend is voor de finale kwaliteitscontroleresultaten. Het C_{18}-UHPLC-systeem, met kolomtemperatuur 30°C en met TFA in de mobiele fase, was geïdentificeerd als het meest geschikte systeem. Mobiele fasen die TFA bevatten zijn compatibel met “single quad” massaspectrometrie (MS) detectorsystemen, waarvan het routinematig gebruik tijdens de kwaliteitscontrole van peptiden werd aangetoond, aangezien het informatie kan verschaffen over de identiteit en de zuiverheid van de pieken in de bekomen chromatogrammen. Voor alle peptiden waarvan het BBB-transport onderzocht werd, lag de zuiverheid boven de vereiste 95% en werd hun identiteit bevestigd met behulp van HPLC-UV/MS.

De hoofdonderzoeksvraag van deze thesis werd beantwoord in **Hoofdstuk V**, waarin de *in vivo* BBB-transporteigenschappen van de CPPs wordt beschreven. The herseninflux, verdeling naar het hersenparenchym en -capillairen en efflux uit de hersenen van vijf “traditionele” CPPs, nl. pVEC, TP10, TP10-2, SynB3 en Tat 47-57, en “nieuwe” CPPs, meer bepaald vier korte, proline-rijke antimicrobiële peptiden (PrAMPs), apidaecin Api137, oncocin, drosocin en drosocin Pro5Hyp, en drie disulfide-rijke (cyclische) peptiden, MCoTI-II, cVc1.1 en chlorotoxin, werden kwantitatief onderzocht. De “nieuwe” CPPs zijn peptiden die ook cel-penetrerende eigenschappen bezitten en gelijkaardige chemische eigenschappen vertonen als de CPPs. De resultaten tonen aan dat de onderzochte

peptiden uiteenlopende BBB-transporteigenschappen vertonen, gaande van een zeer hoge tot zeer lage herseninflux, van hoofdzakelijk distributie naar het hersenparenchym tot captatie in de endotheelcellen van de capillairen en in sommige gevallen efflux uit de hersenen. De weefseldistributie, die sterk verschilde tussen de onderzochte peptiden, alsook de *in vitro* metabole stabiliteit van de peptiden, werd onderzocht. Uitgaande van deze resultaten kan geconcludeerd worden dat peptiden met cel-penetrerende eigenschappen de BBB passeren op een selectieve manier.

Tot slot, werd volgens de traditie op het DruQuaR labo, een regulatoir aspect van dit onderzoek behandeld. De BBB is verondersteld in tact te zijn tijdens de studie van BBB-transport van peptiden, gezien een gezond en jong muismodel werd gebruikt. Tijdens het verouderingsproces vertoont de BBB een verhoogde permeabiliteit, wat dus een wijziging in BBB-transport kan veroorzaken. Ander orgaansystemen vertonen ook functionele veranderingen met ouder worden, wat gevolgen heeft voor het medicatiegebruik bij ouderen, een populatiegroep waarvan, wereldwijd, het aantal exponentieel toeneemt. Daarom werd in **Hoofdstuk VI** onderzocht hoe deze leeftijdsgebonden functionele veranderingen in rekening worden gebracht tijdens de ontwikkeling van geneesmiddelen voor geriatrische patiënten en welk regulatoir kader momenteel wordt geboden. De kijk van de verschillende betrokken partijen hierop werd geanalyseerd en de uitdagingen geïdentificeerd. Er kan geconcludeerd worden dat vandaag, een enorme lacune bestaat in de informatie over de risico-batenverhouding van het gebruik van geneesmiddelen door ouderen, doordat ze vaak minimaal geïncludeerd worden in klinische studies. Niet-bindende richtlijnen zijn beschikbaar, maar de regulatoire autoriteiten zijn zich bewust van deze informatielacune. Alle betrokken partijen, die elk een verschillend aspect van de ontwikkeling van geriatrische geneesmiddelen vertegenwoordigen, zouden betrokken moeten worden bij het regulatoire proces met als ultieme doel het voorzien van veilige en effectieve geneesmiddelen voor deze patiëntenpopulatie.

Op basis van de onderzoeksresultaten kan de hoofdonderzoeksvraag van deze thesis, nl. **"In welke mate passeren CPPs selectief the BBB?"**, beantwoord worden: **JA**, CPPs passeren de BBB in verschillende mate. De onderzochte modelpeptiden verschilden chemisch en vertoonden een verschillende mate van celopname, numeriek uitgedrukt door de CP-respons. Voor de onderzochte peptiden kon niet worden aangetoond dat de CP-respons gecorreleerd was met de mate van BBB-influx, uitdrukt door de BBB_{in}-respons. Daarom kan geconcludeerd worden dat cel-penetrerende eigenschappen van peptiden niet automatische efficiënte herseninflux impliceren.

Tijdens het beantwoorden van de hoofdonderzoeksvraag van dit Ph.D.-project doken nieuwe onderzoeksmogelijkheden op. Een eerste vraag die zich stelt is of een **gelijkaardig mechanisme wordt gebruikt voor celopname als voor BBB-influx**. Indien dit het geval is kan mechanistische informatie over de celopname gebruikt worden om de BBB-influx van CPPs te voorspellen en om het BBB-transportmechanisme van peptiden helpen te ontrafelen. Daarom is het belangrijk om peptiden die in staat zijn om BBB te passeren verder te karakteriseren. Gedetailleerde informatie over de ***in vivo* serum- en hersenmetabolisatie** is ook vereist om een volledig beeld te krijgen van het BBB-transport van peptiden. Zo werd bijvoorbeeld tijdens de *in vitro* incubatie van pVEC in serum de vorming van een metaboliet, zijnde pVEC waarvan de N-terminale hydrofobe aminozuren zijn gekliefd, aangetoond. Op basis van de structuur-activiteitsrelatiestudie van pVEC, is verondersteld dat deze metaboliet geen CPP zal zijn. Als beide peptiden BBB-influx vertonen, kunnen de BBB-transporteigenschappen van CPPs niet enkel toegekend worden aan hun cel-penetrerende eigenschappen. Dit is waardevolle informatie voor de studie van de structurele kenmerken die bepalend zijn voor BBB-transport van (cel-penetrerende) peptiden. Nieuwe, geavanceerde staalvoorbereidingstechnieken en MS-detectiesystemen, ontwikkeld om kleine hoeveelheden van peptiden te kwantificeren, zijn vereist voor de identificatie en kwantificatie van de *in vivo* gevormde metabolieten. De introductie van deze zeer gevoelige MS-systemen en geschikte staalvoorbereidingsmethoden maken bovendien het gebruik van radioactieve labels overbodig.

Tijdens dit onderzoek werd een *in vivo* muismodel gebruikt om het BBB-transport van CPPs te onderzoeken, gezien dit nog steeds geldt als de “gouden standaard”. Daarentegen hebben geschikte ***in vitro* BBB-modellen** aanzienlijke voordelen. De zoektocht naar *in vitro* modellen met goede correlatie met de *in vivo* modellen is niet eenvoudig, wegens de complexe samenstelling van de BBB en het samenspel van BBB met de cellen en andere componenten van de neurovasculaire unit. Een veelbelovend *in vitro* model is de tripel co-cultuur van endotheelcellen, pericyten en astrocyten. Deze *in vitro* modellen kunnen gebruikt worden om grote datasets van BBB-transportresultaten van (cel-penetrerende) peptiden te verkrijgen, wat vereist is om een betrouwbare QSPR-studie te kunnen uitvoeren, maar ze kunnen ook gebruikt worden om de BBB-transportmechanismen op te helderen.

Chemo-moleculaire descriptoren die numeriek de peptidestructuur uitdrukken zijn ook nodig om QSPR-studies uit te voeren. Tijdens dit onderzoek werd vastgesteld dat **peptide-specifieke descriptoren** slechts beperkt beschikbaar zijn, en indien beschikbaar, vertonen ze vaak beperkte toepasbaarheid, voornamelijk doordat ze enkel kunnen berekend worden voor peptiden opgebouwd uit de natuurlijk voorkomende L-aminozuren. Nieuwe descriptoren die de hydrofobiciteit, secundaire structuur en ladingseigenschappen van peptiden uitdrukken, zijn dringend nodig. De huidige

commercieel beschikbare descriptorpakketten zijn ontwikkeld voor kleine organische moleculen, waardoor de interpretatie van de descriptorbetekenis voor de grotere peptidestructuren bemoeilijkt wordt. Het gebruik van peptide-specifieke descriptoren, die zowel voor peptide- als peptoidestructuren kunnen berekend worden, zal QSPR-studies van peptiden naar een hoger niveau tillen en zal toelaten om meer relevante informatie uit deze studies te distilleren.

Peptiden zijn alomtegenwoordig in het menselijk lichaam en kunnen zowel endogeen gevormd worden tijdens metabolisatie van proteinen of kunnen van exogene oorsprong zijn. Peptidestructuren zijn gekarakteriseerd door een hoge specificiteit en potentie, wat impliceert dat een kleine hoeveelheid peptide een langdurig effect kan uitoefenen. Het is daarom van algemeen belang dat we weten **welke peptiden zich toegang kunnen verschaffen tot de hersenen, welke hersendelen ze bereiken, hoe lang ze in het centraal zenuwstelsel verblijven en wat hun mogelijke farmacodynamische effecten zijn**. Modellen die gebaseerd zijn op QSPR-studies kunnen gebruikt worden om peptidestructuren te identificeren die mogelijks de BBB kunnen passeren. Deze evaluatie is van belang tijdens de ontwikkeling van peptidegeneesmiddelen, die steeds meer interesse verwerven van de farmaceutische industrie. Bloed-hersenbarrièretransport van peptiden is een vereiste in het geval van geneesmiddelen voor aandoeningen van het centraal zenuwstelsel, of deze QSPR-modellen kunnen gebruikt worden als instrument om de toxiciteitsprofiel voor het centraal zenuwstelsel van het nieuw geneesmiddel te evalueren. Een andere toepassing van deze modellen is het screenen van proteine- en peptidebibliotheken naar sequenties die mogelijks de BBB kunnen passeren. Deze informatie is relevant voor peptiden die een biologisch effect kunnen uitoefenen en dus ook mogelijks het centraal zenuwstelsel kunnen beïnvloeden. De voorgestelde aanpak laat toe om peptidesequenties verscholen in proteinestructuren, die mogelijks de BBB kunnen passeren, te identificeren. Voor deze verscholen peptidestructuren, de zogeheten cryptische peptiden, kan dan verder onderzocht worden of ze de werking van het centraal zenuwstelsel kunnen beïnvloeden. Beeldvormingsmassaspectrometrie is een vrij recente techniek die toelaat om de **temporale en spatiale distributie van de peptiden in de hersenen** te bestuderen. Deze informatie kan gebruikt worden om de na te gaan of de hersenopname regio-specifiek gebeurt, wat interessant kan zijn voor therapeutische toepassingen of kan helpen bij het ontrafelen van de mogelijke functie van deze peptiden in het centraal zenuwstelsel. De temporale distributie levert informatie op over het tijdsduur dat het peptide in een bepaald hersendeel aanwezig is.

Verouderen is geassocieerd met een verhoogde permeabiliteit van de BBB. Hoewel momenteel vaak niet onderzocht tijdens de ontwikkeling van geriatrische geneesmiddelen, is dit zeer relevant voor de medicinale therapie bij ouderen, gezien het veranderingen in de hersendistributie en bijwerkingen in

het centraal zenuwstelsel kan veroorzaken. De beschikbaarheid van **biomerkers voor de BBB-dysfunctie of modellen voor BBB permeabiliteit** kunnen helpen bij de dosisaanpassing van geneesmiddelen toegediend aan ouderen of ze kunnen gebruikt worden om de potentiële risico's in te schatten van een bepaalde geneesmiddelentherapie bij ouderen. Mogelijke merkers zouden de pro-inflammatoire cytokines kunnen zijn, waarvan de bloedwaarden verhoogd zijn bij ouderen, of de samenstelling van de microflora van de darm, dat de BBB-functie beïnvloedt en wijzigingen vertoont tijdens verouderen. Verschillen tussen man en vrouw zouden ook in acht moeten genomen worden, gezien geslachtshormonen ook de BBB-functie beïnvloeden. De rol van de BBB-dysfunctie in neurodegeneratieve aandoeningen is reeds erkend. Een ander belangrijke vraag is of **BBB-dysfunctie geassocieerd is met de etiologie van andere aandoeningen van het centraal zenuwstelsel** zoals epilepsie, autisme, schizofrenie, depressie of hersenkanker, wat weer nieuwe therapeutische opties zou kunnen bieden.

Met het aantonen van de mogelijkheid van de CPPs om selectief de BBB te passeren, hebben we de fundamenten gelegd voor verder onderzoek. We hebben aangetoond dat de huidige beschikbare studies die zowel de celopname als het BBB-transport van peptiden bestuderen, inconsistentie vertonen in de experimentele opstelling en methodiek. Daarom hebben we universele responsen geïntroduceerd, zowel voor celopname als voor BBB-influx van peptiden. Een **harmonisatie en standaardisatie** van deze protocollen, met onder andere de consequente evaluatie van een positieve en negatieve controle, zouden toelaten om de celopname en de BBB-transporteigenschappen van peptiden op een meer betrouwbare manier met elkaar te vergelijken. Dit zal ook helpen om openstaande vragen te beantwoorden, zoals de gebruikte mechanismen en de vereiste structurele eigenschappen voor celopname en BBB-transport. Tot slot, het feit dat CPPs endogeen kunnen gevormd worden, onderstreept het belang van het **onderzoek van de mogelijke biologische effecten (op het centraal zenuwstelsel)** van deze peptiden.

CURRICULUM VITAE

"Success is not final, failure not fatal:
It is the courage to continue that counts."

Winston Churchill
(°1874 - †1965, Former Prime Minister of the United Kingdom)

CURRICULUM VITAE

SOFIE STALMANS

PERSONALIA

Surname:	Stalmans
First name:	Sofie
Nationality:	Belgian
Place & date of birth:	Brasschaat, 24 February 1988
Private address:	Norbertijnenstraat 36 2040 Berendrecht
Professional address:	Drug Quality & Registration (DruQuaR) laboratory Department of Pharmaceutical Analysis Faculty of Pharmaceutical Sciences Ghent University Ottergemsesteenweg 460 9000 Ghent
Phone:	(+32) 9 264 80 99
E-mail:	Sofie.Stalmans@UGent.be
URL:	http://www.ugent.be/fw/en/research/pharmaceutical-analysis/druquar

EDUCATION

2000 – 2006:	Latin-Sciences at Groenendaalcollege (Merksem)
2006 – 2011:	Master of Science in Drug Development at Ghent University (Ghent)
2011:	"Multivariate Data Analysis & Design of Experiments" at Ghent University
2013:	"Effective Scientific Communication" at Ghent University (Principae)
2013:	"Basisassistententraining" at Ghent University
2014:	"Communication Skills and Negotiation Skills" at Ghent University (T.O.M. bvba)

2013 - 2014: "Registration of Packed Medicines" at Ghent University

2013 - 2014 "Basic course: Laboratory Animal Science (FELASA cat. B)" at HoGent (Ghent)

PROFESSIONAL EXPERIENCE

August 2011 – present: Staff scientist at DruQuaR:

- Research in drug development
- Supporting practical courses (Advanced Drug Analysis and Pharmaceutical Bachelor Dissertation)
- Servicing activities and analyses
- Lab-responsible for the management of the hard-copy and electronic document archiving system and communication with external clients

PUBLICATIONS IN JOURNALS WITH PEER REVIEW

PUBLISHED AND/OR ACCEPTED

Van Dorpe S, Bronselaer A, Nielandt J, Stalmans S, Wynendaele E, Audenaert K, Van De Wiele C, Burvenich C, Peremans K, Hsuchou H, De Tré G, De Spiegeleer B. Brainpeps: the blood-brain barrier peptide database. *Brain Struct. Funct.* 2012; **217**: 687-718.

Novoa A, Van Dorpe S, Wynendaele E, Spetea M, Bracke N, Stalmans S, Betti C, Chung NN, Lemieux C, Zuegg J, Cooper MA, Tourwé D, De Spiegeleer B, Schiller PW, Ballet S. Variation of the Net Charge, Lipophilicity, and Side Chain Flexibility in Dmt[1]-DALDA: Effect on Opioid Activity and Biodistribution. *J. Med. Chem.* 2012; **55**: 9549-9561.

Wynendaele E, Bronselaer A, Nielandt J, D'Hondt M, Stalmans S, Bracke N, Verbeke F, Van De Wiele C, De Tré G, De Spiegeleer B. Quorumpeps database: chemical space and functionality of quorum sensing peptides. *Nucleic Acids Res.* 2013; **41**: D655-D659.

D'Hondt M, Gevaert B, Stalmans S, Van Dorpe S, Wynendaele E, Peremans K, Burvenich C, De Spiegeleer B. Reversed-phase fused-core HPLC modeling of peptides. *J. Pharm. Anal.* 2013; **3**: 93-101.

D'Hondt M, Verbeke F, Stalmans S, Gevaert B, Wynendaele E, De Spiegeleer B. Derringer desirability and kinetic plot LC-column comparison approach for MS-compatible lipopeptide analysis. *J. Pharm. Anal.* 2014; **4**: 173-182.

Stalmans S, Wynendaele E, Bracke N, Gevaert B, D'Hondt M, Peremans K, Burvenich C, De Spiegeleer B. Chemical-Functional Diversity in Cell-Penetrating Peptides. *PLOS ONE* 2013; **8**: e71752.

Wynendaele E, Bracke N, Stalmans S, De Spiegeleer B. Development of Peptide and Protein Based Radiopharmaceuticals. *Curr. Pharm. Design* 2014; **20**: 2250-2267.

Stalmans S, Wynendaele E, Bracke N, Knappe D, Hoffmann R, Peremans K, Polis I, Burvenich C, De Spiegeleer B. Blood-Brain Barrier Transport of Short, Proline-Rich Antimicrobial Peptides. *Protein Peptide Lett.* 2014; **21**: 399-406.

De Spiegeleer A, Wynendaele E, Vandekerckhove M, Stalmans S, Boucart M, Van den Noortgate N, Venken K, Van Calenbergh S, Aspeslagh S, Elewaut D. An *In Silico* Approach for Modelling T-Helper Polarizing iNKT Cell Agonists. *PLOS ONE* 2014; **9**: e87000.

Stalmans S, Willems M, Adriaens E, Remon JP, D'Hondt M, De Spiegeleer B. Flatworm models in pharmacological research: The importance of compound stability testing. *Regul. Toxicol. Pharm.* 2014; **70**: 149-154.

Verbeken M, Wynendaele E, Mauchauffée E, Bracke N, Stalmans S, Bojnik E, Benyhe S, Peremans K, Polis I, Burvenich C, Gjedde A, Hernandez J-F, De Spiegeleer B. Blood-brain transfer and antinociception of linear and cyclic N-methyl-guanidine and thiourea-enkephalins. *Peptides* 2015; **63**: 10-21.

Wynendaele E, Gevaert B, Stalmans S, Verbeke F, De Spiegeleer B. Exploring the chemical space of quorum sensing peptides. *Biopolymers* 2015; doi: 10.1002/bip.22649.

Stalmans S, Gevaert B, Wynendaele E, Nielandt J, De Tré G, Peremans K, Burvenich C, De Spiegeleer B. Towards a unified blood-brain barrier influx (BBB_{in}) response for peptides. *Protein Peptide Lett.* 2015; **22**: 768-775.

Stalmans S, Gevaert B, Verbeke F, D'Hondt M, Bracke N, Wynendaele E, De Spiegeleer B. Quality control of cationic cell-penetrating peptides. *J. Pharmaceut. Biomed.* 2016; **117**: 289-297.

Stalmans S, Bracke N, Wynendaele E, Gevaert B, Peremans K, Burvenich C, Polis I, De Spiegeleer B. Cell-Penetrating Peptides Selectively Cross the Blood-Brain Barrier *In Vivo*. *PLOS ONE* 2015; **Accepted for publication.**

SUBMITTED

Wynendaele E, Verbeke F, Stalmans S, Gevaert B, Janssens Y, Van De Wiele C, Peremans K, Burvenich C, De Spiegeleer B. Quorum sensing peptides selectively penetrate the blood-brain barrier. **Submitted (under review at *PLOS ONE*)**.

De Spiegeleer B, Wynendaele E, Bracke N, Veryser L, Taevernier L, Degroote A, Stalmans S. Regulatory development of geriatric medicines: To GIP or not to GIP? **Submitted (under review at *Ageing Research Reviews*)**.

IN PREPARATION

Veryser L, Taevernier L, Joshib T, Tatkeb P, Wynendaele E, Stalmans S, Peremans K, Burvenich C, Van Risseeuw M, De Spiegeleer B. Gut and blood-brain barrier pharmacokinetics of the plant N-alkylamide spilanthol using *in vitro* and *in vivo* rodent models. **In preparation**.

PRESENTATIONS AT (INTER)NATIONAL CONFERENCES

Stalmans S, Wynendaele E, De Spiegeleer B. Exploring the chemical-functional space of cell-penetrating peptides, *Scientific Afternoon of the Faculty of Pharmaceutical Sciences*, 16 May 2012, Ghent, Belgium.
Poster presentation

Stalmans S, D'Hondt M, Wynendaele E, Bracke N, De Spiegeleer B. Exploring the Brainpeps database, *15th International Symposium on Signal Transduction in the Blood-Brain Barriers*, 13-16 September 2012, Potsdam - Sanssouci, Germany.
Poster presentation

Stalmans S, Wynendaele E, De Spiegeleer B. How the exploration of the chemical space of cell-penetrating peptides helps to understand their functionality, *14th Naples Workshop on Bioactive Peptides*, 12-14 June 2014, Naples, Italy.
Oral presentation

Stalmans S, Bracke N, De Spiegeleer B. Development of geriatric medicines: to GIP or not to GIP?, *TOPRA 11th Annual Symposium*, 13-15 October 2014, Brussels, Belgium.
Poster presentation

Stalmans S, Wynendaele E, Bracke N, De Spiegeleer B. Do cell-penetrating peptides cross the blood-brain barrier?, *33rd European Peptide Symposium*, 31 August - 5 September 2014, Sofia, Bulgaria.
Poster presentation

De Spiegeleer B, D'Hondt M, Stalmans S, Wynendaele E, Van Dorpe S. Blood-brain barrier modelling of bioactive peptides, *13th Naples Workshop on Bioactive Peptides*, 7-10 June 2012, Naples, Italy.
Oral presentation

De Spiegeleer B, Stalmans S, Wynendaele E, Bracke N, Verbeken M, Peremans K, Polis I, Burvenich C. Receptor and blood-brain barrier characterisation of opioid peptides in drug research and early development, *32nd European Peptide Symposium*, 2-7 September 2012, Athens, Greece.
Oral presentation

De Spiegeleer A, Wynendaele E, Stalmans S, Van den Noortgate N, Vandekerckhove M, Van Calenbergh S, Aspeslagh S, Venken K, Elewaut D. A computational high-throughput screening approach of iNKT-agonists: a novel tool to find optimized iNKT cell ligands, *7th International symposium on CD1 and NKT Cells*, 13-19 September 2013, Tours, France.

Poster presentation

Gevaert B, Wynendaele E, Verbeken M, D'Hondt M, Stalmans S, Peremans K, Burvenich C, Delesalle C, De Spiegeleer B. Exploration of the peptide drug space, *33rd European Peptide Symposium*, 31 August - 5 September 2014, Sofia, Bulgaria.
Poster presentation

AWARDS

October 2014: First Poster Prize at TOPRA 11th Annual Symposium (Brussels)